

1984

Ore Types And Fluid Regimes: Macassa Gold Mine, Kirkland Lake

Gordon Peter Watson

Follow this and additional works at: <https://ir.lib.uwo.ca/digitizedtheses>

Recommended Citation

Watson, Gordon Peter, "Ore Types And Fluid Regimes: Macassa Gold Mine, Kirkland Lake" (1984). *Digitized Theses*. 1384.
<https://ir.lib.uwo.ca/digitizedtheses/1384>

This Dissertation is brought to you for free and open access by the Digitized Special Collections at Scholarship@Western. It has been accepted for inclusion in Digitized Theses by an authorized administrator of Scholarship@Western. For more information, please contact tadam@uwo.ca, wlsadmin@uwo.ca.

The author of this thesis has granted The University of Western Ontario a non-exclusive license to reproduce and distribute copies of this thesis to users of Western Libraries. Copyright remains with the author.

Electronic theses and dissertations available in The University of Western Ontario's institutional repository (Scholarship@Western) are solely for the purpose of private study and research. They may not be copied or reproduced, except as permitted by copyright laws, without written authority of the copyright owner. Any commercial use or publication is strictly prohibited.

The original copyright license attesting to these terms and signed by the author of this thesis may be found in the original print version of the thesis, held by Western Libraries.

The thesis approval page signed by the examining committee may also be found in the original print version of the thesis held in Western Libraries.

Please contact Western Libraries for further information:

E-mail: libadmin@uwo.ca

Telephone: (519) 661-2111 Ext. 84796

Web site: <http://www.lib.uwo.ca/>

CANADIAN THESES ON MICROFICHE

I.S.B.N.

THESES CANADIENNES SUR MICROFICHE



National Library of Canada
Collections Development Branch

Canadian Theses on
Microfiche Service

Ottawa, Canada
K1A 0N4

Bibliothèque nationale du Canada
Direction du développement des collections

Service des thèses canadiennes
sur microfiche

NOTICE

The quality of this microfiche is heavily dependent upon the quality of the original thesis submitted for microfilming. Every effort has been made to ensure the highest quality of reproduction possible.

If pages are missing, contact the university which granted the degree.

Some pages may have indistinct print especially if the original pages were typed with a poor typewriter ribbon or if the university sent us a poor photocopy.

Previously copyrighted materials (journal articles, published tests, etc.) are not filmed.

Reproduction in full or in part of this film is governed by the Canadian Copyright Act, R.S.C. 1970, c. C-30. Please read the authorization forms which accompany this thesis.

**THIS DISSERTATION
HAS BEEN MICROFILMED
EXACTLY AS RECEIVED**

AVIS

La qualité de cette microfiche dépend grandement de la qualité de la thèse soumise au microfilmage. Nous avons tout fait pour assurer une qualité supérieure de reproduction.

S'il manque des pages, veuillez communiquer avec l'université qui a conféré le grade.

La qualité d'impression de certaines pages peut laisser à désirer, surtout si les pages originales ont été dactylographiées à l'aide d'un ruban usé ou si l'université nous a fait parvenir une photocopie de mauvaise qualité.

Les documents qui font déjà l'objet d'un droit d'auteur (articles de revue, examens publiés, etc.) ne sont pas microfilmés.

La reproduction, même partielle, de ce microfilm est soumise à la Loi canadienne sur le droit d'auteur, SRC 1970, c. C-30. Veuillez prendre connaissance des formules d'autorisation qui accompagnent cette thèse.

**LA THÈSE A ÉTÉ
MICROFILMÉE TELLE QU'ELLE
NOUS L'AVONS REÇUE**



ORE TYPES AND FLUID REGIMÉS: MACASSA GOLD MINE,
KIRKLAND LAKE

by

Gordon Peter Watson

Department of Geology

Submitted in partial fulfillment
of the requirements for the degree of
Doctor of Philosophy

Faculty of Graduate Studies
The University of Western Ontario
London, Ontario
September, 1984

© Gordon Peter Watson 1984

ABSTRACT

The Macassa Mine is the only remaining gold producer of seven inter-connected mines which comprise the Kirkland Lake mining district. This district has produced more than 710,000 kg Au since 1913 from quartz veins and lodes within the Archean Timiskaming Group, a south-facing sequence of wacke, conglomerate, and trachytic flow and pyroclastic rocks intruded by a composite syenite stock.

There are 3 types of gold ore at the Macassa Mine: 1) native Au in chloritic fault gouge or small quartz lenses within a prominent, subvertical, thrust-fault system traversing the mine and the entire Kirkland Lake district. This is called Break ore. 2) gold-bearing quartz veins in both hanging and footwalls of this fault system. This is called Vein ore. Veins consist of quartz, wallrock fragments, some Ca-, Fe-, Mg-, and Mn-carbonate minerals, 2 to 3% disseminated pyrite, precious and base-metal telluride minerals and fine grained, native Au. Molybdenite with or without graphite coats fractures in the quartz. 3) several zones up to 15 m wide in the deep west part of the mine which are very fractured, bleached, silicified and pyritized rock containing lenses and pods of quartz with native Au and telluride minerals. Molybdenite coats fractures throughout. This is called Breccia ore.

In addition to gold concentrations, the most significant chemical features of all three types of gold ores at

the Macassa Mine are the minor overall S; in conjunction with sporadic large contents of Te, Mo, and W ($29 \text{ ppm} \pm 25 \text{ } 1\sigma$). Gold/silver averages about 5. Cu and Zn are trace metals, whereas Pb is a minor element. Arsenic ($5.7 \text{ ppm} \pm 3.2 \text{ } 1\sigma$) and Sb ($4.2 \text{ ppm} \pm 2.6 \text{ } 1\sigma$) contents are minor and variable. Calculations of chemical mass balance indicate the principal chemical transfers in hydrothermal alteration of wall rocks adjacent to ore involve additions of CO_2 , but minor additions or subtractions of Fe_2O_3 , MnO , MgO and CaO , which alters Fe, Mg, Ca, Mn-silicate minerals in wall rocks to Fe, Mg, Ca, Mn-carbonate minerals. Additions of K_2O along with depletions of Na_2O reflect the hydrolysis of albite to muscovite, and minor gains of SiO_2 plus S are evident in the coprecipitation of quartz and pyrite.

Geostatistical analysis of gold distribution within a type zone of breccia ore at Macassa indicates a general continuity which can be approximated by theoretical semi-variogram models. This area has a greater spatial continuity than either break ore or vein ore. However, experimental semivariograms calculated along three principal directions within the type zone: along strike, across strike, and down dip; have zonal, directional and proportional effect anisotropies. The distribution of gold content is therefore only quasistationary. The inhomogeneity of gold distribution within the type zone of breccia ore is interpreted to reflect syn- and post-ore faulting

and fracturing, evidence of a tectonically active environment of gold deposition.

The $\delta^{18}\text{O}$ and δD of rocks and mineral separates in these 3 ore types suggest the ore was precipitated from hydrothermal fluids of $\delta^{18}\text{O}$ +7 to +9.6 per mil, δD -35 to -85 per mil, and at 380 to 490°C. These data are consistent with fluids evolved by dehydration of volcanic and sedimentary rocks during accumulation and burial, which ascended by seismic pumping along pre-existing faults and fractures. These fluids repeatedly leached and scavenged Au from primary and secondary auriferous areas within older volcanic and sedimentary rocks of the Kirkland Lake district and deposited gold within faulted and fractured syenites and Timiskaming Group rock.

Isotopic abundances and the oxidation state of iron in rocks contained within the major faults suggest that the initial hydrothermal regime was followed by downward penetration of oxidising, sulphate-bearing fluids, $\delta^{18}\text{O}$ 0 to +2 per mil, δD -20 to -70 per mil and of probable marine origin with or without meteoric water, initially at temperatures of <200°C, waning to 50°C or less. A third fluid regime is indicated for quartz-magnetite-chlorite veins which have mineral pair fractionations corresponding to fluids of -4.0 to -0.5 per mil $\delta^{18}\text{O}$ and 210 to 260°C, consistent with hydrothermal fluids of meteoric origin. These three hydrothermal fluid regimes are interpreted to

reflect a sequence of crustal compression, relaxation and finally uplift above sea level.

ACKNOWLEDGEMENTS

Considerable and extended assistance was provided the writer throughout all aspects of this thesis study. Supporting funds from Lac Minerals Ltd. (Macassa Division), unrestricted access to the mine and its records and the competent assistance of the mine staff are gratefully acknowledged. Mr. D. Sheehan, Vice-President Exploration and Mr. G. Nemcsok, Area Chief Geologist are thanked for their personal interest, involvement and consideration.

Financial assistance was received from the Mineral Deposits Branch of the Ontario Geological Survey. Special thanks are due to Drs. A. C. Colvine and M. E. Cherry for their valuable discussions, encouragement and guidance.

The writer is also grateful for the time and effort extended by Dr. R. Froideveaux, D. S. Robertson and Associates Ltd., in assisting the development and analysis of the geostatistical study.

Particular thanks are due to Dr. R. W. Hodder who acted as thesis advisor. His patience and incisive geologic and editorial criticism proved invaluable and are deeply appreciated. The expertise and diligent efforts of Dr. R. Kerrich also merit special acknowledgement. His important contributions to all aspects of the research and the chemical and isotopic studies in particular have added significantly to the final product.

The writer acknowledges the special contributions made

by Dr. R. G. Roberts of the University of Waterloo. His valuable comments and criticisms of an earlier version of this thesis have resulted in a much improved final product. I am grateful to L. Willmore for analytical assistance. The care and diligent attention of Mrs. G. McIntyre who typed the several versions of this manuscript deserves special thanks.

This thesis is dedicated by my wife, Patricia, whose patient endurance made it all worthwhile.

Surely there is a mine for silver,
and a place where they refine gold.
Men search the limits of dark places,
Venturing into their remotest bounds
to obtain the ore.

But where can wisdom be found,
and where is the place of understanding?
Pure gold can not purchase it;
Neither can silver be weighed as its price.

Job 28: 1, 3, 12, 15
(Modern language)

Happy is the man that findeth wisdom,
and the man that getteth understanding.
For the merchandise of it is better than
the merchandise of silver, and the gain
thereof than fine gold.

Proverbs 3: 13, 14

TABLE OF CONTENTS

	Page
CERTIFICATE OF EXAMINATION	ii
ABSTRACT	iii
ACKNOWLEDGEMENTS	vii
TABLE OF CONTENTS	x
LIST OF PHOTOGRAPHIC PLATES	xiii
LIST OF TABLES	xiv
LIST OF FIGURES	xv
CHAPTER 1. INTRODUCTION	1
1.1 General Statement	1
1.2 Location and Access	2
1.3 History and Development of the Kirkland Lake District	3
1.4 History and Development of the Macassa Mine	10
1.5 Past and Present Production of the Macassa Mine	14
1.6 Previous Work	16
1.7 Scope and Purpose of Thesis	17
CHAPTER 2. REGIONAL GEOLOGY	20
2.1 General Statement	20
2.2 General Geology of the Abitibi Greenstone Belt	21
2.3 Geology of the Kirkland Lake District	28
2.3.1 Stratigraphy	29
2.3.2 Structure	40
2.3.3 Metamorphism	43
2.3.4 Radiometric Age Determinations	43
CHAPTER 3. MINE GEOLOGY	46
3.1 General Statement	46
3.2 Rock Types in the Mine	53
3.2.1 Timiskaming Group	53
3.2.2 Intrusive Rocks	59
3.3 Folding	69
3.4 Faulting and Fracturing	71
3.4.1 Pre-Ore Faulting	72
3.4.2 Post-Ore Faulting	77
3.4.3 Fracturing	80
3.5 Gold Occurrence at Macassa	88
3.5.1 Mineralogy	88
3.5.2 Wallrock Alteration	92
3.5.3 Types of Gold Occurrences	98
3.5.3.1 Break Ore	98
Main Break	99
O4 Break	99
R-2 Break	102

	South Break	102
	S- and E-Breaks	103
3.5.3.2	Vein Ore	103
	Hanging Wall Vein Ore	
	- South Dipping	104
	Hanging Wall Vein Ore	
	- North Dipping	108
	Footwall Veins	109
3.5.3.3	Breccia Ore	110
CHAPTER 4. CHEMICAL COMPOSITION OF MINE ROCKS		
	AND ORES	117
4.1	General Statement	117
4.2	Chemical Composition of Mine Rocks'	117
	4.2.1 Timiskaming Group Sedimentary Rocks ..	117
	4.2.2 Intrusive Rocks and Trachytic Tuffs ..	130
	4.2.3 Gold-Bearing Rocks	146
4.3	Chemical Effects of Wallrock Alteration	147
	4.3.1 Chemical Mass Balance Equation	148
	4.3.2 Changes in Major and Minor Element	
	Abundances During Hydrothermal	
	Alteration	150
	4.3.2.1 Break Ore	151
	4.3.2.2 Vein Ore in Syenite	156
	4.3.2.3 Breccia Ore in Augite	
	Syenite and Tuff	159
	4.3.3 Changes in REE Abundances During	
	Hydrothermal Alteration	163
	4.3.4 Oxidation State of Iron	163
CHAPTER 5. OXYGEN AND HYDROGEN ISOTOPE ABUNDANCES		
	AND FLUID INCLUSION DATA'	168
5.1	General Statement	168
5.2	Calculation of Temperature and Isotopic	
	Composition of Hydrothermal Fluids	172
	5.2.1 $\delta^{18}O$ of Syenite and Trachytic Tuffs ...	174
	5.2.2 $\delta^{18}O$ and δD of Ores	175
	5.2.2.1 Break Ore	175
	5.2.2.2 Vein Ore'	178
	5.2.2.3 Breccia Ore	181
5.3	Data from Fluid Inclusions	181
	5.3.1 Break Ore	184
	5.3.2 Vein Ore	185
	5.3.3 Breccia Ore	185
	5.3.4 Quartz-Magnetite Stringer Veins	188
CHAPTER 6. GOLD DISTRIBUTION IN BRECCIA ORE - A		
	GEOSTATISTICAL STUDY	189
6.1	General Statement	189
	6.1.1 The Study Area	190
	6.1.2 The Data Base	101
	6.1.3 Preliminary Appraisal	203

6.2	Geostatistical Appraisal	208
6.2.1	General Statement	208
6.2.2	Reconstruction of the Data Base	209
6.2.3	Data Statistics and Stationarity Check	211
6.2.4	Experimental Semi-Variograms	215
6.2.5	Preliminary Analysis	228
6.2.6	Final Variography and Modelling	229
6.3	Concluding Statement	238
CHAPTER 7. CONCLUSIONS FROM EVIDENCE		240
CHAPTER 8. SIGNIFICANCE OF MACASSA MINE DATA TO GOLD DEPOSITION IN THE KIRKLAND LAKE DISTRICT		245
8.1	General Statement	245
8.2	Source of Gold	247
8.2.1	Magmatic Fluid Source	248
8.2.2	Country Rock Source	249
8.3	Transport Agents and Media	253
8.4	Deposition - The Role of Structures	257
8.4.1	Mine Scale	258
8.4.2	Regional Scale	258
8.5	Seismic Pumping - The Active Role of Structure	259
8.5.1	Seismic Pumping Model	260
8.5.2	Geologic Evidence for Seismic Pumping	261
CHAPTER 9. GENETIC MODEL FOR THE KIRKLAND LAKE DISTRICT		264
9.1	General Statement	264
9.2	A Sequence of Events	264
* * * * *		
APPENDIX A.	ANALYTICAL METHODS	278
APPENDIX B.	CRITERIA FOR DISTINGUISHING THE ORIGIN OF FLUID INCLUSIONS	284
APPENDIX C.	GEOSTATISTICAL CONCEPTS	289
APPENDIX D.	FORTRAN IV PROGRAM LISTINGS	297
REFERENCES	321
VITA	340

LIST OF PHOTOGRAPHIC PLATES

Plate	Description	Page
3-1	Boulder and pebble conglomerate from the Macassa Mine and area	58
3-2	Tuffs and agglomerates from the Macassa Mine	61
3-3	Syenites from the Macassa Mine	66
3-4	Mechanical alteration of wallrocks at the Macassa Mine	94
3-5	Mineral changes during wallrock alteration at the Macassa Mine	97
3-6	Break ore in the Macassa Mine	101
3-7	Vein ore in the Macassa Mine	106
3-8	Breccia ore in the Macassa Mine	112
5-1	Fluid inclusions in vein ore, Macassa Mine	187

LIST OF TABLES

Table	Description	Page
1-1	Milling statistics for the Macassa Mine 1933-1982	15
2-1	Stratigraphy of the Kirkland Lake district	38
3-1	Microprobe analyses of feldspars in syenites, Macassa Mine	68
3-2	Minerals of the Kirkland Lake ores	90
4-1	Abundances of major and trace elements for unaltered rocks at the Macassa Mine and environs	118
4-2	Abundances of major and trace elements for altered rocks associated with vein ore, breccia ore and break ore at the Macassa Mine	126
4-3	Abundances of major and trace elements for altered rocks associated with break ore at the Macassa Mine	128
4-4	Average abundances of major and trace elements for unaltered rocks at the Macassa Mine	152
4-5	Ferrous to total iron ratios for selected rocks, Macassa Mine and area	165
5-1	Oxygen and hydrogen isotope composition of whole rocks and mineral separates from the Macassa Mine and environs	170
6-1	Distribution of diamond drill holes and samples	203
6-2	Statistical summary unweighted assay values	204
6-3	Histogram statistical data summary - 0.01 ounce Au limit	212
6-4	Histogram statistical data summary - 0.04 ounce Au limit	213
6-5	Histogram statistical data summary - 0.04 ounce Au limit, log transformed data	216

LIST OF FIGURES

Figure	Description	Page
1-1	Location of the Kirkland Lake area in northeastern Ontario	5
1-2	Location of major gold mining properties in Kirkland Lake	9
1-3	Longitudinal section of the Macassa Mine	13
2-1	Geology of the Abitibi Greenstone Belt	23
2-2	Tectonic setting of the Abitibi Orogen	27
2-3	Geology of the Timmins-Kirkland Lake area	34
3-1	Generalized geology of the Kirkland Lake district	48
3-2	Distribution of facies associations and rock types in the Kirkland Lake district	51
3-3	General geology of the Macassa Mine	56
3-4	Geologic section through No. 1 shaft of the Macassa Mine	64
3-5	Structural plan of the 4250' level, Macassa Mine	76
3-6	Geologic plan and section of the 5150' level, Macassa Mine	83 & 85
3-7	Structural plan of 42-S-2 antiformal vein, Macassa Mine	87
3-8	Geologic section along 30W, Macassa Mine	115
4-1	Alkali-silica diagram for syenites and rocks of the Timiskaming Group from the Macassa Mine and area	134
4-2	Larsen diagram for syenites and rocks of the Timiskaming Group from the Macassa Mine and area	136

Figure	Description	Page
4-3	Harker diagram for syenites and rocks of the Timiskaming Group from the Macassa Mine and area	140
4-4	Chondrite normalized rare earth element abundances for syenites and altered rocks at the Macassa Mine	143
4-5	Gains and losses of chemical components during alteration of brecc ore	155
4-6	Gains and losses of chemical components during alteration of vein ore	158
4-7	Gains and losses of chemical components during alteration of breccia ore	162
6-1	Schematic diagram of breccia ore study area in the Macassa Mine	192
6-2	Schematic diagrams of study area on 5025', 5150', 5300' and 5450' levels, Macassa Mine	195
6-3	Histogram and cumulative frequency distribution of all unweighted gold abundances in the study area	206
6-4	Normal probability plots of log transformed gold abundances	218
6-5	Average experimental semi-variograms, one dimensional	223
6-6	Experimental semi-variograms and models a) across strike; b) along strike; c) down dip	233
7-1	Isotopic composition of hydrothermal fluids from the Macassa Mine	243
9-1	Schematic diagrams of proposed sequence for gold deposition in the Kirkland Lake district	266

CHAPTER 1

INTRODUCTION

1.1 General Statement

Gold has traditionally been sought by many of the world's geologists. With the significant and sustained increase in price which followed destandardization of the gold price in the 1970's, the search has intensified. However, gold deposits are probably the most difficult of exploration targets. Economic occurrences have an absolute Au content of 5 to 10 ppm and most have no simple geo-physical or geochemical expression. Therefore, the identification of essential ore-related geological features and the environments of deposits is of particular importance in gold exploration.

Geology is not a static discipline but is rather in a constant flux of changing ideas and fashions. This has been readily apparent in the evolution of genetic models applied to gold deposits. The classic magmatic hydro-thermal model of Lindgren (1933) with its emphasis on structure and epigenetic mineralization has been supplanted in more recent years by models emphasizing the role of syn-

2

genetic concentration in the sedimentary and volcanic environments. Both model types have enjoyed periods of popularity when all gold deposits were fitted to their respective molds, sometimes at the expense of geologic observations.

The gold mines in the Kirkland Lake district, Ontario are important examples of Archean lode gold deposits. They are spatially associated with a long, linear zone of fractured, faulted and altered rocks, termed 'breaks'. The gold occurs in complicated fault and fracture systems within a composite syenite stock and adjacent sedimentary and volcanic rocks. These characteristics are not compatible with syngenetic volcanogenic models of gold deposition.

After 50 years of production, the Macassa Mine is the only gold mine still in operation in Kirkland Lake. As such it afforded an excellent opportunity to update previous geological descriptions, implement new studies and reassess the sequence of geologic events for gold concentrations at Kirkland Lake.

1.2 Location and Access

The town of Kirkland Lake is in Teck township, district of Timiskaming, Northeastern Ontario at latitude 48°09' north and longitude 80°03' west (Fig. 1-1). The area is well served by Highways 11, 66, 142 and 624 and many logging, concession and recreation roads that extend from

these highways. The village of Swastika, 9 km to the southwest of Kirkland Lake, is on the Ontario Northland Railway line. A small commercial airport immediately north of Kirkland Lake has scheduled air service by Norontair.

Teck Township is the west part of a gold producing area that extends east for 150 km into northwestern Quebec. The entire area is within the Abitibi greenstone belt, the largest continuous Archean greenstone belt in the Canadian Shield.

Lac Minerals Ltd. (Macassa Division) is the only remaining operational mine of seven original gold producers of Kirkland Lake. Its holdings are fifty-four mining claims on the west edge of Kirkland Lake.

1.3 History and Development of the Kirkland Lake District

The discovery and gradual expansion of the Kirkland Lake gold camp has been well described in several publications (eg. Burrows and Hopkins, 1914, 1920, 1923; Todd, 1928). The interested reader is referred to these for details along with a more complete list of publications dealing with the Kirkland Lake area found within the reference list. An historical synopsis and summary of development for each of the seven gold producers of the Kirkland Lake camp dealing with mining activity to 1947 appeared in Thomson et al. (1950). Charlewood (1964) updated this report, covering development to 1962.

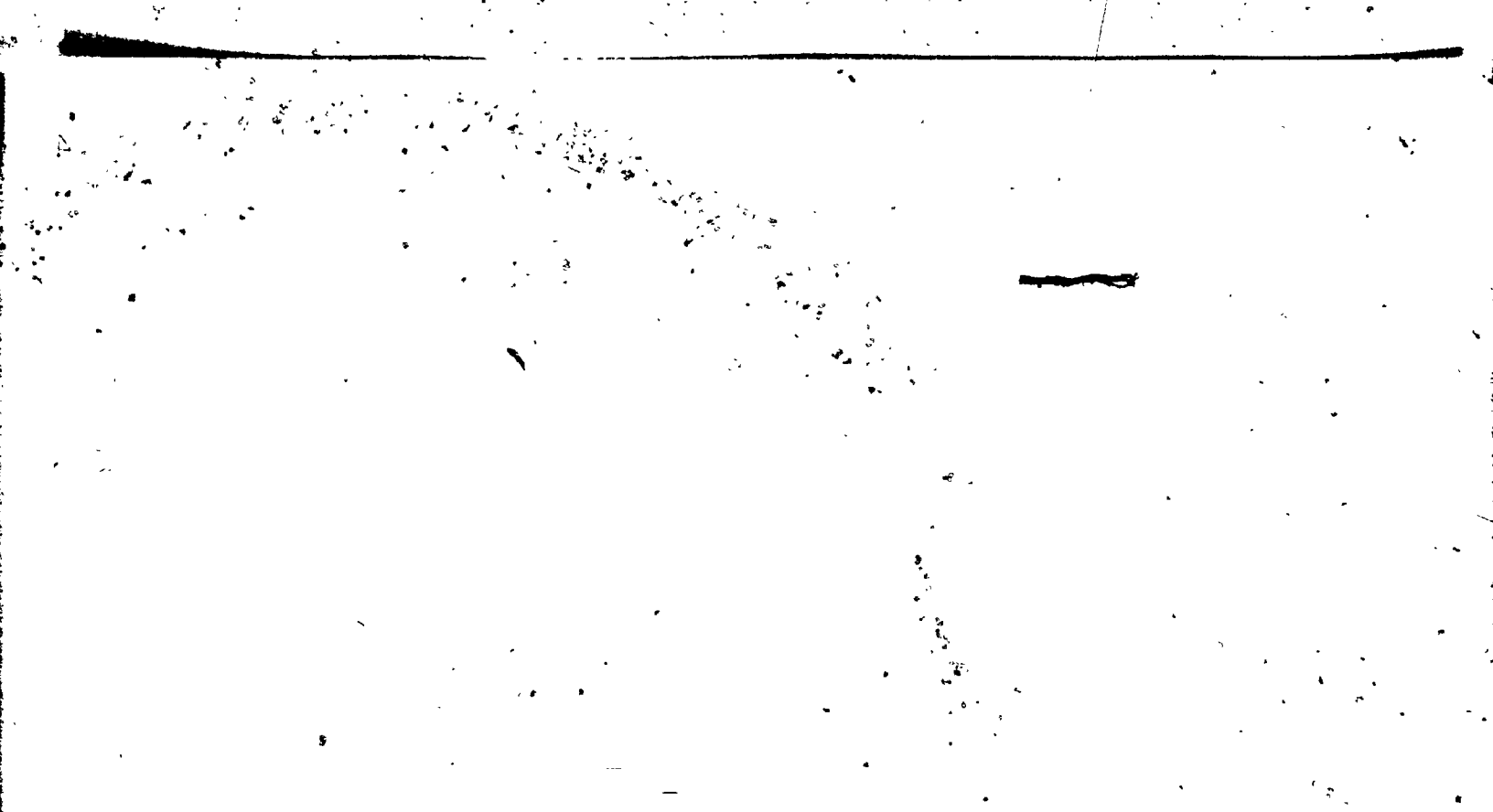
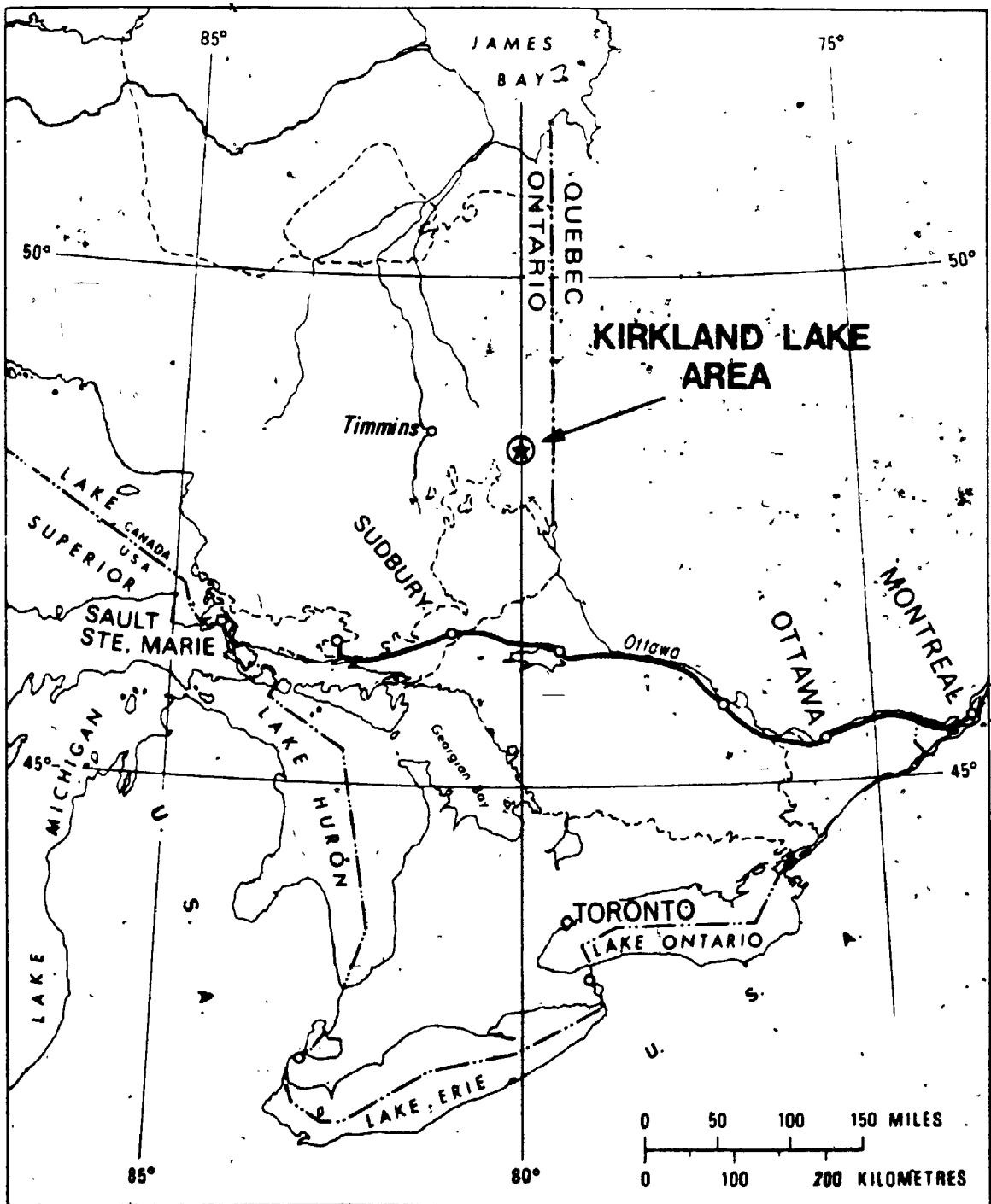


Figure 1.1. Location of the Kirkland Lake area in north-eastern Ontario.



One of the earliest mining exploration ventures in northeastern Ontario was established in New Liskerd at the turn of the century when a number of local people pooled their resources to finance prospectors in various sections of the region. Silver was discovered in Coleman township, 160 km north of the town of North Bay, in the summer of 1903. Construction of a railway to the north of Lake Timiskaming led to the discovery of silver-bearing arsenide near a lake then known as Long Lake, later renamed Cobalt Lake (Bruce, 1933).

Gold was initially discovered in the vicinity of Larder Lake in 1906 by prospectors fanning out from Cobalt. Also in 1906, gold was discovered at Swastika. Limited mining operations were carried on at the Swastika and Lucky Cross properties and small mills were erected which produced some gold (Thomson, 1950). It was not until 1911 that attention was focused on Kirkland Lake when W. H. Wright made the initial find of gold-quartz veins that later became the Wright-Hargreaves mine. The development of mines resulting from this and later discoveries over the next 30 years created the economic base for Kirkland Lake and other towns east to Larder Lake.

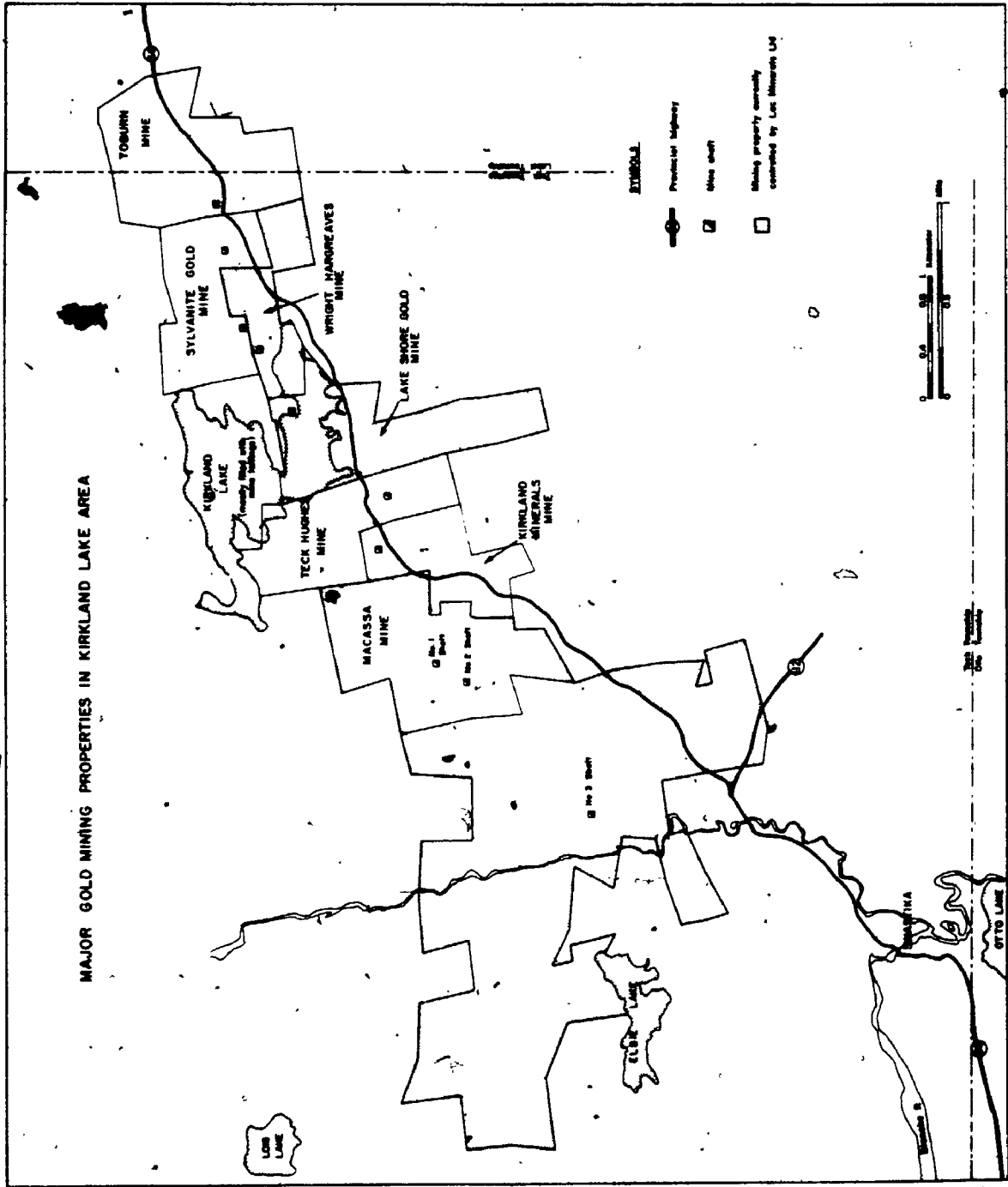
The operating mines of the Kirkland Lake camp, from west to east along the 6 km main ore zone, were: Macassa, Kirkland Lake Gold (later Kirkland Minerals), Teck-Hughes, Lake Shore, Wright-Hargreaves, Sylvanite and Tough-Oakes

Burnside, (later Toburn) (Fig. 1-2). First production from the Toburn property was in 1913, from Teck-Hughes in 1917, from Lake Shore in 1918, from Kirkland Minerals in 1919, from Wright-Hargreaves in 1921, from Sylvanite in 1927 and from Macassa in 1933.

During the decade preceeding World War II, the Kirkland Lake area was one of the most flourishing in Canada. At the peak of mine production in the late 1930's, Kirkland Lake had 35,000 inhabitants, more than double the present population. To the end of 1948, the seven mines had milled 30,840,000 tonnes of ore and produced 480,000 kg of gold and 84,000 kg of silver, valued at \$516,743,288 (Thomson et al., 1950).

Throughout the war years, operations were severely hampered by the chronic labour shortage. After the war, steadily increasing production costs were not sufficiently offset because the price of gold was fixed at \$35/oz. Additionally, all of the mines were forced to develop at deeper and deeper levels as more accessible ore zones were depleted. Faced with increased depth of mining with its attendant difficulties, and general decline of the size and average grade of ore-bodies at depth, six of the seven mines ceased operations after 1948: Toburn in 1953; Kirkland Minerals in 1960; Sylvanite in 1961; Lake Shore and Wright-Hargreaves in 1965 and Teck-Hughes in 1968. Total production of all mines in Kirkland Lake since 1913

Figure 1.2. Location map of major gold mining properties in Kirkland Lake including the Macassa Mine and other mining properties currently owned or controlled by Lac Minerals Ltd.



is over 710,000 kg of Au (Lovell and Ploeger, 1980), second only to the Porcupine district in North America (Bertoni, 1981).

1.4 History and Development of Macassa Mine

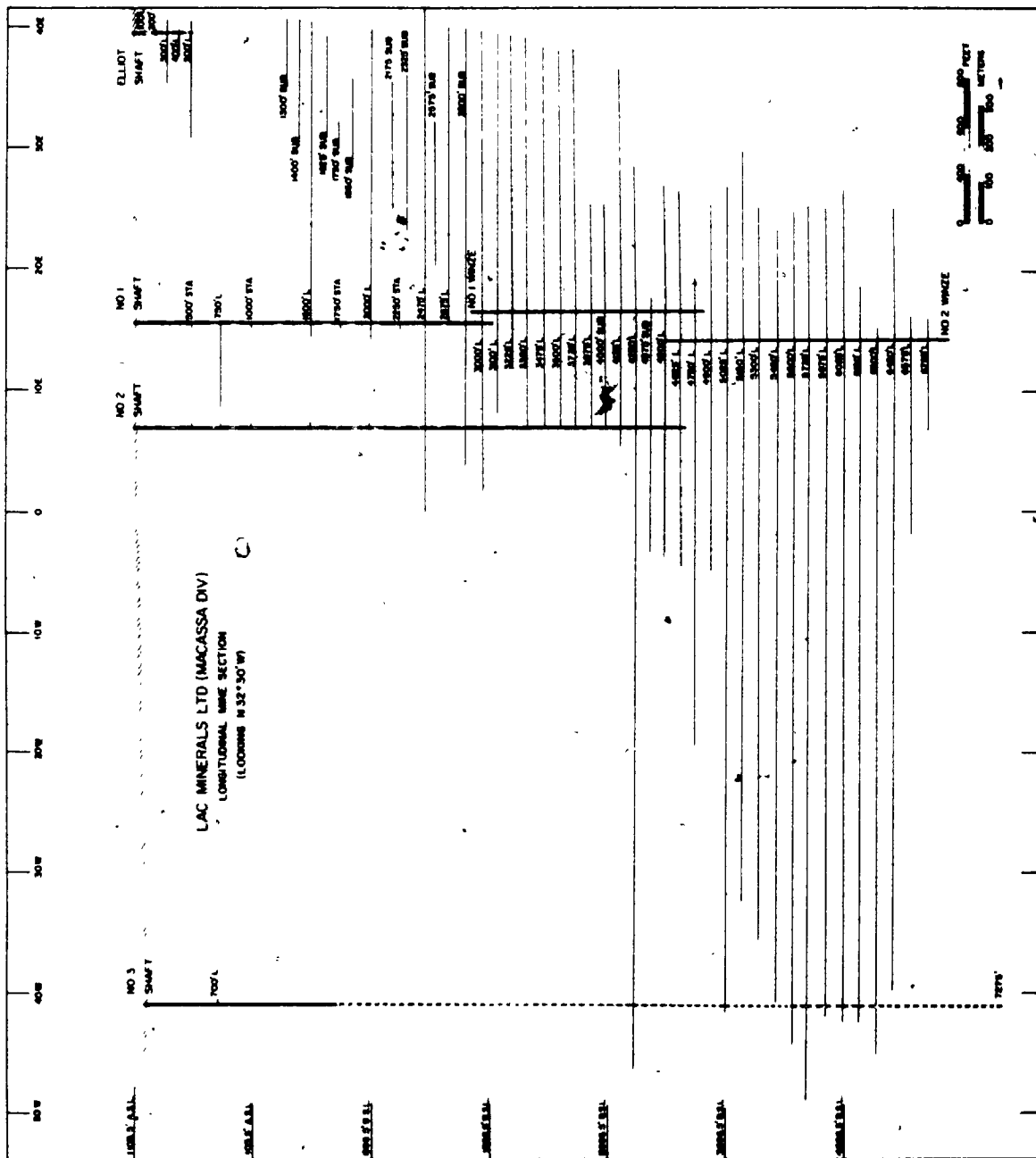
The original Macassa Mines Ltd. was organized in 1926 and, in 1933, acquired the assets of United Kirkland Gold Mines Ltd. Following this, the company was amalgamated in 1962 with Bicroft Uranium Mines Ltd. and Renable Mines Ltd. to become Macassa Gold Mines Ltd. Final amalgamation with Willroy Mines Ltd. and Willecho Mines Ltd. took place in November, 1970 with parent control by Little Long Lac Gold Mines based in Toronto. From 1970-1976 management rights were optioned to Upper Canada Mine Ltd. Corporate reorganization of Little Long Lac Mines Ltd. in December, 1982 resulted in the formation of Lac Minerals Ltd. (Macassa Division) which owns and operates the Macassa Mine.

The original Macassa Mines Ltd. was made up of 11 claims but an additional 20 claims were acquired from Jeck Corporation Ltd. and Oakdale Mines Ltd. (formerly Tegren Goldfields Ltd.) in 1977. Adjacent to these Tegren mining claims, Lac Minerals Ltd. controls the seven mining claims which made up the former McIvor Gold Mines property. Ten additional mining claims further west were acquired from private sources with retained production royalties. A

profit sharing agreement is in effect with Queenston Gold Mines Ltd. for six mining claims to the west. New underground development and mining is in progress on the former Lake Shore and Wright Hargreaves properties. In addition, short term options are presently in effect for mining of the former Kirkland Minerals and Teck-Hughes properties. Current lands owned and controlled by Lac Minerals Ltd. are shown in Figure 1-2.

First underground work was done by Elliott Kirkland Gold Mines, Ltd. which sank a shaft and did limited development on five levels. Macassa Mines Ltd. did further work on the 500-foot level in 1926 and 1927 (Ward and Thomson, 1950). The property was successfully developed in 1931 when arrangements were made to drive westward from the adjoining Kirkland Minerals property on their 2475' level. Ore was encountered along a major fault system and in subsidiary hanging-wall veins. In the meantime, No. 1 shaft was sunk to connect with the workings at this horizon. Since then, two additional internal winzes have been put down (No. 1 winze from 3000' to 4625' levels; No. 2 winze from 4625' to 6875' levels). A second shaft was sunk from surface on the property some 1000' southwest of No. 1 and extends to a depth of 4625'. At the time of this writing, a third shaft (No. 3 Shaft) is being sunk from surface at the far west end of the mine workings to improve access, ventilation and production (Fig. 1-3).

Figure 1-3. Longitudinal section of the Macassa Mine with shaft and winze location and underground development (looking 327° 30').



Sinking of No. 3 shaft began May 1st, 1983 and has presently advanced beyond 1500 feet (550 m) in depth. Proposed depth of the completed, four-component shaft is 7275 ft (2668 m) which will make it the deepest, single-lift shaft in the Western Hemisphere.

To date, active workings begin at the 2325' sublevel and extend to the lowest active level at 6450'. In a horizontal plane, these workings are spread from about 1 km east of No. 1 shaft to about 2.2 km west of No. 1 shaft.

1.5 Past and Present Production of the Macassa Mine

A 200 ton per day mill was constructed and began production in October, 1933. Later, this was increased to 425 tons per day and, during 1956, to a capacity of 500 to 525 tons daily. The present mill capacity is about 350 to 450 tons per day. The main production schedule, upon completion of No. 3 Shaft in 1985, is expected to rise from 126,000 tons per year to 180,000 tons per year or approximately 500 tons per calander day.

Macassa Mine milling statistics compiled from mine records for the period 1933 to 1982 are summarized in Table 1-1. To the end of 1982, 5,152,270 tonnes have been milled giving a total metal production of 82,210 kg of gold. Ore reserves at the end of 1983 are 1,257,738 tonnes with an average gold content of 15.05 grams Au per tonne.

Table 1-1. Milling Statistics for the Macassa Mine 1933-1982.

Year	Production Tons Milled	Calc. grade oz. Au.	oz. Au. Recovered	Rec. grade oz. Au.	Percent Recovery	Milling Cost per ton
1933	8,101		3,683	.455		2.03
1934	86,557		30,977	.465		1.70
1935	68,627		32,117	.468		1.49
1936	70,878		35,155	.496		1.51
1937	90,617	.4896	41,921	.463	94.49	1.46
1938	110,718	.4915	51,648	.466	94.91	1.40
1939	148,398	.4434	62,392	.420	94.91	1.13
1940	150,674	.4859	69,749	.463	95.27	1.12
1941	142,332	.4771	64,497	.453	94.97	1.17
1942	120,400	.4904	55,832	.464	94.56	1.25
1943	103,259	.4352	42,414	.411	94.39	1.33
1944	83,392	.4584	36,193	.434	94.68	1.54
1945	71,988	.4143	28,155	.391	94.40	1.53
1946	87,383	.4373	35,931	.411	94.03	1.42
1947	97,507	.4623	39,319	.403	94.58	1.32
1948	103,650	.4156	40,792	.394	94.71	1.39
1949	126,511	.3974	47,264	.374	94.01	1.33
1950	129,710	.3476	41,898	.326	93.64	1.41
1951	135,440	.3500	44,638	.329	94.17	1.38
1952	139,660	.3337	43,984	.315	94.37	1.42
1953	144,175	.3409	46,388	.322	94.48	1.32
1954	145,286	.3657	50,358	.347	94.79	1.45
1955	142,860	.4475	60,258	.422	94.26	1.61
1956	140,743	.4370	58,030	.412	94.35	1.57
1957	141,115	.4896	64,963	.460	93.89	1.75
1958	164,262	.4452	68,452	.417	93.60	1.79
1959	158,130	.4672	69,367	.439	93.90	1.73
1960	149,862	.4061	69,778	.466	93.85	1.91
1961	153,171	.4759	68,242	.446	93.61	1.91
1962	139,618	.4645	60,483	.433	93.26	2.16
1963	140,800	.4833	63,625	.452	93.50	2.03
1964	141,408	.4755	62,801	.444	93.40	2.20
1965	116,791	.4621	58,838	.430	93.08	2.40
1966	130,909	.4463	54,416	.416	93.14	2.56
1967	108,331	.4661	47,557	.439	94.19	2.85
1968	102,593	.5423	52,470	.511	94.30	2.84
1969	96,265	.5023	40,976	.475	94.57	3.43
1970	76,998	.5180	37,481	.487	93.98	3.55
1971	78,532	.6412	47,350	.603	94.03	3.79
1972	98,425	.7319	68,212	.693	94.69	3.91
1973	98,976	.5416	50,955	.515	95.05	5.10
1974	90,186	.5082	43,610	.484	95.15	7.14
1975	88,008	.5325	44,776	.509	95.54	7.97
1976	92,244	.5677	50,111	.543	95.69	7.98
1977	102,437	.5642	55,675	.544	96.33	8.16
1978	111,416	.5096	54,388	.488	95.79	6.53
1979	105,510	.5167	52,798	.500	96.85	10.22
1980	110,975	.4657	50,000	.451	96.74	8.31
1981	115,161	.4608	91,190	.445	96.47	10.90
1982	117,507	.4682	53,357	.454	96.97	11.84

1.6 Previous Work

The geology and mineral resources of the Kirkland Lake area have been described by geologists and engineers at intervals dating back to initial prospecting activity. The first geological reports of the Kirkland Lake area are found in Burrows and Hopkins (1914, 1920, 1923), Tyrrell and Hore (1926) and Todd (1928). The earliest major study with detailed geology of Teck township and the main ore zone of Kirkland Lake camp is in Thomson (1950) and Thomson et al. (1950).

Gradually this work expanded to include general geological relations in the Matachewan area to the west - Dyer (1936), Marshall (1947), Lovell (1967) and Ridler (1975); and the Skead area to the south - Hewitt (1949), and Ridler (1969, 1970). Other important additions to the investigations of the Kirkland-Larder Lakes area are in Hewitt (1963), Cooke (1966), Cooke and Moorehouse (1969), Jensen (1976, 1978a, 1978b), Jensen and Langford (1983), Tihor and Crockett (1977), Hyde and Walker (1977) and Hyde (1980).

In 1975, field work was begun on a regional stratigraphic correlation of the Timmins-Kirkland Lake map sheet by Jensen and Pyke of the Ontario Geological Survey. Beginning in 1980, a three-year multi-disciplinary gold deposit study was initiated in the immediate Kirkland Lake area by the Ontario Geological Survey.

To date, the only geological investigations focussed

on the Macassa property are Ward and Thomson (1950), Charlewood (1964), and most recently Watson and Kerrich (1983) and Kerrich and Watson (1984).

1.7 Scope and Purpose of Thesis

This thesis is based on investigations carried out at the Macassa Mine during two and a half summers mapping and sampling underground and laboratory research conducted at the University of Western Ontario. While at Macassa, the writer worked as a mine geologist which afforded good opportunity to examine, map, sample and photograph/exposures underground and in surface outcrop.

Some 500 kg of host rock and gold ore was obtained from more than 150 locations underground and on surface. Of these, 48 samples were selected for detailed whole rock chemical analysis of major, minor and trace element abundances. Major element and some transition metal abundances were determined by X-Ray Assay Labs and Barringer Magenta Labs respectively. Precious metals and related element abundances were determined by Neutron Activation Services as were rare earth element abundances. Trace element abundances were determined by the writer using XRF at the University of Western Ontario. Chemical compositions of feldspar, chlorite, biotite and carbonate minerals from unaltered and ore-related rocks were determined by the writer using the electron microprobe. Ferrous

iron abundances in a selected number of altered and unaltered rocks were determined titrimetrically by the writer using the metavanadate method described by Wilson (1955).

The geostatistical study is the result of a special project conducted by the writer for Lac Minerals Ltd. to test the application of geostatistics to problems of gold distribution and grade control at the Macassa Mine. The data on isotopic abundances is the result of a joint investigation by the writer and Dr. R. Kerrich, University of Western Ontario, and has been published in Watson and Kerrich (1983) and Kerrich and Watson (1984).

The focus of this thesis has been deliberately restricted to the Macassa Mine in particular and, to a lesser degree, the six other former gold producing mines in the immediate vicinity of Kirkland Lake. The prime purpose is to reassess the nature and characteristics of gold occurrences at the mine in light of the additional data and changes in ore deposit models since the initial description summarized by Thomson et al. (1950). This purpose was accomplished through examination, sampling and analysis of rocks and ores from the Macassa Mine. Valuable insight into details of the physical distribution of gold within the most spatially continuous ore type, breccia ore, was provided by geostatistical analysis. A secondary purpose was to examine evidence regarding the nature and origin of hydrothermal fluids implicated in the formation of gold

ores at the Macassa Mine and, by inference, the Kirkland Lake area. This purpose was accomplished by chemical mass balance calculations based on the precursor and products of hydrothermal alteration in wallrocks adjacent to ores, determination of oxygen and hydrogen isotope abundances in unaltered and altered host rocks and ores. These were supplemented by fluid inclusion studies, and determination of ferrous to total iron ratios for selected unaltered and altered wallrocks.

Naturally, new data generated by this study should be incorporated in a larger scale regional framework. The final chapter of this thesis attempts to do this using a regional model proposed by Jensen (1980). While the adaptation of Jensen's model is convenient, no attempt is made to deny the healthy disagreements which currently exist regarding proper interpretation of regional stratigraphy. The various regional interpretations will be briefly discussed in Chapter 2. To mediate between any of the conflicting interpretations or to propose a new version would require extensive regional geologic study beyond the scope of this thesis.

CHAPTER 2

REGIONAL GEOLOGY

2.1 General Statement

The Kirkland Lake mining district is in the Abitibi greenstone belt, one of the largest and best preserved Archean greenstone belts in the world. In addition to producing base metals, silver, gold and iron, there are numerous sub-economic occurrences of other metals. Excellent exposure of a variety of Archean rock types along with significant metal concentrations makes the Kirkland Lake district a prime source of information on Archean geological processes.

The geology of the Abitibi belt has been described by Wilson et al. (1956) and Goodwin and Ridler (1970). Recent detailed investigations include those dealing with stratigraphy (Hewitt, 1963; Hyde, 1978, 1980; Jensen, 1978, 1980; Jensen and Lanford, 1983), petrography (Bass, 1961; Boutcher et al., 1966), metamorphism (Jolly, 1974) and economic geology (Ridler, 1969, 1970, 1976; Tihor and Crockett, 1977; Lovell and Ploeger, 1980; Ploeger, 1980, 1981; Ploeger and Crockett, 1982). The following is

intended as a brief synoptic overview of the general geology of the Abitibi belt and the salient aspects of the geology of the Kirkland Lake district drawing on these previous efforts.

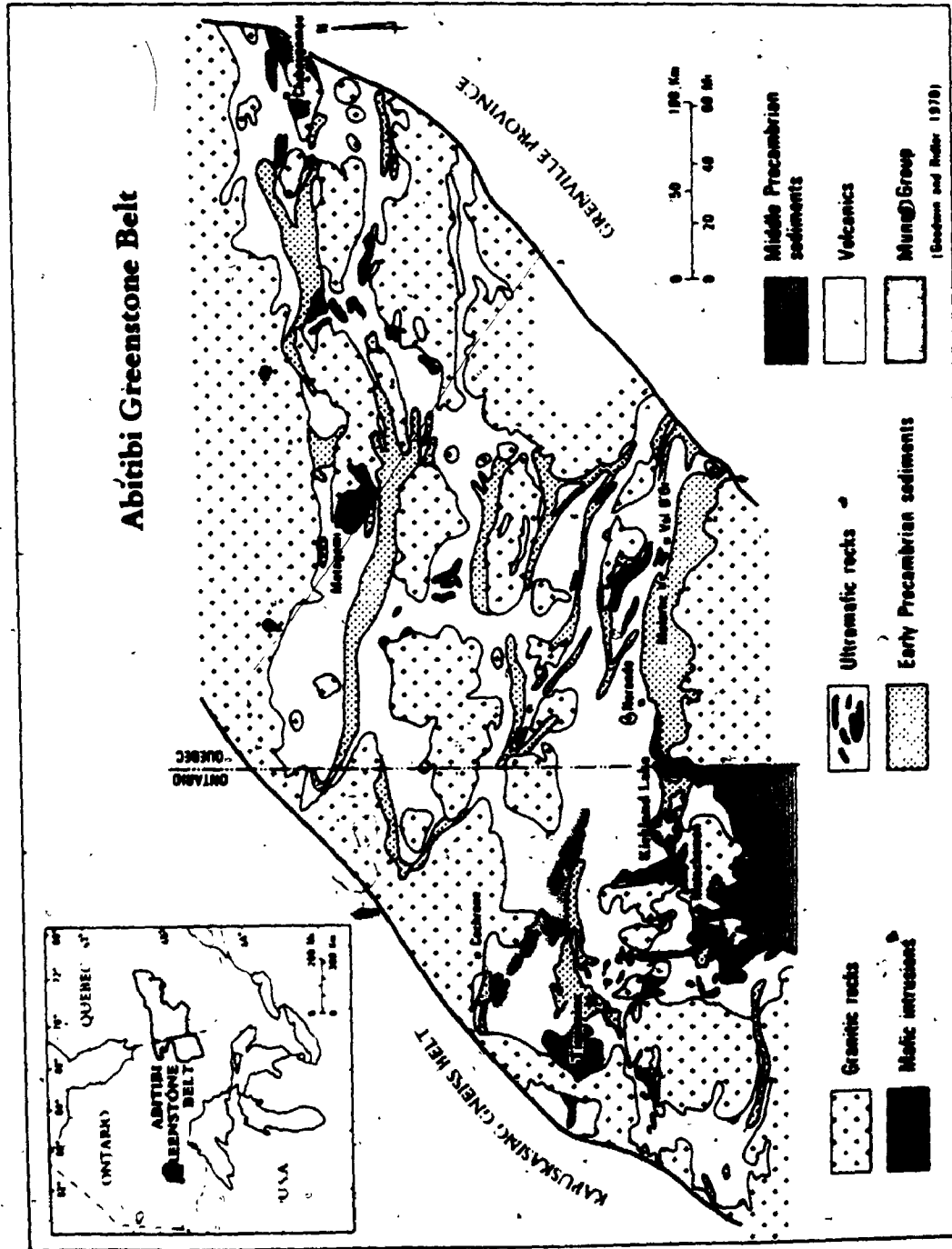
2.2 General Geology of the Abitibi Greenstone Belt

The Abitibi greenstone belt, in the southeast part of the Superior tectonic province, is approximately 725 km long and 240 km wide (Fig. 2-1). This east-trending belt is truncated to the east and the west by the northeast trending crystalline rocks of the Grenville province and the Kapuskasing subprovince respectively.

The Abitibi lithic assemblage is characteristic of many Archean greenstone belts of the Canadian Shield. Older supracrustal and intrusive rocks, now deformed and commonly of greenschist facies of regional metamorphism have been intruded by felsic to mafic stocks and batholiths of late-Archean age. Numerous Precambrian diabase dikes, younger by about 10 Ma and including many of the Matachewan and Keweenaw swarms, are present. Several tongues of flat-lying Proterozoic rocks protrude upon the Abitibi belt from the south.

The supracrustal rocks are predominantly volcanic, particularly mafic to felsic flows and pyroclastic rocks of tholeiitic to calc-alkaline affinity. These are typically in several mafic to felsic cycles or sequences. Overlying

Figure 2-1. Geology of the Abitibi Greenstone Belt (after Goodwin and Ridler, 1970).



the great apparent thicknesses of mafic volcanic rocks are numerous concentrations of felsic volcanic rocks, each concentration characteristically representing an eruptive centre or cluster of related centres. Principal concentrations occur at Val d'Or, Noranda, Kirkland Lake, Timmins and Chibougamau. In addition, the regional volcanic accumulation includes many thin, extensive felsic tuff horizons attributed to periodic explosive eruptions of volcanic ash.

Sedimentary rocks are predominantly of turbiditic nature, in broad, generally east-trending, folded zones, principally south of Noranda, east of Kirkland Lake, near Timmins, northeast of Lake Abitibi, south and southwest of Matagami and west of Chibougamau (Goodwin and Ridler, 1970). This includes facies of greywacke, argillite, lithic sandstone, conglomerate, breccia, chert and iron-formation ranging up to 3 km thick. Chaotic textures and polymict, unsorted materials are distinctive features and are characteristic of very active tectonic zones. Most sedimentary and volcanic rocks are structurally conformable. Local unconformities have been established at Kirkland Lake and Timmins (eg. Thomson, 1946; Roberts, 1981).

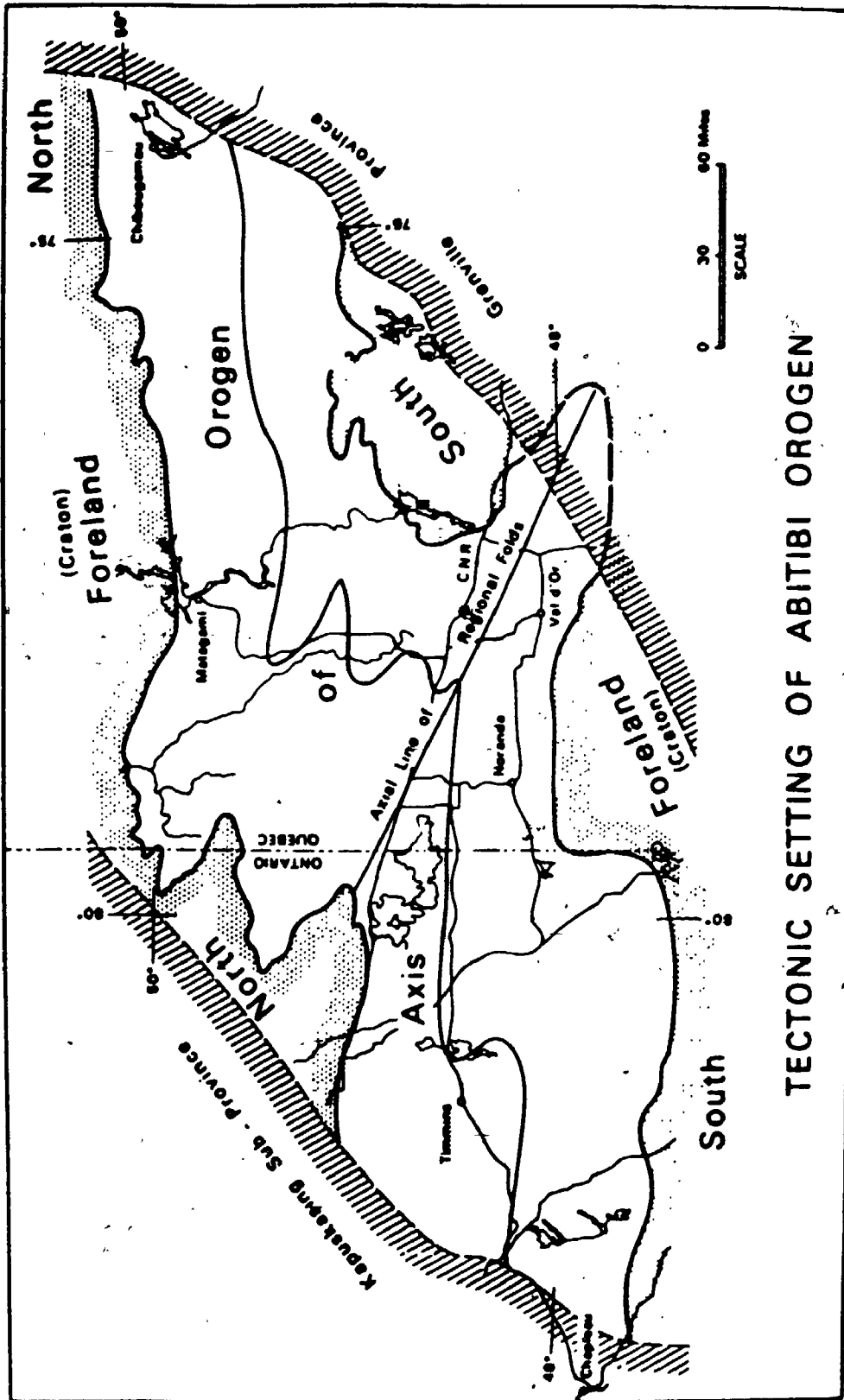
Foliated to massive granitic rocks commonly underlie the margins of the region. When intrusive relations are apparent, the granitic rocks post-date the volcanic and sedimentary rocks. The large granitic complexes along the

north and south boundaries may include primitive, crystalline basement. Granitic plutons are also widely distributed within the Abitibi belt. There are nine major plutons, each 60-160 km in diameter. Most of these are in the north part of the Abitibi belt. Several smaller plutons, enclosed within volcanic rocks, are associated with the felsic volcanic rocks (eg. Noranda, Malartic, Kirkland Lake, Chibougamau) and may represent coeval intrusive equivalents. Numerous sills, dikes and irregular masses of mafic to ultramafic rocks are present, particularly in the lower, mafic parts of volcanic sequences.

Goodwin and Ridler (1970) have interpreted the Abitibi belt as a remnant of a bilaterally symmetrical, intracratonic orogen. The orogen proper is between two postulated cratonic forelands, the boundaries of which are defined on the basis of the preponderant granitic rocks (Fig. 2-2). The first order structure of the Abitibi belt is an S-shaped regional fold which is delineated by the boundary surface of the orogen. Two conspicuous, second-order, S-shaped folds which form part of the regional fold, are present on both boundary surfaces. The axial lines of the regional folds trend northwest. Folding of the compositional layering within the orogen is widespread. These folds have east-trending axes, are characteristically isoclinal, doubly-plunging and bifurcate along strike (Goodwin and Ridler, *op. cit.*).

102

Figure 2-2. Tectonic setting of the Abitibi Orogen (from Goodwin and Ridler, 1970).



TECTONIC SETTING OF ABITIBI OROGEN

2.3 Geology of the Kirkland Lake District

Physically, the Archean rocks of the Kirkland Lake district are divided into three by a central, east-trending belt of sedimentary rocks and interlayered trachytic flows and pyroclastic rocks intruded by a composite syenite stock. To the north, unconformably beneath the rocks of the central belt, there are mafic to felsic volcanic rocks and subvolcanic intrusions. South of the central belt there is a complex suite of ultramafic to felsic volcanic rocks and related intrusive rocks overlain conformably by and interlayered with sedimentary rocks. Correlation with, and structural relations to, rocks of the other belts is controversial.

Early mapping in the Kirkland Lake district described a great thickness of mafic and intermediate volcanic rocks overlain by sedimentary rocks with interbedded alkaline volcanic rocks (Todd, 1928). Volcanic rocks were grouped together and correlated with the Keewatin Series described from the Lake of the Woods area. In 1911, Miller named a series of sedimentary rocks containing pebbles and boulders of Keewatin rocks in the Cobalt area the Timiskaming Series. In 1914, Miller extended the usage to include sedimentary rocks of Kirkland Lake, applying it to areas mapped earlier by A. G. Burrows, P. E. Hopkins, M. E. Wilson and R. W. Brock. Miller and Knight (1914) applied the same term to many other regions in southern Ontario.

Miller's simple two-fold classification of the Archean into a predominantly volcanic series, the Keewatin overlain by a predominantly sedimentary series, the Timiskaming, persisted for over 40 years.

However, in other areas of the Archean, further detailed field work indicated that the old two-fold division of rock types alone was not supported by new observations. Thick sedimentary horizons were found interbedded with the volcanic Keewatin Series, and it became apparent that the Keewatin was more complex than first interpreted (Hewitt, 1963). Additionally, various workers have long recognized that the Timiskaming of the Kirkland Lake area is represented by volcanic and sedimentary rocks differing from the type sedimentary section described on Lake Timiskaming (Cooke and Moorhouse, 1969).

2.3.1 Stratigraphy

Stratigraphic relations in the Kirkland Lake district are a matter of some controversy in the literature. Three major schemes of interpretation have been advanced since the first systematic program of detailed mapping was done in the 1930's by the Ontario Department of Mines (Thomson, 1946, 1948; Thomson and Griffiths, 1941; McLean, 1944; Hewitt, 1949). Major proponents of these interpretations have been J. E. Thomson, R. H. Ridler and L. S. Jensen. The following section provides a brief synopsis of the

chronologic development of their stratigraphic interpretations.

As stated previously, first investigations of Precambrian rocks in the Superior Province below the Huronian Supergroup resulted in the definition of the Keewatin and the Timiskaming series. The Keewatin series consisted of volcanic rocks with minor interbedded sedimentary rocks. The Timiskaming series consisted of dominantly clastic sedimentary rocks.

The first geologic mapping done by the Ontario Department of Mines in the Kirkland Lake district have a lower sequence of mafic volcanic rocks and related diorite to the south with minor interlayered sedimentary rocks. The volcanic rocks were overlain by greywacke with interbedded conglomerate and distinctive alkalic volcanic rocks. Also interlayered with the sedimentary rocks were mafic volcanic rocks markedly similar to those of the lower sequence. Thomson (1946) showed there was a profound angular unconformity at the base of the upper sequence in Lebel Township and to the west. Elsewhere the contact was apparently conformable due to coincidence of structures.

The presence of the angular unconformity led Thomson to correlate the upper sedimentary rocks with the Timiskaming series and the underlying volcanic rocks with the Keewatin. Thomson viewed the structure of the district as an asymmetric remnant of a great synclorium cut by a

major fault which he referred to as the Larder Lake Fault. The primary evidence for the fault was the existence of a broad zone of shearing and carbonate alteration and that south-facing Keewatin volcanic rocks occurred south of the south-facing, ostensibly younger, Timiskaming sedimentary rocks. Thomson acknowledged the probable equivalence of the Larder Lake Fault with the Cadillac-Bouzan Fault to the east in Quebec and suggested a possible continuation of the structure to the west, under areas overlain by Huronian sedimentary rocks. He viewed the displacement on the fault as great with the south side being upthrust and eroded.

In the late 1960's R. H. Ridler (1969, 1970) re-examined the Kirkland Lake district as part of a Geological Survey of Canada study of the Abitibi Greenstone belt. Ridler made substantial revisions to Thomson's stratigraphic and structural interpretation using A. M. Goodwin's (1965) concept of volcanic cycles and related iron formations. The key to Ridler's interpretation was the recognition of carbonate facies iron formation among the carbonate-rich rocks of the Larder Lake Fault. He denied the existence of a fault along this zone of carbonate-rich rocks, attributing the extensive shearing in the area to the incompetent nature of carbonate facies iron formation. Ridler correlated this carbonate facies with oxide facies iron formation in Boston township and included both in the upper part of the Timiskaming sedimentary rocks. The

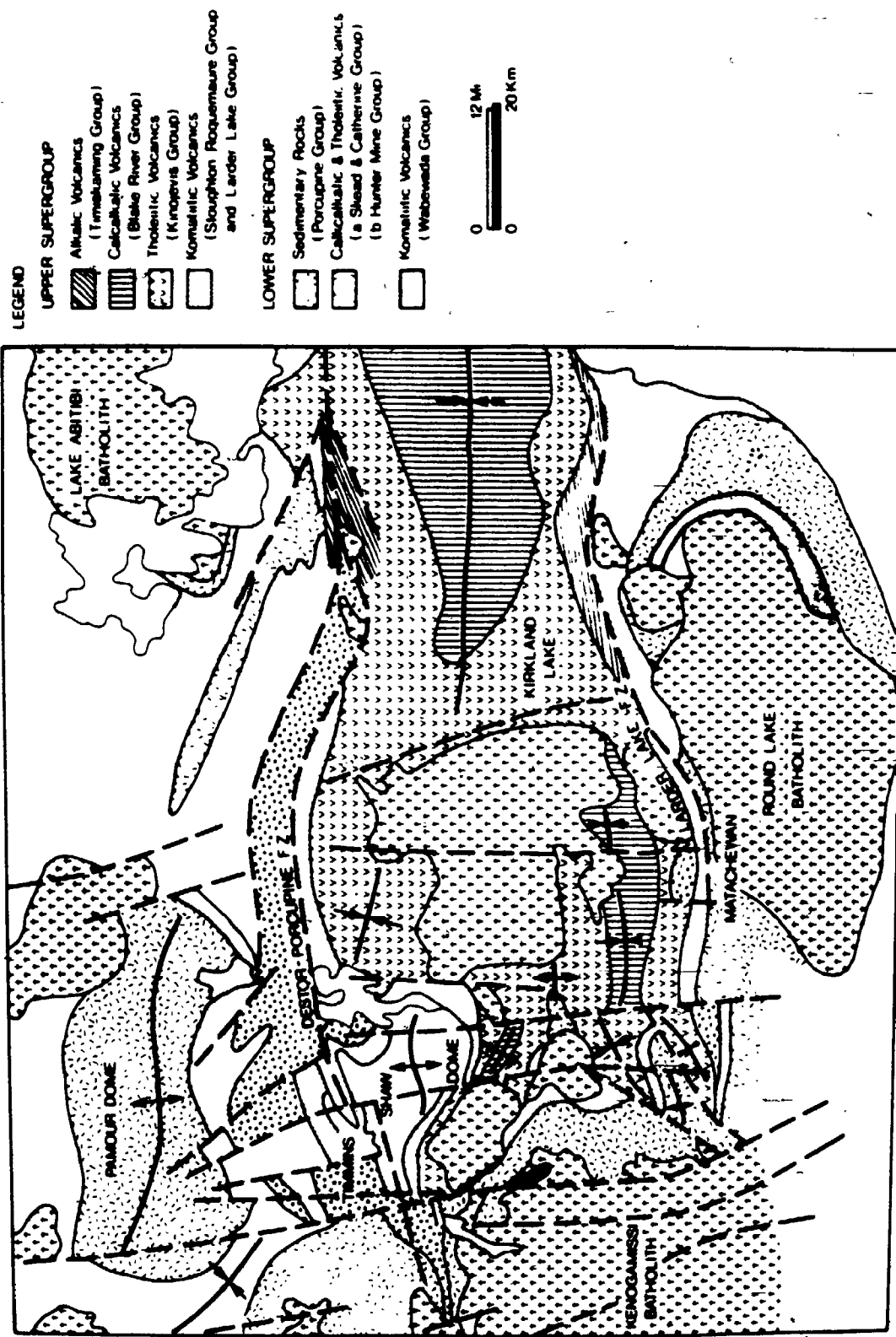
correlation was supported by the presence of alkali-rich basalts near the oxide facies iron formation in Boston township suggesting affinities with the alkalic volcanic rocks of the Timiskaming series.

The Keewatin-like volcanic rocks that structurally overlie Timiskaming sedimentary rocks west of Kirkland Lake were said to be younger and called the Highway 11 basalts. Ridler made major subdivisions in the previously undivided Keewatin volcanic rocks below the Timiskaming. The importance of the angular unconformity at the base of the Timiskaming was deemphasized as not necessarily representing any great gap in time. Ridler's revised stratigraphic interpretation eliminated the asymmetric nature of the synclorium proposed by Thomson and appeared to provide a simpler, more consistent model.

In the 1970's, L. S. Jensen and D. R. Pyke of the then Ontario Department of Mines started a systematic revision of the geology of the Timmins-Kirkland Lake area. They made extensive use of whole rock major element abundances of volcanic rocks to define cycles of volcanism similar to those defined by Goodwin (1965). Each cycle had a komatiitic base, a tholeiitic middle, and a calc-alkalic upper part passing upwards into intercycle sedimentary rocks including iron formation.



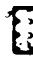

Jensen (1976) and Meyn (1977) examined the oxide facies iron formation in Boston township. They found the

Figure 2-3. Geology of the Timmins-Kirkland Lake area (from Jensen, 1980).


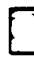



LEGEND

UPPER SUPERGROUP

-  Alkalic Volcanics (Timiskaming Group)
-  Calcalkalic Volcanics (Blake River Group)
-  Tholeiitic Volcanics (Kinopvis Group)
-  Komatiitic Volcanics (Stoughton, Roguemaure and Larder Lake Group)

LOWER SUPERGROUP

-  Sedimentary Rocks (Porcupine Group)
-  Calcalkalic & Tholeiitic Volcanics (a) Shead & Catherine Group (b) Hunter Mine Group)
-  Komatiitic Volcanics (Wabewanda Group)



iron formation was interlayered with both calc-alkalic felsic tuffs and komatiitic ultramafic flows. The implied stratigraphic position of this iron formation was clear, between two major volcanic cycles. It was equally clear that the iron formation occurred below rocks that the Timiskaming rocks overlie with profound angular unconformity regardless of the time significance of the unconformity. Thus the Boston township oxide facies iron formation could not be correlative with the Timiskaming rocks.

Jensen interpreted whole rock element abundances to suggest that the alkali basalts in Boston township are the result of alkali metasomatism associated with the Lebel syenite stock. This is significant in that Ridler justified correlation of these basalts with Timiskaming rocks on the basis of their alkalic affinities.

Ridler's interpretation was also superseded somewhat by work of Tihor and Crocket (1977) on the carbonate-rich rocks of the Larder Lake area. They recognized relict spinifex textures in some of these rocks. Hence, at least some if not much of the carbonate-rich rocks are altered volcanic rocks and not carbonate facies iron formation.

The Highway 11 basalts of Ridler (1969) were included by Jensen in a tholeiitic unit overlying the basal komatiitic rocks which include the Boston township oxide iron formation. It is thus interpreted as older than Timiskaming rocks and separated by the Larder Lake Fault

from the younger but structurally lower sedimentary rocks as originally interpreted by Thomson. The identification of older rocks structurally above Timiskaming rocks brought the Larder Lake Fault back to its former prominence.

Below and south of the basal komatiitic rocks mentioned above there is a thick, complete komatiitic to calc-alkalic volcanic cycle. Jensen's interpretation here did not differ substantially from that of Ridler.

The following description of stratigraphy in the Kirkland Lake district is essentially that of Jensen. It is this writer's opinion that Jensen's interpretation is current, coherent and most suitable for the area immediately surrounding Kirkland Lake and hence the more restricted area of the Macassa Mine property, the focus of this study.

In the Kirkland Lake district, volcanic, sedimentary and associated intrusive rocks form a large east-plunging synclorium between the Lake Abitibi batholith and the Round Lake Batholith (Fig. 2-3). Two cycles of volcanism, each with associated sedimentary and intrusive rocks occur in the area: these are referred to by Jensen (1978a, b; 1980) as the Lower and Upper Supergroups. Each are composed of komatiitic rocks at the base, overlain in turn by tholeiitic and calc-alkalic rocks: the second cycle or Upper Supergroup is capped by an upper alkalic sequence. They are separated from each other by sedimentary rocks containing conglomerate, argillite, chert and iron-

formation. The upper-alkalic sequence is preserved along the Kirkland-Larder Lake Fault and is alkalic rocks of the Na and K series (Jensen, 1978). Total apparent stratigraphic thickness is greater than 35 km. The stratigraphy of the Kirkland Lake district is summarized in Table 2-1 and the following nomenclature and descriptions are taken from Jensen (1978, 1980).

The basal komatiitic sequence of the first cycle, which is referred to as the Lower Supergroup (Jensen and Langford, 1983), is called the Wabewawa Group and is ultramafic komatiite, basaltic komatiite and Mg-rich tholeiitic basalt. This group overlies calc-alkalic tuffs, called the Pacaud tuffs (Ridler, 1975), which are interlayered with argillite, chert and iron-formation along the south margin of the regional synclinorium adjacent to the Round Lake Batholith. The Pacaud tuffs may represent the top of an older volcanic cycle. Overlying the Wabewawa Group is a tholeiitic sequence of Mg-Fe rich basalt known as the Catherine Group. The Catherine Group is overlain, in turn, by calc-alkalic basalt, andesite, dacite and rhyolite of the Skead Group. Total apparent maximum thickness of the first volcanic cycle is about 15 km.

At the top of the first volcanic cycle, the calc-alkalic tuffs and tuff breccias are interlayered by conglomerate, greywacke, argillite, chert and iron-formation. Flows of ultramafic and basaltic komatiite occur

Table 2-1.

Stratigraphy of the Kirkland Lake District.*

Group	Volcanic Rocks	Sediments	Intrusive Rocks	Relationships
Timiskaming Group (Kirkland Lake- Larder Lake Section) 3,000 m	Na- and K-rich mafic to felsic alkalic volcanic rocks and K-rich subalkalic felsic volcanic rocks	Fluviatile conglomerate, wacke and argillite of material derived locally and from LLG	Mafic to felsic syenodiorite and syenites	Unconformably overlies BRG, KG and in places LLG. Mainly a fault contact with LLG
Blake River Group (BRG) 10,000 m	Calc-alkalic basalt, andesite, dacite and rhyolite flows and pyroclastic rocks Minor Mg-rich tholeiitic basalt	Volcaniclastic turbidites derived by slumping off volcanic edifices	Gabbro, diorite, quartz diorite and rhyolite domes	Conformably overlies KG
Kinojevis Group (KG) 10,000 m	Mg-rich and Fe-rich tholeiitic basalt with minor tholeiitic andesite, dacite and rhyolite flows	Hyaloclastite and argillite, chert and graphite	Gabbro	Conformably overlies BRG
Larder Lake Group (LLG) Thickness unknown 5,000 m	Peridotitic and basaltic komatiite and Mg-rich tholeiitic basalt, minor Fe basalt, calc-alkalic rhyolite tuff toward base of group	Turbiditic conglomerate wacke, argillite of material derived locally from komatiitic flows and distally from SR graphite, carbonate and iron formation Pebble conglomerate with syenite clasts	Dunite, perido- pyroxenite and gabbro Syenite intrusion?	Disconform- ably overlies CG
Skead Group (SG)	Calc-alkalic basalt, andesite, dacite and rhyolite flows and pyroclastics	Cherts and iron formation	Rhyolite porphy- ries	Conformably overlies CG
Catharine Group (CG)	Mg-rich and Fe-rich tholeiitic basalt	Minor argillite	Gabbro	Conformably overlies WC
Wabewawa Group (WG)	Peridotitic and basaltic komatiite and Mg-rich tholeiitic basalt Minor rhyolite-tuff*	?	Dunite, perido- tite pyroxenite and gabbro	Overlies calc-alkalic tuffs (Pacaud tuffs)

*From Jensen (1940).

interlayered with these sedimentary rocks and become predominant upward in the stratigraphic sequence. These komatiitic volcanic rocks are the Larder Lake Group and form the basal section of the second volcanic cycle referred to as the Upper Supergroup (Jensen and Langford, 1983). Above the Larder Lake Group there is a sequence of tholeiitic rocks (Mg-Fe rich basalt and some andesite, dacite and rhyolite toward the top) called the Kinojevis Group. This group is about 10 km thick. Above the tholeiitic sequence are the calc-alkalic volcanic rocks of the Blake River Group. These are Mg-rich tholeiitic basalt, plus calc-alkalic basalt, andesite, dacite and rhyolite flows and pyroclastic rocks derived from two or more volcanic centres represented by massive rhyolite domes at the centre of the synclorium. The Blake River Group is about 10 km thick.

Unconformably overlying the Kinojevis Group, the Blake River Group and possibly the Larder Lake Group, is the Timiskaming Group. The Timiskaming Group includes both sedimentary and volcanic rocks consisting of conglomerates, sandstones, siltstones, argillite, chert, iron-formation, lavas, agglomerates and tuffs (Hyde, 1980). The volcanic rocks are dominately trachytes and phonolites. Cooke and Moorhouse (1969) identified leucite-bearing volcanic rocks within the Timiskaming Group. The maximum exposed thickness of the Timiskaming Group is about 5 km in east Label

Township (Hewitt, 1963).

2.3.2 Structure

The dominant structural elements of the Kirkland Lake district are two steeply inclined, east-trending irregular shear zones: the Destor-Porcupine Break in the north and the Larder Lake Break in the south. They follow contacts between sedimentary and volcanic rocks. Recent field studies have cast doubt on their continuity and magnitude of dislocation (Goodwin, 1965). Their exact nature, whether they represent faults of undetermined movement, carbonate-rich exhalative sedimentary rocks (Ridler, 1969), carbonatite flows (Stricker, 1978) or carbonatized ultramafic flows (Pyke, 1975), or a combination of these and other relationships, remains a matter of interpretation.

The Larder Lake Break extends from south of Kenogami Lake on the west to the Rouyn-Noranda area on the east where it is called the Cadillac-Bouzan Break. This fault system is obscured by only slight movement in the younger Proterozoic rocks. The older the rocks, the greater is the displacement (Jensen, 1980). This suggests that the fault system has been an active influence throughout the deposition of volcanic and sedimentary rocks and their subsequent intrusion by granite and syenite. Where identified in the Kirkland Lake district, the Break is at or close to the

south edge of the Timiskaming Group. In Teck Township, south of the Macassa Mine, it is close to the south contact. To the east, however, the Break is mainly within Timiskaming Group sedimentary rocks (see ODM map 2205, 1972). The Break has been variably defined as: 1) a major thrust fault with attendant hydrothermal carbonatization (Thomson, 1950); 2) a sedimentary zone of carbonate exhalative iron-formation marking the change from oxide to carbonate facies (Ridler, 1969, 1975); and 3) a volcanic zone wherein many of the carbonate rocks may be shown to be ultramafic flows on the basis of remnant textures and structures (Jensen, 1978).

The first definition is favoured here based on the following evidence in diamond drill core from the south edge of the Macassa Mine property: a surface diamond drill hole collared north of the Larder Lake Break and drilled south after approximately 250-300 m encountered a zone of very fractured and bleached mafic rock rich in carbonate minerals 10 m wide which was terminated down hole by a steeply dipping chloritic gouge 10 cm wide. This structure was assumed to be the down dip extension of the Larder Lake Break. The hanging wall rocks had little or no carbonate minerals and appeared much less altered and fractured. The asymmetric pattern of fracturing and alteration around the structure is interpreted to reflect post alteration movement of unknown magnitude.

Numerous northwest to northeast trending fractures transect the supracrustal rocks. No consistent patterns of horizontal offset have been established. The fractures are considered to cover a wide age range and represent several separate, possibly repeated periods of development and movement.

The Round Lake batholith is another major structural element of the Kirkland Lake region. The batholith is mantled by the Skead Volcanic rocks. Ridler (1969) suggested that the batholith, which is itself metamorphosed and mylonitized near its margins is in part the basement upon which the Skead volcanic rocks were originally deposited and both basement and volcanic rocks have been moved to their present position.

The Timiskaming Group of volcanic and sedimentary rocks form an east trending narrow continuous belt (0.5 to 8 km wide) on the northeast of the Round Lake batholith. They are a south-facing, monoclinial sequence. There are strike faults, cross-faults and oblique faults in the Timiskaming Group. Parts of the older komatiitic sequence to the south have been faulted in with the Timiskaming Group in several places.

The upper contact of the Timiskaming Group is a fault. This fault truncates several of the upper units and several of the syenitic bodies which intrude both Timiskaming Group and volcanic rocks to the south.

2.3.3 Metamorphism

In a study of metamorphism of part of the Abitibi greenstone belt, Jolly (1974) was able to subdivide the region according to metamorphic facies and distinguish between regional and contact metamorphic effects. He found that burial metamorphism of much of the pre-Timiskaming volcanic rocks was to the prehnite-pumpellyite facies. Jolly also found that the Timiskaming Group contains prehnite-pumpellyite only in detrital lithic fragments and is largely chloritic wherever the sedimentary rocks are remote from igneous intrusions. Thus, the Archean volcanic and sedimentary rocks of the Kirkland Lake district are metamorphosed to the sub-greenschist and greenschist facies except near the margins of large intrusive bodies where amphibolite-facies rocks are found (Jolly, 1978).

2.3.4 Radiometric Age Determinations

In the Kirkland Lake district, the Upper Supergroup consists of a series of volcanic cycles in an easterly plunging synclinalorium. On the north limb, the basal Hunter Mine Group has been dated by the U-Pb method on zircons at 2710 ± 2 Ma (Nunes and Jensen, 1980). Unconformably overlying the Hunter Mine Group are the komatiitic volcanic rocks at the Stoughton-Roquemare Group (Jensen, 1976, 1978) which have been correlated with the Larder Lake Group of the Kirkland Lake district (Jensen and Pyke, 1980), at the

base of the Upper Supergroup. The felsic volcanic rocks of the Blake River Group at the top of the Upper Supergroup has been dated by the U-Pb method on zircons at 2703 ± 2 Ma (Nunes and Jensen, 1980). These are upper concordia intercept model ages, which probably represent minima given the absence of xenocrystic zircons (Nunes and Jensen, 1980). These data from rocks which span the volcanic stratigraphy of the Upper Supergroup with an apparent cumulative thickness of 30,000 m signify a time interval of 7 ± 3 Ma for development of much of the Kirkland Lake section of the Abitibi greenstone belt.

Overlying the Blake River Group are intrusive and extrusive alkalic igneous rocks of the Timiskaming Group, which host the principal gold deposits. There are as yet no precise age determinations on zircons from igneous rocks of this Group although work is currently in progress by the Ontario Geological Survey.

Major granitic batholiths in the Abitibi greenstone belt are thought to be broadly contemporaneous with volcanic activity. Krogh et al. (1982) report that the majority of batholiths have ages in the narrow interval of 2675 to 2685 Ma (U-Pb determinations on zircons). The Lake Dufault granodiorite at Noranda has an age of 2701 Ma (U-Pb isotopic determinations on zircons by Krogh, quoted in Nunes and Jensen (1980), and the Round Lake batholith south of Kirkland Lake has a Rb-Sr isochron age of 2,390 Ma,

although this is probably a cooling age ($^{87}\text{Sr}/^{86}\text{Sr}$ initial = 0.7009 ± 0.0009 , Purdy and York, 1967).

A lower age constraint on Abitibi belt igneous activity is provided by a Rb-Sr whole rock isochron age of $2,690 \pm 93$ Ma ($^{87}\text{Sr}/^{86}\text{Sr}$ initial = 0.700 ± 0.001) on the Matachewan diabase dike swarm, which transects all rock types, batholiths and some of the ore deposits in the Timmins area (Gates and Hurley, 1973).

CHAPTER 3

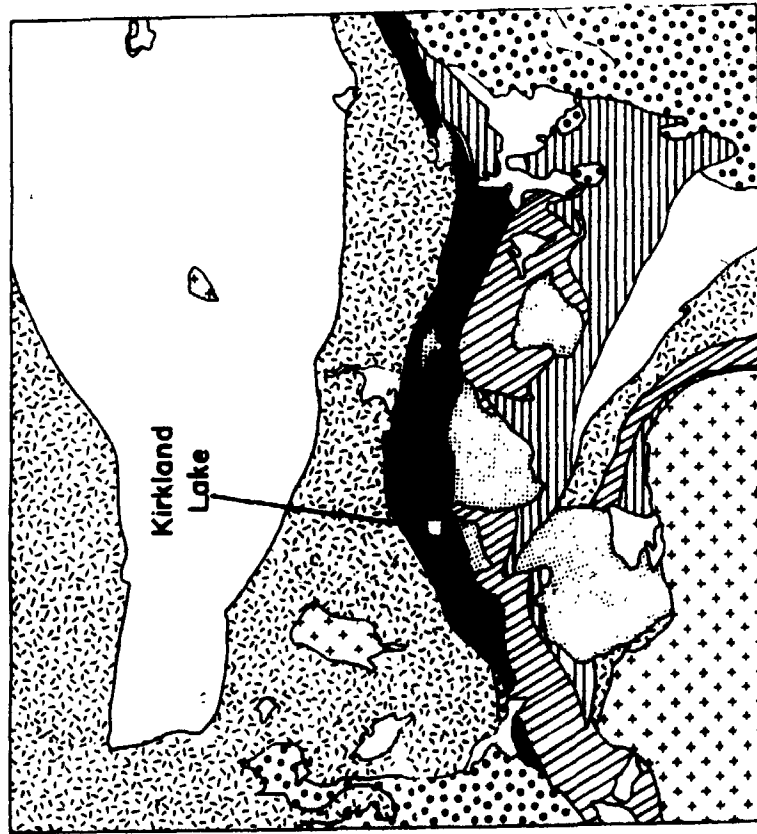
GEOLOGY OF THE MACASSA MINE

3.1 General Statement

The town of Kirkland Lake and the surrounding district is underlain by Timiskaming Group sedimentary and volcanic rocks. These rocks extend from Kenogami Lake, through Teck Township and further east (Fig. 3-1). The Timiskaming rocks form two east-trending belts (informally called the north and south belts) which are separated by a synclinal axis, syenitic stocks and the Larder Lake Fault. In Teck Township, in the north belt, the sequence is a south-facing homoclinal succession about 3.5 km thick and striking approximately 065°.

Hyde (1978, 1980) subdivided Timiskaming Group sedimentary and volcanic rocks into 12 facies based on grain size, nature and thickness of bedding, type and size of sedimentary structures and vertical sequence of sedimentary structures. Four of these sedimentary facies were grouped together to form a Non-marine Association, which is dominated by pebble and cobble conglomerate and sandstone of braided river origin. Smaller amounts of floodplain,

Figure 3-1. Generalized geology of the Kirkland Lake district (from Jensen, 1978b).



- Proterozoic - Cobalt Group
- Syenitic rocks
- Troghjemitic rocks
- Alkalic volcanic rocks and sedimentary rocks - Timiskaming Group
- Intercycle sedimentary, volcanic and intrusive rocks
- Calc-alkalic volcanic rocks
- Tholeiitic volcanic rocks
- Komatitic volcanic rocks



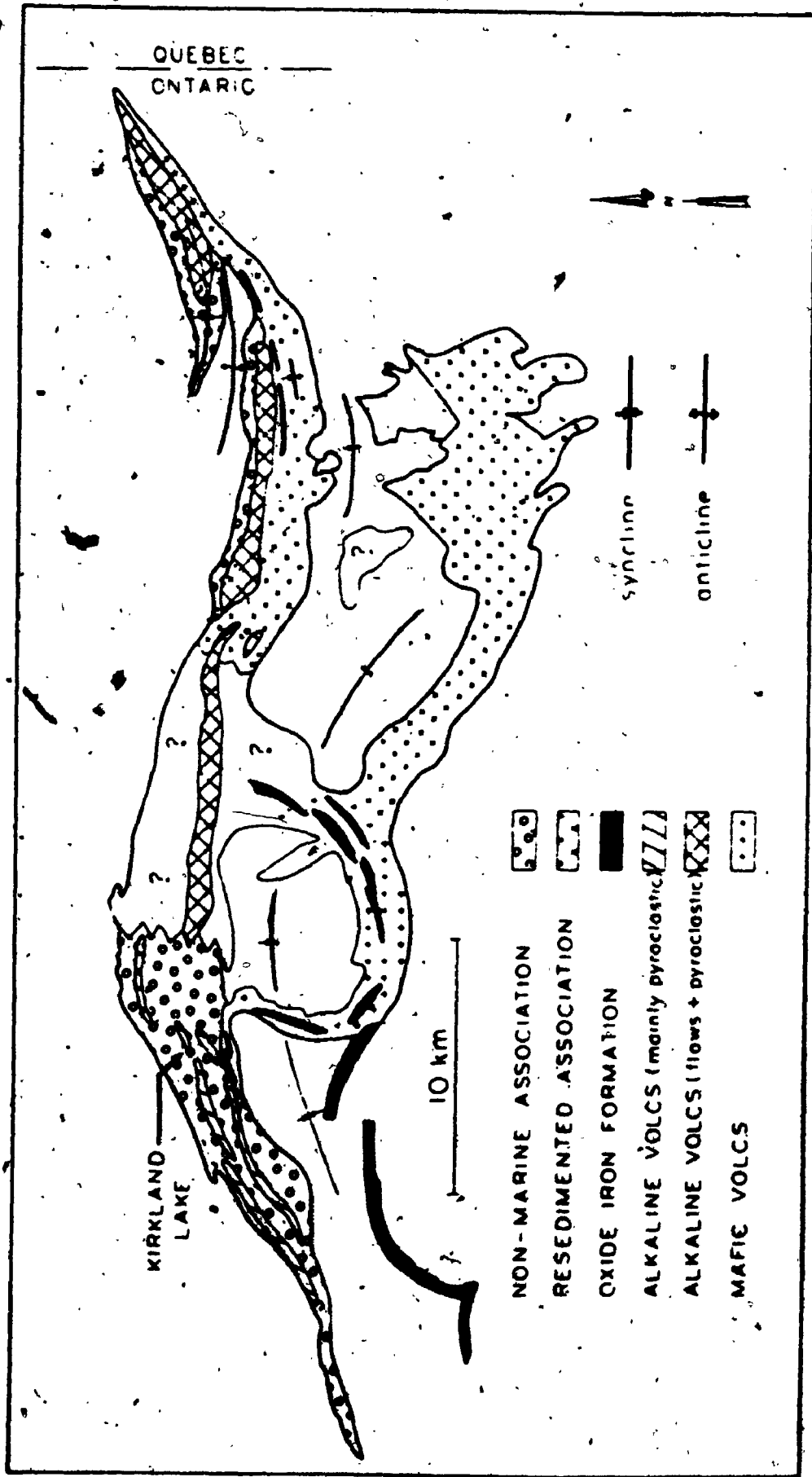
lacustrine, and eolian deposits are also present. A Resedimented Association consists of four other facies, and includes graded and ungraded conglomerates, sandy turbidites, sandy and silty, laminated turbidites, and oxide iron-formation. These facies were interpreted to represent deposition within submarine fans.

Sedimentary and pyroclastic rocks underlying Kirkland Lake, most of Teck and Lebel Townships are dominated by those facies assigned to the Non-marine Association whereas areas further east are characterized by Resedimented Association facies (Fig. 3-2). More than 95 percent of volcanic rocks near Kirkland Lake are pyroclastic in contrast to areas further east where massive and porphyritic trachytic flows, including altered leucitic porphyritic flows, commonly occur.

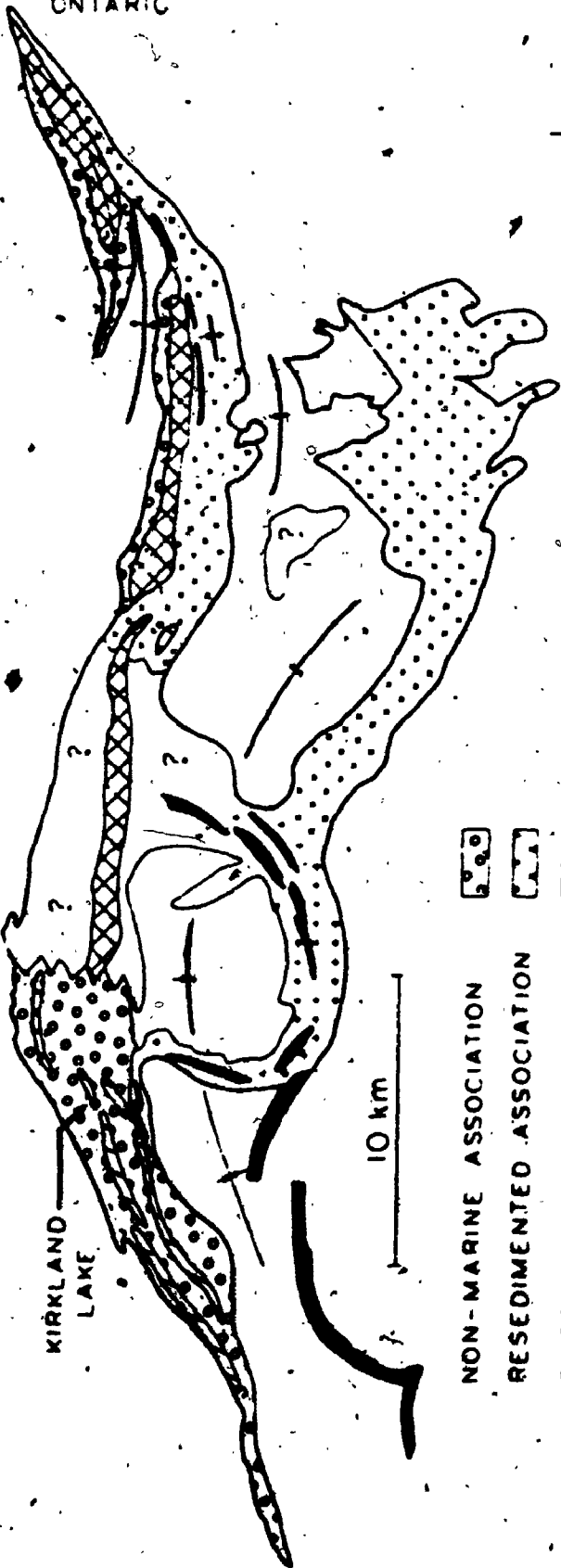
The Timiskaming Group sedimentary and volcanic rocks are intruded by a composite syenitic stock centered on the town of Kirkland Lake. The long axis of this stock and its satellitic dikes is roughly parallel to the strike of the Timiskaming rocks. In plan it is somewhat wedge-shaped, broadening to the east. The dip is steeply to the south with the north contact being somewhat steeper than the south resulting in a general widening of the complex with depth. In longitudinal section, the intrusive complex plunges down to the west at approximately 45°.

The syenite stock is made up of three main phases:

Figure 3-2. Distribution of facies associations and rock types of the Timiskaming Group
in the Kirkland Lake district (from Hyde, 1980).



QUEBEC
ONTARIO

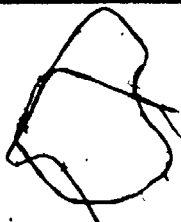


KIRKLAND
LAKE

10 km

- NON-MARINE ASSOCIATION
- RESEDIMENTED ASSOCIATION
- OXIDE IRON FORMATION
- ALKALINE VOLCS (mainly pyroclastic)
- ALKALINE VOLCS (flows + pyroclastic)
- MAFIC VOLCS

syncline
anticline



augite syenite, massive or felsic syenite and porphyritic syenite. The augite syenite was the earliest of these phases and forms irregular tabular lenses and dike-like bodies. It typically contains more than 15% augite phenocrysts. Massive syenite occurs in an irregular pipe-like form the dimensions of which are 250 m x 500 m at surface. This phase plunges westward at approximately 40° and contains less than 15% augite phenocrysts. In drill core and underground exposure, massive syenite is transitional into augite syenite with increasing augite content or may have a sharp, well-defined intrusive contact. The relative age relationship between massive syenite and augite syenite is therefore ambiguous. Porphyritic syenite transects both augite syenite and massive syenite with well-defined intrusive contacts and is therefore the youngest phase of the composite intrusive complex. The main porphyritic syenite body forms a central elongated plug, which also has a steep westerly plunge, from which numerous dikes and irregularly shaped bodies emanate. This rock is distinctly porphyritic with 2-4 mm sodic plagioclase as the dominant phenocrysts.

The principal gold-bearing zones of Kirkland Lake occur along a major fault system called the Main Break or the Kirkland Lake Fault. The Main Break fault system is a thrust fault which has been traced across Teck Township and a short distance into Label township. Its overall strike

is about 067° . This is approximately parallel to the long axis of the composite syenite stock and the trend of Timiskaming Group sedimentary and volcanic rocks. The system generally has a steep dip to the south (75° - 80°). The main plane of movement has been traced in underground workings to a depth of more than 8,000 ft (2650 m). Estimates of the amount of vertical displacement on the Main break were made by Tyrell and Hore (1926), Todd (1928) and the geologists of the Kirkland Lake mines. All have agreed that it is a thrust fault in which the south or hanging-wall side has moved upward with respect to the north or footwall side. Thomson et al. (1950) summarize displacement on the Main break as rotational, amounting to about 1500 ft (460 m) at the Macassa mine in the west and about 350 ft (110 m) at the Toburn mine in the east.

The following sections describing the geology of the Macassa Mine are based on underground and surface mapping and sampling, and petrographic investigation conducted during the course of this study, compilation of existing mine maps and records, discussions with mine geologists and published data in the literature.

3.2 Rock Types in the Mine

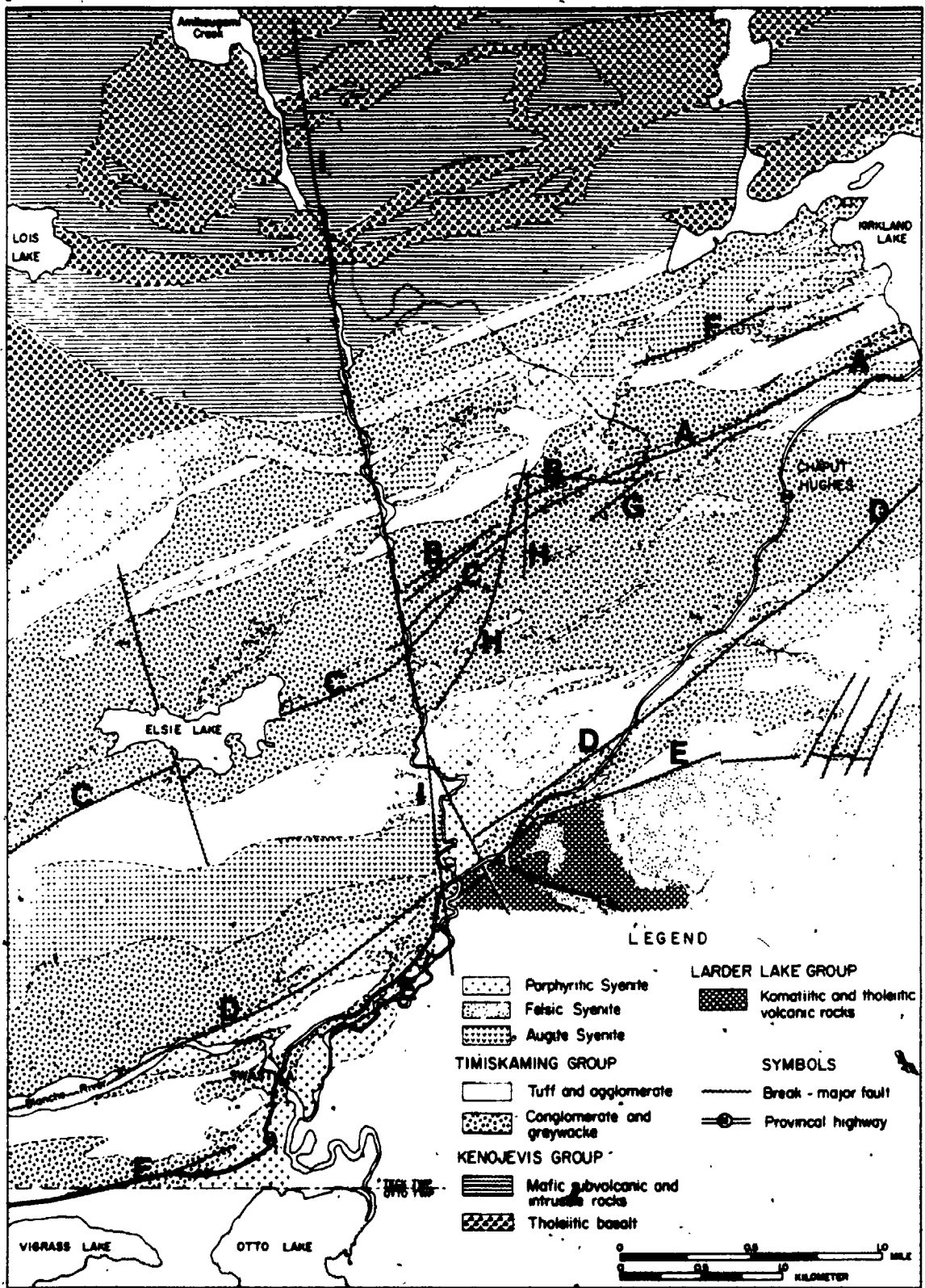
3.2.1 Timiskaming Group

The Timiskaming Group is represented by sedimentary

and volcanic rocks on surface and underground in the Macassa Mine workings (Fig. 3-3). There are both pebble and boulder conglomerates exposed as widths up to 100 m along cross-cuts extending both north and south from the bottom of the No. 1 shaft and to a lesser extent in drifts, crosscuts and drilling to the west. Pebbles and boulders of massive and porphyritic syenite, granite, rhyolite, trachyte, diorite, gabbro, quartz, jasper, chert and spinifex-bearing ultramafic lavas have been noted (Plate 3-1) (Thomson, 1948). Matrix is normally fine to medium-grained sandstone or greywacke. Hyde (1980) has interpreted these rocks as representing a Non-marine facies association.

Greywackes and tuffs are common on the north and south margins of the composite syenite stock in the east and central parts of the mine. Increasing amounts of these rocks are present in areas to the west, away from the main stock. Greywacke is typically a massive, medium to fine-grained (0.20-0.80 mm) rock with <15% angular quartz and quartz fragments, 10 to 15% angular feldspar fragments in a matrix of quartz, chlorite, biotite, feldspar, and minor carbonate minerals. Fresh samples are mostly dark grey and well indurated. With increasing quartz content the grey colour becomes progressively whiter. Samples with abundant secondary carbonate minerals are buff coloured. The generally minor quartz content and scarcity of metamorphic

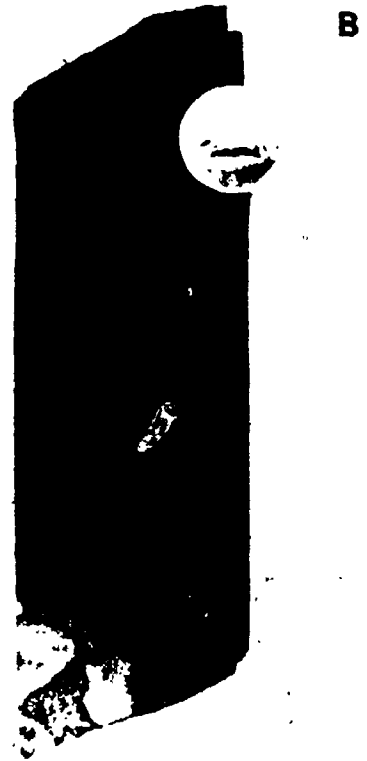
Figure 3-3. General geology of the Macassa Mine with distribution of rock types and major structures. Geology modified from ODM map 1945-1, stratigraphic nomenclature after Jensen, 1980. A = Kirkland Lake Fault - Main Break; B = North Break; C = '04 Break; D = Amalgamated Kirkland Mud Break; E = Kirkland-Larder Lake Fault Zone (Break); F = Narrows Break; G = 'Q' Fault; H = Tegren crossfault system; I = Amikougami crossfault.



7e

Plate 3-1. Boulder and pebble conglomerate from the
Macassa Mine and area.

- a. Outcrop of pebble conglomerate interlayered with lapilli tuff of the Timiskaming Group. Road cut on Highway 66 approximately 0.75 km southeast from No. 1 shaft. Scale bar is approximately 0.5 m.
- b. Polished hand specimen of pebble conglomerate in diamond drill core from the Macassa Mine showing the variety of rock types making up the clasts.
- c. Polished hand specimen of pebble conglomerate in diamond drill core from the Macassa Mine showing large central clast with spinnifex-texture.
- d. Photomicrograph of spinnifex-textured pebble in c. with radiating patterns of clinopyroxene minerals. Scale bar is approximately 1 mm.



rock fragments and minerals suggest that these rocks represent detritus from a source area dominated by volcanic rocks.

There are both fine-grained cherty tuffs and a variety of medium to coarse-grained volcanoclastic rocks including agglomerates, lapilli tuffs and tuffaceous conglomerate (Plate 3-2). Tuffs contain up to 60% altered sodic feldspar, hornblende, pyroxene pseudomorphous after augite, secondary carbonate minerals, and 2-5% opaque minerals. The opaque minerals are almost always iron-oxides. Samples of unaltered tuff from the 5425 ft level contain enough magnetite to be discernable with a hand magnet. Rock fragments are the most abundant constituent of agglomerates and tuffaceous conglomerates. Most fragments are composed of cryptocrystalline feldspar and chloritic material. Mafic volcanic fragments and quartz-bearing volcanic fragments are rare but fragments with feldspar, hornblende or pyroxene are common. Some rocks contain enough rock fragments to be called lithic tuffs.

In addition to these rocks, there are small amounts of arkosic greywacke, and massive and amygdaloidal trachytic flows exposed underground.

3.2.2 Intrusive Rocks

There are three main intrusive rock types in the Macassa Mine: augite syenite, syenite and porphyritic syen-

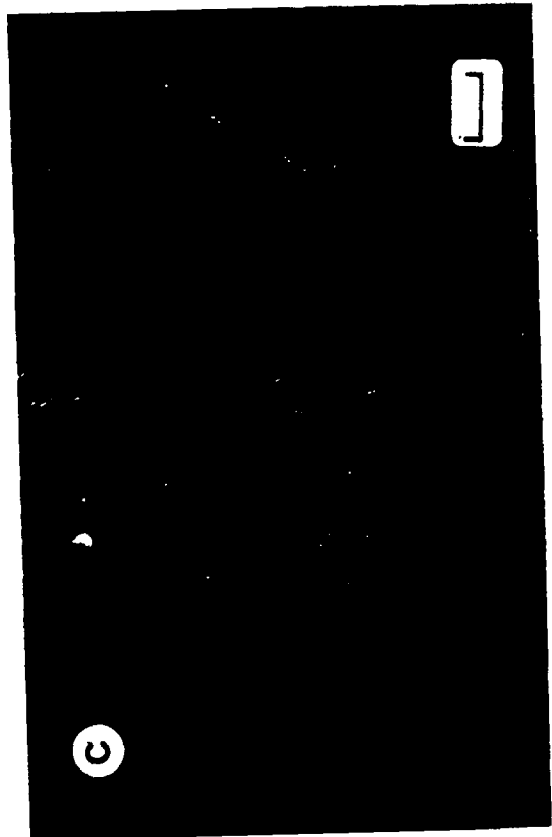
Plate 3-2. Tuffs and agglomerates from the Macassa Mine.

a. Fine-grained cherty tuffs (centre) interbedded with lapilli tuffs. Underground exposure in the Casakirk cross-cut, 3000' level, Macassa Mine, looking east. Scale bar is approximately 0.5 m.

b. Detail of layered lapilli tuff in the back at Casakirk cross-cut, 3000' level, Macassa Mine.

c. Agglomeratic section exposed in the Casakirk cross-cut, 3000' level, Macassa Mine. Very large, irregular clasts (outlined in white chalk) in a fine tuff matrix. Scale bar approximately 0.5 m.

d. Detail of agglomerate clasts in 3-2c, showing both amygdaloidal and massive textures.



ite. The long axes of all the intrusive rocks strike, 060-080° and are generally parallel to the strike of the sedimentary and volcanic rocks of the Timiskaming Group.

Intrusive rocks have dips which are steeper than those of adjoining sedimentary and volcanic rocks (Fig. 3-4). This cross-cutting relationship between the syenitic complex and Timiskaming Group rocks indicates the intrusions to be the later, younger rocks.

Augite syenite is the oldest and most wide spread of the intrusive rocks. The main body intrudes Timiskaming Group conglomerate at surface in a narrow, elongate tabular mass, dips 75 to 85° south to about the 2,000' level and appears to bulge on its south side and generally flatten in dip (Ward and Thomson, 1950). The fresh rock is dark green to black coloured commonly with a medium to coarse, almost granitoid texture (Plate 3-3a). The essential ferromagnesian mineral, augite, makes up 15-35% of this rock, although this is generally pseudomorphed by chlorite, Fe-Mg carbonate, magnetite and actinolite (Plate 3-3b). Feldspar, occurring in approximately similar proportions, is generally about Ab₉₀An₁₀ (Table 3-1) but is commonly replaced by fine, mosaic orthoclase. Biotite, olivine and alkali feldspar occur in minor amounts. Accessory minerals are magnetite, apatite and titanite. The augite syenite contains subradial interstitial growths of secondary alkali feldspar, uranite, sericite, carbonate and leucocoxene (Cooke

80

Figure 3-4. Geologic section through No. 1 shaft of the Macassa Mine with distribution of major rock types and relationships with faults (looking 065°). A = Main Break (Kirkland Lake Fault); AB = Main Break - South Branch; AC = Main Break - North Branch ('E' or R-2 Break); B = '04 Break; C = North Break (Narrows Break?)

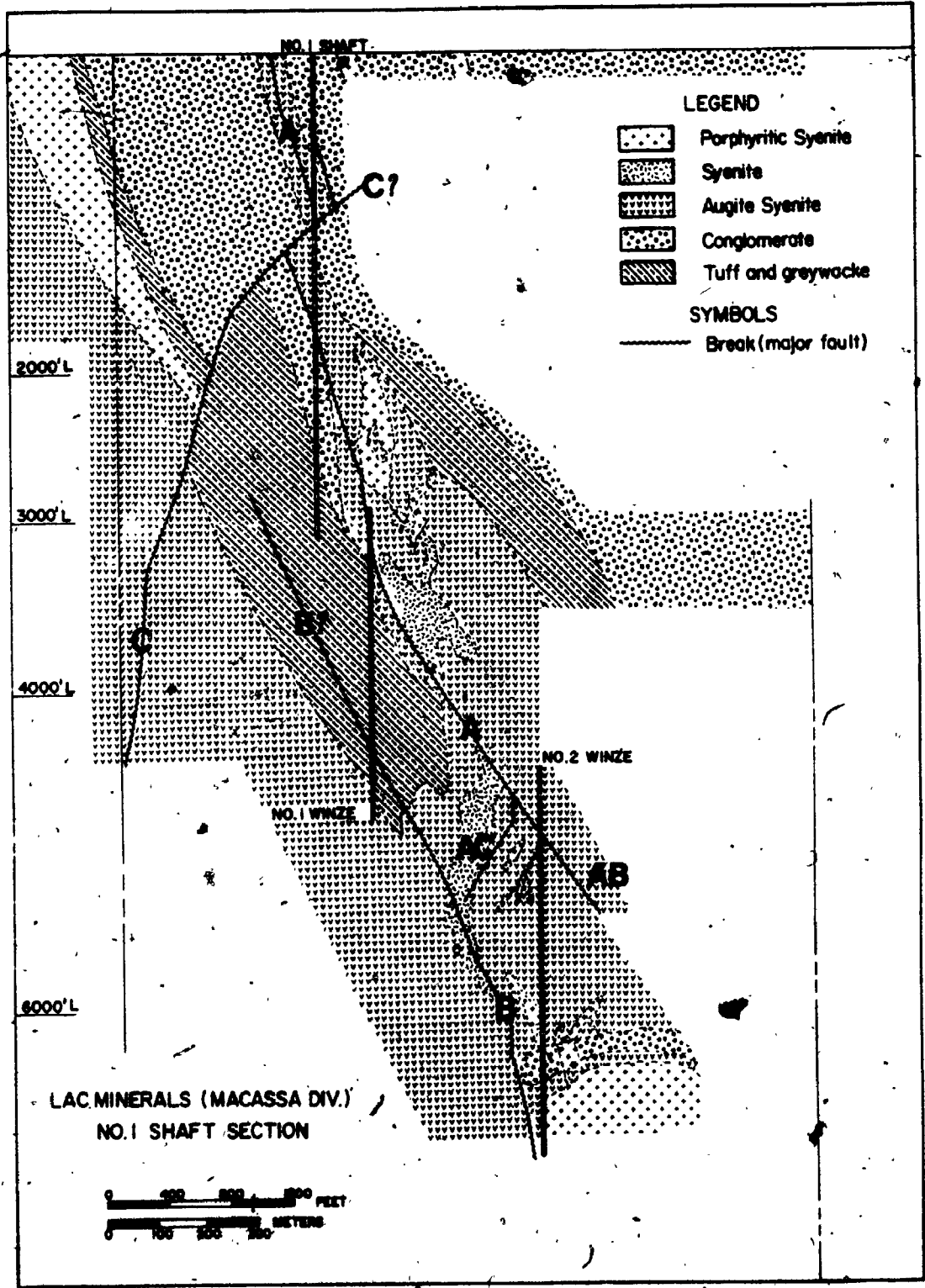
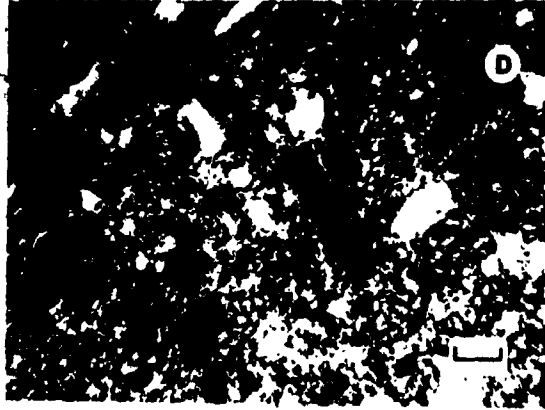
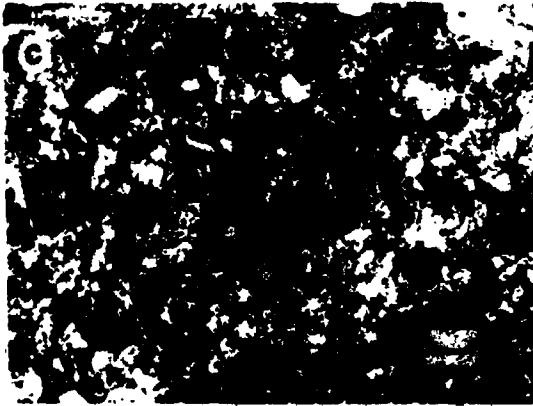
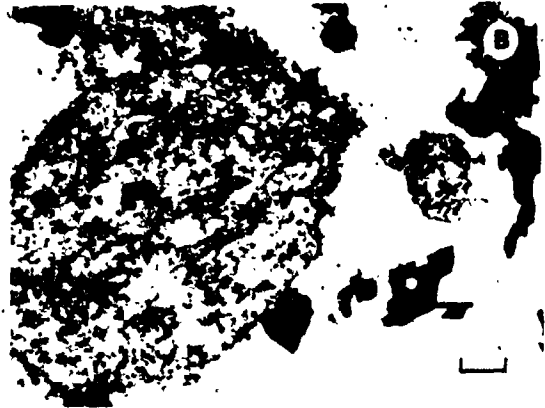


Plate 3-3. Syenites from the Macassa Mine.

- a. Photomicrograph of augite syenite with large subhedral to euhedral augite phenocrysts and smaller, darker laths of biotite in feldspar-rich matrix. Plane-polarized, transmitted light. Scale bar is approximately 1 mm.
- b. Detail of relict augite phenocryst in augite syenite now made up of secondary carbonate minerals, chlorite and minor subhedral magnetite (opaque). Plane-polarized, transmitted light. Scale bar is approximately 0.5 mm.
- c. Photomicrograph of massive (felsic) syenite with typical granitic texture and zoned orthoclase phenocryst. Plane-polarized, transmitted light. Scale bar is approximately 1 mm.
- d. Detail of massive (felsic) syenite with accessory apatite (grey euhedral lath, center of frame) and scattered, euhedral magnetite grains (opaque). Plane-polarized, transmitted light. Scale bar is approximately 0.1 mm.
- e. Polished hand sample of porphyritic syenite with typical plagioclase porphyrocrysts and large, anhedral xenolith at top of sample.
- f. Photomicrograph with typical porphyritic texture of zoned and twinned plagioclase phenocrysts in a fine feldspar matrix. Plane-polarized, transmitted light. Scale bar is approximately 1 mm.



and Moorhouse, 1969).

Syenite occurs primarily as a west pitching pipe-like mass which enters the Macassa mine from Kirkland Minerals property on the 1,300' level in the east. The rock has a granitic texture and is mostly orthoclase with 10% intergrown oligoclase (Plate 3-3c) (Table 3-1). Chlorite, Fe-Mg carbonate, leucoxene and sericite are pseudomorphous after biotite, augite and feldspar. Accessory minerals are apatite, magnetite and ilmenite (Plate 3-3d). In drill core and underground exposure, syenite may be transitional into augite syenite with increasing augite content or may have a sharp, well-defined intrusive contact. The relative age relationship between syenite and augite syenite is therefore ambiguous.

The main body of porphyritic syenite forms a central elongated plug that extends eastward 2.4 km from the Lake Shore Mine. To the west, in the Macassa Mine, porphyritic syenite occurs as dikes and small irregularly shaped sills which transect both syenite and augite syenite with well-defined intrusive contacts. The porphyritic syenite is therefore the youngest phase of the composite intrusive complex. This rock is red to grey in colour and distinctly porphyritic with plagioclase (Ab80-Ab95) as the dominant phenocryst (Table 3-1). Phenocrysts of orthoclase are rare but have been noted (Hawley, 1950). Biotite, hornblende and chlorite are the common ferromagnesian minerals.

Table 3-L. Representative microprobe analyses of Feldspars in Augite Syenite, Syenite and Porphyritic Syenite, Macassa Mine.

	1	2	3	4	5	6	7	8	9
SiO ₂	69.21	69.90	68.95	69.19	69.11	69.68	68.96	68.95	64.69
Al ₂ O ₃	19.44	19.40	18.95	19.04	19.27	19.23	19.15	19.36	17.79
CaO	0.10	0.04	0.11	0.11	0.07	0.09	0.07	0.07	0.00
Na ₂ O	11.72	11.63	11.26	11.25	11.80	11.65	11.62	11.85	0.19
K ₂ O	0.22	0.09	0.37	0.16	0.24	0.07	0.13	0.70	16.48
Total	100.69	101.06	99.64	99.75	100.49	100.72	99.93	100.43	99.15
Si	12.010	12.060	12.078	12.078	12.022	12.066	12.045	12.003	12.068
Al	3.795	3.944	3.912	3.920	3.950	3.924	3.942	3.971	3.911
Na	3.493	3.890	3.824	3.811	3.980	3.911	3.935	4.000	0.069
Ca	0.019	0.007	0.021	0.021	0.013	0.017	0.013	0.013	0.00
K	0.049	0.020	0.083	0.036	0.053	0.015	0.029	0.044	3.921
Total	19.366	19.921	19.918	19.866	20.018	19.996	19.964	20.031	19.969
Ab	98.32	99.31	97.37	98.55	98.36	99.18	98.94	98.58	1.72
An	0.46	0.19	0.53	0.53	0.32	0.42	0.33	0.32	0.00
Or	1.21	0.51	2.10	0.92	1.32	0.39	0.73	1.09	98.28
	10	11	12	13	14	15	16	17	18
SiO ₂	64.05	65.06	64.54	64.86	67.75	66.04	66.66	67.39	65.90
Al ₂ O ₃	18.29	18.14	18.54	18.11	19.76	19.63	21.12	20.13	20.75
CaO	0.02	0.00	0.05	0.83	0.44	0.95	2.30	1.17	2.26
Na ₂ O	0.29	0.29	1.21	0.89	7.83	8.03	9.93	10.38	9.66
K ₂ O	15.23	16.19	14.77	15.53	4.20	3.87	0.45	0.91	1.25
Total	98.88	99.68	99.11	100.22	100.48	98.52	100.46	99.98	99.82
Si	11.979	12.048	11.972	11.969	11.931	11.868	11.654	11.831	11.646
Al	4.031	3.958	4.052	3.938	4.100	4.157	4.351	4.164	4.321
Na	0.105	0.104	0.435	0.318	2.673	2.798	3.366	3.533	3.810
Ca	0.004	0.00	0.010	0.164	0.177	0.183	0.431	0.220	0.428
K	3.872	3.824	3.494	3.655	0.943	0.887	0.100	0.204	0.282
Total	19.991	19.934	19.963	20.089	19.824	19.893	19.902	19.952	19.987
Ab	2.64	2.65	11.05	7.70	70.46	72.34	86.37	89.29	82.34
An	0.10	0.00	0.25	2.97	4.67	4.73	11.06	5.56	10.65
Or	97.26	97.35	88.70	88.34	24.86	22.93	2.57	5.15	7.01

Analyses 1 - 8 albitic feldspar phenocrysts in augite syenite.

9 fine, mosaic orthoclase replacing phenocryst margin and in matrix of augite syenite.

10 - 13 orthoclase phenocrysts from syenite.

14 oligoclase margin on phenocryst 13.

15 oligoclase in matrix.

16 - 18 plagioclase phenocrysts from porphyritic syenite.

Accessories are apatite, magnetite, ilmenite, sphene and zircon. Primary quartz is rare to absent. The matrix is a fine aggregate of plagioclase. The porphyritic syenite commonly has scattered xenoliths which are from 0.5 to 10 centimetres in diameter (Plate 3-3e, f).

These xenoliths, diagnostic of porphyritic syenite in areas of very altered rocks, are typically angular to sub-rounded mafic rock fragments with chloritic selvages and may have been derived from the underlying pre-Timiskaming Group volcanic rocks. Some have a linear fabric suggesting a sedimentary or bedded pyroclastic source rock. In one unusual instance, a rounded granitic cobble was found to be included in porphyritic syenite immediately west of a major north-trending crossfault, the Amikougami Fault, on the 5725' level approximately 1.8 km west of the No. 1 shaft.

In addition to the three main phases of syenite, there is a nearly vertical diabase dike averaging 2.5 m wide and striking 165° approximately 325 m west of No. 1 shaft. This dike cross-cuts all other rock types and therefore, post-dates them. Two other narrow, sub-vertical diabase dikes have been noted immediately west of No. 2 winze on the lower levels.

3.3 Folding

Timiskaming Group rocks exposed underground and on surface at the Macassa Mine are generally south facing with

an average dip of 60° south. Detailed mapping of these rocks in long cross-cuts on the 3000' level both north and south of No. 1 Shaft showed only limited variations in dip (45° to 65° south), consistent top indicators (graded beds, load casts, cross-bedding) and unchanging strike direction.

Thomson (1950) and Thomson et al. (1950) described Timiskaming Group rocks throughout the Kirkland Lake area as a south-dipping homoclinal sequence. This was interpreted to represent the north limb of an east trending syncline, the south limb having been removed by reverse faulting along the Kirkland Lake-Larder Lake fault followed by erosion.

Although the major structural style of the Timiskaming Group rocks is homoclinal, several types of minor folds have been described in the former Kirkland Lake Gold and Lake Shore Mines (Thomson et al., 1950).

A zone of folded Timiskaming Group rocks is also known in the Macassa mine from mapping conducted during this study between the 4150' and 4500' levels, immediately south of No. 1 winze. Here, 0.5 m to 1 m thick beds of tuff are folded into a 25 m to 30 m wide, east-trending synform about an axis plunging 15° to 20° west. The central part of this synform is characterized by numerous carbonate-filled fractures and faults oriented subparallel to the axial plane of the fold, which cut the layered tuffs into a series of fault blocks. These blocks are progress-

ively down-faulted moving in from the fold limbs toward the central axis. The synform is bordered north and south by augite syenite.

It is most probable that this synform was created during the emplacement of the syenitic rocks as a result of drag along the north and south margins of the Timiskaming Group rocks and restricted foundering around the central axis. There is no evidence yet known from the Macassa mine or elsewhere in the Kirkland Lake area to support an interpretation of this synform as representing a distinct folding event.

3.4 Faulting and Fracturing

There are 2 groups of faults and fractures: pre-ore and post-ore. Detailed analysis of the various forms and patterns of faulting and fracturing within the Kirkland Lake camp are in Thomson et al. (1950) and Charlewood (1964).

Two differing interpretations of the Kirkland Lake Fault have been proposed previously. The first, detailed in Ward et al. (1948), describes one continuous, main-fault plane which crosses the entire Kirkland Lake mining camp. All other faults and fractures are considered subsidiary to this main structure. This interpretation did not account for areas within all of the mines where the structure defined as the main fault would dwindle into a series of

weak fractures and slips along strike and down dip making positive identification of any single branch as the "Main Break" impossible. This objection was raised by Thomson et al. (1950) citing specifically evidence from underground exposure at the Lake Shore Mine.

A second interpretation regards the Kirkland Lake Fault as a complex system of discontinuous, interconnecting faults and fractures having prominent branches which can be traced over varying distances. In the west part of the Kirkland Lake district the system is generally a single or double fault plane with local anastomosing and parallel slips. To the east it becomes more complicated as the fault system tends to subdivide into more and more branches, each with less displacement and the number of post- or cross-faults increases particularly east of the Lake Shore Fault.

The latter concept of the Kirkland Lake Fault system best accounts for the structural complexity at the Macassa Mine. In the following synopsis, adapted from Nemcsok (1980), the term "break" is intended to mean an anastomosing network of chlorite-filled faults, slips and brecciated seams up to 5 m wide.

3.4.1 Pre-Ore Faulting

The Kirkland Lake Fault system, or Main Break, traverses the entire length, 3.2 km, of the Macassa proper-

ty (Fig. 3-3). Thomson (1950) has noted the relatively insignificant appearance of this structure on surface. A branch of the Main Break is exposed near the rear of the Macassa Mine office building where there is a shallow, drift-filled depression about 1 foot wide along the contact between augite syenite and Timiskaming conglomerate. Underground, the Main Break is generally a zone of mylonitized and sometimes brecciated wallrock, chloritic schist and mud or gouge. There is a vertical displacement of approximately 1,500' (450 m) in the west end of the Macassa Mine (Thomson et al., 1950) with the south (hanging wall) side up in relation to the north (footwall).

The strike of the Main Break averages 065° and dips 80° south to above the 3475' level where it has a gradual flattening in dip to about 50° . The deeper levels of the mine have a branching fault system with an open split to the west below the 4,125' level, forming a north and south branch to the Main Break. The south branch has a slightly flatter dip and is considerably south of the mine workings. It has been tested by diamond drilling to about the 5,300' level and is not known to be ore bearing below the 4,750' level. The north branch is productive in the west part of the mine to the bottom of the present workings (6,450' level).

Another fault of major importance, known as the '04 Break, is subparallel to the Main Break. The '04 is con-

nected to the north branch of the Main Break via the S, R-2 and E Breaks (Fig. 3-5). Striking about 060° and dipping 70° - 80° south, the '04 Break has been explored from the 4,500' level to the 6,500' level. Over the past 25 years, the '04 Break and its branches have been the main source of ore for the Macassa Mine.

Near the west end of the mine, commencing just west of the post-ore Tegren Cross fault, there are two faults. One is called the '04 Break, although direct evidence is lacking that this is indeed the faulted extension of the '04 Break to the east, and the other to the south is called the South Break. The South Break is the more important of these two and has been traced from just above the 5,025' level down to the 5,725' level where it appears to recombine with the '04 Break. The Crossover Fault splits off the '04 Break at the low angle, just west of the Tegren Crossfault and crosses over to the South Break.

North and south of the Main Break there are other more or less parallel faults (Fig. 3-3). A strong, north-dipping fault is known approximately 375 m north of No. 1 Shaft on the 3000' level at Macassa (Fig. 3-4). This structure has been previously called the Narrows Break at Macassa but recent investigation conducted by this writer and mine geologists suggests it does not correlate with the fault described as the Narrows Break in Thomson et al. (1950) which is further north of the Main Break. ~~Map~~

Figure 3-5. Structural plan of the 4250' level, Macassa Mine with relationships between the '04 and Main Breaks, and other major pre-ore faults and post-ore crossfaults. Compiled from mine records.

of No. 1 Shaft conducted during this study has shown that the Main Break has been shifted between the 750' and 1700' levels by several north-dipping faults which are interpreted to be the up dip extension of this north (Narrows?) break.

South of the Main Break, the Amalgamated Kirkland Mud Break and the Kirkland Lake Larder Lake Fault Zone are the most prominent structures (Fig. 3-3).

3.4.2 Post-Ore Faulting

Major north-striking faults displace both sedimentary and volcanic rocks, along with pre-ore structures described above. Four major post-ore faults of the Macassa Mine are: The Q Fault, the Boundary Fault, the Tegen Crossfault system and the Amikougami Crossfault (Fig. 3-5).

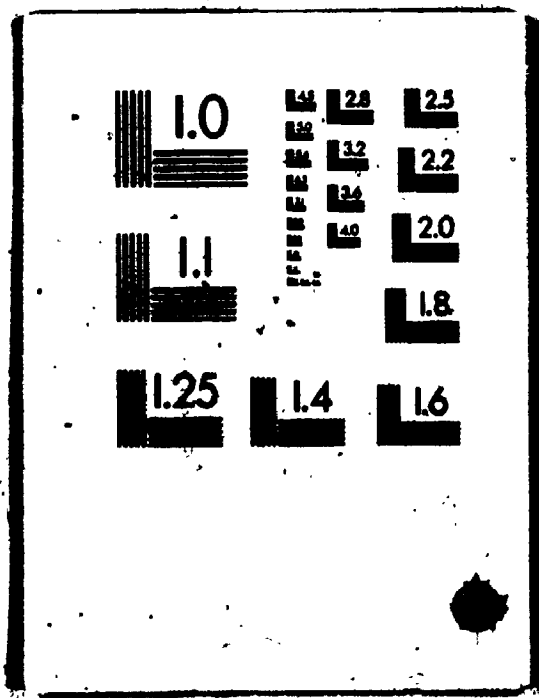
The Q Fault is a brecciated, chlorite-filled fault generally 0.2 m to 0.4 m wide located approximately 300 m west of No. 1 Shaft. It has a strike direction of 035° to 040° and dips steeply (85°) to the east. The structure has been traced in underground workings between the 2475' and 6000' levels. The Q Fault is known to transect the R- and S-Breaks and is suspected to cut the Main Break although clear evidence is lacking underground. The chloritic gouge typically contains angular fragments of altered wallrock and discontinuous lenses of distinctive pink coloured carbonate minerals and lenses of white quartz. The wall-

rocks are slightly red coloured up to 1 meter away from this fault.

The Boundary Fault is a narrow, brecciated fault striking due north and dipping 75° west near the west end of the original Macassa property boundary approximately 0.65 km from No. 1 Shaft. This fault has been traced underground between the 4250' and 5025' levels. Wallrock alteration is typically weak to absent. The fault contains minor amounts of carbonate minerals and no quartz. Movement on the Boundary Fault is unknown as most of the upper levels in the Macassa workings are no longer accessible.

The Tegen Crossfault system is composed of two or three branching, sub-parallel fault segments approximately 1.1 km west of No. 1 shaft. These segments strike approximately 016° and dip 75° to 85° east. The Tegen system has been traced from surface to the lowest levels in the Macassa underground workings. A major branch of the Tegen system was found to transect No. 3 Shaft between 73 and 85 metres below surface during mapping by this writer and mine geologists. The fault segments are strong and brecciated and are typically 0.3 m to 1.2 m wide. The fault gouge has abundant chlorite with many discontinuous lenses of bright pink-coloured carbonate minerals and patches of white quartz. Fault segments are typically surrounded by a red alteration halo which extends from 1 to 2 meters into surrounding wallrocks. As there are no definitive marker

2



horizons which can be correlated across this fault system, only the relative displacement of ore segments immediately adjoining can be used to indicate the sense of movement. There is an approximate displacement of 90 m vertical (west side up) and 60 to 75 m horizontal (west side south).

The Amikougami Crossfault is a normal fault at the extreme west end of the Macassa Mine approximately 1.85 km west of No. 1 Shaft. It strikes approximately 165° and dips 85° east. The structure has been traced from surface to below the 5725' level. It is a more prominent fault than those described above, having well-developed shearing and fracturing of immediately adjacent wallrocks, and a distinct chloritic mud gouge. The main fault is approximately 2.0 meter wide. There are eight associated sub-parallel faults and fractures up to 35 m east of this main fault. The Amikougami Crossfault has a red alteration halo extending up to 1.5 m into the wallrocks similar to the Tegren system. However, in contrast to the Tegren system, the Amikougami Crossfault has little or no carbonate and quartz entrained within the fault gouge. A diabase dike has apparently been emplaced along this fault as discontinuous lengths of it have been found within and on the west side of the fault on the 5725' level. Movement on the Amikougami Crossfault is not known to be present as there is only one opening into the structure on the 5725' level but slickensides observed by the writer on the hanging wall

plunge 10° north indicating a subvertical component of translation.

In addition to these major, post-ore crossfaults there are several post-ore strike faults in the Macassa property which have separated different mineralized zones. There is also evidence of post-ore strike movement on major faults like the Main and '04 Breaks. Thomson et al. (1950) characterize post-ore strike faults in some mines adjacent to Macassa as containing late barren quartz, calcite and occasionally barite and gypsum. Isolated lengths of the '04 Break at Macassa have a fault gouge of large masses of semi-transparent selenite crystals up to 4 cm wide and massive, dark green chlorite. This unusual mineral combination is interpreted as a disequilibrium assemblage superimposed upon the pre-existing sericite, pyrite, carbonate-mineral and chlorite fault-filling.

3.4.3 Fracturing

All of the major faults and breaks described previously have associated subsidiary fractures. Many of these fractures are tensional structures created during fault movement. On the upper levels, subsidiary fractures branch off the Main Break both vertically and horizontally. Most are on the south side or hanging wall of the Main Break. Hanging wall fractures generally parallel the strike and have dips 10° to 20° flatter than the main fault. They

typically refract in toward the main fault going up dip on section and going west on plan. These fractures were probably produced as the south side of the fault system was thrust upward over the north side. In areas where there is a pronounced change in dip or a roll in the main structure, as on the Main Break around the 3475' level, there is a tendency for fractures to branch off the crest of the deflection on the main fault. These fractures are generally more steeply dipping and make contact down dip with the main fault plane.

On lower levels, in the east part of the mine another favourable location for tension fractures is in the wedge-shaped block of ground between the '04 and Main Breaks. Here, these fractures typically extend between the major faults with relatively shallow dips to the north but in some instances do not connect directly with the bounding faults (Fig. 3-6).

A unique set of fractures was noted by the writer in an antiformal structure on the 4250' level. Here the fractures, now represented by the 42-S-2 vein, are curved into a crude semi-circle on plan (Fig. 3-7) about an antiformal axis plunging 026° southeast. A similar antiformal vein-fracture was described on the 4450' level in the former Kirkland Minerals mine (Thomson et al., 1950) where fractures are curved or horseshoe-shaped on plan and conform with enclosing rocks in strike and dip. Although

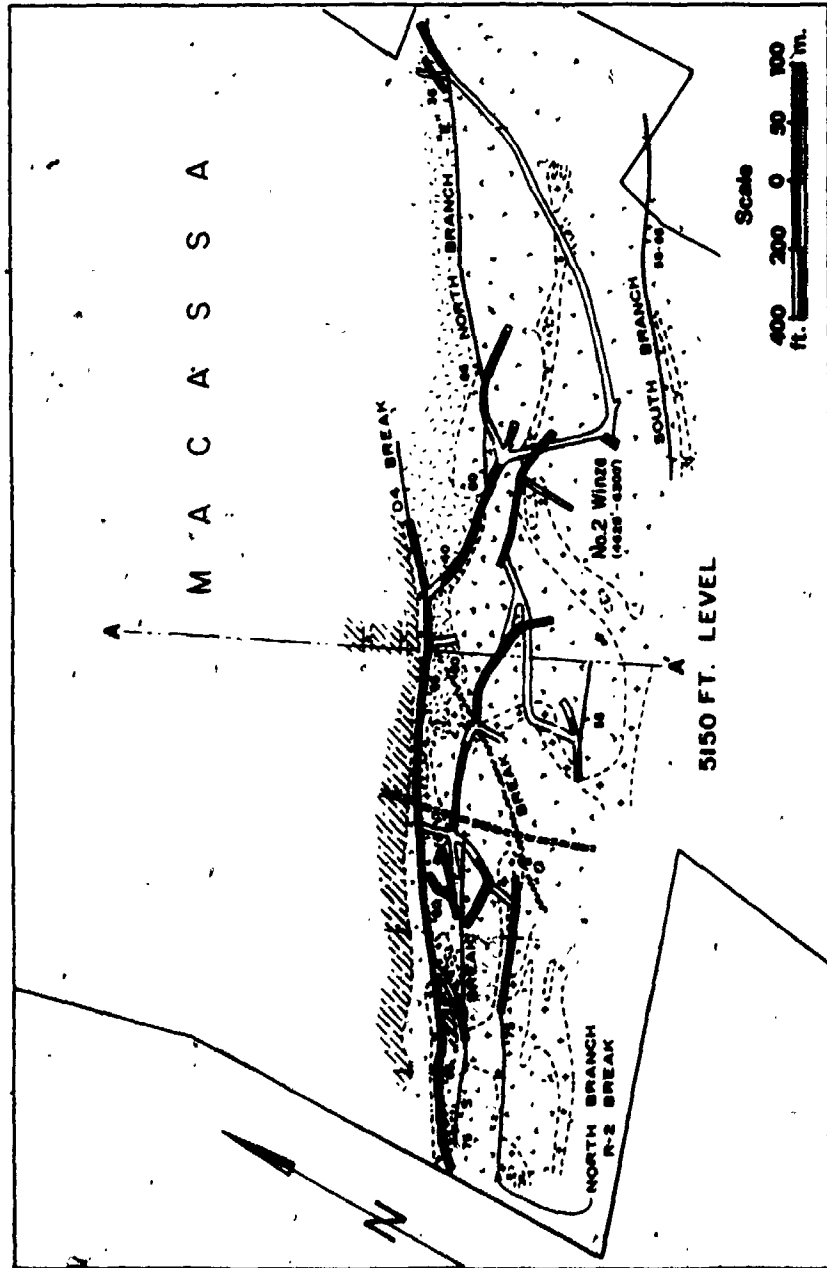
Figure 3-6. a) Geologic plan of the 5150' level, Macassa Mine, with relationship between '04 and Main Breaks, S and R-2 Breaks and location of section A-A' (from Charlewood, 1964).

LEGEND

	Porphyritic Syenite
	Syenite
	Augite syenite
	Conglomerate and greywacke
	Tuff

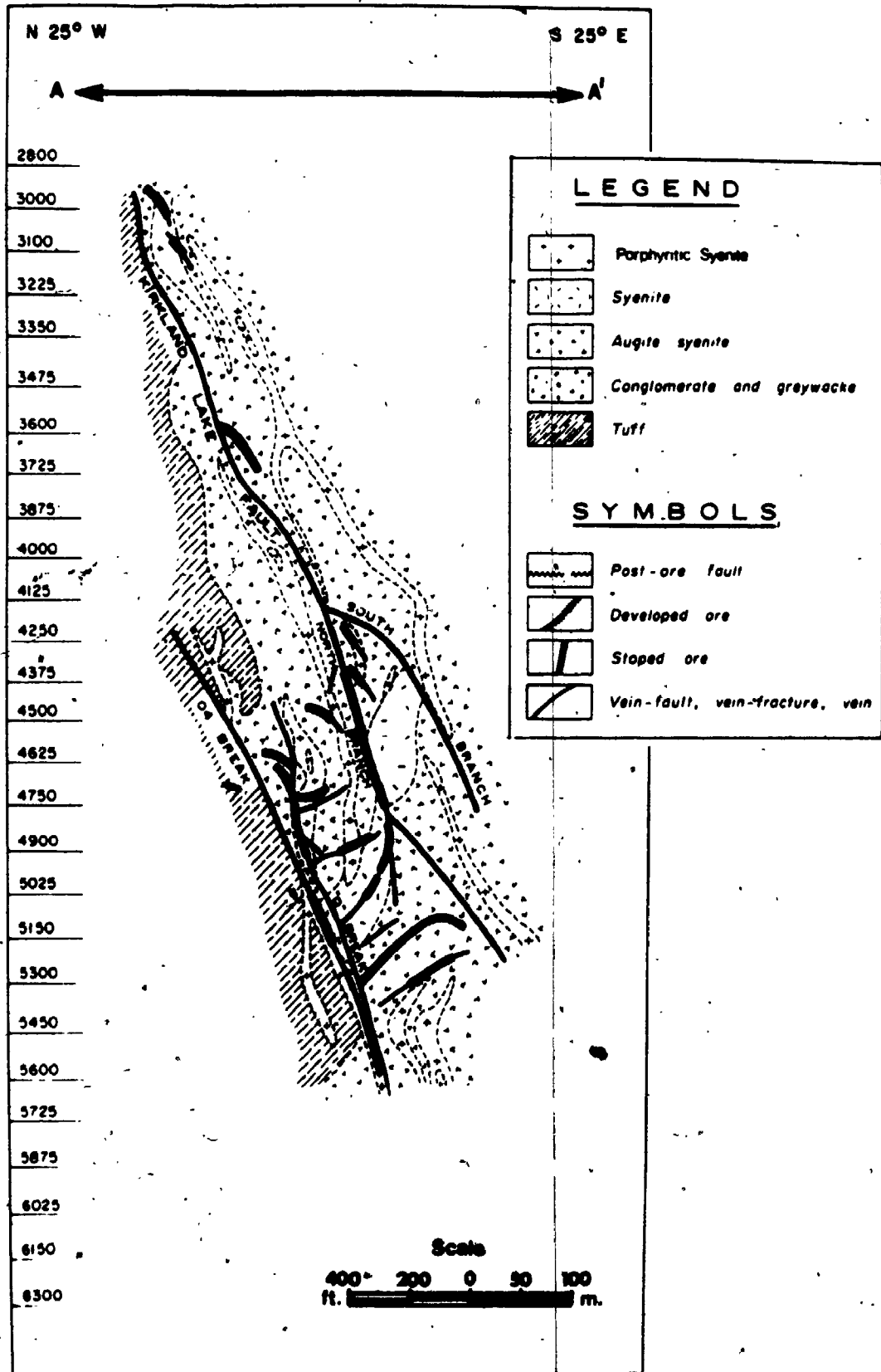
SYMBOLS

	Post-ore fault
	Developed ore
	Stopped ore
	Vein-fault, vein-fracture, vein



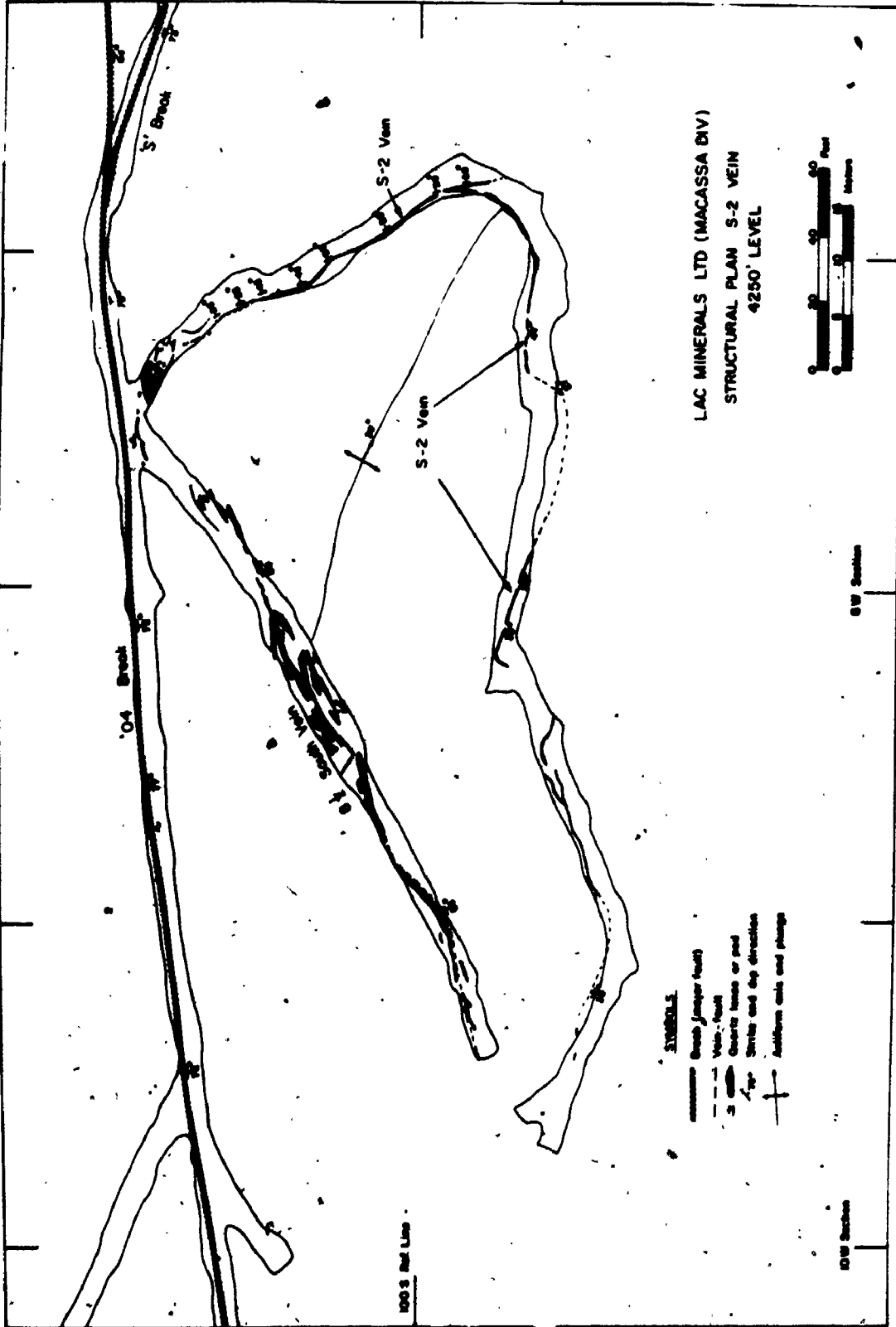
18

Figure 3-6. b) Geologic section along A-A' (Figure 3-6a) with fracture pattern between the Main Break and '04 Break (from Charlewood, 1964).



00

Figure 3-7. Structural plan of the 42-S-2 antiformal vein on 4250' level, Macassa Mine.



the 42-S-2 vein-fracture system has a similar shape it transects syenitic intrusive rocks and layered Timiskaming Group tuffs and does not conform in any way with bedding attitudes in the latter. These curvilinear planes may be the result of the deflection of fractures as they propagated through rocks of differing competency. Alternatively, they may have resulted from a compensational destressing of rocks adjacent to dilatent zones associated with major fault zones in a manner analagous to the spalling off of curved slabs of roof and wall rocks in tunnel excavations.

There is some evidence from old mining records at Macassa that this phenomenon of veins following curvilinear fracture sets is more widespread than appreciated at present. Some of the vein systems described in the following sections may represent corresponding "limbs" of large scale antiformal and synformal structures. It is stressed, however, that there is no evidence yet known to suggest that any of the fault and fracture systems in the Macassa mine or in any other area of Kirkland Lake have been folded.

3.5 Gold Occurrence at Macassa

3.5.1 Mineralogy

The ores of the Kirkland Lake mines have proven to be uniform in mineral content both vertically and laterally and are characterized by exceptionally fine-grained metal-

lic species seldom exceeding one millimeter in diameter. Although the bulk composition is somewhat governed by the wall-rock types and the percentage dilution during mining, silica content from all sources averages 50 to 60 percent, but iron, calcium and magnesium carbonate minerals account for 15 to 20 percent. The remainder is provided by aluminium silicates in the form of feldspar, mica, hornblende and chlorite (Hawley, 1950).

All known metallic (21) and non-metallic (13) minerals identified to 1950 appear in Table 3-2. Within the first group, magnetite-ilmenite, pyrite, molybdenite, telluride minerals and native gold make up the most important species. Magnetite-ilmenite grains, observed in thin section samples as graphically intergrown, primary constituents of all phases of syenite from the Macassa Mine, are generally replaced by pyrite to varying degrees. Pyrite, the most abundant sulphide mineral, comprises less than 2 percent of the ore, and occurs as exceptionally fine grains ranging from 0.001 mm to less than 0.5 mm. It was observed in thin sections of wall-rock adjacent to the ores or in wallrock inclusions, more rarely within microfractures and intergranular boundaries of gold-bearing quartz. Extremely fine-grained inclusions of gangue, carbonate minerals, gold, chalcopyrite, and altaite suggest contemporaneous deposition or replacement of pyrite by these species. The gold was not found to be restrict-

Table 3-2
Minerals of the Kirkland Lake Ores*

METALLICS

<u>Type</u>	<u>Mode of Occurrence</u>	<u>Mineral</u>	<u>Remarks</u>
MAGMATIC.....		Magnetite-ilmenite	In graphic inter-growths; primary constituents of syenites and porphyry
HYDROTHERMAL.	Elements..	Gold.....	Alloyed with minor silver
		Graphite.....	Minor
	Oxides....	Specular hematite.....	
		Red dusty hematite.....	
		Magnetite.....	Rare
	Tellurides.	Altaite, PbTe.	
		Calaverite, AuTe ₂ .	
		Coloradoite, HgTe.	
		Melonite, NiTe ₂	Rare
		Betzite, (Ag,Au) ₂ Te.....	Ag: Au=3:1
Sulphides...	Tetradymite, Bi ₂ Te ₂ S.....	Locality unknown	
	Joseite, Bi ₃ TeS.....	Locality unknown	
	Pyrite.		
	Arsenopyrite.....	Very rare	
	Chalcopyrite.		
	Pyrrhotite.....	Very rare	
	Molybdenite.		
	Sphalerite.....	Very rare	
	Galena.....	Very rare	

NON-METALLICS

<u>Occurrence</u>	<u>Mineral</u>	<u>Remarks</u>
IN VEINS	Quartz.	
	Albite.....	Very rare
	Ferruginous dolomites....	Of variable iron content
	Calcite.	
	Barite.	
	Celestite.....	Rare
	Gypsum.....	Rare
	Sericite.	
	Chlorite.	
	IN ALTERED WALL ROCKS....	Tourmaline.....
Biotite.		
Sericite.		
Carbonates.		
Chlorite.		

*After Hawley, 1950.

ed or related to any particular generation of pyrite. Molybdenite, though making up only a fraction of one per cent of the ores is widespread throughout all Macassa Mine workings. Much of it is closely associated with gold and telluride minerals. It was observed in thin section and hand specimen as bluish-black coatings along slip planes in quartz or wallrocks. Seven species of telluride minerals are listed in Table 3-2. The two gold-bearing species calaverite and petzite accounted for 17 to 19 percent of the ore at Lakeshore Mine (Thompson, 1950) and locally for as much as 61 percent on the 12th level of the Teck-Hughes (Todd, 1928).

The two most commonly observed telluride minerals at the Macassa Mine are altaite ($PbTe$) and calaverite ($AuTe_2$).

Altaite was the most abundant telluride mineral identified in hand specimen and thin section samples of gold ore at the Macassa Mine. It was observed as disseminations and irregular blebs 0.01 to 0.1 mm wide and as coarse bands 1 to 2 cm wide. On fresh surfaces in hand specimen, altaite is pale yellow in colour and a bright, blue-white colour in polished thin section. Some hand specimens contained a bright, blue-coloured mineral which was tentatively identified as coloradoite ($HgTe$), a telluride mineral which was found only infrequently at Macassa. However, X-ray diffraction study showed the mineral to be altaite with an uncharacteristic blue tarnish. Calaverite,

the next most abundant telluride mineral at Macassa, typically occurred intergrown with and as inclusions in altaite.

Native gold which is the form taken by much of the precious metal, occurs in a variety of habits, all of which suggest that it may have replaced or filled fractures in many of the earlier formed minerals. Commonly, native gold as fine veinlets, inclusions and rims is intimately associated with the base metal telluride minerals colbradoite and altaite. Repeated opening and closing of the tension and shear fractures forming simultaneously with the deposition of minerals may be the principal reasons for replacement and fracture-filling of older grains by later ones (Hawley, 1950).

3.5.2 Wallrock Alteration

Gold in the Kirkland Lake district is in the pre-ore fault and fracture systems described in the preceding sections. The structures are more continuous than the gold concentrations. Host rocks to the gold occurrences may be any of the types known to underlie the Kirkland Lake district except for the late diabase dikes. Wallrock adjacent to gold concentrations are generally altered, but the altered rocks do not in themselves contain sufficient gold to be classified as ore. They do however provide a practical guide to ore in areas of inconsistent or dissi-

pating fractures. Wallrock alteration is the result of two processes: 1) the mechanical disruption of rocks adjacent to major structures during fault movement, and 2) chemical and mineralogical changes in wallrocks through which fluids flowed.

Massive and crystalline rocks adjacent to major faults and some gold-bearing veins have been changed to a banded, brecciated and streaky rock (Thomson et al., 1950). The degree of mechanical alteration is directly related to the amount of movement on each structure. Wallrock near major faults are first cracked and sheared subparallel to the fault, then undergo progressive transgranular fracturing (Plate 3-4a, b). These effects are preserved at both the macro- and microscopic scales depending on proximity to the plane of movement (Plate 3-4c, d). Wallrock adjacent to simple, dilatant fractures have little or no mechanical alteration.

The alteration mineral assemblage in wallrock to ore consists of chlorite, sericite and leucoxene along fractures subparallel to the main fracture. Secondary Ca-, Fe-, and Mg-carbonate minerals occupy primary ferromagnesian minerals, pyrite is after magnetite and sericite after plagioclase feldspar (Plate 3-5). A more detailed account of the progressive mineral changes has been provided by Hawley (1950). The chemical effect of wallrock alteration will be discussed in detail in a following

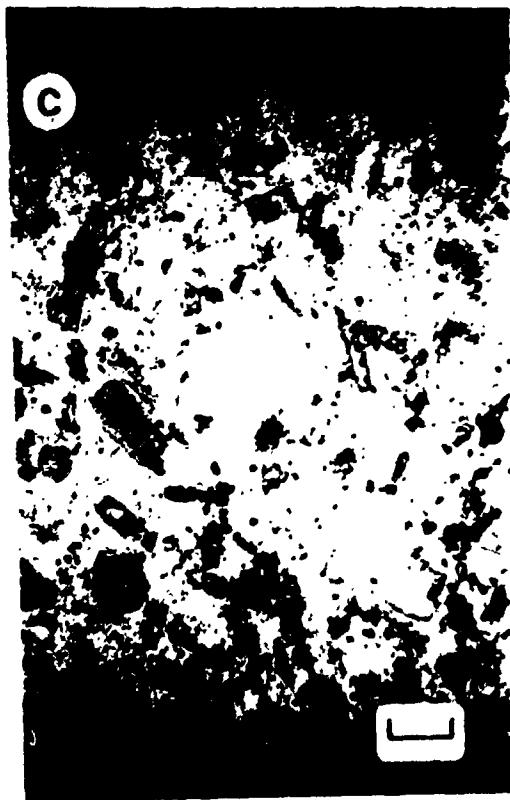
Plate 3-4. Mechanical alteration of wallrocks at the Macassa Mine.

- a. Detail of chloritic, schistose wallrock immediately adjacent to a major fault marked by a central core of chloritic gouge. North Break (Narrows?), 3000' level, Macassa Mine.
- b. Polished sample of diamond drill core with subangular wallrock fragments incorporated into fine-grained fault gouge, Main Break, Macassa Mine.
- c. Photomicrograph illustrating progressive fracturing, shearing of wallrock immediately adjacent to a fault (light areas in lower half of photo). Note also cataclastic gouge (dark) with small rounded quartz clasts and disaggregated wallrock inclusions. Plane-polarized, transmitted light. Scale bar is approximately 1 mm.
- d. Photomicrograph of small and large wallrock fragments (light) in granular matrix of pulverized rock immediately adjacent to a fault margin (not shown). Plane-polarized, transmitted light. Scale bar is approximately 0.5 mm.



Plate 3-5. Mineral changes during wallrock alteration at the Macassa Mine.

- a. Photomicrograph of altered augite syenite with replacement of primary augite phenocrysts by secondary Ca-, Fe-, and Mg-carbonate minerals and the development of opaque minerals around crystal margins and along fracture planes. Plane-polarized, transmitted light. Scale bar is approximately 1 mm.
- b. Photomicrograph of incomplete replacement of magnetite (centre) by pyrite (rim). Plane-polarized, reflected light. Scale bar is approximately 0.1 mm.
- c. Photomicrograph of altered porphyritic syenite with remnant outlines of plagioclase phenocrysts completely occupied by sericite. Plane-polarized, transmitted light. Scale bar is approximately 1 mm.
- d. Photomicrograph of altered syenite with incomplete alteration of biotite to chlorite along cleavage planes. Cross-polarized, transmitted light. Scale bar is approximately 0.1 mm.



section.

The net result of alteration processes is the production of fine-grained, discoloured rocks adjacent to ore zones associated with strong faults. These altered rocks are variously reddish, pale green, bleached and siliceous depending on the original wallrock type and degree of alteration. Wallrocks adjacent to ore unrelated to prominent faults are commonly bleached and siliceous but with original granitoid textures.

3.5.3 Types of Gold Occurrences

There are three types of gold occurrences: 1) native Au in chloritic fault gouge or quartz lenses within sections of the major fault system i.e. the Main Break and '04 Break; 2) gold-bearing quartz veins in both hanging and footwalls of this fault system and 3) several relatively wide, up to 15 m areas in the deep western areas of the mine of very fractured, bleached rock containing lenses and pods of quartz with native Au and tellurides. These types are known as break-ore, vein-ore and breccia-ore respectively.

3.5.3.1 Break Ore

Irregular and discontinuous lengths of major branches of the various faults have been mined for gold at Macassa. Gold commonly occurs associated with erratic lenses of grey

and white quartz within the fault gouge or sheared and fractured rock bordering the fault (Plate 3-6). Occasionally, native gold occurs within the chloritic gouge itself with no quartz present. However, such instances are exceptions to an apparent relationship between large concentrations of gold and lenses of well-fractured quartz. These lenses and masses of quartz are on either or both of the hanging wall and footwall margins of these major faults and appear to have been deposited along the faults as opposed to being incorporated from other areas during fault movement.

Main Break

Gold has been mined from the Main Break system between the 1100' and 4500' levels from 41E section to 10E section. These areas provided most of the ore milled from the mine during the first 20 years of operation. Grades were typically 8.6 to 12.0 grams Au per tonne. Ore shoots have a maximum strike length of 200 m and widths of 2.5 to 3.0 m. Wallrock alteration associated with ore along the Main Break is characterized by a bleached halo extending from 2 m to 8 m away from the fault contact with patchy zones of red alteration.

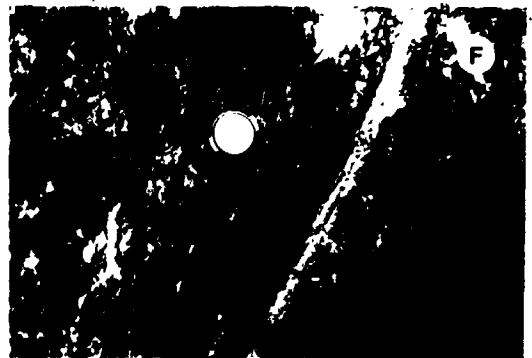
'04 Break

The '04 Break system has been mined for gold in areas

Plate 3-6. Break ore in the Macassa Mine.

- a. North Break (Narrows?) in the Casakirk, cross-cut, 3000' level, Macassa Mine with relatively wide band of sheared and altered rock (center) with quartz-and carbonate mineral-filled subsidiary fractures in wallrock. Scale bar is approximately 0.5 m.
- b. Section of the Main Break on east end of 5250' level, Macassa Mine, with narrow, chlorite-filled fault gouge surrounded by very fractured and altered wallrocks. Scale bar is approximately 0.5 m.
- c. Detail of massive quartz lens within chlorite-filled section of North Break (Narrows?), 3000' level, Macassa Mine. Scale bar is approximately 0.25 m.
- d. Wide section of massive, very fractured quartz on south margin of the 04 Break, 5300' level, Macassa Mine.
- e. View of east portion of the North Break (Narrows?), 3000' level, Macassa Mine, with subparallel, mud-filled fault (480) adjacent to the main fault branch (770) and scattered lenses of quartz in wallrocks.
- f. Detail of 3-4a showing mud-filled fracture in very schistose chloritic wallrock.

—



bounded laterally by 16E and 48W mine section lines and between the 4300' and 6400' levels. Generally the grade has been 15 grams Au per tonne although some areas are significantly richer. The Central Pillar area between 0 and 3E sections and 4600' and 5000' levels has continuous ore of up to 26 grams Au per tonne. Gold along the '04 Break is more continuous than the Main Break system, with maximum strike length of over 400 m. Mining widths are 7 m to 8 m. Commonly, the only metallic minerals present are abundant pyrite with lesser amounts of fine, native gold, although some telluride minerals, notably altaite, have been identified. Wallrocks are typically red coloured up to 0.75 m from the fault grading outward to minor bleaching in hanging wall rocks.

R-2 Break

Gold on the R-2 Break is between the 4600' and 5800' levels from 6E to 7W sections. Ore lengths are not continuous and have widths varying from 0.3 to 1.3 m. Average grade for ore along the R-2 Break is 14 grams Au per tonne. Alteration associated with this R-2 Break is a distinctly red halo extending from 1.5 to 3 m into adjacent wallrock.

South Break

Ore shoots on the South Break are in scattered lenses.

of fractured quartz on the footwall of the structure from the Tegren Crossfault system and 40W section line between the 5025' and 5700' levels. Gold concentrations are generally narrow, up to 0.75 m wide, and have an average gold content of 17 grams Au per tonne. Gold occurs as fine native metal and in the Au-telluride calaverite (AuTe_2). Wallrock changes from light red in the lower parts of the South Break, near the 5700' level, to bleaching near the upper parts.

S- and E-Breaks

These are less important structures than those already described in that gold-bearing zones only occur in association with the coincidence of either hanging wall or footwall veins. Gold content is generally minor, less than 10 grams Au per tonne, and wallrock alteration is similar to that described for the R-2 occurrence.

3.5.3.2 Vein Ore

Gold is in quartz-filled fractures occupying the pre-ore fractures described previously. This is vein ore and is in both the hanging and footwalls of the major faults. The Main Break in the east section of the mine has relatively more subsidiary veins associated with it than the '04 Break to the west. Vein-ore occurs as single, well-defined quartz filled fractures from 5 cm to 0.5 m

wide (Plate 3-7a) to intricately connected composite veins or lodes, sheeted zones, stockworks and vein breccias up to 10 m wide (Thomson, 1950). This change from relatively narrow, simple veins to wide, complex zones typically reflects increasing proximity to major faults (Plate 3-7b, c). Vein-ore consists of several different generations of quartz, wallrock fragments, some Mg-Fe carbonate and calcite, 2 to 3% disseminated sulphide minerals (chiefly, pyrite), precious and base metal tellurides and fine native gold (Plate 3-7d, e). Sericite and chlorite occur in the ore and wallrocks. Molybdenite with or without graphite is confined to slips in fractured vein quartz. Gold appears commonly in fractures in vein quartz perpendicular to the vein contacts (Plate 3-7f). Telluride minerals are typically in narrow bands parallel to and along the outer edges of veins or as disseminations in the vein-quartz and carbonate minerals. The most common telluride minerals are altaite (PbTe) and calaverite (AuTe₂).

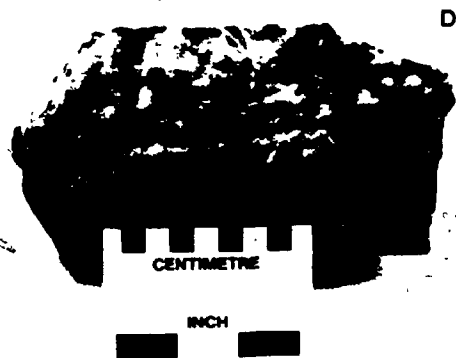
Some of the vein-ore in the east part of the mine has distinctive mineral associations.

Hanging Wall Vein Ore - South Dipping

A series of quartz-filled fractures dipping 35° to 75° south in the hanging wall of the Main Break are termed the 'G-' and 'H-' Vein systems. These veins found between the 1500' and 3100' levels of the mine from 25E to 40E

Plate 3-7. Vein ore in the Macassa Mine.

- a. Example of simple, quartz-filled fracture. Section of 'A'-vein system on 5025' level, Macassa Mine.
- b. Faulted section of 'A'-vein system on 5025' level near No. 2 winze, Macassa Mine. Scale bar is approximately 0.5 m.
- c. Irregular lenses and pods of vein-quartz adjacent to the North Break (Narrows?), 3000' level, Macassa Mine. Scale bar is approximately 0.25 m.
- d. Polished hand sample of 26-6 vein with wallrock inclusions and altered syenite wallrock.
- e. Polished hand sample of 58-E vein showing subrounded inclusions of early quartz (vein center) caught up in massive lense of latter quartz.
- f. Hand specimen of 'X'-vein from 5450' level, Macassa Mine, with small leaf of native gold (right, rear of specimen) protruding above the surface of the sample in fracture perpendicular to vein margin.



sections, curl into the Main Break up dip and merge with the Main Break at a shallow angle to the west. They vary in width from 5 cm to 0.75 m, commonly contain visible gold and tellurides and have average gold content of over 15 grams Au per tonne. Particularly large concentrations of gold occur near the top of these vein sets as they curl into the Main Break. Wallrocks are typically red for 0.3 m to 1 m beyond vein margins.

The 'G'- and 'H'-Vein systems are continuous with the Nos. 5 and 6 Vein systems from sections 20E to 30E between the 2100' and 3300' levels. These dip steeply about 75° south and strike subparallel to the Main Break. The Nos. 5 and 6-Vein systems are 1 cm to 0.75 m wide and contain in hand specimen a varied mineral assemblage including minor amounts of galena, chalcopyrite, specularite and fluorite in addition to native gold and telluride minerals in a quartz gangue. Pyrite content of both the veins and reddish wallrocks is approximately 2% to 3%. Gold content of these vein sets is usually greater than 17 grams Au per tonne.

The 'P'-vein is also in the hanging wall of the Main Break between the 3600' and 3700' levels from 7E to 10E sections. It dips south 45° to 50°, is 5 cm to 45 cm wide and has a relatively large gold content of 26 to 34 grams Au per tonne. The 'P'-vein is distinct from the 'P'-vein system which is in the hanging wall of the R-Break. The

'P' system is between the 4125' and 4600' levels from 10E to 0 sections. These veins have an average width of 15 cm to 65 cm and an average gold content of 12 to 15 grams Au per tonne.

The 'X'-vein system extends 50 m to 80 m into the hanging wall of the '04 Break from the 5400' level to below the 6000' level between 15W and 23W sections. These veins are 2.5 cm to 30 cm wide, contain approximately 20 grams Au per tonne in scattered patches of visible native gold and more abundant telluride minerals.

Many of the individual veins and vein sets described above narrow to a tight fracture or slip in the host rock down dip. At such terminations there is no precious or gangue minerals remaining in the fracture which has a restricted, altered and often pyrite-bearing selvage.

Hanging Wall Vein Ore - North Dipping

Some of the vein-ore in the east part of the mine has distinctive mineral associations. The 'E'-vein system, a set of vertical to north-dipping quartz veins in the hanging wall of the Main Break near the Kirkland Minerals property has actinolite, Ca-garnets, Mg-Fe carbonate, epidote and calcite as both vein-filling and within surrounding wallrocks. This vein set also has minor amounts of scheelite, <5%, in addition to gold. Another vein set with distinctive mineral association is the 50-04

east quartz-magnetite-chlorite vein on the 5000' level of the mine. This set has moderate amounts of narrow native gold and appears to postdate other gold bearing veins. The 'E'-vein system is between the 4700' and 5700' levels from 30E to 16E sections. The veins are 5 cm to 1 m wide and have dips varying from 45° to 75° N. Gold content is greater than 17 grams Au per tonne and is empirically related to the presence of abundant actinolite.

The 'A'-vein system is between the 4600' and 5800' levels from 21E to 5E section. It is a set of quartz-filled fractures dipping to the north from 45° to 60° and plunging east 40°, in the hanging wall of the '04 Break between the '04 and Main Breaks. These are 1 m to 1.5 m wide and occur as single veins or braided networks. The average gold content is 10 to 15 grams Au per tonne. The wallrocks are reddish up to 1 m away from vein margins.

Other, less important north-dipping hanging wall veins are the Nos. 87, 69 and 70 veins between the 3100' and 3700' levels from 40E to 30E sections and Nos. 01, 02 and 03 veins between the 4200' and 5000' levels from 12E to 2W sections.

Footwall Veins

The only set of footwall veins of importance at the Macassa mine is the 'T'-vein system. This is a series of east plunging stacked veins dipping into the '04 Break at

450 to 600 south between 0 section and 24W section from the 5300' to 6400' levels. The 'T' veins are 25 cm to 2 m wide and are noted for the common, visible gold and abundant telluride minerals. Gold content is greater than 24 grams Au per tonne. Wallrocks are moderately reddish.

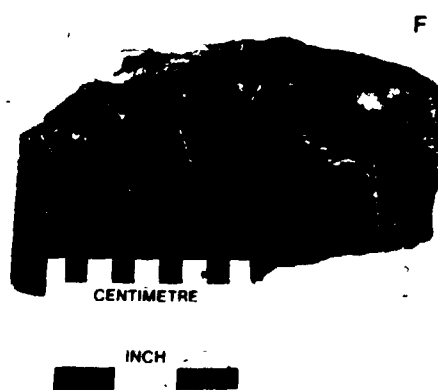
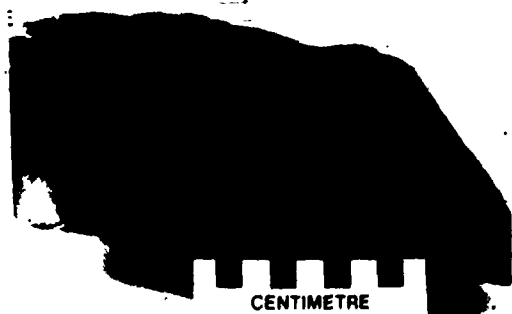
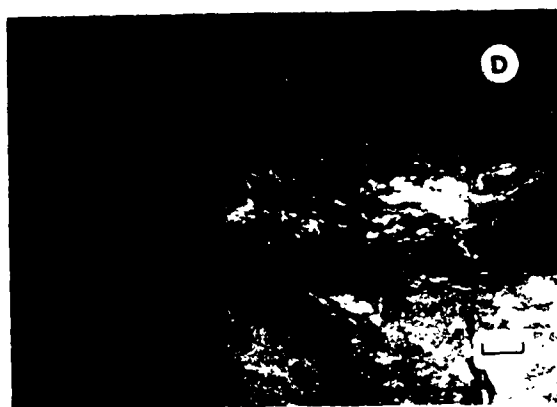
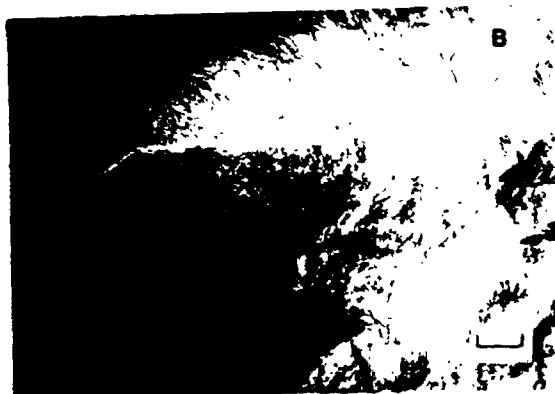
3.5.3.3 Breccia-Ore

Breccia-ore is principally in the deep, western third of the mine workings. Since 1980, over 40% of the unbroken ore reserves have been classed as breccia ore. It is hosted by a mixture of augite syenite and tuff which exist in a complex, interfingering relationship and lesser amounts of porphyritic syenite. The ore is characterized by an erratic distribution of white and grey quartz pods and lenses which contain native gold and tellurides (Plate 3-8). Pyrite and sericite are abundant and molybdenite coats fractures in both host rock and quartz lenses. Breccia-ore is typically confined on the north and south by major faults in four areas of the Macassa mine.

Not only is the gold ore limited by the major confining faults but the host rocks north and south of these structures are typically not fractured, are less siliceous and light coloured. Apparently, the major faults enclose lensoid areas which were very sheared and broken because of differential movement on the faults. During and subsequent to these episodes of ground preparation, altering, gold-

Plate 3-8: Breccia ore in the Macassa Mine.

- a. Underground exposure of breccia ore 5150' level of Macassa Mine with erratic distribution of fractured lenses and pods of quartz and poorly developed linear fabric.
- b. View of rocks hosting breccia ore with large mass of altered augite syenite (dark) with an included fragment of altered tuff (outlined in white chalk). Scale bar is approximately 0.25 m.
- c. View of back of stope on 5150' level, Macassa Mine, with occurrence of isolated pods of white quartz in mass of dark grey quartz.
- d. Breccia ore cut by several directions of post-emplacement faults, 5300' level, Macassa Mine. Scale bar is approximately 0.25 m.
- e. Polished hand specimen of breccia ore with small fragments of white quartz in brecciated augite syenite.
- f. Polished hand specimen of breccia ore with altered and brecciated tuff fragments (light) in fractured augite syenite (dark).



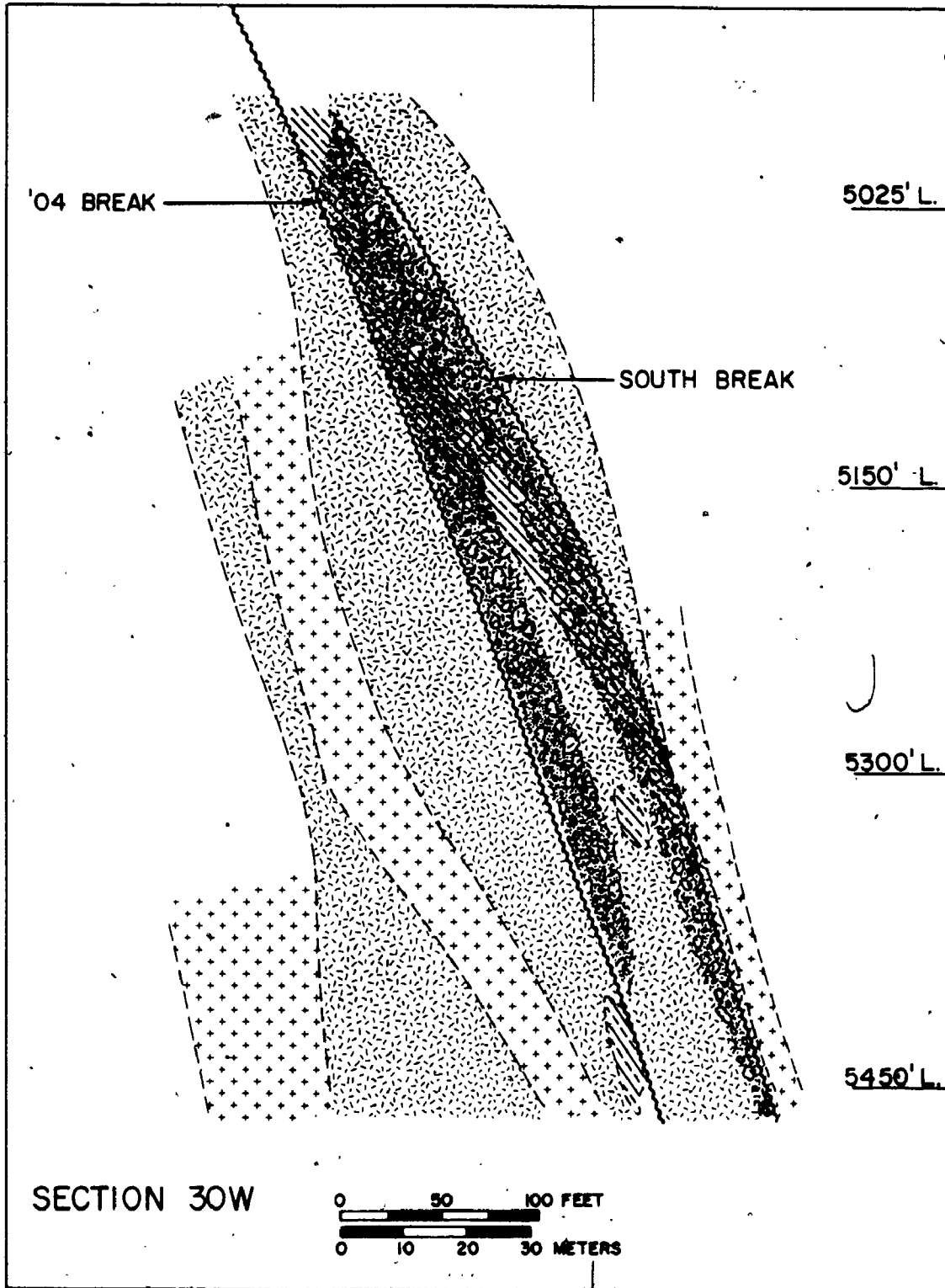
bearing hydrothermal fluids moving along the faults invaded the broken rocks. Gold abundances are not continuous within areas of breccia-ore but rather are very erratic (see Chapter 6). Although, the entire area may have widths of 15 to 20 m, narrower lenses of gold concentration 3 to 5 m wide are contained within. Although the fracture pattern within areas of breccia-ore is complex, there is commonly a poorly developed, linear fabric subparallel to the major fault planes (Plate 3-8a).

Breccia-ore is present between the 5025' and 5400' levels from 28W to 34W sections. The major confining structures are the '04 Break to the north and South Break to the south. This area is terminated by the incomplete convergence of these two structures approximately 20 m above the 5025' level and ranges from 5 m to 15 m wide (Fig. 3-8).

Breccia-ore also occurs between the 5700' and 6300' levels between sections 21W and 25W. The confining structures are the '04 Break to the south and a prominent footwall fault to the north for a width of approximately 7 m to 10 m. Tuffaceous rock fragments are bleached, syenite fragments are reddish and there is 2 to 4% disseminated pyrite. Unlike other examples of breccia-ore, there is little or no molybdenite on fracture surfaces. Average grade for this zone is 14 to 17 grams Au per tonne.

A third example of breccia ore is from 33W to 38W

Figure 3-8. Geologic section along 30W, Macassa Mine with relationship of breccia ore to major faults. Compiled from mine sections and drill hole logging by Watson.



AUGITE SYENITE



PORPHYRITIC SYENITE



TUFF



BRECCIA ORE



BREAK (major fault)

sections between the 6100' and 6400' levels. It is also approximately 7 m to 10 m wide. This zone is confined by the '04 Break to the south and an unnamed footwall fault to the north. Gold abundance is slightly greater than average at 19 grams Au per tonne. Wallrock alteration near the '04 Break is characterized by reddishness whereas wallrocks near the north fault are predominantly bleached.

The fourth area of breccia-ore is in the hanging wall of the '04 Break between the 4700' and 5400' levels from 17W to 21W sections. There is no known confining structure to the south. This zone is 3 m to 8 m wide. Gold abundance is from 12 to 14 grams Au per tonne. It is accompanied by both intense reddishness and bleaching in wallrocks.

CHAPTER 4

CHEMICAL COMPOSITION OF MINE ROCKS AND ORES

4.1 General Statement

Forty eight representative samples of the major rock types, ore types and associated altered wallrocks from the Macassa Mine were analysed for their major, minor, selected trace element and rare earth element abundances (Tables 4-1 to 4-3, appendix A). Other analytical data for intrusive rocks from the mine provided by F. R. Ploeger of McMaster University are included along with selected previously published analyses of rocks from other mines in Kirkland Lake (Thomson et al., 1950). The following discussion deals with the chemical composition of the unaltered rocks and gold-bearing ore rocks at the mine and changes in composition of the whole rock caused by alteration adjacent to gold-bearing breaks, veins and breccias.

4.2 Chemical Composition of Mine Rocks

4.2.1 Timiskaming Group Sedimentary Rocks

Hyde (1978) has discussed the chemical composition of

	366	332	247	278	171	170	175	172	308	380
Cr										
Co	53	52	26	28	21	21	20	18	29	33
Mn	118	121	57	59	41	39	42	40	76	104
Cu	15	16	106	89	98	104	88	79	75	90
Zn	125	136	106	112	102	105	102	92	110	120
W	4	40								
Pb	21	29	14	16	15	28	24	16	10	17
U	2.2									3.0
Th	11	31								7.6
Rb	209	312								
Sr	629	1622								
Y	22	23								
Zr	145	170								
Nb	6	20								
Ba	1166	2183	2200	2040	1660	1980	1680	2020	1820	1750
S.G. ^{*2}	2.77	2.79	2.79	2.78	2.73	2.80	2.72	2.73	2.78	2.78

LOI^{*1} = weight percent loss on ignition at 1000°C

S.G.^{*2} = specific gravity (2 σ ± 0.02)

9.4^{*3} = Total iron expressed as Fe₂O₃

Analyses:

- 1: Augite syenite, unaltered and unmineralized, 5450 ft. level Macassa Mine.
- 2: Augite syenite, unaltered and unmineralized, 6425 ft. level Macassa Mine.
- 3-10: Augite syenite, unaltered and unmineralized, 3000 ft. level Casakirk cross-cut, Macassa Mine (data from F.R. Ploeger, McMaster University, Analyses by O.G.S. Geoscience Laboratories, Toronto).

TABLE 4-1(11) Cont'd

Analysis No.	11	12	13	14	15	16	17	18	19	20
Sample No.	6	71	72	74	143	2473	2475	2476	PL-190	PL-190
SiO ₂	50.2	63.8	63.6	60.3	60.9	63.8	65.2	63.8	64.5	57.4
TiO ₂	0.93	0.40	0.39	0.50	0.40	0.39	0.33	0.34	0.99	0.98
Al ₂ O ₃	16.4	15.3	15.2	13.8	14.4	14.6	15.1	14.8	15.5	18.8
Fe ₂ O ₃	2.8	3.8 ³	3.7	4.6	4.0	3.5	2.8	3.0	1.3	1.3
FeO	4.5									
MnO	0.16	0.05	0.07	0.09	0.08	0.05	0.05	0.08	0.05	0.07
MgO	3.8	1.7	1.6	3.6	2.1	1.9	1.4	1.4	1.7	1.2
CaO	5.8	2.9	3.0	4.2	3.3	2.4	3.2	2.5	2.0	
K ₂ O	5.8	3.2	3.3	3.1	4.0	3.4	3.4	3.6	2.8	7.8
Mn ₂ O	3.4	5.6	5.5	4.6	5.0	4.4	5.5	5.0	4.4	3.3
P ₂ O ₅	0.51	0.18	0.18	0.3	0.20	0.16	0.15	0.16	0.15	0.30
LOI ₅₁	1.9	2.0	2.3	3.5	4.3	3.1	2.4	3.8	2.2	4.2
Total	99.8	99.0	98.7	98.8	98.6	98.3	98.6	99.2	98.3	100.8
CO ₂	3.4	1.0	1.5	2.75	3.8	2.2	1.8	4.0	1.1	3.9
S	1039	1457 ⁴	1243	238	506	104	202	2000	100	
As(prob)	58	17	<1	<1	15	<1	<1	<1	<1	<1
Pb	<1	<1	<1	<1	<1	<1	<1	<1	<1	<1
Ag	4	2	2	4	5	1	2	3	3	3
Cu	0.9	0.8	0.8	0.9	3	4	1	5	1	5
Sc	14									
V	95	102	137	125	112	66	75			

Cr	165	147	279	185	228	173	169	51	6
Co	35	29	54	33	36	38	30	7	8
Mn	29	29	82	46	43	31	35	21	1
Cu	12	10	12	12	12	10	10	8	64
Zr	51	57	73	66	72	45	36	33	60
W	4	3	<1	5	8	1	<1		
Pb	26	27	55	26	20	22	24	11	
U	3.7	3.7							
Th	7.6	13							
Rb	78	84	106	144	98	72	101		
Sr	1815	1263	1809	1400	2030	968	1262		
Y	48	19	21	15	18	10	22		
Zr	175	171	180	171	158	155	166		
Nb	2	10	5	1	2	1	16		
Ba	2376	1987	2164	2360	2500	1565	1656	2760	2020
S.G. ^{*2}	2.82	2.66	2.67	2.67	2.68	2.67	2.64	2.70	2.71

LOI^{*1} = weight percent loss on ignition at 1000°C

S.G.^{*2} = specific gravity (2σ = ± 0.02)

3.0^{*3} = Total iron expressed as Fe₂O₃

Analyses

- 11: Aegite syenite, unaltered and unmineralized, average of 5 samples (from Thomson et al, 1948).
- 12-14: Porphyritic syenite, unaltered and unmineralized, 5450 ft. level Macassa Mine.
- 15: Perphyritic syenite, unaltered and unmineralized, 3000 ft. level Casakirk cross-cut, Macassa Mine.
- 16-18: Porphyritic syenite, unaltered and unmineralized, Wright-Hargreaves Mine, Kirkland Lake.
- 19-20: Porphyritic syenite, unaltered and unmineralized, 3000 ft. level Casakirk cross-cut, Macassa Mine. (data provided by F.R. Pileger, McMaster University. Analyses by O.G.S. Geoscience Laboratories, Toronto).

TABLE 4-1 (111) Cont'd

Analysis No. Sample No.	21 PL-199	22 PL-200	23 PL-201	24 PL-202	25 8	26 70	27 86	28 86A	29 7
SiO ₂	62.9	64.0	66.2	65.9	62.2	56.2	56.7	56.8	57.0
TiO ₂	0.89	0.77	0.76	0.72	0.44	0.66	0.55	0.63	1.9
Al ₂ O ₃	14.7	14.5	14.7	14.3	14.9	18.8	19.2	18.8	18.3
Fe ₂ O ₃	2.0	1.8	1.7	1.8	1.4	4.4*3	4.1	3.7	1.0
FeO	1.4	1.2	1.0	1.5	2.0				2.7
MnO	0.06	0.05	0.05	0.05	0.13	0.07	0.08	0.08	0.17
MgO	1.8	1.7	1.4	1.9	2.3	1.0	0.8	0.9	1.0
CaO	3.0	2.4	2.3	2.7	3.9	2.1	1.4	2.0	2.0
K ₂ O	2.9	3.3	2.6	2.6	3.8	7.8	7.6	7.0	7.4
Mn ₂ O	4.3	4.7	4.7	4.85	4.9	4.1	4.3	4.7	4.2
P ₂ O ₅	0.16	0.12	0.10	0.13	0.37	0.24	0.21	0.21	0.37
LOI ₁	4.4	4.2	3.9	3.0	1.05	3.2	3.4	4.0	4.1
Total	98.9	99.1	99.8	99.7	100.1	98.6	98.4	98.8	100.0
CO ₂	3.8	3.6	3.4	2.0	2.8	3.1	2.5	3.5	3.1
S	1400	1000	2400	1800		104	658	135	
Au (ppb)						25	18	8	
Ag						<1	<1	<1	
As						2	12	5	
Sb						3.2	4	2	
Sc						8			
V						77	100	97	

Cr	59	56	53	65	71	87	83
Co	8	7	6	9	10	29	33
Mn	23	23	18	28	16	21	20
Cu	15	12	8	13	24	14	12
Zn	75	50	41	75	61	38	69
V					2	5	2
Pb	17	16	20	24	23	41	33
U					4.0	2.0	3.7
Th					28	6.4	12.5
Rb					190	230	200
Sr					720	430	540
Y					22	23	18
Zr					240	320	238
Nb					8	28	12
Ba	2150	2040	3480	2980	976	732	745
S.G. ^{*2}	2.72	2.72	2.70	2.70	2.73	2.58	2.60
					2.58	2.58	2.73

LOI^{*1} = weight percent loss on ignition at 1000°C.

S.G.^{*2} = specific gravity (20 ± 0.02).

4.4^{*3} = Total iron expressed as Fe₂O₃.

Analysis

21-24: porphyritic syenite, unaltered and unmineralized, 3000 ft. level Casakirk cross-cut, Macassa Mine. (data provided by F.R. Ploeger, McMaster University. Analyses by O.G.S. Geoscience Laboratories, Toronto).

25: porphyritic syenite, unaltered and unmineralized, average of 4 samples (from Thomson et al, 1948).

26-28: felsic syenite, unaltered and unmineralized, 2475 ft. level Macassa Mine.

29: felsic syenite, unaltered and unmineralized, average of 2 samples (from Thomson et al, 1948).

TABLE 4-1 (iv) Cont'd

Analysis No.	30	31	32	33	34	35	36	37	38	39
Sample No.	141	142	77	79	83	80	85	3140	1	2
SiO ₂	48.9	52.4	49.9	47.2	55.9	53.6	42.4	50.8	45.6	47.7
TiO ₂	0.78	1.1	0.79	0.89	0.41	0.73	1.2	0.93	1.0	1.7
Al ₂ O ₃	16.2	13.7	15.5	16.2	13.9	19.9	13.4	12.6	10.6	11.9
Fe ₂ O ₃	7.1*3	8.9	8.2	7.14	3.8	7.9	11.6	10.1	4.7	6.4
FeO									3.8	4.7
MnO	0.19	0.14	0.16	0.27	0.14	0.25	0.24	0.18	0.17	0.16
MgO	1.0	1.6	3.3	2.7	0.8	0.8	3.8	4.5	6.1	3.4
CaO	6.2	4.3	7.1	5.4	2.7	5.6	8.5	6.9	10.3	6.1
K ₂ O	9.5	10.1	7.7	7.4	7.3	10.4	9.0	2.6	3.5	5.8
Mn ₂ O	1.7	0.4	1.6	2.8	4.4	1.5	0.6	3.0	2.1	2.1
P ₂ O ₅	0.22	0.9	0.34	0.15	0.2	0.42	0.6	0.85	0.52	0.99
LOI-1	7.2	5.0	3.6	8.8	3.0	3.8	7.0	6.7	10.0	9.3
Total	99.0	98.5	98.2	98.7	98.6	98.9	98.2	99.1	100.2	100.2
CO ₂			12.8	8.0	2.6	4.2	6.8	5.0	40.0	8.3
S	169	183	358	113	156	1254	409	92		
Au(ppb)	110	14	22	52	10	19	6	13		
Au	<1	<1	<1	<1	<1	<1	<1	<1		
As	10	36	13	17	6	19	15	9		
Sb	10	16	2	14	1	11	34	1		
Sc							35			
V	413	506	299	440	125	407	508	428		

Cr	79	103	133	119	49	92	141	176
Co	1	1	12	10	24	1	1	49
Mn	20	31	39	43	19	24	49	54
Cu	27	34	37	17	15	26	37	16
Zn	82	50	102	142	60	173	154	140
K	1	1	1	1	2	5	2	3
Pb	57	66	41	53	39	77	48	36
U				15.1				
Th				52			54	
Rb	254	233	194	323	262	333	285	69
Sr	2774	1275	3007	2136	2078	1580	3058	1303
Y	37	37	33	52	24	27	45	40
Zr	442	378	470	784	547	278	411	403
Nb	22	12	14	31	32	20	14	11
Ba	5304	5757	3443	4208	8386	3212	4725	2076
S.G. ^{*2}	2.73	2.71	2.74	2.72	2.69	2.65	2.59	2.73
							2.76	2.82

LOI^{*1} = weight percent loss on ignition at 1000° C

S.G.^{*2} = specific gravity (2 n = ± 0.02)

7.1^{*3} = Total iron expressed as Fe₂O₃

Analysis

- 30-31: trachytic tuff, unaltered and unmineralized, 3000 ft. level Macassa Mine.
- 32: black tuff, unaltered and unmineralized, 3050 ft. level Macassa Mine.
- 36: black tuff, unaltered and unmineralized, 4250 ft. level Macassa Mine.
- 37: trachytic tuff, unaltered and unmineralized, surface outcrop near Don Lou Motel, Kirkland Lake.
- 38-39: bedded tuff, unaltered and unmineralized, Macassa Mine property (from Thomson et al., 1948).

Cr	70	196	327	292	267	282	63	331	310	302	264
Co	0	68	24	27	7	15	0	49	72	29	28
Ni	17	64	67	38	16	14	36	85	69	12	12
Cu	15	10	26	16	13	39	44	24	24	23	10
Zn	96	88	135	100	21	187	70	85	61	19	23
V	41	2	4	23	25	15	66	23	12	12	5
Pb	30	24	16	98	85	107	75	23	22	99	66
U	3.1				1.5						
Th	21		27		24	16		28	31	8	
Rb	280	83	85	88	88	60	400	165	147	27	28
Sr	311	1060	154	1713	2670	340	960	1640	1426	1426	148
Y	14	24	10	14	15	14	34	24	22	6	10
Zr	185	182	111	70	126	93	492	144	140	55	25
Mb	13	15	0	5	0	1	28	14	8	<1	6
Ba	531	1347	1091	268	3908	5209	1578	811	976	2746	286
S.G.	2.62	2.62	2.75	2.77	2.64	2.70	2.70	2.79	2.78	2.67	2.67

- *1 LOI - Weight percent loss on ignition at 1000° C.
 - *2 S.G. - Specific gravity (Z₀ = ± 0.02).
 - *3 I-IV - Vein ore and breccia ore sample groupings referred to in text.
 - Fe₂O₃ (T)^{*4} - Total iron expressed as Fe₂O₃.
- Analysis
- 1-2: felsic syenite, altered and mineralized, wallrock from 26A vein, 2475 ft. level Macassa Mine.
 - 3: aegite syenite, altered and mineralized, wallrock from 58E vein, 5875 ft. level Macassa Mine.
 - 4: 58E vein material, 5875 ft. level Macassa Mine.
 - 5-6: tuff breccia ore, 5450 ft. level Macassa Mine.
 - 7-10: aegite syenite breccia ore, 5450 ft. level Macassa Mine.
 - 11: brecciated quartz from '04 break, 4625 ft. level Macassa Mine.
 - 12: blue-gray quartz from Kirtland Lake Main Break (1911 discovery site of M.H. Wright), Wright-Hargreaves property.

TABLE 4-3 Abundances of major and selected trace elements for altered rocks associated with Break ore at Macassa mine. (Major elements in weight percent, trace elements in ppm except as noted)

Sample No.	O4 Break					Narrows Break					Main Break		
	108	121	1212	1214	1216	135	137	138	139	117A	116	115	
SiO ₂	43.2	47.5	49.2	47.8	49.7	47.5	52.0	50.0	52.3	48.0	47.4	47.6	
TiO ₂	0.71	0.8	0.8	0.8	0.8	0.8	0.7	0.70	0.72	0.8	0.8	0.8	
Al ₂ O ₃	11.90	13.1	13.8	12.5	13.0	11.6	16.4	15.0	15.0	11.7	12.1	13.6	
Fe ₂ O ₃ (T)	7.9	9.9	8.8	9.0	9.8	8.6	5.7	6.0	4.9	9.3	9.2	7.8	
MnO	0.14	0.17	0.12	0.15	0.13	0.13	0.10	0.12	0.11	0.16	0.14	0.11	
MgO	5.5	5.6	5.7	6.4	6.9	6.5	2.0	3.9	3.6	5.3	6.4	5.1	
CaO	7.2	5.5	5.9	7.0	5.3	6.9	4.4	5.7	5.7	7.6	6.6	7.4	
K ₂ O	5.5	4.2	6.7	6.3	6.5	5.9	7.1	5.9	4.1	4.1	4.4	5.5	
Mg ₂ O	2.3	3.9	2.7	2.5	2.6	0.3	3.4	2.9	4.1	2.6	2.8	2.4	
P ₂ O ₅	0.16	0.54	0.6	0.53	0.56	0.53	0.4	0.4	0.43	0.6	0.54	0.5	
LOI ¹	13.8	7.5	5.62	6.0	4.5	11.7	6.9	9.3	8.95	10.4	9.8	9.2	
TOTAL	98.3	98.7	99.9	99.0	99.8	100.5	99.9	99.9	100.3	100.8	100.2	100.0	
CO ₂	14.0	7.0	4.8	5.0	3.5	11.0	5.6	6.8	6.3	10	6.5	8.3	
S	110.5	1078	190	189	326	93.6	80.3	55	48	89	83	106	
Au (ppb)	74	11	31	4	3	6	6	7	19	8	1	6	
Ag	<1	1	1	1	1	0.5	0.5	0.5	0.5	0.5	0.5	0.5	
As	10	13	5	6	4	6	10	9	8	26	7	8	
Sb	2.3	2.4	2	3.4	1.6	23	28	23	16	2.7	2.1	4	
SC	23	23	21	22	23	22	10	13	15	23	22	17	
V	328	406	388	360	390	354	198	238	291	356	342	307	

Cr	333	328	325	302	332	271	118	141	178	257	293	251
Co	60	56	52	43	52	79	48	78	72	33	55	64
Mn	92	108	110	111	121	88	38	46	50	78	99	83
Cu	19	49	19	21	16	21	14	14	10	18	20	22
Zn	85	108	132	134	136	92	55	66	60	69	88	82
N	90	79	51	47	40	49	81	87	60	57	100	110
Pb	22	94	37	31	29	21	38	34	31	50	30	34
Th		31	31	34	31	30	29	33	32	32	27	33
Nb	165	103	256	300	312	188	211	211	256	98	100	92
Sr	1004	1477	1066	1040	1622	754	533	490	444	538	964	1050
V	19	26	26	28	23	21	24	24	17	22	26	30
Zr	149	164	175	168	171	139	206	206	196	153	155	184
Mb	7	8	19	25	20	6	21	26	9	8	9	18
Ba	1410	2610	1314	1162	2183	1141	1129	955	1014	1342	1491	1656
S.G. #2	2.73	2.77	2.75	2.76	2.79	2.78	2.75	2.74	2.74	2.77	2.76	2.74

*1 LOI = weight percent loss on ignition at 1000°C

*2 S.G. = specific gravity (20 ± 0.02)

Timiskaming sandstone and argillite from the Kirkland Lake district. Included were samples from rocks he assigned to the Chaput-Hughes Formation immediately south of the Macassa Mine. Hyde noted that the abundance of total Fe, MgO, CaO, Na₂O and K₂O, when compared to a dacite, an average rock of similar SiO₂ content, suggests sediment contribution from a mafic source terrain. Also, when compared to an average greywacke (Pettijohn, 1963), Timiskaming Group sandstones have more MgO and Na₂O and slightly less K₂O. These chemical compositions were attributed to nature of the source rock (Hyde, op. cit.).

The chemical composition of Timiskaming Group rocks from the Macassa Mine (samples 30 to 39, Table 4-1), is most similar to those determined by Cooke and Moorhouse (1969, their Table 1) for trachytic flows in and east of Kirkland Lake. The Macassa Mine samples are trachytic tuffs characterized by SiO₂ content of 48 to 56 wt. %, large absolute amounts of K₂O, 7.3 to 10.4 wt. %, abundant TiO₂, total Fe, MnO, P₂O₅, and Na₂O:K₂O ratios of 0.04 to 0.38. Large concentrations of mafic affiliated trace elements such as V and Cr and reflect the presence of augite with or without hornblende in these rocks.

4.2.2 Intrusive Rocks and Trachytic Tuffs

Analysis of unaltered augite syenite, massive syenite and porphyritic syenite rocks from the Macassa Mine

(samples 1 to 29, Table 4-1), are generally atypical of syenites. SiO_2 varies from 48.9 to 53.7 wt. %, 56.2 to 58.0 wt. %, and 57.4 to 66.2 wt. % in augite syenite, massive and porphyritic syenites respectively. Porphyritic syenite contains less K_2O than the other two rocks, 2.5 to 4.0 wt. % versus 4.4 to 7.8 wt. %. Relatively abundant concentrations of augite with or without hornblende phenocrysts is reflected in greater abundances of TiO_2 , total Fe, MnO , CaO and MgO in augite syenite in comparison to porphyritic syenite. Large concentrations of V, Cr, Co, Ni and Sc in augite syenite samples also reflect the greater proportion of mafic minerals. Porphyritic syenite contains more Na_2O than the other two types of syenite phases, from 3.3 to 5.6 wt. %, with an average of 4.8 wt. % versus 2.3 to 4.7 wt. %, with an average 3.7 wt. %.

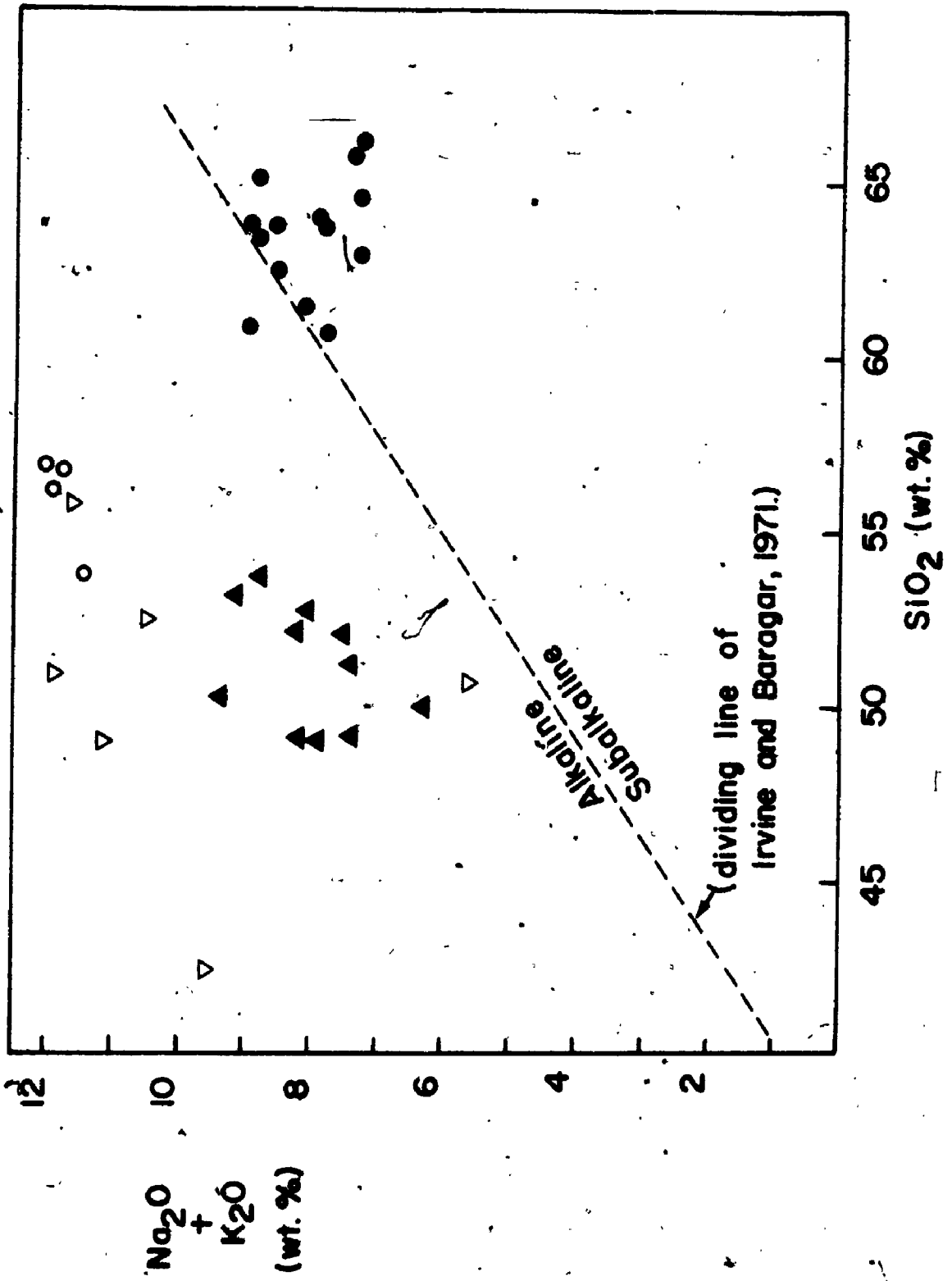
The suite of syenitic rocks from the Macassa Mine differs in several important respects from the composition of typical syenitic rocks (cf. Sorenson, 1974; Gerasimovsky, 1974). Specifically, the minor absolute Zr and Nb abundances result in high Ti/Zr for syenites, 13-35 compared to typical ratios of about 7; and Nb/Y of 0.2 to 0.5 which are less by a factor of 5 to 10 than is typical for alkaline igneous rocks (cf. Floyd and Winchester, 1978). Another aspect of interest is the relatively large thorium contents of porphyritic and massive syenite, 18 to 26 ppm, contrasting with normal Th abundance for augite

syenite of 9 ppm.

The three different phases of syenites constitute distinct populations in terms of some major element oxide abundances. On an alkali-silica diagram (Fig. 4-1) these rocks plot in both the alkaline and subalkaline fields. Augite syenite and massive syenite are clearly alkaline as are the Timiskaming pyroclastic and sedimentary rocks of the Timiskaming Group. Porphyritic syenite, although plotting close to the line dividing alkaline and subalkaline fields (Irvine and Baragar, 1971), is predominantly subalkaline with only 1 analysis in 14 above that line.

In a Larsen diagram, the abscissa parameters reflect the variation of major oxide constituents with differentiation. Where smooth curves result from plots of a group of rock analyses, these rocks are co-magmatic (Fig. 4-2). The data set has a coherent trend for TiO_2 , Al_2O_3 , total Fe, MgO, CaO and Na_2O reflecting the differentiation of the syenites from the mafic to more felsic end members. However, the variations of SiO_2 , K_2O and MnO suggest the existence of two separate groups of comagmatic rocks. The augite syenite and massive syenite phases together with trachytic tuffs of the Timiskaming Group belong to one group and the porphyritic syenite to another. This is partly supported when the same data is plotted on a Harker diagram with wt. % SiO_2 as the abscissa ordinate (Fig. 4-3). Again, there is a distinct grouping of data points

Figure 4-1. Alkali-silica diagram for syenites and rocks of the Timiskaming Group from the Macassa Mine and area. Solid triangles = augite syenite; solid circles = porphyritic syenite; open circles = massive syenite; open, inverted triangles = trachytic tuffs. Data from Table 4-1; Thomson et al., 1950, their Table 5.



2810

Figure 4-2. a) Larsen diagram for syenites and rocks of the Timiskaming Group from the Macassa Mine and area. Solid triangles = augite syenite; solid circles = porphyritic syenite; open circles = massive syenite; open, inverted triangles = trachytic tuffs. Data from Table 4-1; Thomson et al., 1950, their Table 5.

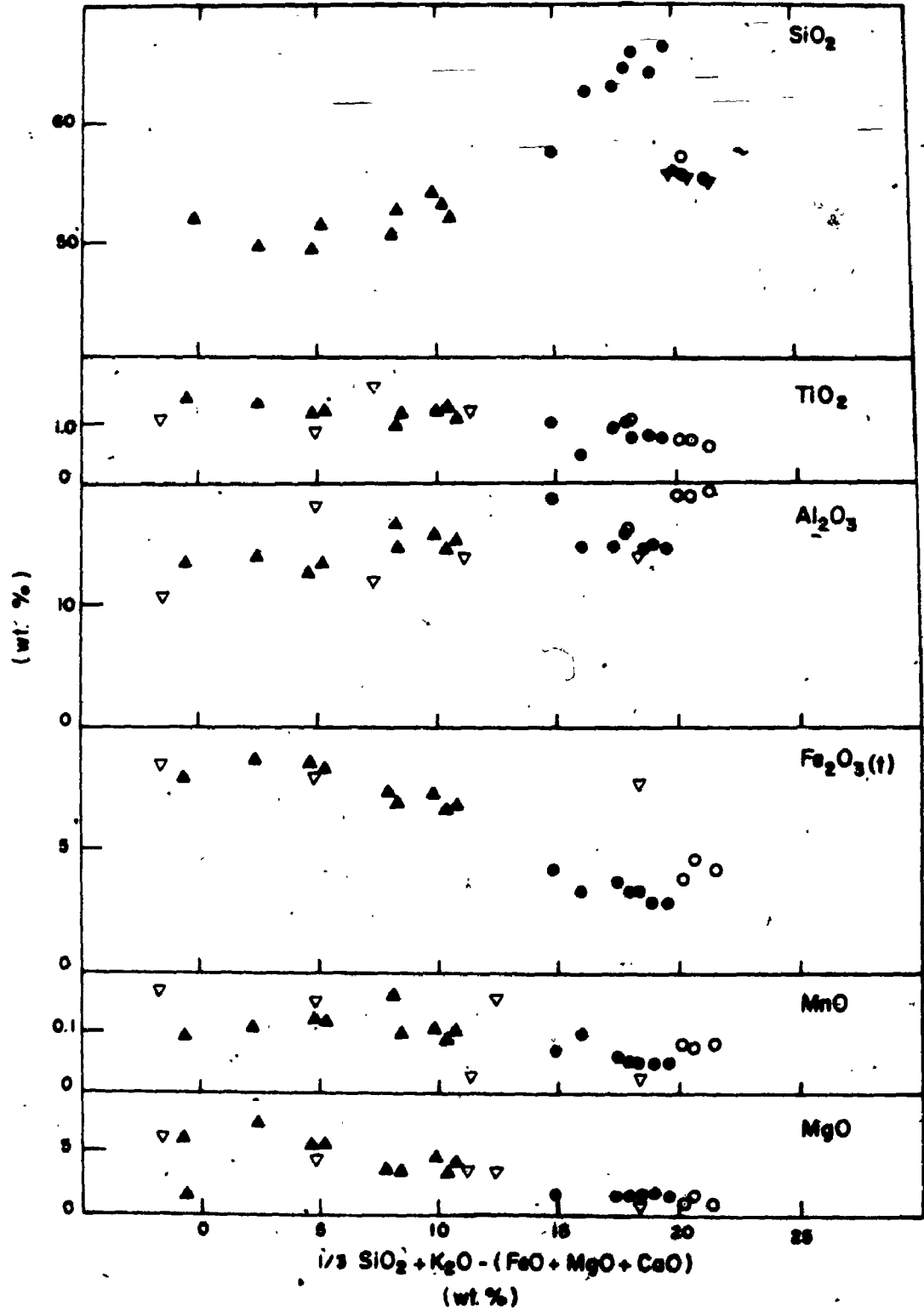


Figure 4-2. b) Larsen diagram continued.



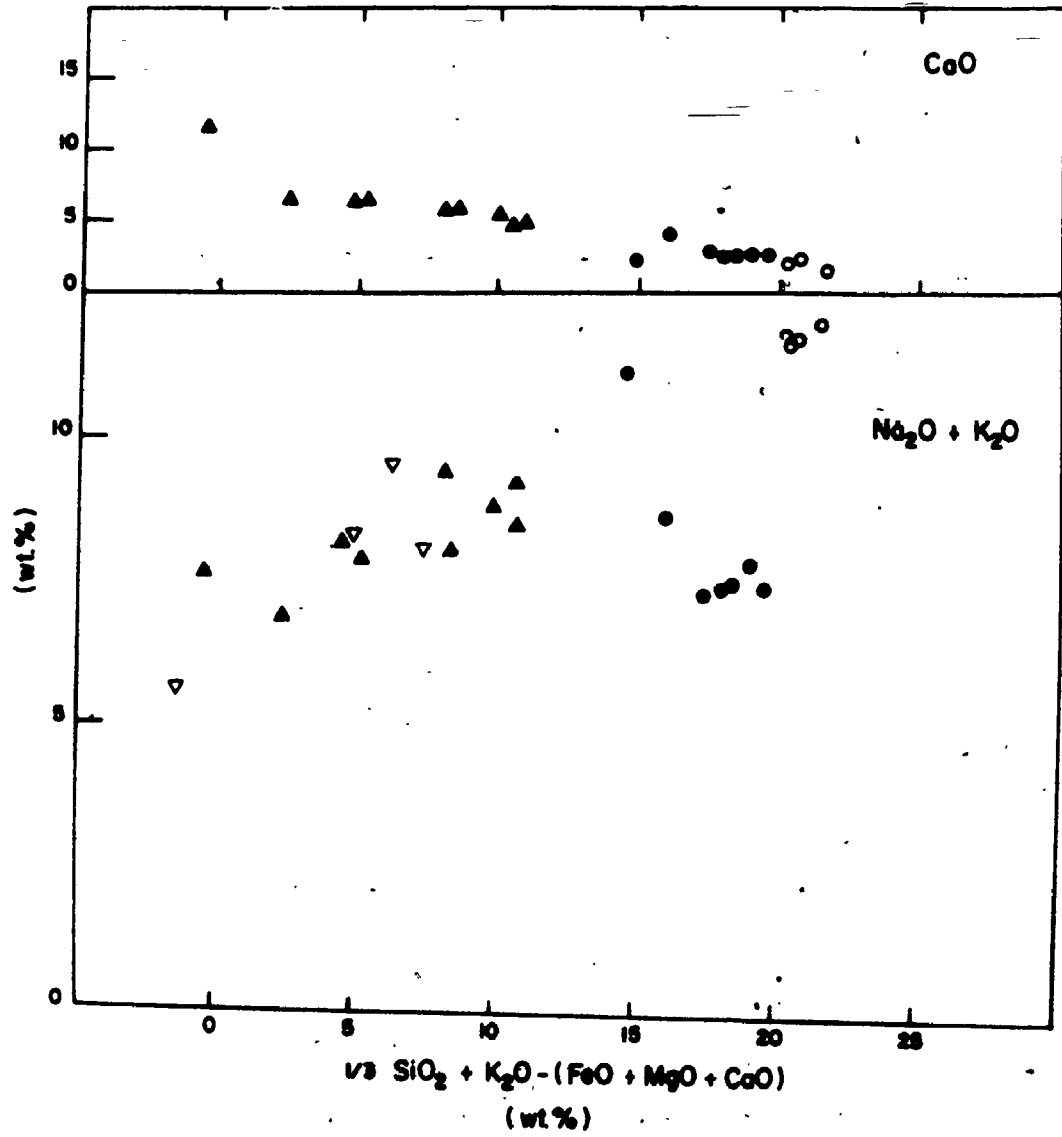
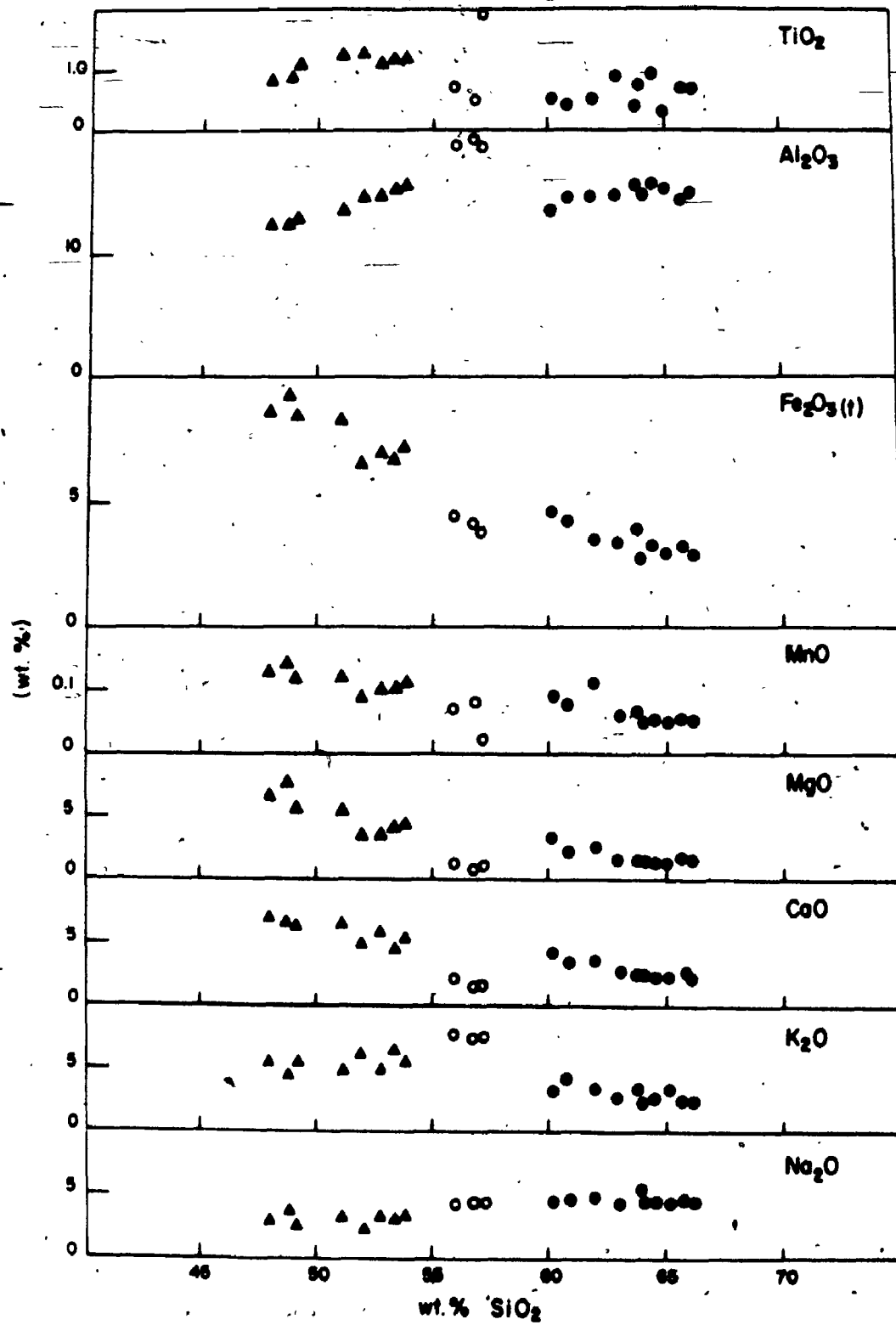


Figure 4-3. Harker diagram for syenites and rocks of the Timiskaming Group from the Macassa Mine and area. Solid triangles = augite syenite; solid circles = porphyritic syenite; open circles = massive syenite; open, inverted triangles = trachytic tuff. Data from Table 4-1; Thomson et al., 1950, their Table 5.



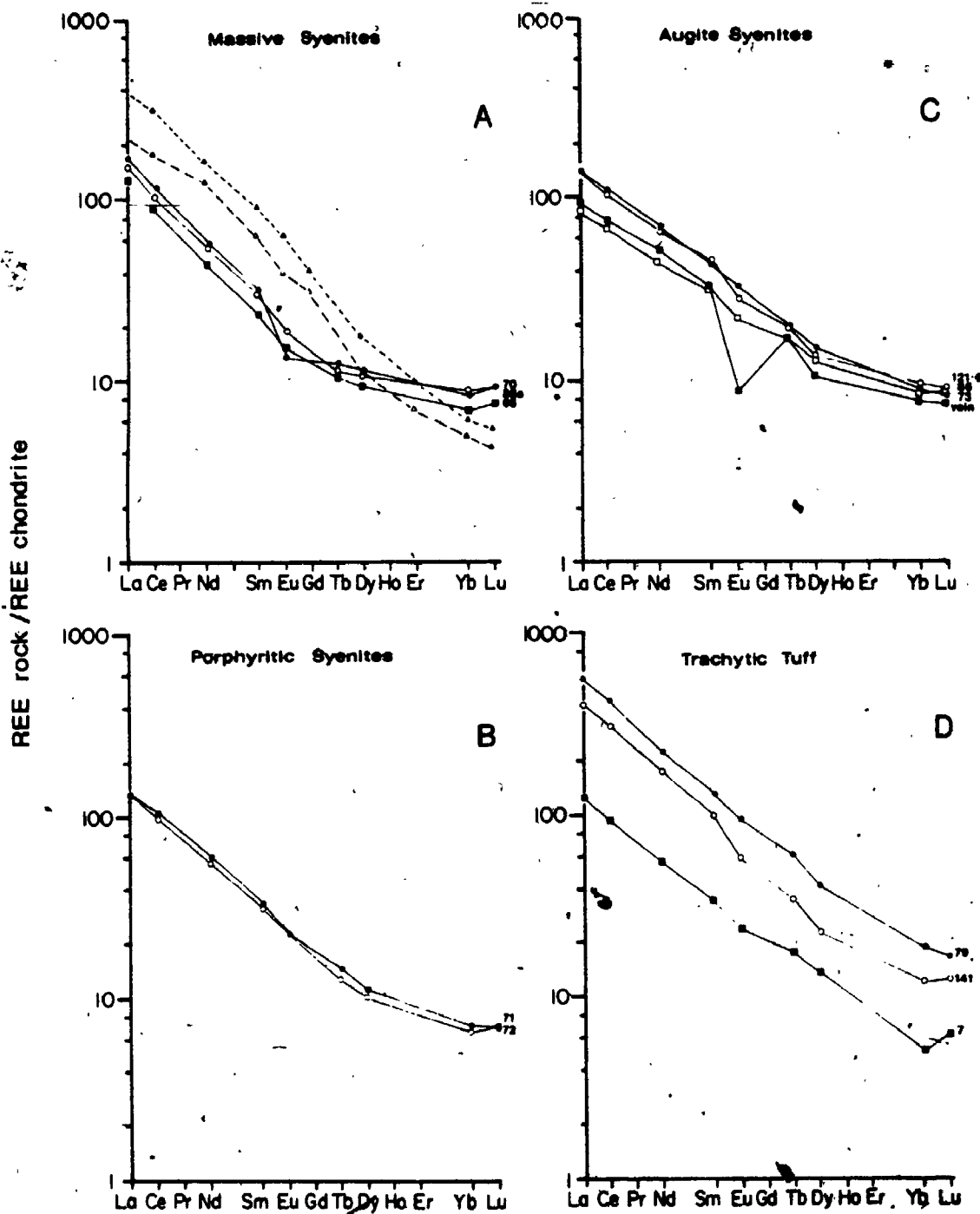
for Al_2O_3 and K_2O which differentiate between porphyritic syenite and the other two syenites. This grouping is not evident for TiO_2 , total Fe, MnO , MgO , CaO and Na_2O .

Similar analysis of data for volcanic and intrusive rocks of the Kirkland Lake district led Cooke and Moorhouse (1969, page 130) to conclude "on the basis of their form, distribution and chemical composition, the mafic syenite (ie. augite syenite) and syenite (ie. massive syenite) intrusions were contemporaneous with the Timiskaming phase of volcanism". The porphyritic syenites which definitely cross-cut the volcanic rocks and other syenites are compositionally distinct and may belong to a post-Timiskaming period (Cooke and Moorhouse, op. cit.). The Macassa samples only partially support the separation of augite syenite and massive syenite from porphyritic syenite on the basis of their major element abundances and the suggested existence of two distinct magma sources for these rocks. There are some apparent chemical affinities between the former two syenites and pyroclastic rocks of the Timiskaming Group from the mine.

Rare earth element patterns for unaltered examples of the augite-, massive and porphyritic-syenites are remarkably uniform, with La 100 to 200 times chondritic, and the HREE about 10 times chondrite abundances (Fig. 4-4). This implies a common magma parentage. It is suggested here that the weight of evidence from major element oxide and

571

Figure 4-4. Chondrite normalized rare earth element abundances for varieties of syenites and their hydrothermally altered counterparts at Macassa. A - Massive syenites, samples 70 and 86A unaltered, sample 65 altered. The dashed lines are the REE envelope for Archean syenites, as reported by Condie (1980). B - Porphyritic syenites. C - Augite syenites, samples 73 and 121.6 unaltered, sample 86 altered, vein = k-feldspar actinolite vein in altered augite syenite. D - Syenitic trachytic tuffs, samples 79 and 141 unaltered, 7 altered (from Kerrich and Watson, 1984).



REE abundances is in favour of a common magmatic source for all syenites from the Macassa Mine. The uniformity of absolute abundances results in consistent La_N/Yb_N of 15. Relative to Archean syenite in general, for which the REE envelope is depicted (Fig.4-4), Kirkland Lake rocks have lower chondrite normalized ratios of the light to intermediate REE, but larger ratios for the HREE (Condie, 1981; Taylor et al., 1978). This is in accord with the previous observations that the compositions of Kirkland Lake alkalic rocks differ in several important respects from conventional syenites.

All of the syenites analysed in this study are enriched in gold by a factor of 3 to 8 times crustal abundances. This contrasts with observations of Ploeger (1980) who concluded that the syenitic rocks of Kirkland Lake did not contain more than crustal abundances. Sporadic minor enrichments of As (1 to 5x), Sb (5 to 50x) and W (2 to 100x) are also present in the unaltered rocks but sulphur is present at normal content for syenite (cf. Turekian and Wedepohl, 1961; Gerasimovsky, 1974). It is difficult to establish whether these anomalies are i) indigenous to the parental magma, ii) the result of magma assimilation of auriferous country rock, or iii) reflect post-crystallization penetration of auriferous hydrothermal fluids into syenite along microfractures. The third alternative is favoured here based on the presence of

carbonate-bearing microveinlets in some syenite samples and the observation that rocks which appear fresh in underground exposure and hand specimen commonly have carbonate minerals pseudomorphing primary minerals (Kerrick and Watson, 1984).

Trachytic tuffs are enriched in incompatible elements, including Ti, P, U, Th, Rb, Sr, Y, Zr, Nb and Ba, compared to the augite and porphyritic syenite. Specifically, the tuffs have more Ti and significantly greater Zr, resulting in lower Ti/Zr. A prominent aspect of their composition is the extremely abundant U, up to 15 ppm, and Th (26-54 ppm) consistent with their overall relative enrichment in incompatible elements. Thorium and uranium vary sympathetically, resulting in uniform Th/U of 2.0 to 3.5. These ratios are within the magmatic Th/U range (Maynard, 1983), suggesting that the greater absolute abundances are inherently a primary feature of the magmas (Kerrick and Watson, 1984).

Such abundances of large ion lithophile (LIL), or incompatible elements, in volcanic rocks are common in alkaline plutonic-extrusive complexes, probably because of the preferential concentration of the incompatible elements plus volatiles into an explosive extrusive phase (Taylor et al., 1981). This enrichment is also reflected in the REE abundances of the trachytic tuffs which have La contents 400 to 600 times chondrite, or about 5 times that of the

other syenites (Fig. 4-4). Overall, the REE have greater absolute abundances in the trachytic tuffs, but LaN/YbN is about 25, indicating some systematic fractionation of the REE between intrusive and extrusive phases.

Smith (1979) and Hildreth (1979) have shown that certain incompatible elements such as Nb, Ta, Th, U, Cs, Rb, Li, Sn, Be, B, W, Mo, F, Pb, Zn and Sn may be concentrated upward in high level compositionally zoned magma chambers, and are therefore preferentially incorporated into early extrusive phases. On the other hand, in such systems Ti, Cr, Co, Sc, and Cu are concentrated downward, being characteristically enhanced in late extrusive volcanic rocks. Trachytic tuffs at Kirkland Lake only partly follow this LIL enrichment pattern, and do not have the REE fractionation between early and late phases described by Hildreth (1979).

4.2.3 Gold-Bearing Rocks

Representative analyses of gold-bearing rocks from the Macassa Mine and previously published data for bulk ore samples from other mines in the Kirkland Lake district (Tables 4-2, 4-3, Thomson et al., 1950, their Table 5) have major element abundances similar to that of the adjacent wallrock. In addition to greater gold content, the most significant feature of these rocks is the minor overall S, together with sporadic content of tellurium. Gold/silver

in these samples average about 5. Charlewood (1964, Table IV), citing production data for the Macassa Mine from 1948 to 1962, calculates an overall average gold/silver of 6.5:1 with an average bullion fineness of 782 for gold. The relatively minor base metal content of the ore samples is indicated by Cu, 22 ppm \pm 21 1 σ , and Zn, 79 ppm \pm 37 1 σ . Pb, 67 ppm \pm 35 1 σ , is more abundant and reflects the presence of the lead telluride, altaite, in the ore samples. Arsenic, 5.7 ppm \pm 3.2 1 σ , and Sb, 4.2 ppm \pm 2.6 1 σ , are present at low levels but W, 29 ppm \pm 25 1 σ , is significantly enriched over normal abundance which averages 3 ppm in syenitic rocks at the Macassa Mine and 0.4 ppm in basaltic rocks generally (Helson et al., 1978). Transition metals, including V, Sc, Cr, Co and Ni are present at abundances which reflect the amount of wallrock incorporated into ore.

In summary, Macassa gold ores have the same overall metal distribution as Archean gold deposits in general, with large to moderate enrichments of rare elements including Au, Ag, As, Sb, W, Sc, Te coupled with minor to negative enrichments of the base metals Cu, Pb, and Zn (for a review see Kerrich, 1983).

4.3 Chemical Effects of Wallrock Alteration

Bruce (1933) and Thomson et al. (1948) citing analytical data originally published by Todd (1928) describe the effect of hydrothermal alteration of wallrock for the mines

of the Kirkland Lake district. They describe overall increases in CaO, MgO, CO₂ and FeO abundances and overall decreases of other major element oxides within the wall-rocks as a result of their alteration. These changes were deduced by direct comparison of the chemical composition of fresh wallrock to that of altered samples with the assumption of constant volume relations during the alteration process.

Such simple inspection and analysis of chemical data is generally not satisfactory for deducing real changes in elemental abundances. Because the major element oxides are constrained to a constant sum (100%), no single component is independent of the others and an infinite number of solutions exists (Kerrick, 1983). Gresens (1967) has pointed out that the tacit assumption of constant volume relations is untenable if alteration is accompanied by deformation with or without changes of volatile content as at the Macassa Mine.

4.3.1 Chemical Mass Balance Equation

Gresens (op. cit.) derived a general equation that expresses change in element abundances accompanying the transformation of a given parent to its complement daughter rock. This mass balance equation incorporates analyses of the whole rock, specific gravity, and a deduced volume change accompanying alteration.

Gresens mass balance equation is:

$$\Delta X_i = f(a, \beta^d, \beta^p, x_i^p, x_i^d, F_v)$$

$$\Delta X_i = a(F_v x_i^d (\beta^d / \beta^p) - x_i^p)$$

where the parameters are:

ΔX_i = Chemical change: the change in abundance of element i.

a = Initial quantity of parent rock, prescribed 100 gms.

F_v = The volume change: ratio between the final and initial volumes of rock masses.

x_i^p, d = Weight fraction of element i in parent and daughter rock, respectively.

β^p, d = Specific gravity of parent and daughter rock, respectively.

A unique solution to the general equation is obtained by measuring the composition and specific gravity of parent and daughter rocks, and inferring the change in volume accompanying the transformation in question. The volume factor is found by:

- 1) Estimating the volume change based on independent evidence such as changes in the shape of relict textures or structures;
- 2) Establishing the isochemical behaviour of two or more elements. Two elements probably remained immobile

during rock alteration if their ratio in parent and daughter rocks is the same. Component lines for immobile elements will cross the zero mass change axis in a composition-volume diagram at the same point (Gresens, 1967); or

- 3) Assuming a reasonable volume factor or chemical change for some element.

In the notation used by Gresens (op. cit.), $f_v = 1$ signifies constant-volume metasomatic alteration of reactants to products; $f_v = 0.8$ and $f_v = 2.0$, for example correspond to 20% volume reduction and 100% volume increase, respectively. The significance of calculations can be deduced by comparing the results of several pairs of parent-daughter rocks which describe the same transformation process: Consistent negative or positive quantities for X_i of a particular element i indicates leaching or addition, respectively, of the element in question.

4.3.2 Changes in Major and Minor Element Abundances During Alteration

Representative samples of wallrock associated with each of the three types of gold ore i) vein, ii) breccia and iii) break-ore (Tables 4-2 and 4-3) were used to determine and compare absolute changes in composition of the whole rock using Fortran programs ENTRY.FOR and ROCKI.FOR (Note: All computer programs used in this study

are listed in Appendix D). These rocks were compared with equivalent average parent rocks (Table 4-4) whose composition is a mean of unaltered and least altered rock analyses previously discussed (Tables 4-1 and 4-2). In the altered rocks at the Macassa Mine the volume factors for TiO_2 , Al_2O_3 and Zr typically cluster. An average of their fv's has been applied in calculations of mass balance relations.

For altered wallrocks associated with break ore, it was possible to sample in a direction perpendicular to the fault. These spatially related samples were used to define the net changes in composition of altered rock and also the lateral extent of alteration. For both vein ore and breccia ore related samples, individual altered samples were compared directly with appropriate average parent rock compositions (Kerrick and Watson, 1984).

4.3.2.1 Break ore

For Break ore it was possible to systematically sample in a direction perpendicular to the ore boundaries, in order to define both the nature and lateral extent of alteration. In general, the discernable chemical changes of alteration diminish rapidly within 2 to 10 m of ore (Fig. 4-5).

Significant additions of CO_2 , but minor variations of Fe_2O_3 , MnO , MgO and CaO abundances about zero corresponds

TABLE 4-4 Average abundances of major and selected trace elements for unaltered rocks at Macassa Mine (Major elements in weight percent, trace elements in ppm except as noted).

Sample No.	Felsic Syenite				Augite Syenite				Tuff				
	\bar{x}	PI	n	σ	\bar{x}	P2	n	σ	\bar{x}	P3	n	σ	
	70				73	1216						85	
SiO ₂	56.6	3	0.32	56.2	48.2	3	0.78	48.9	49.7	49.6	5	4.4	42.4
TiO ₂	0.61	3	0.06	0.66	0.90	3	0.05	0.85	0.81	0.94	5	0.2	1.15
Al ₂ O ₃	18.9	3	0.23	18.8	12.6	3	1.0	12.4	13.0	14.0	5	1.3	13.4
Fe ₂ O ₃ (T)	4.1	3	0.35	4.41	8.7	3	0.8	9.4	9.8	9.1	5	1.8	11.6
MnO	0.08	3	0.01	0.07	0.13	3	0.02	0.14	0.13	0.2	5	0.04	0.24
MgO	0.90	3	0.13	1.04	6.6	3	1.4	7.9	6.9	2.3	5	1.7	3.8
CaO	1.9	3	0.37	2.08	7.2	3	0.5	6.45	5.3	6.3	5	1.6	8.5
K ₂ O	7.5	3	0.41	7.8	5.5	3	0.74	4.50	6.5	9.8	4	0.6	9.00
Na ₂ O	4.4	3	0.31	4.06	3.1	2	0.78	3.5	2.6	1.03	4	0.6	0.6
P ₂ O ₅	0.22	3	0.02	0.24	0.52	3	0.03	0.54	0.60	0.69	4	0.2	0.6
LOI	3.60	3	0.41	3.23	5.2	2		4.33	4.47	6.0	5	1.5	7.0
TOTAL	98.8			98.6	98.7			98.9	99.8	100.0			98.2
CO ₂	3.03	3	0.53	3.10	4.4	3	1.9	3.25	3.5	5.4	5	1.02	6.7
S	119.7	2		104	121.6	3	38.7	166	326	148	3	49	408
Au (ppb)	17	3	8.54	25	6	1		48	3	13	4	5.4	6
Ag					0.5	1			1				
As	3.5	2		2.0	8.7	3	2.3	10	4	13.2	4	4.6	11.9
Sb	3.1	3	3.2	3.6	3.6	2		2.8	1.6	12.3	3	3.2	15
Sc	8.1	1		8.1	28.3	3	15.5	46	23	35	1		35
V	91	3	12.8	76	367	3	26.2	350	390	452	5	50.4	508

Cr	80	3	8.5	70	318	2	366	332	91	3	12	205		
Co	24	3	12.3	10	50	3	53	52	0	4		0		
Mg	18	3	2.4	16	96	3	118	121	36	5	15	67		
Cu	16	3	6.7	24	19	3	15	16	31	4	5.45	37		
Zn	56	3	15.8	61	99	3	125	136	156	3	17	154		
V	3	3	1.7	2	4	1	4	40	3	5	1.6	2		
Pb	32	3	9.1	22	25	3	21	29	52	4	12.5	48		
U	3.2	3	1.1	4.0	2.6	2	2.2	3.0	15.1	1				
Th	26	1		28	9	3	11	31	54	2		41		
Nb	206	3	20.8	190	166	3	209	312	276	4	43	285		
Sr	562	3	145	718	692	2	629	1622	2097	5	820	3060		
Y	21	3	2.6	22	24	3	22	23	37	5	7.6	45		
Zr	265	3	47.1	240	156	3	145	170	436	5	66	411		
Mn	10	2		8	6	2	6	20	15	4	5.1	14		
Ba	817	3	131	976	132	3	1166	2183	5261	3	517	4724		
S.G. ⁰²		2.58	3	0.01	2.58	2.78	3	0.02	2.77	2.79	2.72	3	0.02	2.50

⁰¹ LOI = weight percent loss on ignition at 1000° C.

⁰² S.G. = specific gravity (2σ = ± 0.02).

⁰³ P1, P2 and P3 represent average felsic syenite, augite syenite and tuff rock composition. For each, \bar{x} = average major and trace element abundance, n = number of analyses in average, σ = 1 standard deviation from calculated average value.

401

Figure 4-5. Gains and losses of chemical components accompanying hydrothermal alteration of break ore (expressed as percentage changes relative to abundances in parent rock). Altered products are arranged according to distance from the break. Small bars indicate variations in gain or loss about the data points, arising from one standard deviation of the mean volume factor (from Kerrich and Watson, 1984).

to the hydrolysis of Fe, Mg, Ca, Mn-silicate minerals to Fe, Mg, Ca, Mn-carbonate minerals during alteration; and further signifies that hydrothermal fluids depleted the CO_2 whereas the bivalent metal cations were indigenous to wall rocks. K_2O and Na_2O have minor variable gains or losses in which they behave antipathetically, reflecting the hydrolysis of albite to muscovite accompanying additions of potassium from the hydrothermal fluids. As for the other ore types discussed below, Cr, Ni, Cu and Zn vary little, with Pb as the only base metal having pronounced additions. Significant introduction of S is evident for the '04 Break and Narrows breaks, whereas sulfur is actually leached from the Main Break wall rocks (Kerrick and Watson, 1984).

4.3.2.2 Vein ore in syenite

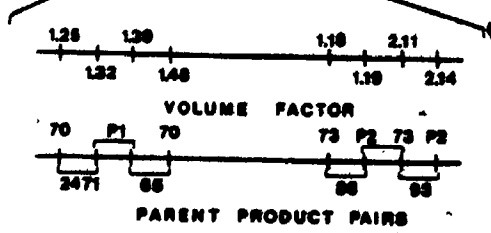
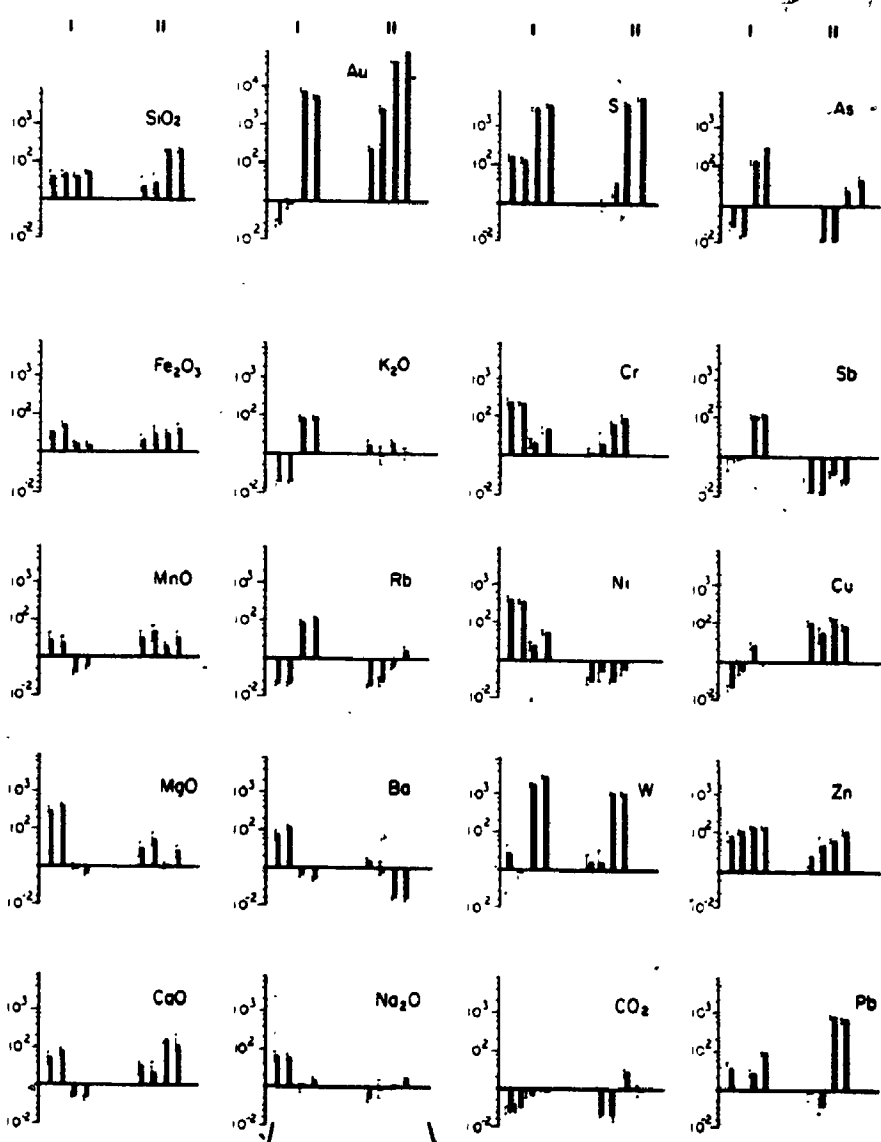
Transfers of chemical components during hydrothermal alteration of the syenite traversed by the 26A vein (Group I samples) and of syenite adjacent to the 58E vein (Group II samples) are illustrated in Fig. 4-6. The syenites have been altered according to deduced volume factors of 1.2 to 1.5 and 1.2 to 2.1 respectively, which represent volume increases of 20-50% in the former host rock and 20-110% in the latter.

Massive gains of gold and sulfur, reflected in the presence of native gold and pyrite, are the salient

Figure 4-6. Gains and losses of chemical components during hydrothermal alteration associated with 26A vein (group I) and 58E vein (group II) ore (expressed as percentage changes relative to abundance in average parent rock and selected individual parent rocks). Altered products are arranged in order of increasing volume factor. Small bars indicate variations in gain or loss about the solid bars, arising from one standard deviation of the mean volume factor (from Kerrich and Watson, 1984).

Vein Ore Alteration

Percentage gains and losses relative to parent rock



features of alteration in these rocks. Additions of iron are minor compared to sulfur, suggesting that much of the iron present in pyrite is derived from hydrolysis of Fe-Mg silicate minerals indigenous to the parental syenites, whereas 98% of the sulfur has been added from solution. Small net gains of SiO_2 correspond to the presence of vein quartz, and of Fe_2O_3 , MnO , MgO plus CaO to the precipitation of Fe, Mn, Mg, Ca-carbonate minerals.

Sodium and potassium have variable minor gains or losses, expressed in the relative proportions of albite and muscovite respectively: Rb and Ba vary broadly with K_2O . Of the transition and base metals, Cr plus Ni have been added overall, residing in chlorite and muscovite, whereas there is a massive addition of tungsten as the ubiquitous scheelite. Copper, Zn and Pb have all been added to a variable extent, whereas As and Sb have erratic minor variations about zero gain/loss.

Altered syenite adjacent to veins are neither extensively hydrated nor have significant fixation of CO_2 - consistent with the minor amounts of hydroxy or carbonate minerals observed.

4.3.2.3 Breccia ore in augite syenite and tuff

Introduction of gold and sulphur on a massive scale are the most pronounced chemical transfers involved in the hydrothermal alteration accompanying breccia ore within the

augite syenite and tuff (Fig. 4-7). Iron and S behave in a manner comparable to alteration about vein ore.

Fixation of SiO_2 is more pronounced in breccia in the tuff versus breccia in augite syenite, consistent with a greater proportion of massive quartz in the former. Small gains or losses of Fe_2O_3 , MnO , MgO and CaO reflect variability in the relative abundance of Fe, Mn, Mg, Ca-carbonate minerals. Potassium and Rb have comparable minor overall gains, but whereas Ba covaries with K_2O in the tuff-hosted breccia ore it behaves erratically in the brecciated augite syenite. Given that K_2O is predominantly in feldspar and biotite in parental rocks, but is incorporated into muscovite in altered equivalents, and further that for the ore, Ba plus Rb do not reside in minerals other than muscovite, these relations collectively suggest that the micas are not unusually Rb or Ba-rich, a conjecture confirmed by electron microprobe analysis.

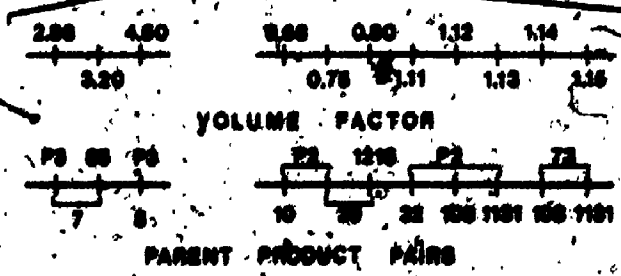
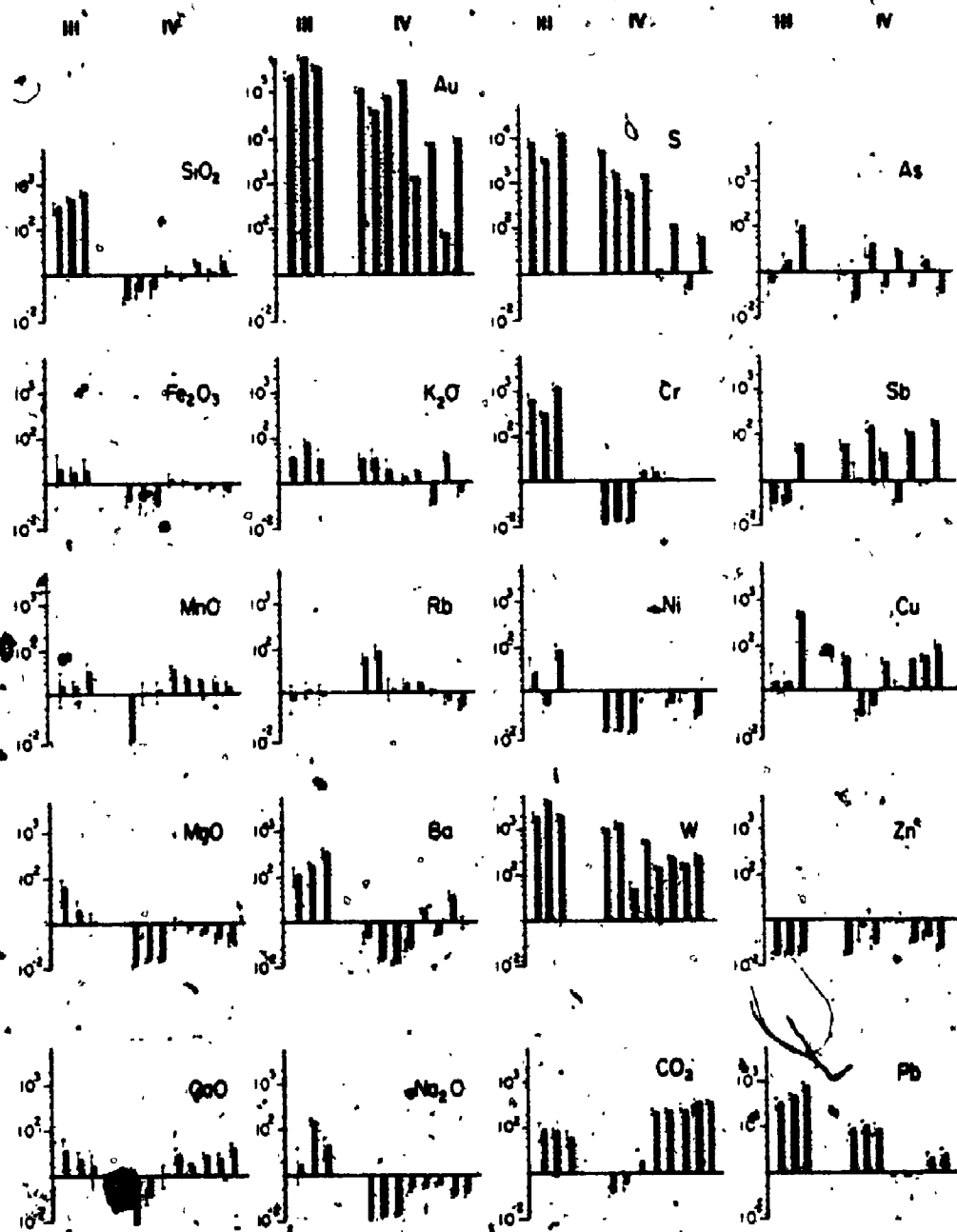
Chromium and Ni have been added in minor amounts to breccia ore in tuff, where they substitute in chlorite and muscovite; however, these elements are leached from breccia ore in augite syenite. As for the vein ore counterparts, massive introduction of tungsten is represented by the presence of scheelite. Arsenic and Sb abundances are essentially comparable to those for the vein ores.

101

Figure 4-7. Gains and losses of chemical components during hydrothermal alteration associated with tuff breccia (group III) and augite syenite breccia (group IV) ore (expressed as percentage changes relative to abundance in average parent rock and selected individual parent rocks). Altered products are arranged in order of increasing volume factor. Small bars indicate variations in gain or loss about the solid bars, arising from one standard deviation of the mean volume factor (from Kerrich and Watson, 1984).

Breccia Ore Alteration

Percentage gains and losses relative to parent rock



4.3.3 Changes in REE abundances during hydrothermal alteration

Rare earth element abundances in altered rocks remain close to those of parent syenite, and overall, hydrothermal fluids have not fractionated the REE during interaction with wall rocks (Fig. 4-4). A single exception to this is the 58E vein, a K-feldspar, actinolite, quartz, chlorite fracture selvage, which possesses a pronounced negative Eu anomaly relative to unaltered augite syenite (Fig. 4-4): this may result from hydrolysis of plagioclase.

Behaviour of the REE during hydrothermal alteration associated with Archean lode gold deposits has been discussed by Kerrich and Fryer (1979) and Kerrich (1983). It appears that in this alteration the REE are relatively immobile, except under conditions of intense carbonatization where the HREE are preferentially taken into solution. For the 58E vein specifically, and at the Macassa Mine in general, carbonatization is not intense, such that the relatively undisturbed patterns in rocks that have reacted with the hydrothermal fluids, is consistent with essentially isochemical behaviour in the REE.

4.3.4 Oxidation State of Iron

The oxidation state of iron in rocks, expressed as the ratio of ferrous iron to total iron (Fe^{2+}/Fe_{total}), is a sensitive indicator of fluid flow. Changes in ferric to

ferrous iron can occur in rocks that have reacted with large volumes of fluid bearing oxidizing or reducing agents.

The abundance of ferrous iron in 19 selected unaltered and altered rocks from the Macassa Mine was determined titrimetrically by the method described in Wilson (1955). From this and other previously published and unpublished data cited at the beginning of this chapter, the ratios of Fe^{2+}/Fe_{total} were calculated (Table 4-5).

Unaltered syenite has an average Fe^{2+}/Fe_{total} ratio of 0.61. Unaltered tuffs of the Timiskaming Group are less reduced than the syenite with an average ratio of 0.45. In contrast, altered syenite adjacent to gold ore is moderately to very reduced with ratios varying from 0.64 to 0.93. Similarly, samples from the Main Break, vein ore and breccia ore zones are reduced with respect to unaltered rocks. These data suggest the influence of fluids capable of reducing the wallrocks.

However, samples from the '04 and Narrows Break have Fe^{2+}/Fe_{total} less than the average 0.60 indicating these rocks are less reduced with respect to unaltered rocks. In both instances, samples taken at increasing intervals away from the break itself have a gradual return to near normal Fe^{2+}/Fe_{total} within 4 to 5 m. These data suggest the influence of fluids capable of oxidizing the wallrocks.

It is unlikely that reducing and oxidizing fluids

TABLE 4 - 5(a) Ferrous to Total Iron Ratios For Selected Unaltered Rocks, Macassa Mine and Area.

Rock Type	Sample No.	FeO (wt.%)	Fe ₂ O ₃ (wt.%)	Fe ₂ O ₃ * ¹ Total (wt.%)	Fe ²⁺ /ΣFe
<u>Augite Syenite</u>					
	PL-188	4.54	3.55		0.59
	PL-189	5.10	3.33		0.63
	PL-191	4.05	2.67		0.63
	PL-192	3.73	3.40		0.55
	PL-193	4.05	2.76		0.62
	PL-194	4.05	2.51		0.64
	PL-196	4.70	3.19		0.62
	PL-197	4.86	3.92		0.58
	Thomson No.6* ²	4.48	2.77		0.64
	Av.North Suite* ³	4.60	3.34		0.60
	Av.Main Suite* ³	4.24	3.86		0.55
<u>Felsic Syenite</u>					
	Thomson No.7* ²	2.67	0.98		0.75
	Av.Main Suite* ⁴	2.69	1.89		0.61
<u>Porphyritic Syenite</u>					
	Thomson No.8* ²	2.03	1.38		0.62
	Av.North Suite* ³	1.67	1.69		0.52
	Av.Main Suite* ³	1.70	1.52		0.55
<u>Trachytic Tuffs</u>					
	Thomson No.1* ²	3.84	4.73		0.47
	Thomson No.2* ²	4.71	6.36		0.45
	G-80	3.11		7.89	0.44
	G-85	4.56		11.6 ²	0.44

*¹ Total iron expressed as Fe₂O₃.

*² Data from Thomson et al (1950); their Table 5.

*³ Data from Ploeger (1981), Table 1.

Table 4 - 5(b) Ferrous to Total Iron Ratios for Selected Altered Rocks and Ores, Macassa Mine and Area.

Rock Type	Sample No.	FeO (wt.%)	Fe ₂ O ₃ (wt.%)	Fe ₂ O ₃ * ¹ Total (wt.%)	Fe ²⁺ /ΣFe
<u>Altered Augite</u>					
<u>Syenite</u>	1211	4.32		9.89	0.48
	1212	4.63		8.79	0.59
	1214	4.07		9.04	0.50
	1216	5.50		9.82	0.62
	Thomson No. 12* ²	7.10	3.00		0.72
<u>Altered Felsic</u>					
<u>Syenite</u>	2471	2.43		4.46	0.60
	Thomson No. 11* ²	4.78	0.97		0.84
<u>Altered</u>					
<u>Porphyritic</u>					
<u>Syenite</u>	Thomson No. 9* ²	1.16	1.08		0.54
	Thomson No. 10* ²	2.41	0.94		0.74
<u>Main Break</u>					
	113	5.48		8.26	0.74
	117A	5.99		9.54	0.70
	116	4.79		9.19	0.58
	115	3.79		7.76	0.54
<u>Narrows Break</u>					
	140	2.32		5.57	0.46
	139	2.58		4.94	0.58
	138	3.91		6.00	0.72
	137	3.02		5.71	0.59
	135	5.56		8.62	0.72
<u>58-E Vein</u>					
	93	4.31		5.83	0.82
	86	5.48		9.50	0.64
<u>Breccia Ore</u>					
	5.14			7.99	0.71
	Thomson No. 18* ²	6.07	1.49		0.82
	Thomson No. 19* ²	3.00	0.91		0.78

*¹ Total iron expressed as Fe₂O₃.

*² Data from Thomson et al (1950), their Table 5.

would co-exist within the same hydrothermal system. It is suggested that the oxidation state of iron in the altered rocks is the effect of two distinct fluid systems. Further evidence on the nature of these systems will be discussed in following sections on the relative abundance of oxygen and hydrogen isotopes.

CHAPTER 5

OXYGEN AND HYDROGEN ISOTOPE ABUNDANCE AND FLUID INCLUSION DATA

5.1 General Statement

Because H_2O is the dominant constituent of ore forming fluids, a knowledge of its origin is fundamental to any theory of ore formation (Taylor, 1979). Any naturally occurring water is potentially an ore-forming fluid if it becomes heated as a result of deep circulation in the crust or through interaction with a magma body. Investigation of hydrogen and oxygen isotope abundances of natural waters, fluid inclusions trapped in hydrothermal minerals, and rock-forming minerals have identified four different sources of H_2O in the earth's crust (Taylor, 1974, 1979). These water reservoirs, each with characteristic δDH_2O and $\delta^{18}OH_2O$, are designated as primary magmatic, metamorphic, seawater and connate and meteoric waters.

The oxygen isotope abundances of the whole rock and separate minerals of the syenites and three types of gold ore described previously at the Macassa Mine were determined by Dr. R. Kerrich at the University of Western

Ontario following the analytical methods outlined in Appendix A. Hydrogen isotope analyses, conducted by Dr. J. Bowman, Salt Lake City, were done for a limited number of chlorite and actinolite mineral separates from selected gold-bearing samples. Homogenization temperatures of fluid inclusions within quartz from selected gold ores were studied using a Linkham TH600 Fluid Inclusion stage at the University of Western Ontario.

A limited number of samples were selected from the larger suite of igneous and volcanoclastic rocks and principal gold ore types collected from the Macassa Mine during the course of this study. Samples of unaltered rock were selected to determine the origin and extent of isotopic reequilibration. Samples of gold ores were selected to evaluate thermal conditions and fluid reservoirs implicated in gold mineralization.

Given the variety of ore types and the multistage nature of quartz veining and fracturing, a large number of isotopic and fluid inclusion analyses would ideally be required to understand the ore forming system in detail. Because of the difficulty and expense of obtaining isotopic analyses, only 65 analyses are presented (Table 5-1). Because of the difficulty of obtaining suitable materials for fluid inclusion study, only data on homogenization temperatures as a first approximation to trapping temperatures are presented.

TABLE 5-1 Oxygen and hydrogen isotopic compositions of whole rocks and mineral separates from the Macassa Mine and environs, Kirkland Lake, Ontario.

Sample description	Sample Number	Sample location	$\delta^{18}O$ whole rock	$\delta^{18}O$ quartz/feldspar	$\delta^{18}O$ chlorite/muscovite	$\delta^{18}O$ amphibole/epidote	$\delta^{18}O$ magnetite mineral	$\delta^{18}O$ quartz/mineral	T°C	$\delta^{18}O$ fluid
PRINCIPAL TONNESQUE ROCK TYPES										
Felsic syenite	G-80-70 G-86	2075' level	8.63 9.20			6.02 (h)				
Amphibole syenite	G-80-73 G-80-95 G-80-114	5450' level, 28 W	6.74 6.66 6.12	7.38 (f) 6.60 (f)		5.05 (ag) 4.39 (ag)		2.32 (f-ag) 2.21 (f-ag)		
Perthitic syenite	G-80-143 G-3475	3000' level, Casalfrk X-cut 7200' level, W-epidote/graves	9.96 6.56	11.04 (f)		5.71 (h)		5.33 (f-h)		
Troctolite syenite tuff	G-80 G-80-85 G-80-124	3000' level, E 4250' level, near S2 vein 5300' level by pass drift	9.60 7.74	10.93 (f)		5.58 (h)		5.35 (f-h)		
BIOTIC ORE										
Fault group: massive syenite with chlorite, other quartz, + magnetite	A	5450' level (M Break)		13.96*	1.7 ⁹ (c)			+ 2.96*	-70 (c)	12.3 (q-c) 11.0 (q-m) 200 440 +0.5 +9.6
Massive quartz from fault group	B			12.50 v 12.21 m				0.82*		11.7 (q-m) 430 +8.0
Altered epide syenite. (Fault) to A,B	C			8.59	10.33 m			11.39		
Drainaged epide syenite	D(G-80-113)	2000' level (N in Break)	9.15					5.60		
Quartz fragments and fault group	E	3000' level, Casalfrk (Barron Break)		12.48 v 12.61 m	3.09 (c)			-87 (c)	9.4 (q-c)	250 +0.2.2.
Fault group and breccia (subunit)	H(G-80-125)	5725' level, 20 W (M Break)		11.26*				4.26		

WEIR ONE										
High grade vein in felsic syenite	26-SA	F	12.63 v 11.63 m							
Vein quartz	42-52 vein	G-80-82	13.64							
High grade vein	42-52 vein	G-80-60	12.63 v 9.78 (ms) 6.03 (c)						3.8 (q-ms) 6.6 (q-c)	300 +7.0
E WEIR SYSTEM (amphibole, garnet, W association)										
Altered amphibole syenite	5075 level, footwall of E vein	G-80-88	11.89	5.97	5.00 (a)	1.93	-60 (a)	6.9 (q-a) 10.0 (q-m)		490 +0.5
Vein quartz	50-E vein	G-80-92	11.52 v 11.56 m		4.81 (a)		-105 (a)	6.7 (q-a)		
E-feldspar-actinolite-quartz-chlorite vein	50-E vein	G-80-71	11.90 v 9.74 (r)		6.39 (a)	1.30		2.1 (q-f) 6.0 (q-c) 5.5 (q-a)		420 +7.2
QUARTZ-AMPHIBOLE STRONGERS										
Vein Quartz, with amphibole, biotite	50-E-17 57-E-16 system	G-80-130	12.37 m							
Quartz-amphibole vein	50-04 E	G-82-150	12.12	-0.4 (c)		-11.80		12.6 (q-c) 23.9 (q-m)		260 -4.0 to 210 -0.5
DRIFT										
Quartz fragments from buff horizon, with amphibole	5475 drift, 31-5 W	G-80-8	12.56							
Buff breccia ore	54-32 slope (50' above G-80-8)	G-80-38	12.91			7.58				
Partially microfractured amphibole syenite	5475' level, 32 W	G-80-32	12.57			0.54		12.0 (q-m)		420 7.9

(q-c) = quartz-chlorite; (q-a) = quartz-actinolite; (q-m) = quartz-muscovite; (r-ag) = feldspar-amphibole; (r-h) = feldspar-hornblende.
 Isotopic temperatures and $\delta^{18}O$ rigid calculated from the fractionation equations reported by Clayton et al. (1972) for quartz-water; Berman and Taylor (1971) for chlorite-water; Jørgensen (1977) for quartz-amphibole; Friedman and O'Neill (1977) for quartz-muscovite; O'Neill and Taylor (1967).
 The postscript v signifies vein quartz, and m matrix quartz from the adjacent wall rock.
 * The $\delta^{18}O$ chlorite values have been estimated from isoscape analysis of ultrafine grained chlorite plus quartz mixtures and their relative proportions (see analytical methods).
 * Composite quartzite.
 ag = amphibole; f = feldspar; h = hornblende; c = chlorite; ms = muscovite.

5.2 Calculation of temperature and isotopic composition of hydrothermal fluids

Ambient hydrothermal temperatures for the various ore types at the Macassa Mine have been calculated from oxygen isotope fractionations between mineral pairs or triplets, employing appropriate mineral-water fractionation equations, according to conventional procedures (for a discussion see Taylor, 1974, 1979; Bottinga and Javoy, 1975; and Javoy, 1977). This study utilized the experimentally, and empirically determined mineral-water equations for quartz, K-feldspar, amphibole, and chlorite as reported by Clayton et al. (1972), O'Neil and Taylor (1964), Javoy (1977) and Wenner and Taylor (1971) respectively. Isotopic temperatures from quartz-magnetite fractionations were interpreted using the graphs of Friedman and O'Neil (1977).

It is important to emphasize that ~~triple~~ isotopic concordancy is required among three coexisting minerals in order to obtain a reliable temperature estimate. Concordant temperatures were assigned to those samples for which TOC quartz-K feldspar, TOC quartz-chlorite and TOC K feldspar-chlorite agree to within an uncertainty in Δ quartz-K feldspar, Δ quartz-chlorite, etc., where the error in mineral pair fractionations $\epsilon\Delta = (\epsilon_{\delta}^2 + \epsilon_{\delta}^2)^{0.5} = \pm 0.17$ per mil, and the reproducibility of δ -values is ± 0.12 per mil (cf. Bottinga and Javoy, 1973).

Triple isotopic concordancy is present in two of the vein samples where three or more minerals could be separated. For the remaining samples only two minerals were isolated for analysis, and thus isotopic concordancy could not be demonstrated. However, in these samples the isotopic temperatures calculated from the fractionation between two minerals was found to be close to those derived from triply concordant assemblages, and with independent estimates of temperature based on hydrothermal mineral assemblages and fluid inclusion filling temperatures. Taylor (1974) emphasizes that isotopic disequilibrium relations are the rule and not the exception in hydrothermal ore deposits. Despite this, valid conclusions can be made of fluid isotopic abundances provided a mineral resistant to post-formation reequilibration, like quartz, is used (Clayton et al., 1968; Taylor, 1974) and an independent estimate of temperature, like fluid inclusion homogenization temperature, is available.

Calculation of fluid $\delta^{18}\text{O}$ was based on the measured mineral δ -value, and temperatures as estimated above, in conjunction with the appropriate mineral-water fractionation equation, generally the quartz-water curve of Clayton et al. (1972). Water δD was calculated by the same means as for $\delta^{18}\text{O}$ H_2O , employing the measured δD mineral, a temperature estimate, coupled with the appropriate mineral-water fractionation equation (see Taylor, 1974,

1979). For chlorite, the chlorite-water curves of Taylor (1974) and Marumo et al. (1980) were utilized. There is little information on hydrogen isotope fractionation between amphiboles and water. Thus for actinolites at the Macassa Mine, the data of Graham and Sheppard (1978) on aluminous pargasitic hornblende was used as a first approximation.

Suzuki and Epstein (1970, 1974) and Taylor (1974, 1979) have emphasized that D/H fractionations among silicate minerals are primarily a function of the Mg, Al and Fe contents of the minerals. For instance Mg-rich and Al-rich minerals concentrate deuterium relative to Fe-rich minerals under the same conditions. For this reason, and given some uncertainties in temperature, a range of calculated $\delta D H_2O$ is given below.

5.2.1 $\delta^{18}O$ of Syenite and Trachytic Tuffs

Syenite that is relatively fresh has oxygen isotope compositions for the whole rock from 6.6 to 10‰ (Table 5-1). This includes the entire span of $\delta^{18}O$ for isotopically 'normal' felsic plutonic rocks, defined as $+6‰ < \delta^{18}O < +10‰$ (Taylor, 1978), and indicates that no significant component of high $\delta^{18}O$ metasedimentary or hydrothermally altered igneous rocks participated in the source region melting, or contaminated a primary igneous syenitic magma. For syenite specifically, Taylor (1968)

reported that whole rock typically has 6.0 to 7.00/00; K-feldspar, 6.5 to 8.80/00; and augite, 5.5 to 5.90/00. Hence the syenites at Kirkland Lake are isotopically similar to, or enriched by less than 30/00 relative to fresh counterparts.

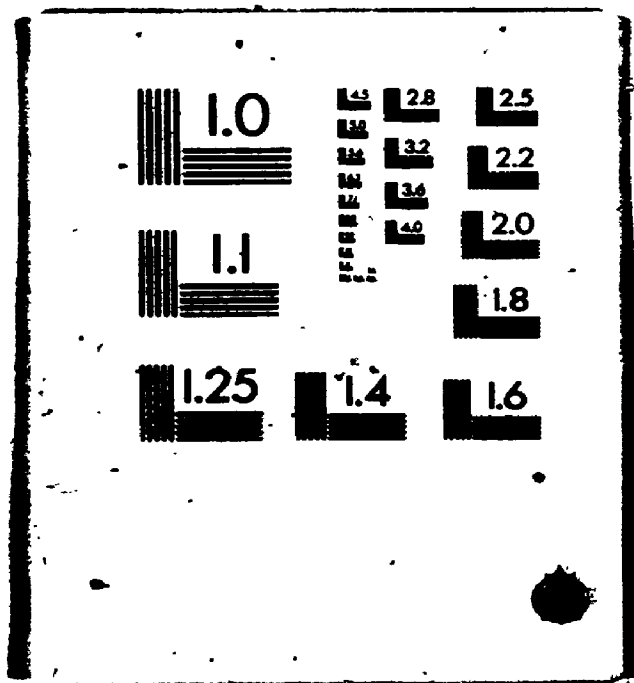
Overall, the augite syenite has the least ^{18}O , as is expected from its greater proportion of mafic minerals and their lesser ^{18}O content relative to coexisting feldspar at equilibrium. The greatest content, 9.20/00 in felsic syenite, 10.00/00 in porphyritic syenite, and 9.60/00 in tuff, likely represent a trend of ^{18}O enrichment from primary igneous abundance during sub-solidus, partial oxygen isotope exchange with a fluid reservoir. Various possible fluid regimes that would be consistent with the deduced trend of sub-solidus ^{18}O enrichment include pristine marine water ($\delta^{18}O \approx 00/00$) at 200°C, or an isotopically heavier reservoir such as evolved marine water, formation brines, or metamorphic fluids at greater temperatures. This multiplicity of possible fluid-alteration regimes is generally resolved by measuring $\Delta^{18}O$ quartz-feldspar, an approach that is not possible for the case of quartz-free syenites (Watson and Kerrich, 1983).

5.2.2 $\delta^{18}O$ and δD of Ores

5.2.2.1 Break Ore

Massive quartz from the break ore has a relatively

3



narrow range of $\delta^{18}O$ at 12.2 to 12.5 (Table 5-1). Quartz isolated from the neighbouring wall rocks is isotopically similar to breccia matrix counterparts, signifying close isotopic equilibrium between fluids, breccia matrix quartz, and wall rock quartz; and in addition a fluid dominated system along fracture conduits now occupied by ores.

On the other hand, minor quartz isolated from brecciated syenite at $\sim 11.50/00$ (samples C, H), and accessory quartz present in chlorite- or selenite-dominated break ore at $140/00$ (sample A), are systematically lighter and heavier respectively than the massive variety of quartz in break ore. The isotopic abundances of magnetite is very variable in rocks enclosing break ore. Magnetite present in small quantities in rocks is known to undergo partial retrograde isotope exchange with coexisting minerals toward more $\delta^{18}O$, and this effect may account for the observed spread of $\delta^{18}O$ abundance in magnetite of rocks about break ore, where the greatest $\delta^{18}O$ is in rocks with < 5 weight percent magnetite. Accordingly, only those samples with abundant magnetite have been utilised for computing isotopic temperatures from quartz-magnetite fractionations: these are $440^{\circ}C$ (A) to $430^{\circ}C$ (B). The calculated $\delta^{18}O$ of fluids in equilibrium with quartz and magnetite is 8.0 to $9.60/00$ (Table 5-1). Such isotopic abundances in fluids are consistent with either magmatic or metamorphic hydro-

thermal solutions, but are isotopically heavy compared to meteoric or marine waters that have undergone high temperature isotope exchange with crustal rocks (c.f. Taylor, 1974).

Quartz-chlorite fractionations of 11.3 and 9.40/00 for samples A and E correspond to temperatures of 200 and 250°C respectively; and a fluid in equilibrium with the chlorite of +0.5 and 2.20/00 for the specified temperatures (Table 5-1). Two samples of chlorite from the break analyzed for their hydrogen isotope composition have a δD of -87 (sample E) and -70 per mil (sample A). Assuming an equilibration temperature of 200°C for fluids and hydrogen in silicate minerals, the calculated δD H₂O would be -70 to -20 per mil (Table 5-1). This range of fluid δD and $\delta^{18}O$ could plausibly reflect low-temperature evolved meteoric water.

The large differences in temperatures and fluid isotopic abundances deduced from Δ quartz-magnetite and Δ quartz-chlorite in sample A (Table 5-1) signify isotopic disequilibrium between the three minerals. Such relations are to be anticipated in view of the observed coexistence of selenite and pyrite in sample A indicating mineralogical and redox disequilibrium. Furthermore, two varieties of quartz are present in some samples which could have distinct isotopic signatures; for instance A contains white and citrine quartz, but white and rose quartz are present in sample H. Taking these features into consideration,

along with the inference that, whereas quartz does not readily undergo oxygen isotope exchange at $<300^{\circ}\text{C}$, chlorite may do so in the presence of large water/rock, then the quartz-chlorite fractionations yield both maximum temperatures and fluid $\delta^{18}\text{O}$ abundance.

The disequilibrium mineral association and oxygen isotope fractionations of some break ore may reflect multi-stage fluid regimes: an earlier episode of fluids with higher $\delta^{18}\text{O}$ of probable metamorphic origin implicated in the precipitation of Au, quartz, chlorite and magnetite, followed by a subsequent episode involving incursion of SO_2 -bearing oxidising fluids initially at $<200^{\circ}\text{C}$ for an anhydrous sulphate-precursor to selenite, finally waning to 50°C for stability of selenite itself.

5.2.2.2 Vein Ore

Gold-bearing quartz in vein ore has a $\delta^{18}\text{O}$ of 12.6 to 13.6 per mil. Quartz in wall rocks to veins is isotopically similar to that of neighbouring vein quartz, indicating close isotopic equilibrium among fluids, vein quartz and wall rock quartz; and also signifying a fluid dominated system in rocks bounding veins (Table 5-1). In one sample (G80-60) quartz, muscovite and chlorite are in triply concordant equilibrium, with fractionations corresponding to an isotopic temperature of 380°C . The calculated $\delta^{18}\text{O}$ of water in equilibrium with quartz at the specified

temperature is +7 per mil.

Quartz of the E vein system has uniform isotopic abundances of 11.5 and 11.9‰ (Table 5-1), or about 1.5‰ lighter than those characteristic for gold-bearing vein ore discussed below (quartz-magnetite veins excluded). Quartz in the wall rocks is isotopically similar to vein quartz (c.f. sample G-80-92, Table 5-1). Triply concordant isotopic equilibrium is present between quartz, K feldspar, and chlorite in sample G80-71, defining an isotopic temperature of 420°C, and a calculated $\delta^{18}\text{O}$ H₂O of +7.2 per mil, assuming equilibrium between quartz and the fluid (Table 5-1). Magnetite in this rock is close to isotopic equilibrium with the other minerals, but as for examples discussed above where magnetite is present in small quantities, there is a tendency for it to selectively re-equilibrate toward greater ¹⁸O abundance. If the magnetite in G-80-88 is in isotopic equilibrium with co-existing quartz, then the mutual fractionation of 10.0 per mil corresponds to precipitation temperatures for the veins of 490°C (cf. Friedman and O'Neil, 1977) and a fluid isotopic composition of +8.5 per mil. In view of the inference that magnetite in other samples has undergone variable degrees of re-equilibration toward greater δ -abundance, the above Δ quartz-magnetite should be considered as a minimum, thus yielding maximum estimates of temperature and fluid $\delta^{18}\text{O}$.

The magnetite-bearing veins contain a coexisting amphibole which is actinolitic in composition and isotopically uniform at 4.8 to 5.00/00 (Table 5-1). No experimental mineral-water calibration exists for amphiboles, and thus it is difficult to establish whether or not the quartz, amphibole and magnetite are isotopically concordant. Javoy (1977) gives the equation $10^6 \ln \alpha_{\text{quartz-hornblende}} = -0.30 + 3.15 \times 10^6 T^{-2} (\text{OK})$, deduced on a combined theoretical and empirical basis for igneous rocks at high sub-solidus temperatures. Use of this equation gives temperatures of 400°C for the magnetite-amphibole-quartz veins which is not in close agreement with that deduced from quartz-magnetite. Such apparent isotopic disequilibrium has previously been reported for hydrothermal actinolite and cummingtonite (Costa, 1980), and it seems likely either that extrapolation of the quartz-hornblende equation to lower temperatures is invalid, or that this equation is inappropriate for other amphibole compositions.

The δD of two actinolitic amphibole separates from the E vein system are -60 (G90-92) and -105 per mil (G80-88) respectively (Table 5-1). Assuming an equilibration temperature of 400 to 450°C for H₂O with the hydrogen in silicate minerals, the calculated fluid δD would be -85 to -35 per mil.

The quartz-magnetite-chlorite vein has distinctively

minor $\delta^{18}O$ in chlorite and magnetite compared to any other minerals analysed (Table 5-1). In sample G-82-150 quartz, chlorite and magnetite approach triple concordancy, with the mineral pair fractionations corresponding to temperatures of 210 to 260°C and fluids of -4.0 to -0.50/00. The isotopic abundance of the fluid is consistent with a hydrothermal reservoir of meteoric origin ($\delta^{18}O < 00/00$), and may signify downward penetration of surface groundwaters from terrain above sea level.

5.2.2.3 Breccia Ore

Quartz from the matrix of breccia ore is isotopically uniform at 12.6 to 12.90/00. This is in close compliance with what is believed to be single stage and isotopically least disturbed massive quartz samples from break ore (Table 5-1). As for the instance of rocks of break ore, magnetite in breccia ore has a wide spread in $\delta^{18}O$ abundance; in this ore type, 70/00, from 0.5 to 7.60/00. If the quartz and abundant magnetite present in sample G-80-32 are assumed to be in equilibrium, then the quartz-magnetite fractionation of 12.00/00 corresponds to a temperature of 420°C and an isotopic ratio of the fluid 7.90/00.

5.3 Data from Fluid Inclusions

Fluid inclusions are small, usually microscopic volumes of fluid trapped within crystals during their

growth from the fluid. Although usually trapped as a homogenous fluid at the temperature (and pressure) of growth, they are generally multiphase when examined at room temperature.

Inclusions that form as the host crystal is growing are called primary. Secondary inclusions originate from healing of cracks within crystals and trapping of later fluids different from those associated with crystal formation. Some secondary inclusions are trapped in fractures that occur while the host crystals are still growing - these are termed pseudo-secondary inclusions. The criteria for distinguishing the three types of fluid inclusions are summarized in Appendix B from Roedder (1979).

Fluid inclusion study can provide direct data on the time and space variations of temperature, pressure, density and composition of fluids in geologic environments. Such use is based on the following major assumptions (from Roedder, 1967):

- 1) as a crystal grows in a fluid medium irregularities in growth will cause the trapping of small pockets of fluid.
 - 2) the fluid within an inclusion is representative of the fluid at the time of trapping.
 - 3) there has been no significant gain or loss of material within the inclusion since the time of trapping.
- Roedder (1967, 1976) has discussed these assumptions and their limitations.

Study of fluid inclusions from selected gold-bearing rocks of the Macassa Mine was limited to determination of homogenization temperatures (T_h) as a first estimate of the temperature of formation (T_f) or inclusion trapping. The latter is called also a "corrected temperature of homogenization". On cooling from the temperature of formation, the fluid within an inclusion shrinks and an inclusion that originally contained a single, homogenous fluid phase generally forms a vapour bubble. The homogenization temperature (T_h) is the temperature of disappearance of this bubble as determined on a microscope heating stage. If the pressure on a fluid at the time of trapping was greater than the vapour pressure of the fluid in the inclusion at the moment of homogenization, the inclusion will homogenize at a temperature below that at which it was initially formed. The difference between T_h and T_f is a pressure correction. The homogenization temperatures provide a minimum value for T_f (Roedder, 1984).

The data was intended primarily to provide an independent method of verifying hydrothermal fluid temperatures calculated from isotopic data discussed previously. Instrumentation limitations and the difficulty encountered in identifying suitable fluid inclusions in the generally fractured and broken quartz from all three ore types did not allow for fluid inclusion investigation beyond this preliminary stage.

5.3.1 Break Ore

Polished grain mounts of quartz crystals isolated from a chlorite and selenite-bearing section of the '04 Break were used to study fluid inclusions associated with break-ore. Two types of primary inclusions were identified: 1) 2 phase, fluid rich inclusions with filling factors ranging from 30 to 50 percent, and 2) three phase inclusions with a vapour bubble surrounded by a fluid (at room temperature) within a second fluid phase. The liquid surrounding the vapour phase was determined to be CO_2 as it was observed to disappear upon heating from 29.50 to 30.50°C. More than 80% of inclusions observed were of the first type. Both types were identified as primary inclusions on the basis of their isolated, irregular occurrence within individual quartz grains and regular or equant habit. All inclusions were very small, generally ranging from 3 to 6 μ in diameter. Trains of secondary inclusions (all two phase) were localized along microfractures within single grains and commonly were smaller and thinner than primary inclusions.

Provisional studies of 60 two-phase and CO_2 -rich three phase primary inclusions in two samples of '04 Break-related quartz grains yielded homogenization temperatures in the range 180° to 230°C. These data are in good accord with isotopic temperatures based on quartz-chlorite fractionation discussed in the preceding section, taking into account pressure corrections of 100 to 150°C.

5.3.2 Vein Ore

Samples of vein quartz from the 26-A vein system were used to study fluid inclusions related to vein ore. Approximately 40 inclusions in 2 samples were subjected to heating study. Primary inclusions were of two types: 1) two phase, fluid rich inclusion with variable filling factors, tentatively recognized as evidence for phase separation and 2) relatively smaller, 3 phase, CO₂ rich inclusions similar to those described for break-related samples. Fracture-related trains of 2 phase, secondary inclusions were also observed (Plate 5-1).

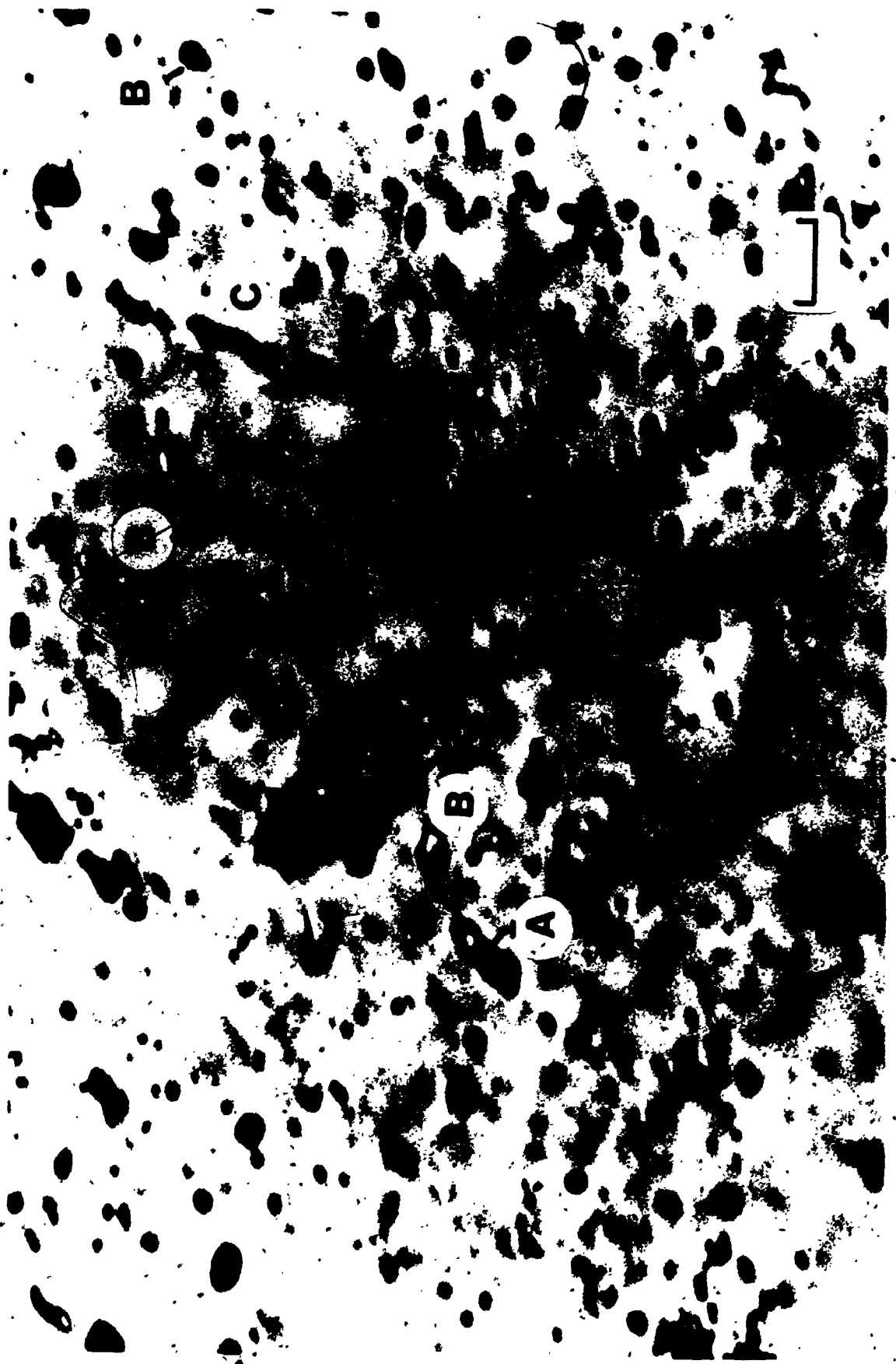
Heating studies showed that both the 2 phase secondary inclusions and three phase CO₂-bearing inclusions homogenized in the range 220° to 235°C. Large 2 phase primary inclusions revealed homogenization temperatures in a higher range, from 425°-440°C. The higher temperature for 2 phase inclusions is in approximate agreement with triply concordant isotopic temperatures of 380°C to 420°C for vein ore samples discussed previously. If the interpretation of variable filling factors in primary inclusions as evidence of phase separation is valid, these homogenization temperatures are essentially equivalent to formation temperatures as no pressure correction is necessary.

5.3.3 Breccia ore

No reliable heating data was obtained for fluid

Plate 5-1. Fluid inclusions in vein ore.

Photomicrograph of fluid inclusions in quartz from 26-A vein, Macassa Mine. A = primary, 3 phase inclusion with CO₂ liquid; B = primary, 2 phase inclusion; C = secondary inclusions along microfracture. Plane-polarized transmitted light. Scale bar is approximately .01 mm.



188

inclusions in breccia ore samples because of the highly fractured nature of all quartz associated with this ore type.

5.3.4 Quartz-magnetite Stringer Veins

Primary inclusions in quartz from the quartz-magnetite-chlorite stringers were very sparse. Some 15 to 20 inclusions in 2 samples were subjected to a limited number of heating runs. All of these small, two phase inclusions homogenized in the range of 110°-230°C.

CHAPTER 6

GOLD DISTRIBUTION IN BRECCIA ORE - A GEOSTATISTICAL STUDY.

6.1 General Statement

The physical distribution of native gold and gold-bearing telluride minerals in the ores of the Macassa Mine is an important characteristic. Not only interesting from an academic perspective, a detailed assessment of amount of gold present, its spatial distribution and continuity are of practical importance to the mine geologist and planning engineer faced with the problems of grade and tonnage calculations in reserve estimation.

One approach to this complex problem is to quantify the statistical characteristics of gold abundances as expressed by assay data from diamond drill core samples. A statistical approach is best applied to a large volume of data taken from a physically large ore zone. Neither the break-ore or vein-ore types as described previously (Chapter 3) had sufficient spatial continuity or sampling density by diamond drilling.

Since 1980, over 40% of the unbroken ore reserves at the Macassa Mine have been classed as breccia ore. This significant part of gold ore at the mine is physically more

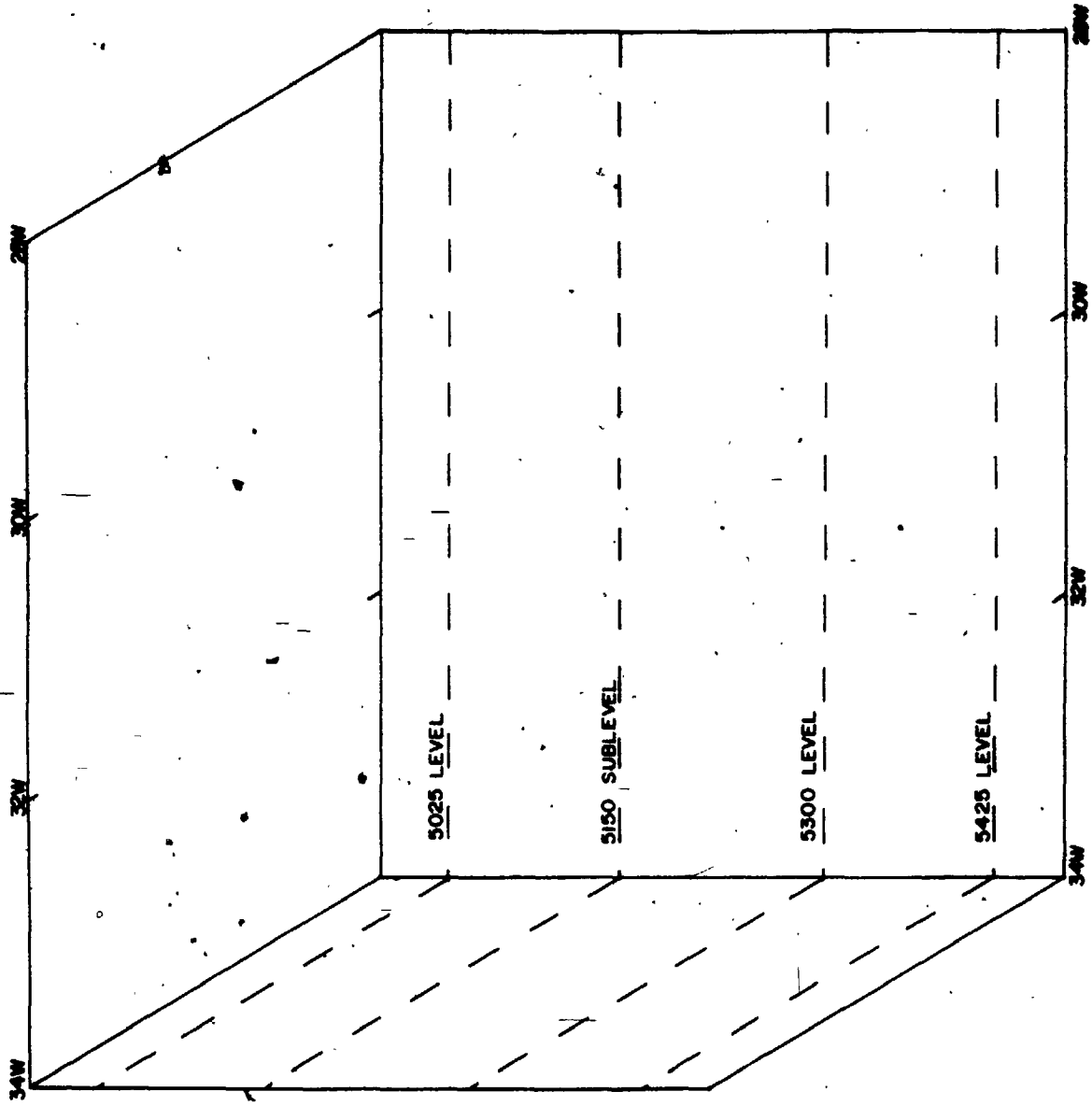
continuous in three dimensions than the previous two ore types. Additionally, as this ore type was not well understood and gold somewhat more erratic than vein or break-ore types, a significantly greater number of samples were required by diamond drilling prior to underground development and extraction of individual ore zones. Thus, breccia-ore was chosen as the best type for statistical investigation of gold distribution.

This chapter details the results of a special study conducted by the writer for Lac Minerals Ltd. to characterize the distribution of gold within a type zone of breccia-ore and to assess controls to gold distribution made by host rocks versus structure.


6.1.1 The Study Area

The area within the mine workings chosen as typical of the breccia-ore (Fig. 6-1) is bounded on east and west by the 28 west and 24 west mine section lines respectively and extends vertically from 50' above the 5025 level to 50' below the 5425 level (see section 3.5.3.3 and Fig. 3-8). The maximum known horizontal width of the ore is approximately 50', the maximum separation of the two confining faults: the '04 Break and South Break (Figs. 6-2A-D). Drill information used in this study includes a horizontal width of 150' in places and includes samples from outside the ore zone. Thus, the approximate dimensions of the

Figure 6-1. Schematic diagram of breccia ore study area in the Macassa Mine.




LEGEND FOR FIGURES 6-2, A-D

 DRIFT OUTLINE

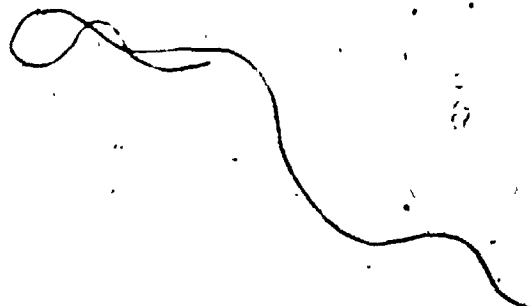
 '04 BREAK

 SOUTH BREAK

 DIAMOND DRILL HOLE

 - horizontal

 - inclined



4

Figure 6-2. a) Schematic diagram of study area on the 5025' level, Macassa Mine, showing the '04 and South Breaks and diamond drilling pattern.

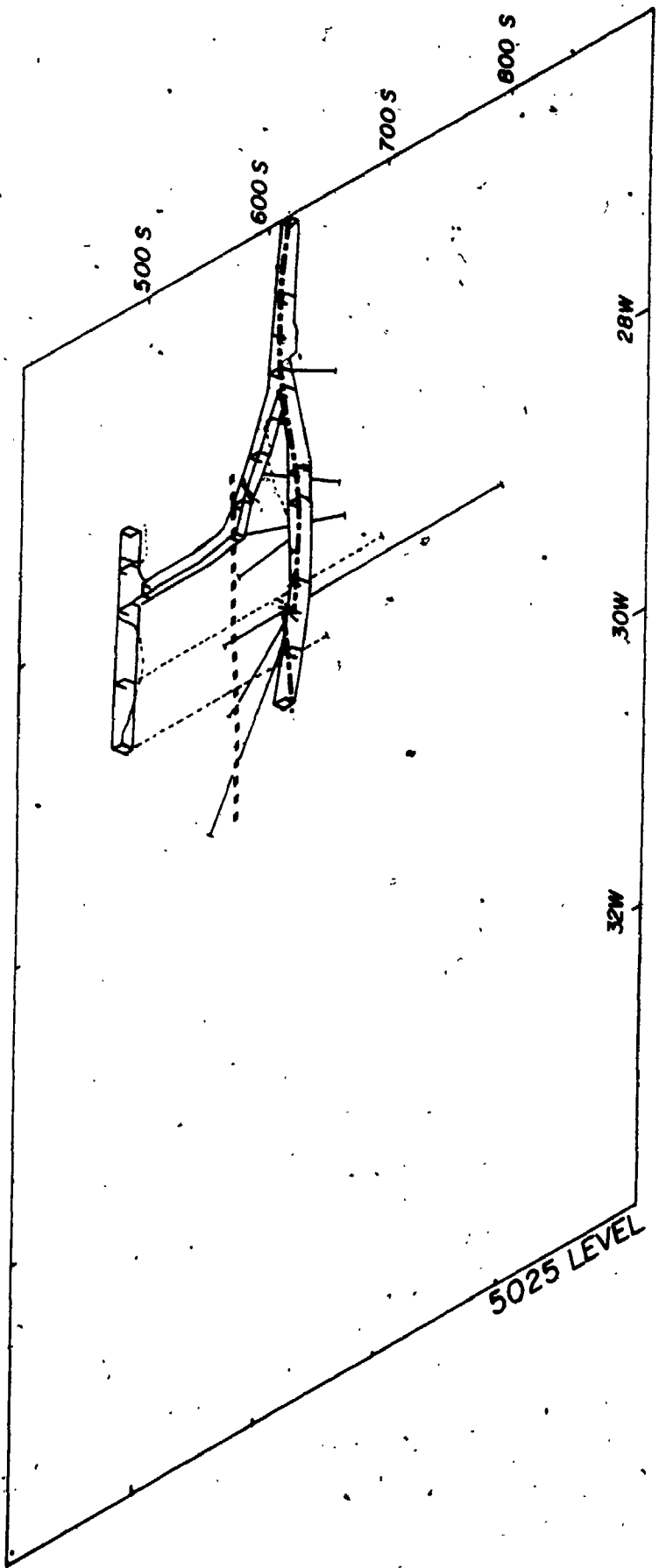


Figure 6-2. b) Schematic diagram of the study area on the 5150' level, Macassa Mine, showing the '04 and South Breaks and diamond drilling pattern.

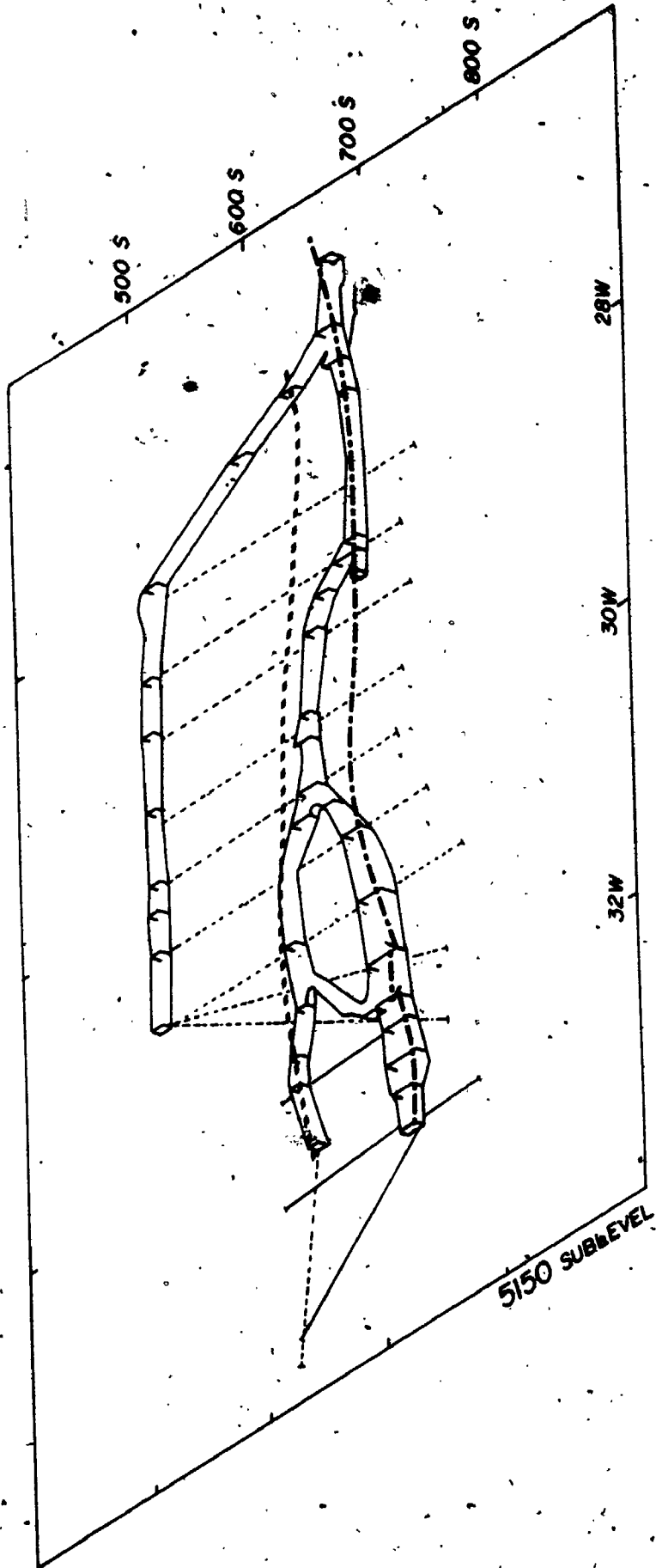


Figure 6-2. c) Schematic diagram of the study area on the 5300' level, Macassa Mine, showing the '04 and South Breaks and diamond drilling pattern.

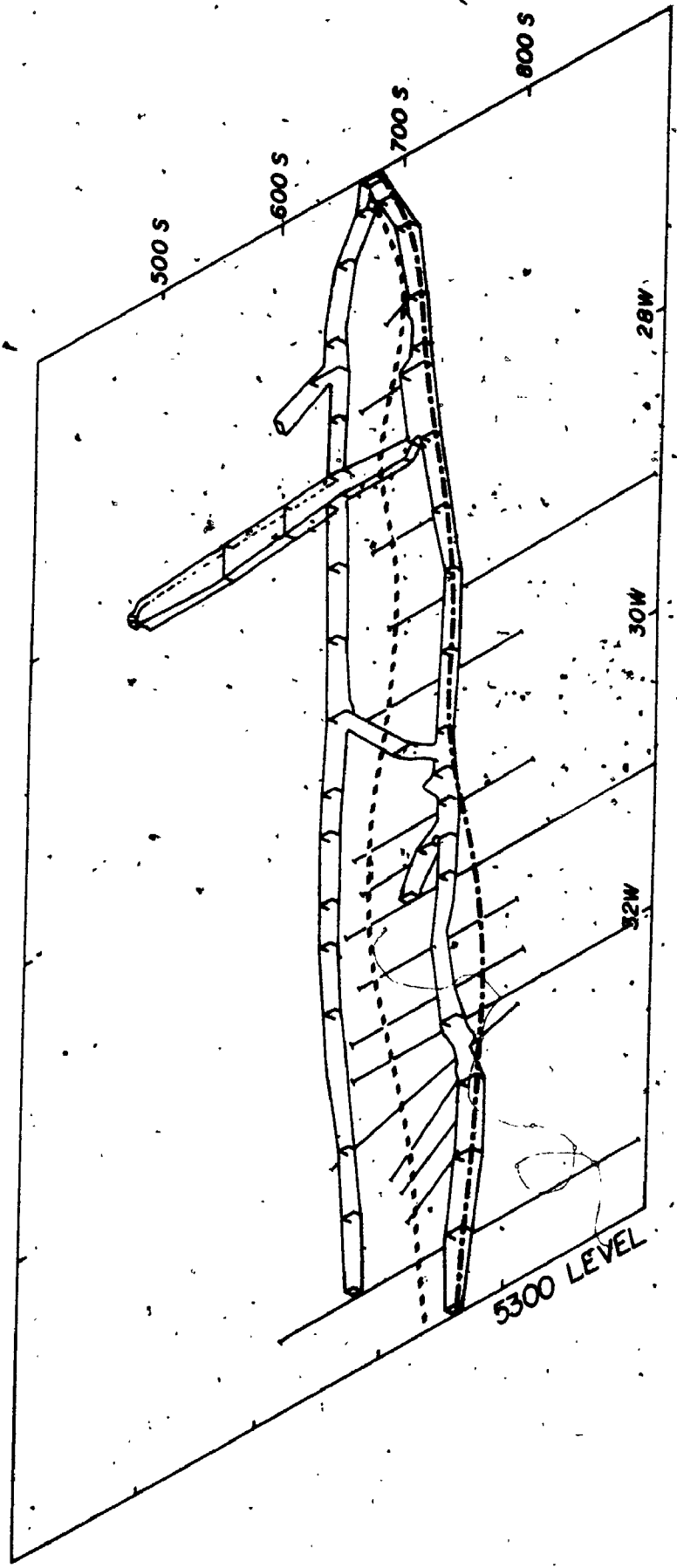
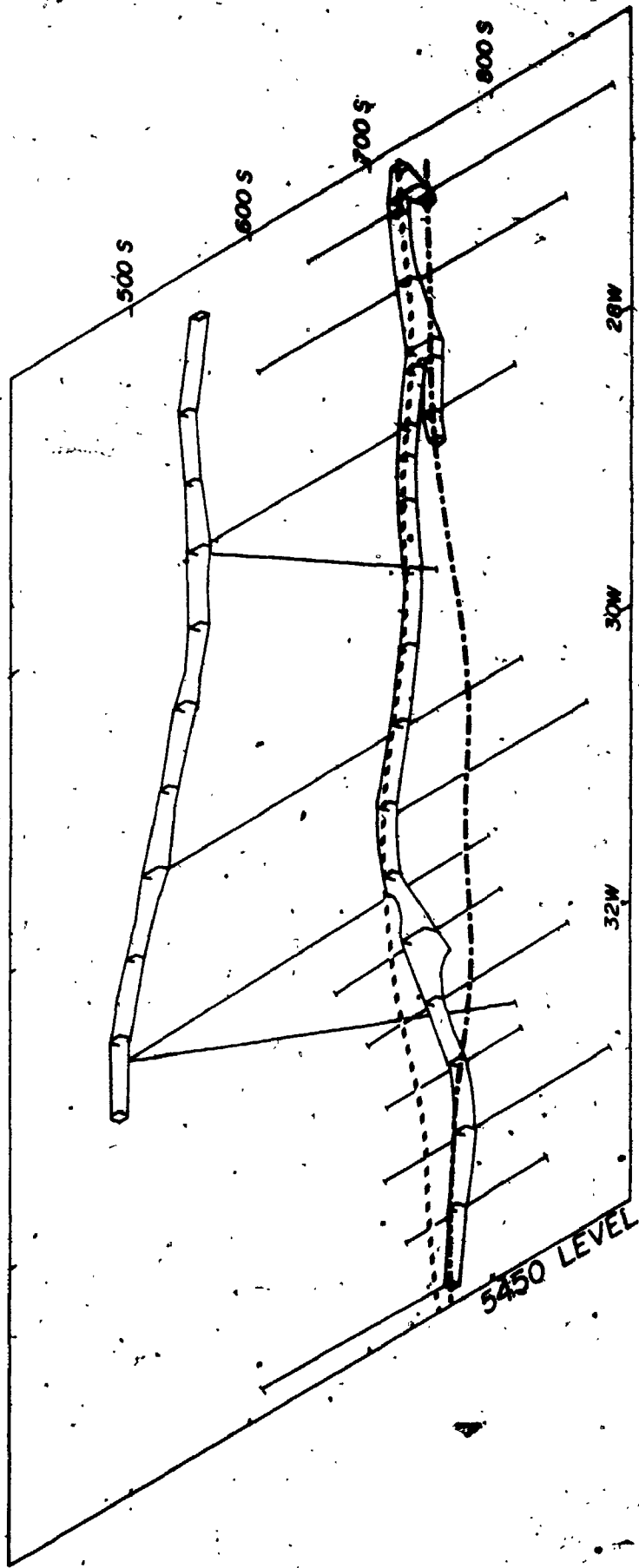


Figure 6-2. d) Schematic diagram of the study area on the 5425' level, Macassa Mine, showing the '04 and South Breaks and diamond drilling pattern.



study area are 600' x 500' x 150'.

6.1.2 The Data Base

The study area was extensively sampled in three dimensions by pre-production underground diamond drilling. The drill hole logs and gold assays from all the diamond drilling within the study zone provided the original information base. This amounted to over 150 drill holes and 2000 individual core sample assays (Fig. 6-2, A-D; Table 6-1). Management of this information required the use of computerized data storage and retrieval using the DEC-10 computing system at the University of Western Ontario.

6.1.3 Preliminary Appraisal

The first appraisal was an elementary statistical analysis of the unweighted assays as they were reported in the diamond drill logs. Histograms were prepared for the entire population including all levels and rock types, then for subpopulations according to rock type and underground level where the drill holes originated. These histograms were summarized in the following simple statistical parameters: population size, mean, standard deviation, maximum, and minimum. Table 6-2 contains these parameters for the entire population and each of the subpopulations.

The histogram and cumulative frequency distribution (Fig. 6-3) for the entire population, typical also of the

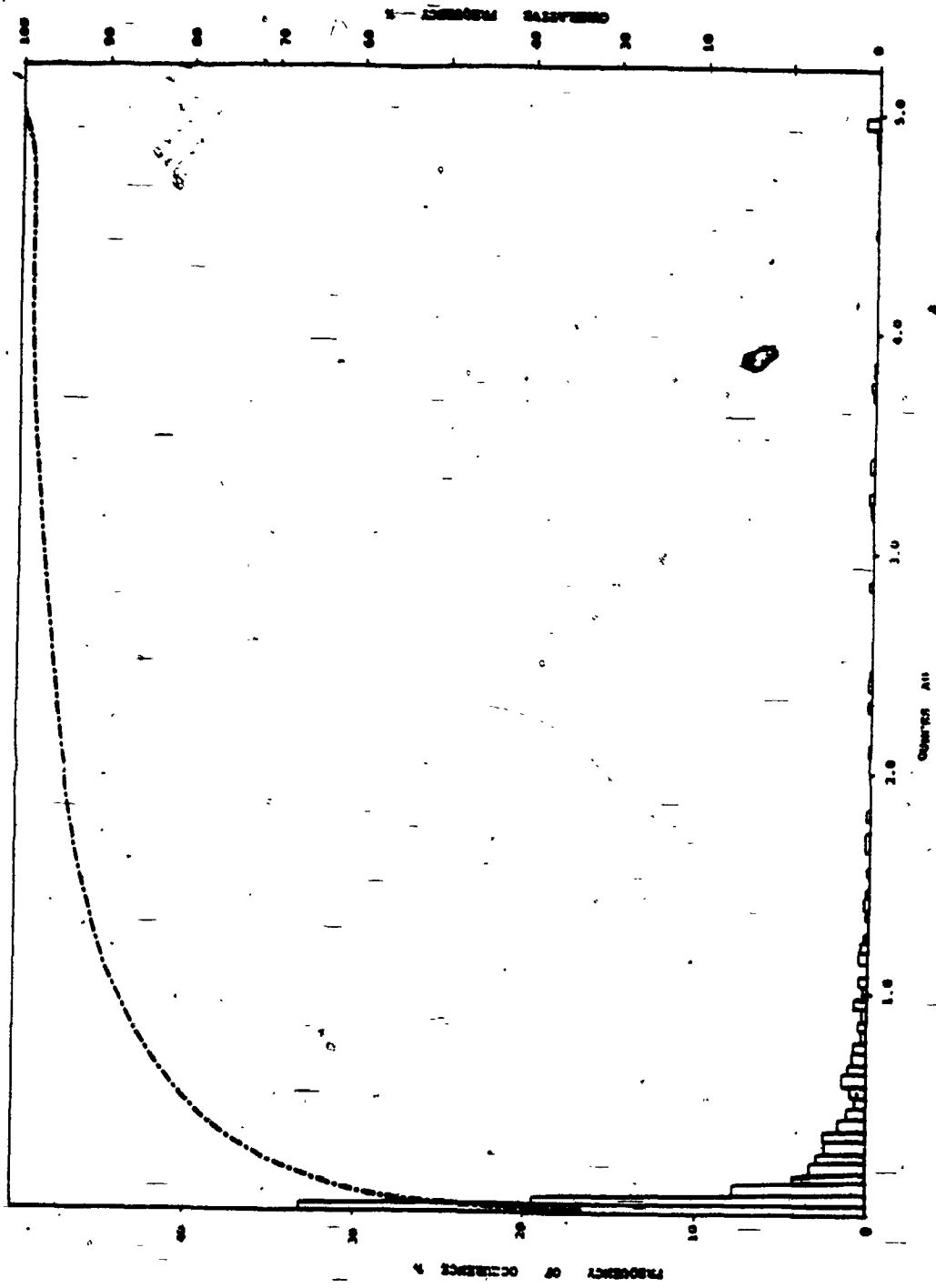
TABLE 6-1. Distribution of Diamond Drill Holes and Samples.

Mine Level	No. of DDH	No. of Samples
5025	29	465
5150	41	1045
5300	64	534
5425	17	51
Total	151	2095

TABLE 6-2 Statistical Summary Unweighted Assay Values

	Augite Syen.	Tuff	Porphyry	All Rocks	
5 0 2 5 L E V E L	N	382	66	1	465
	\bar{Z}	0.42	0.76	0.01	0.48
	Med.	0.04	0.24	0.01	0.05
	St.D.	1.34	1.11		1.31
	C.V.	3.19	1.46		2.73
	Max.	22.2	4.82	0.01	22.2
5 1 5 0 L E V E L	N	743	263	39	1045
	\bar{Z}	0.50	0.45	0.28	0.48
	Med.	0.10	0.11	0.04	0.10
	St.D.	0.98	1.07	0.60	0.99
	C.V.	1.96	2.38	2.14	2.06
	Max.	7.40	10.0	2.79	10.0
5 3 0 0 L E V E L	N	197	243	94	534
	\bar{Z}	0.34	0.33	0.22	0.31
	Med.	0.06	0.08	0.06	0.07
	St.D.	0.86	0.70	0.44	0.73
	C.V.	2.53	2.12	2.00	2.35
	Max.	6.95	4.91	3.40	6.95
5 4 2 5 L E V E L	N	11	34	6	51
	\bar{Z}	0.04	0.28	0.03	0.20
	Med.	0.02	0.05	0.04	0.04
	St.D.	0.05	0.60	0.13	0.50
	C.V.	1.25	2.14	4.30	2.50
	Max.	0.18	3.18	0.04	3.18
A L L L E V E L S	N	1333	606	140	2095
	\bar{Z}	0.45	0.42	0.23	0.43
	Med.	0.07	0.10	0.05	0.08
	St.D.	1.08	0.93	0.48	1.01
	C.V.	2.40	2.21	2.09	2.35
	Max.	22.2	10.0	3.40	22.2

Figure 6-3. Histogram and cumulative frequency distribution of all unweighted gold abundances from the study area.



subpopulations, is very skewed to the left and has a long tapering tail to the right punctuated by erratic high grades. All the populations are unduly influenced by a pronounced peak over the 0.01 ounces/ton Au grade at the origin. This gold content (which is also the mode) merely reflects the lower detection limit of analytical facilities at the mine. The pronounced asymmetry of the histograms is reflected in the order of magnitude difference between the median and mean for each of the larger populations, a situation which reduces the value of the arithmetic mean as an accurate descriptor of these populations. The random high grades in each distribution reflects the erratic nature of the gold distribution itself.

A further indication of the ability of these distributions to accurately estimate the entire population of gold assays within the study zone is provided by the coefficient of variation, i.e., the ratio of the standard deviation to the mean. For all the populations grouped in Table 6-2, this ratio has an average of 2.32. For any case where the coefficient of variation is much greater than 1.0, little or no confidence can be assigned to the statistical parameters as accurate estimators (Journel and Huijbregts, 1978).

Aside from the real limitations imposed by the erratic nature of the preliminary distributions and their resultant inability to accurately portray the distribution of gold,

two other factors are of equal importance in limiting the usefulness of this first approach. The first is that no consideration was given to the relative weight or importance assigned to each sample. In this instance, the relative weight of a given sample is only dependent upon its length as all samples were taken from drill core of the same diameter. Thus, a 50 foot long interval of core with 0.01 oz. Au has a distinctly different physical importance than 0.5 feet at 10 oz. Au even though the resulting grade x width product is identical. The second factor is that no consideration was given to the remaining unsampled lengths of core in each hole which are assumed to have a zero grade. Both of these factors must be accounted for before a meaningful appraisal of gold distribution in the study area can be attempted.

Accordingly, a second, more comprehensive appraisal was initiated using the probabilistic tools and concepts of Geostatistics. Appendix C briefly introduces and describes Geostatistics and its important concepts so as to provide a framework for the analysis which follows.

6.2 Geostatistical Appraisal

6.2.1 General Statement

Classically, a geostatistical study proceeds with the following steps:

i. Data Statistics - elementary statistical appraisal of the data.

ii. Check of Stationary - the stationarity (of order 2) must be checked, i.e., the local mean and variance of the variable under study must be fairly constant throughout the study zone.

iii. Variography (Structural Analysis) - the purpose is to characterize the spatial continuity pattern of the variable.

iv. Kriging - three dimensional estimation and modeling based on initial variography.

v. Resources and reserve estimation and appraisal.

The following sections will consider the first three of these steps.

Full description of the various statistical and geo-statistical tools commonly used can be found in Journel and Huijbregts (1978).

6.2.2 Reconstitution of Data Base

The preliminary statistical evaluation of gold distribution within the study area utilized the unweighted assays of diamond drill core. The original splitting and analysis of core samples was heterogeneous in that sample lengths were not constant and not all the drill core was analysed. The original data set preferentially reflected the character of narrow, distinctly auriferous zones within

the study zone. This is an important consideration in that no systematic information was provided for non-analysed, ostensibly barren sections of core which represent areas of waste rock that will be partially recovered during mining.

One of the first requirements of geostatistical study is that the available data be defined on a constant sample support, in this case a constant length of drill core. To accomplish this, the complete drill log for each of the underground diamond drill holes within the study zone was summarized and stored in computer memory using the Fortran program ENTRY FOR. (Note: all computer programs used in this study are listed in appendix D). Then each hole was reduced to a series of composite samples of equal length using the Fortran program COMPOS FOR. The length chosen initially was 2.0' to provide sufficient detail but not to create an unmanageable data mass. A second data set was generated using 4.0' composites for comparative purposes. Each of the composited samples has 3-dimensional coordinates, Au grade in ounces per ton, and rock type.

All composited lengths of drill core not containing sampled and analysed sections were assigned a zero gold grade to simulate the missing data. This convention was adopted as a conservative and consistent alternative to uncertain extrapolation of data from known points.

6.2.3 Data Statistics and Stationarity Check

Composited data sets (2.0' and 4.0') were subjected to elementary statistical appraisal similar to that previously described for the raw sample data. For the entire population and a series of subpopulations according to the mine levels within the study zone and rock types, a histogram of gold grades was produced and the mean ($Z+$), variance (Var.), coefficient of variation (C.V.), maximum and minimum values were determined. This was done twice using population cut-off limits of 0.01 and 0.04 ounces Au per ton. The statistical parameters for each cut-off value are summarized in Table 6-3 and 6-4.

Several important observations can be made from these data summaries. The coefficient of variation ($\sigma/Z+$) for 0.01 ounce Au limit has an average of 2.23 and 1.89 for the 2.0' and 4.0' sample composites respectively. Where compared to the average coefficient of variation previously calculated for the unweighted, raw assay data (see 6.1.3), it is apparent that there is no significant decrease in the C.V. factor in the composited data using the 0.01 ounce Au limit. However, the average C.V. for composited samples greater than 0.04 ounces Au is 1.62 and 1.36 for the 2.0' and 4.0' composite lengths. Clearly, a reduction in spurious, "noisy" data is evidenced. The coefficient of variation is an important factor in describing the "robustness" or ability of any data set and subsequent semi-variograms

TABLE 6-3 HISTOGRAM STATISTICAL DATA SUMMARY - 0.01 oz. Au limit

	Augite Syen.		Tuff		Porphyry		All Rocks		
	2.0'	4.0'	2.0'	4.0'	2.0'	4.0'	2.0'	4.0'	
5 0 2 5 L	N	619	301	83	37		723	355	
	$\bar{Z}+$	0.218	0.224	0.533	0.503		0.257	0.261	
	VAR.	0.226	0.189	0.657	0.549		0.286	0.234	
	C.V.	2.175	1.941	1.519	1.476		2.080	1.854	
	MAX.	3.076	2.848	3.245	2.786		3.245	2.848	
5 1 5 0 L	N	883	441	288	134	22	11	1242	612
	$\bar{Z}+$	0.289	0.276	0.215	0.198	0.167	0.139	0.267	0.266
	VAR.	0.449	0.275	0.297	0.160	0.810	0.675	0.397	0.283
	C.V.	2.318	1.897	2.532	2.021	1.714	1.867	2.361	1.997
	MAX.	7.727	3.983	4.504	2.541	1.312	0.891	7.727	5.420
5 3 0 0 L	N	574	291	664	324	141	69	1454	763
	$\bar{Z}+$	0.228	0.215	0.229	0.216	0.233	0.229	0.230	0.219
	VAR.	0.305	0.191	0.306	0.183	0.669	0.356	0.337	0.198
	C.V.	2.422	2.028	2.414	1.983	3.514	2.608	2.523	2.034
	MAX.	6.060	3.364	4.958	2.808	9.080	4.540	9.080	4.540
5 4 2 5 L	N	30	14	83	43	27	15	146	77
	$\bar{Z}+$	0.039	0.032	0.145	0.140	0.036	0.035	0.099	0.094
	VAR.	0.007	0.005	0.076	0.057	0.002	0.002	0.045	0.035
	C.V.	0.923	0.668	1.903	1.714	1.161	1.188	2.170	1.984
	MAX.	0.168	0.080	1.480	1.123	0.203	0.169	1.480	1.123
A L L E V E L S	N	2106	1047	1118	538	192	95	3565	1816
	$\bar{Z}+$	0.248	0.241	0.242	0.225	0.195	0.188	0.243	0.238
	VAR.	0.339	0.224	0.319	0.197	0.505	0.270	0.336	0.229
	C.V.	2.347	1.964	2.335	1.974	3.639	2.767	2.387	2.007
	MAX.	7.727	3.983	4.958	2.808	9.080	4.540	9.080	5.420

TABLE 6-4. HISTOGRAM STATISTICAL DATA SUMMARY - 0.04 oz. Au limit

	Augite Syen.		Tuff.		Porphyry		All Rocks		
	2.0'	4.0'	2.0'	4.0'	2.0'	4.0'	2.0'	4.0'	
5 0 2 5 L	N	246	135	62	27			318	173
	$\bar{Z}+$	0.527	0.478	0.708	0.682			0.564	0.518
	VAR.	0.412	0.304	0.760	0.636			0.481	0.353
	C.V.	1.217	1.152	1.230	1.170			1.229	1.146
	MAX.	3.076	2.848	3.245	2.786			3.245	2.848
5 1 5 0 L	N	513	265	158	77	11	4	711	374
	$\bar{Z}+$	0.487	0.449	0.380	0.331	0.312	0.346	0.454	0.432
	VAR.	0.681	0.384	0.483	0.237	0.125	0.135	0.612	0.402
	C.V.	1.696	1.379	1.832	1.468	1.135	1.063	1.721	1.467
	MAX.	7.727	3.983	4.504	2.541	1.312	0.891	7.727	5.420
5 3 0 0 L	N	341	180	432	212	86	47	908	492
	$\bar{Z}+$	0.371	0.337	0.341	0.319	0.368	0.326	0.357	0.329
	VAR.	0.463	0.271	0.434	0.250	1.054	0.497	0.496	0.274
	C.V.	1.832	1.545	1.930	1.564	2.789	2.164	1.974	1.592
	MAX.	6.060	3.364	4.958	2.808	9.080	4.540	9.080	4.540
5 4 2 5 L	N	11	4	49	25	7	4	70	35
	$\bar{Z}+$	0.075	0.062	0.231	0.223	0.081	0.085	0.185	0.182
	VAR.	0.020	0.002	0.112	0.083	0.004	0.004	0.084	0.064
	C.V.	0.571	0.246	1.454	1.289	0.795	0.719	1.565	1.392
	MAX.	0.168	0.080	1.480	1.123	0.203	0.169	1.480	1.123
A L L L E V E L S	N	1111	584	701	341	104	55	2007	1074
	$\bar{Z}+$	0.456	0.418	0.375	0.344	0.343	0.310	0.418	0.390
	VAR.	0.552	0.331	0.462	0.273	0.888	0.435	0.527	0.330
	C.V.	1.629	1.374	1.813	1.519	2.748	2.130	1.736	1.472
	MAX.	7.727	3.983	4.958	2.810	9.080	4.540	9.080	5.420

to accurately portray the structural characteristics of the gold distribution.

Simple comparison of the number of composite samples on the basis of rock type shows the dramatic distinction between tuff and augite syenite versus porphyritic syenite which is volumetrically unimportant (10-12% of total population) and of much lower grade. This supports the geological interpretation of the porphyritic syenite as a later unit which cross-cut the augite syenite and tuff units. The most interesting observation is that there is a marked lessening of average gold grade (Z+) on the lowest level (5425') and an indication of a tendency toward higher average grades in the upper portions of the study zone. This is supported by recent experience of mine staff who have noted a relatively poor grade within development areas around the 5425' level (G. Nemcsok, pers. comm., 1982). This suggestion of a vertical trend in gold distribution within the study zone is significant in that the phenomenon may only be quasi-stationary at best. This possibility must be accounted for in any geostatistical modelling. Further study will establish the reality of this directional anisotropy and evaluate its effect on grade distribution.

The shapes of the histograms generated for all the composited subpopulations at both the 0.01 and 0.04 ounce Au cut-off limits were essentially similar to those

produced for the raw sample data. They are dominated by a large cluster near the origin and rapidly taper-off toward higher values. Their general shape suggested a lognormal type of distribution model for the gold grades. This possibility was checked by plotting the cumulative distribution of log-transformed gold grades (ie. $\ln Z$) on normal probability graph paper for both the 2.0' and 4.0' composite populations (Fig. 6-4 a,b). Except for a few extreme percentiles, the fit by a line is approximated but not strictly adhered to.

A further test of the usefulness of log-transformed gold grades is provided by data summarized in Table 6-5 for log-transformed values greater than 0.04 ounces Au. For most of the subpopulations the coefficient of variation is significantly below 1.0 (average 0.65 and 0.63 for 2.0' and 4.0' samples respectively). Further, the suggested vertical zonation of gold grade within the study zone is particularly marked by the gradual consistent trend from a low of -2.30 (5425 level) to -1.40 (5025 level). Acceptance of a lognormal model on these criteria alone is subjective and will need to be considered against the ease of application of normal (ie. linear) geostatistical models.

6.2.4 Experimental Semi-Variograms

As stated, it is possible to estimate the semi-

TABLE 6-5 HISTOGRAM STATISTICAL DATA SUMMARY - LOGTRANSFORMED - 0.04 oz. Au/limit

	Augite Syen.		Tuff		Porphyry		All Rocks		
	2.0'	4.0'	2.0'	4.0'	2.0'	4.0'	2.0'	4.0'	
S O 2 S L	N	246	135	62	27		318	173	
	\bar{Z}	-1.462	-1.449	-1.136	-1.077		-1.393	-1.363	
	VAR.	1.870	1.600	1.790	1.626		1.866	1.605	
	C.V.	0.935	0.873	1.174	1.184		0.981	0.929	
	MAX.	1.124	1.046	1.177	1.024		1.177	1.047	
S 1 S O L	N	513	265	158	77	11	4	711	374
	\bar{Z}	-1.605	-1.532	-1.763	-1.797	-1.587	-1.428	-1.644	-1.578
	VAR.	1.650	1.450	1.329	1.241	0.906	0.881	1.546	1.407
	C.V.	0.800	0.786	0.654	0.620	0.600	0.657	0.756	0.751
	MAX.	2.045	1.382	1.505	0.933	0.271	-0.115	2.045	1.690
S 3 C O L	N	341	180	432	212	86	47	908	492
	\bar{Z}	-1.812	-1.802	-1.902	-1.858	-1.900	-1.979	-1.858	-1.831
	VAR.	1.340	1.242	1.298	1.218	1.222	1.284	1.307	1.221
	C.V.	0.639	0.618	0.599	0.594	0.582	0.573	0.615	0.603
	MAX.	1.802	1.213	1.601	1.032	2.206	1.513	2.206	1.513
S 4 S L	N	11	6	49	25	7	4	70	35
	\bar{Z}	-2.727	-2.708	-2.109	-2.049	-2.740	-2.655	-2.290	-2.231
	VAR.	0.223	0.108	1.062	0.997	0.462	0.489	0.906	0.849
	C.V.	0.173	0.122	0.490	0.487	0.248	0.263	0.416	0.413
	MAX.	-1.784	-2.171	0.392	0.116	-1.594	-1.778	0.392	0.116
A L L L E V E L S	N	1111	584	701	341	104	55	2800	1074
	\bar{Z}	-1.648	-1.605	-1.817	-1.797	-1.924	-1.988	-1.724	-1.680
	VAR.	1.615	1.436	1.378	1.276	1.182	1.226	1.503	1.372
	C.V.	0.771	0.747	0.646	0.629	0.565	0.557	0.711	0.697
	MAX.	2.045	1.382	1.601	1.032	2.206	1.513	2.206	1.690

Figure 6-4. a) Normal probability plot of log transformed gold abundances - 2.0 ft. composite samples.

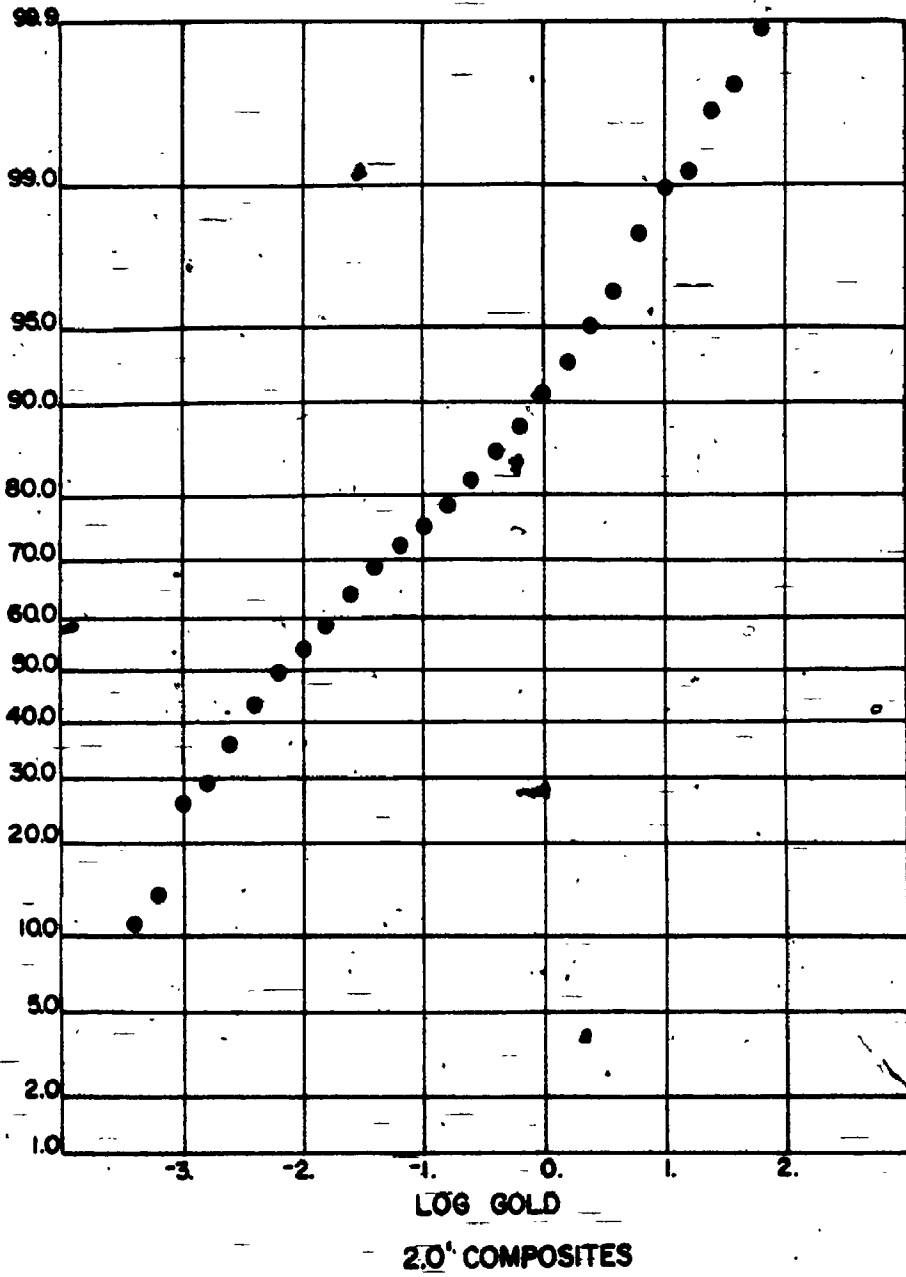
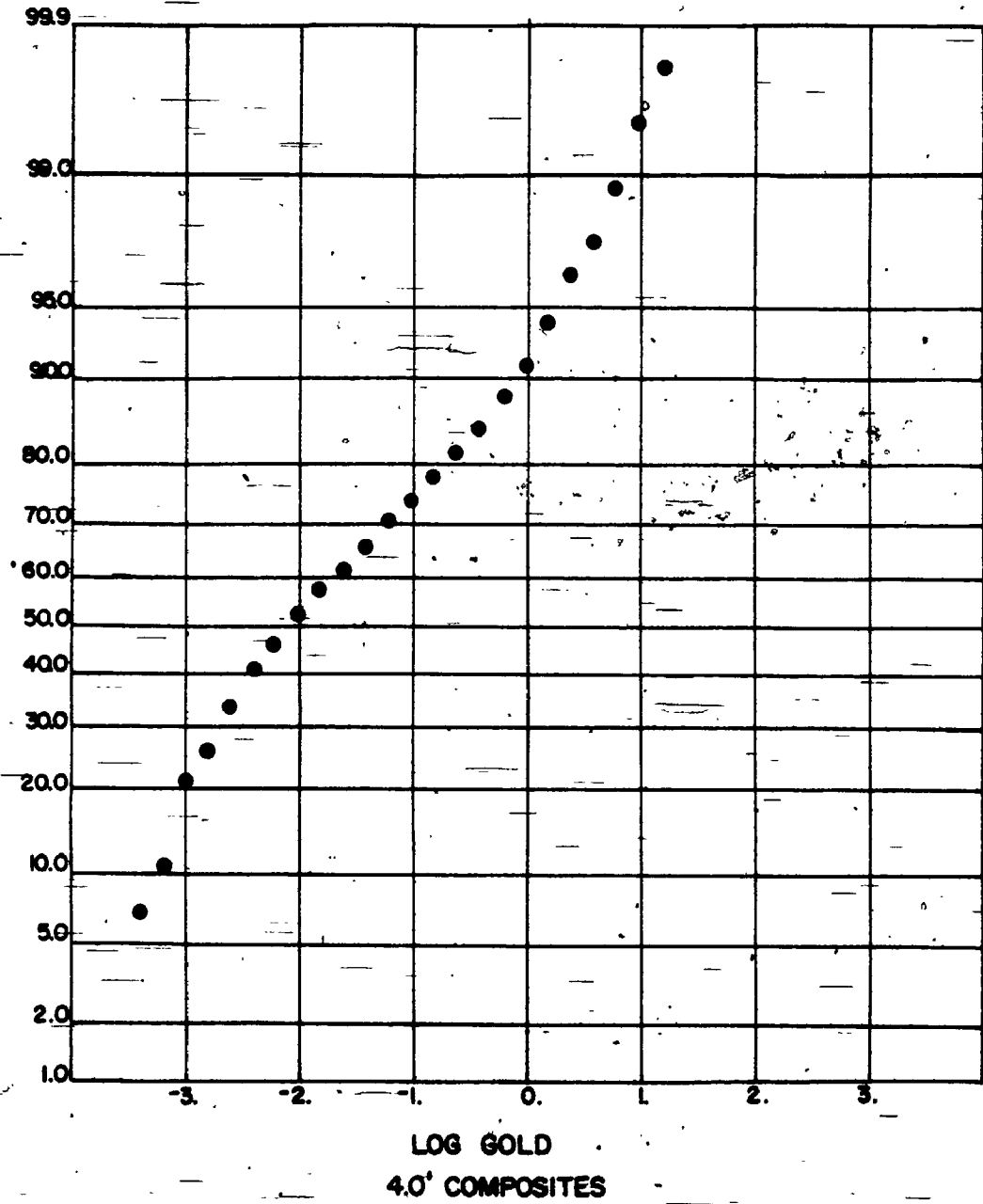


Figure 6-4. b) Normal probability plot of log transformed gold abundances - 4.0 ft. composite samples.

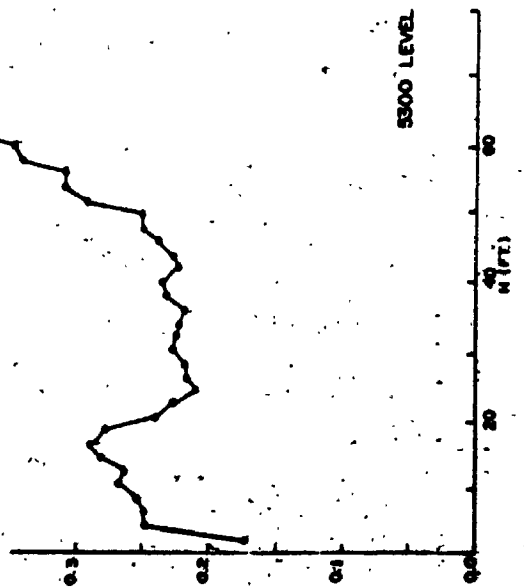
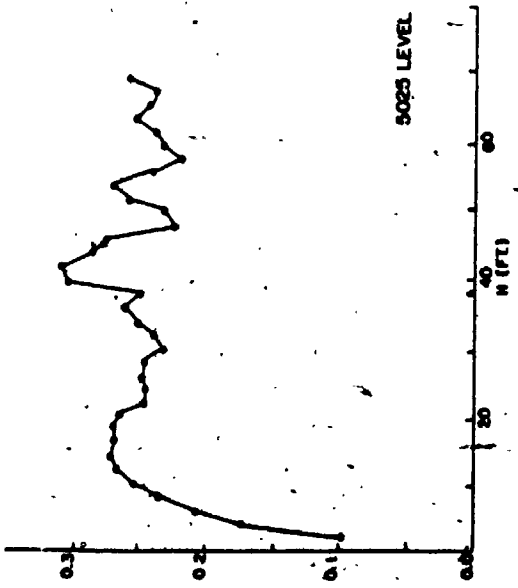
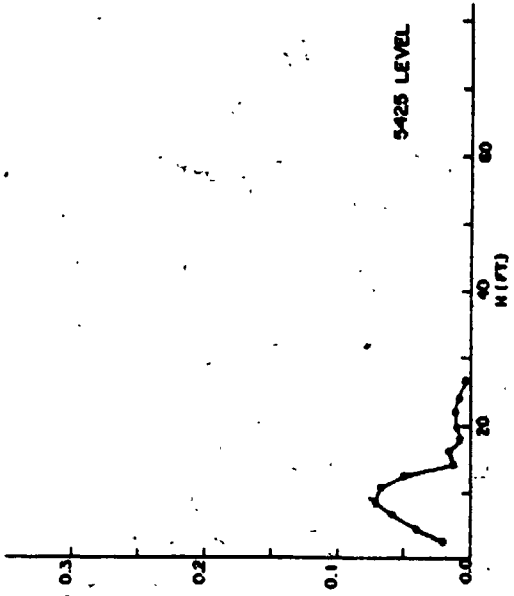
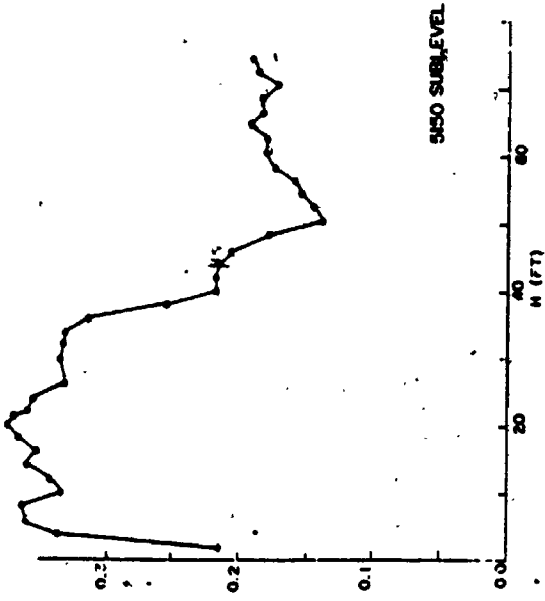


variogram function from the available sample data. The calculation is defined as: take each pair of samples separated by a given distance (assuming a constant direction); determine the squared difference in value between the samples; repeat for all possible sample pairs at the given separation; divide the sum of all squared differences by twice the number of pairs. This procedure is repeated for various increments of distance separating sample pairs, generally up to half of the total sampled dimensions. The reliability of any point on the semi-variogram is, in practice, directly proportional to the number of sample pairs used to calculate it.

In this case, as is true for most three dimensional orebodies, the most detailed and continuous information was provided along the length of the diamond drill holes. Thus, the initial experimental semi-variograms were one-dimensional, ie. calculated "down-the-hole". As the vast majority of holes used in these calculations were drilled in a direction approximately perpendicular to the strike of the breccia-ore within the study zone, the individual, down-the-hole semi-variograms were combined to provide average, one-dimensional semi-variograms for the entire zone and subzones on the basis of mine levels. These average, experimental semi-variograms (Fig. 6-5a, b, c) are shown for the subpopulations summarized statistically in Tables 6-3, 6-4 and 6-5.

535

Figure 6-5a. Average experimental semi-variogram: 0.01 ounce Au lower limit, 2.0 ft. composite samples. One dimensional, i.e. "down-the-hole".



4 1/2 1/2

Figure 6-5. b) Average experimental semi-variogram: 0.04 ounce Au lower limit, 2.0 ft. composite samples. One dimensional, i.e. "down-the-hole".

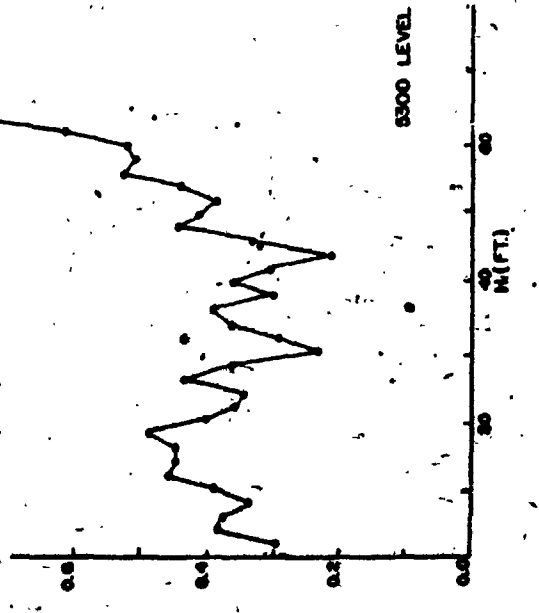
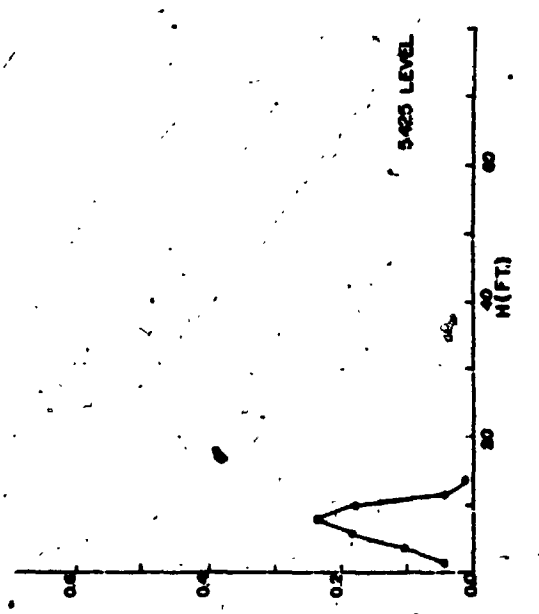
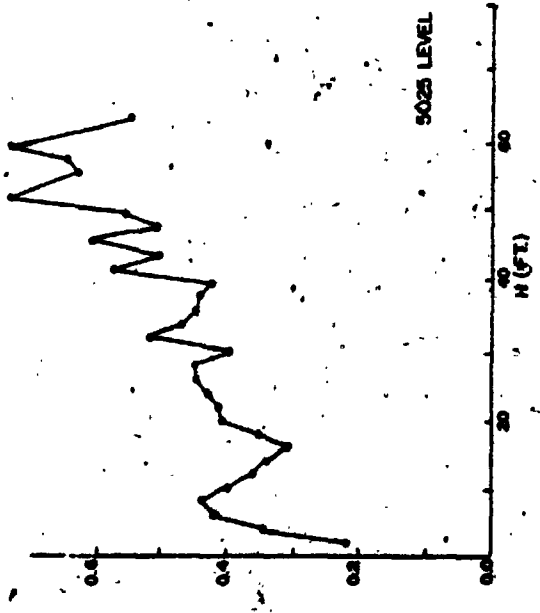
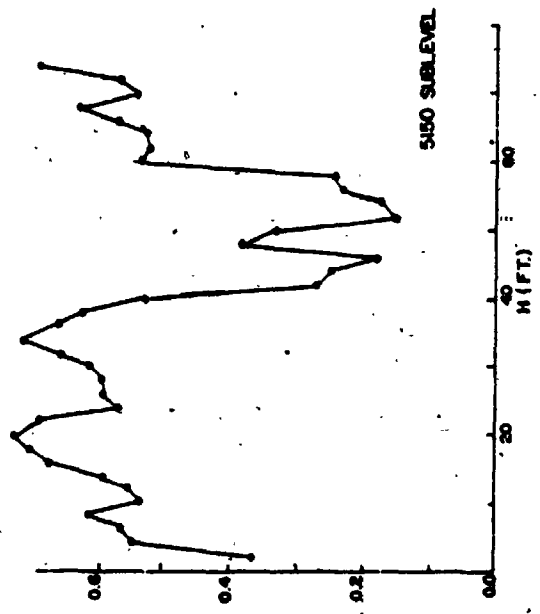
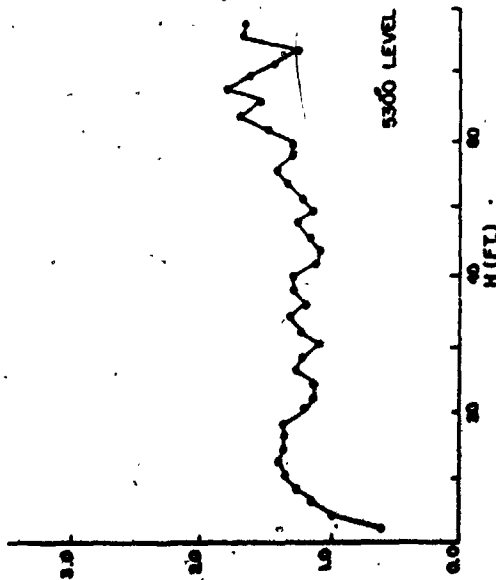
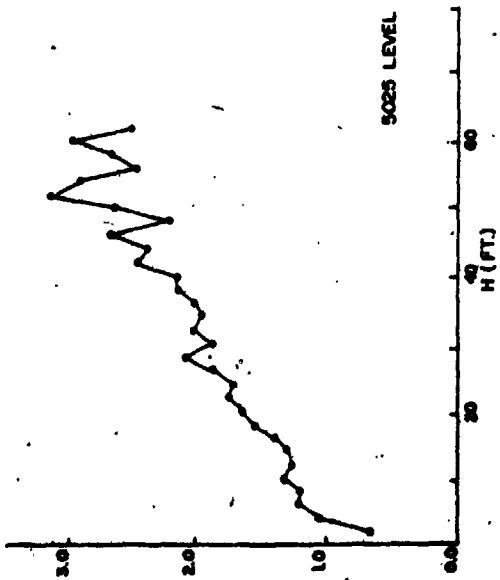
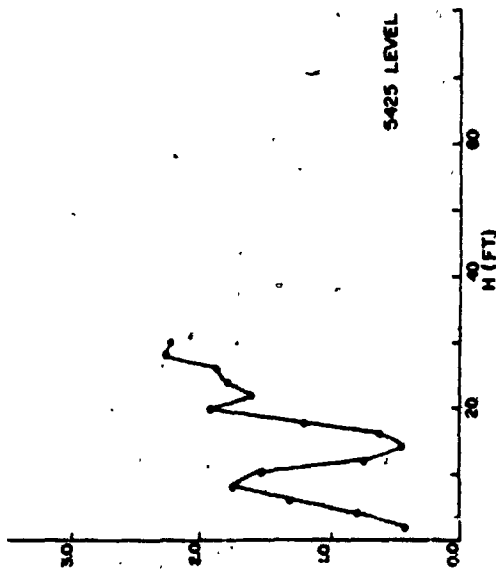
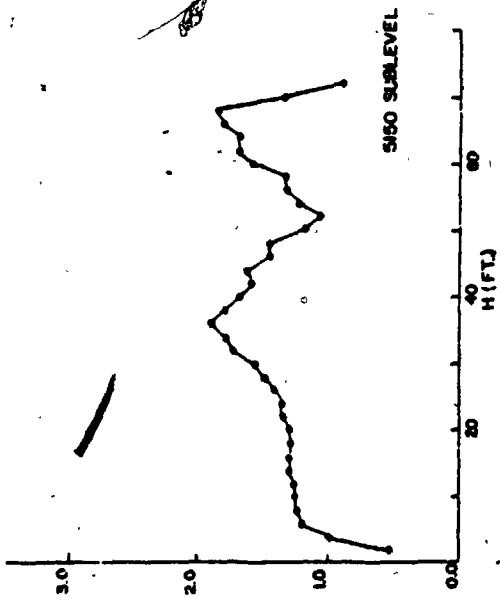


Figure 6-5. c) Average experimental semi-variogram: 0.04 ounce lower limit, 2.0 ft.
composite samples, log transformed data. One dimensional, i.e.
"down-the-hole".



6.2.5 Preliminary Analysis

Inspection of the mean experimental semi-variograms for 0.01 and 0.04 ounce Au cut-off limits (Fig. 6-5a, b), reveals some important preliminary trends. Each level generally has an indication of an initial sill or plateau around 15 ft. and most tend to either break-down into very erratic fluctuations or sharply increase beyond 50 to 60 ft. Thus, a preliminary interpretation would involve an overall range of the measured phenomenon of 50 to 60 ft. which contains a nested structure of approximately 15 to 20 ft. width. These observations correspond favourably with the known geological information in the study zone. The average separation of the '04 and South Breaks, which structurally limit the ore zone is on the order to 50 ft. Within the ore zone, there are known to be lenses of ore which are located near each Break and have widths of 10 to 20 ft.

The pronounced drop in $\gamma^*(h)$ values over the 30 to 50 ft. range for some mean semi-variograms may indicate a hole-effect phenomenon. If so, this could be explained by a mixing of two types of mineralization, ore grade zones with barren material in this case. To this point, no attempt has been made to separate the data points solely within the breccia-ore from all data within the study zone. The generally "noisy" character of the semi-variograms, particularly for 0.04 ounce Au limit, could be

attributed to this mixing of mineralization types.

The sharply attenuated and unusual mean semi-variograms for the 5425' level reflect the small data set and a pronounced difference in the tenor of mineralization already noted on this level. This data will be excluded from further modelling.

The mean semi-variograms for the log-transformed data (Fig. 6-5c) are smoother and more regular than the others due to the damping effect of the log-transform function, i.e. the logarithmic gold distribution is by definition less variable than the actual data. A short range phenomenon is still indicated between 10 to 20 ft. and a longer range changes at 60 to 70 ft. which apparently reflect the known geology. However, the pronounced smoothing effect of the non-linear logarithmic transformation combined with errors introduced when resolving log-transformed variogram functions make this application undesirable. As the linear variogram functions are apparently able to portray the significant details of the gold distribution and known geology, the log-transform approach will not be considered further.

6.2.6. Final Variography and Models

The keystone of any geostatistical study is to create semivariogram models which adequately describe the major features of the variable(s) under study. The particular

spatial regionalization considered here is the distribution of gold abundances in the three-dimensional space represented by the study zone. Thus, a unique 3d model is required which accomodates any directional experimental semivariogram and accounts for major features as anisotropies, proportional effect and hole-effect (Tournel and Froideveaux, 1982).

The experimental semi-variograms previously discussed were all calculated 'down-the-hole', i.e. along the length of the diamond drill core. As the vast majority of drill holes in breccia ore of the study area were oriented parallel to the mine section lines, the 'down-the-hole' direction is generally across the strike of the ore - one of the three principal directions for any orebody. Various experimental semivariograms for the remaining principal directions, along strike and down dip, were calculated using the one and two dimensional programs GAMMA1.FOR and GAMMA2.FOR (Appendix D).

Data for these semi-variograms were based on 4.0 ft composite samples and restricted to the first 3 levels within the study area (5025', 5150' and 5300' levels) for reasons cited previously. Further sorting of data was employed to eliminate values either north of the '04 Break or south of the South Break, the structural limits of the breccia ore in this area. This sorting effectively eliminated the apparent hole-effect phenomena and "noisy"

characteristics observed in the initial mean semi-variograms described above.

Final semi-variograms in all three directions stabilized beyond a range of 10-15 ft (Fig. 6-6 a-c) and did not begin at $\gamma(0) = 0$. Each was therefore interpreted in terms of a spherical model with an added nugget-effect factor. The experimental semi-variogram in the across strike direction (Fig. 6-6a), corresponding to the previous one dimensional semi-variograms, is interpreted in terms of a spherical model with a range of 10 ft, a sill at $\gamma = 0.09$ and a nugget-effect factor of 0.015. The along strike direction (Fig. 6-6b) was interpreted by a spherical model with a range of 12 ft, a sill at $\gamma = 0.135$ and a nugget-effect factor of 0.02. The down dip direction (Fig. 6-6c) was fitted to a spherical model of range = 15 ft, sill at $\gamma = 0.10$, and a nugget-effect factor of 0.015. All of these parameters are readily interpretable in light of known geology of the study area. The down dip range is greatest because it is the most continuous dimension of the breccia ore. The across strike range is shorter than along strike simply because of the relative lengths of these dimensions. In addition to portraying the short-range variability of gold abundances in breccia ore, these models underline the relative constancy in all three principal directions. This relates to an overall consistency in ore mineral assemblage and alteration mineral assemblage noted

Figure 6-6. a) Experimental semi-variogram and model. Across strike direction. $a_1 =$

range; $c_1 =$ sill; $c_0 =$ nugget-effect factor.

EXPERIMENTAL SEMI-VARIOGRAM & MODEL

$C_0 = 0.015$
 $C_1 = 0.09$
 $a_1 = 10$

ACROSS STRIKE

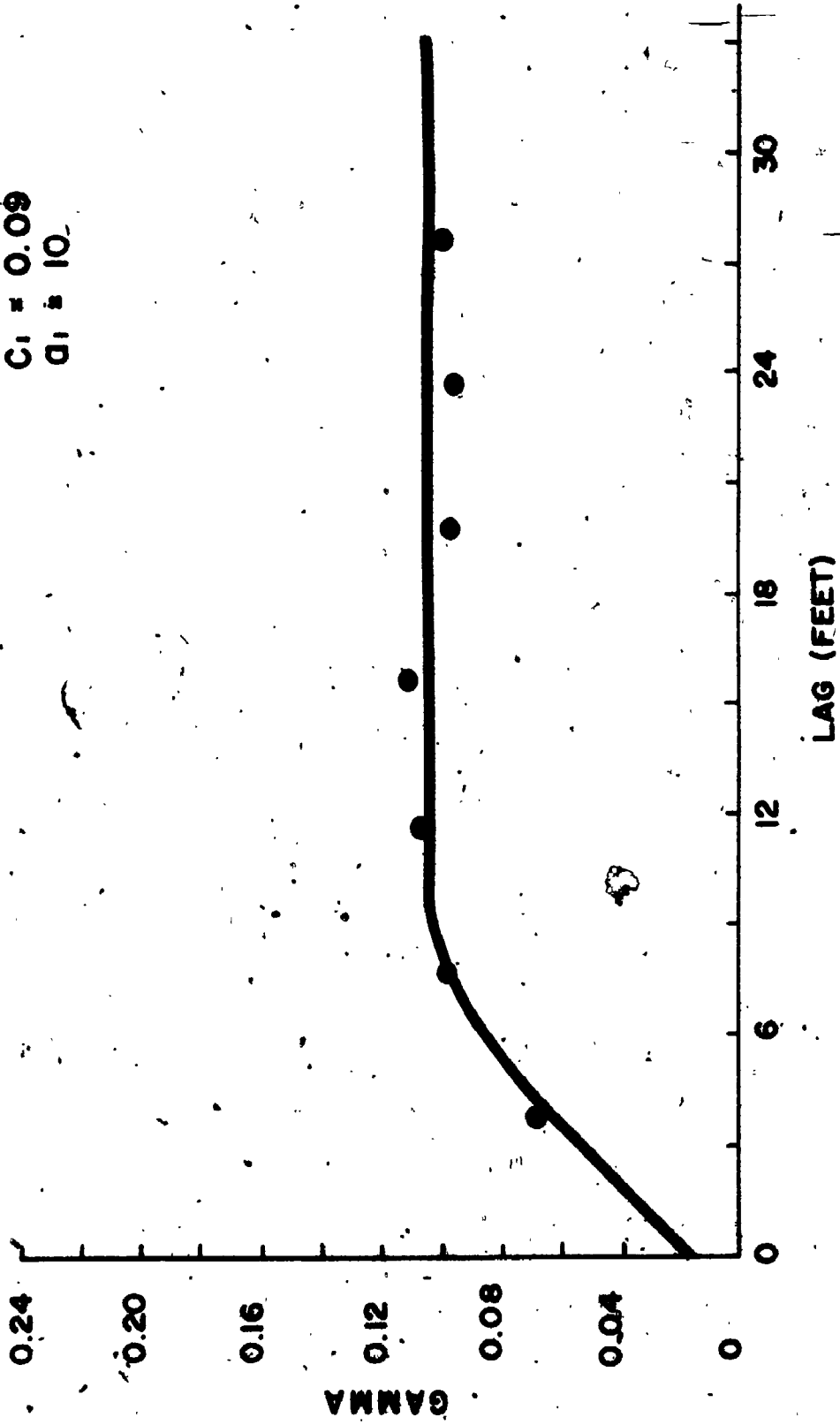


Figure 6-6. b) Experimental semi-variogram and model. Along strike direction. $a_1 =$
range; $c_1 = \text{sill}$; $c_0 = \text{nugget-effect factor}$.

EXPERIMENTAL SEMI-VARIOGRAM & MODEL
ALONG STRIKE

$C_0 = 0.02$
 $C_1 = 0.135$
 $q_1 = 12$

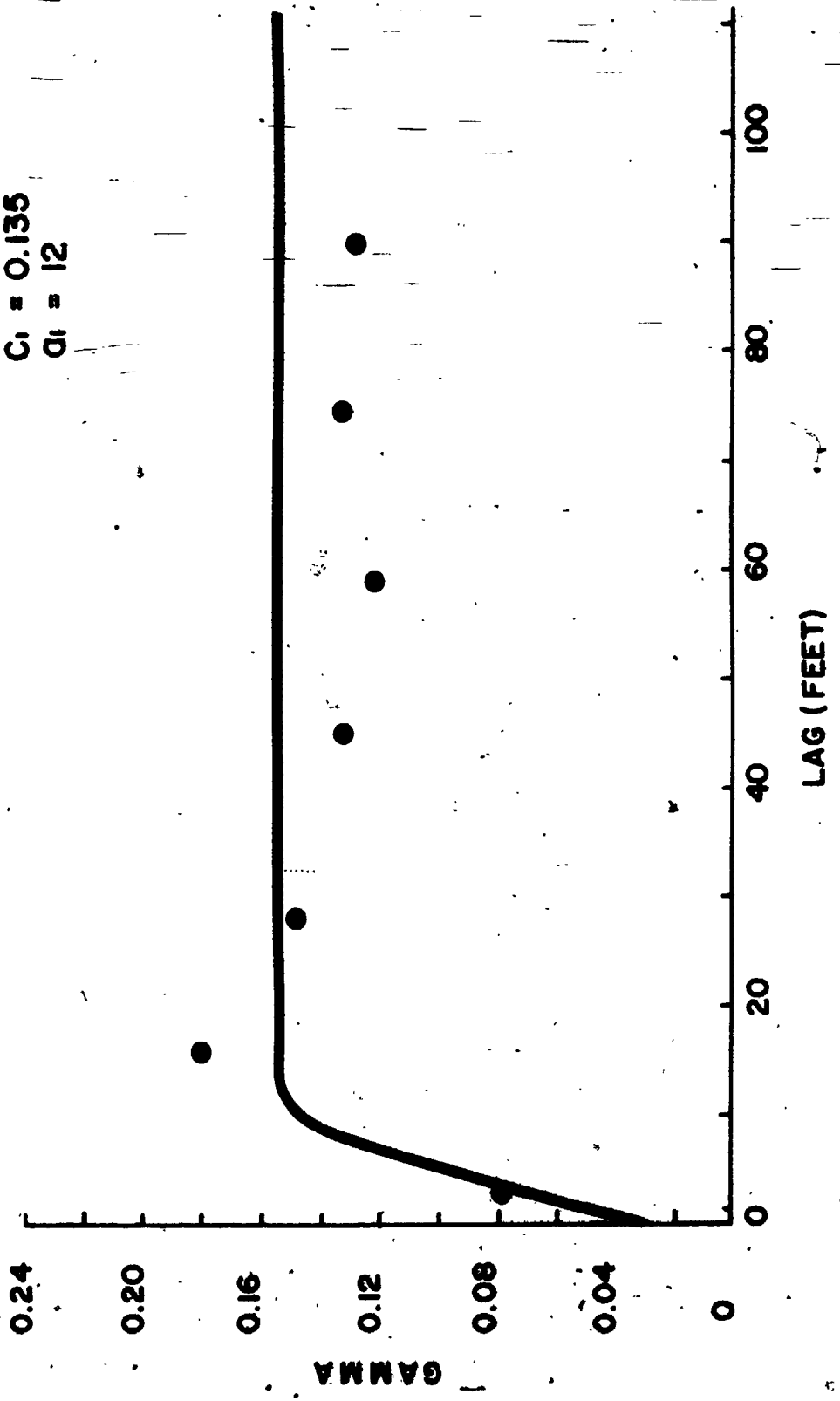
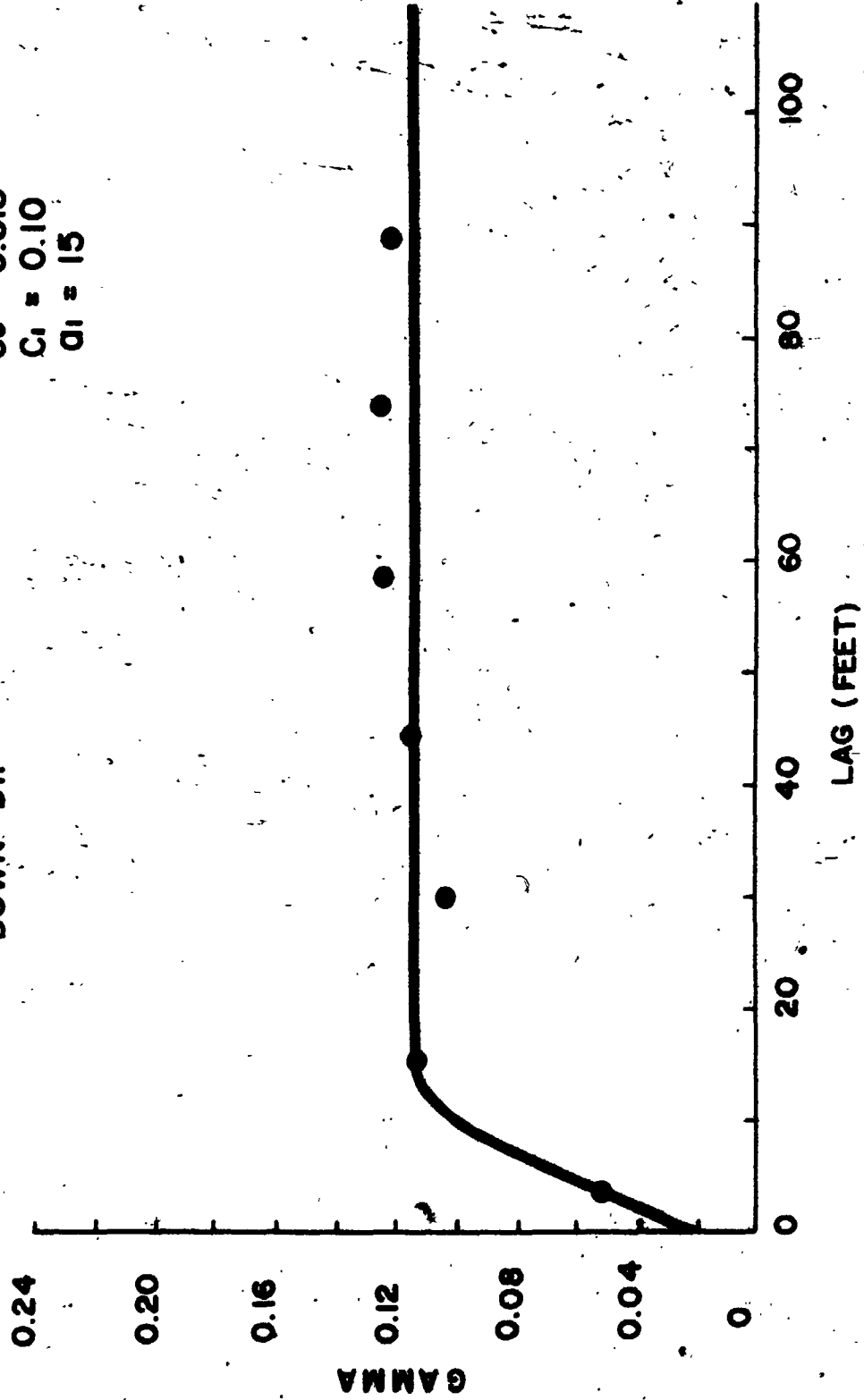


Figure 6-6. .c) Experimental semi-variogram and model. Down dip direction. $a_1 = \text{range}$;
 $c_1 = \text{sill}$; $c_0 = \text{nugget-effect factor}$.

EXPERIMENTAL SEMI-VARIOGRAM & MODEL

DOWN DIP

$C_0 = 0.015$
 $C_1 = 0.10$
 $\alpha_1 = 15$



by others along the length and breadth of all mines in the Kirkland Lake district (Thomson et al., 1950; Hawley, 1950).

6.3 Concluding Statement

The experimental mean semi-variograms calculated for the one-dimensional case in section 6.2.4 had distinctly different sills for the population subgroups based on mining levels. This reflects a general increase in average gold content (Z+) on the 5025' level and 5150' sublevel noted previously in Tables 6-3 and 6-4. The general shapes of these semi-variograms differ from each other by a proportional effect directly with the experimental mean. This is evidence of a general inhomogeneity of gold distribution.

The indication of a hole-effect phenomenon and nested structures in some of these one-dimensional semi-variograms correlated with known geology in that the overall breccia-ore study area, defined by the confining structures approximately 50 to 60 ft wide, contains lenses of gold concentrations about 15 to 20 ft wide. These characteristics are indicative of another type of distribution inhomogeneity known as zonal anisotropy (Journel and Huifbreghts, 1978).

The effects of these two anisotropies were reduced by selective sorting of data exclusively within the ore zone.

The resulting experimental semi-variograms calculated in three principal directions within the study area were interpreted after the spherical model with similar sill values and different ranges. These characteristics are criteria for a third type of inhomogeneity referred to as geometric anisotropy (Journel and Huijbregts, 1978).

One conclusion of this study is that host rock type does not appear to exert any control on gold distribution within breccia-ore. The strongest control appears to be structural. The study area of breccia-ore is confined by major faults, the '04 and South Breaks. The presence of lensoid domains of greater gold abundance within the study area and crudely developed linear fabric may be attributable to internal shearing and dislocation subparallel to the confining structures. The three types of distribution inhomogeneity identified by geostatistical analysis, proportional effect, zonal and geometric anisotropies, are interpreted to reflect faulting and fracturing events which pre-dated, accompanied and post-dated influx of gold-bearing hydrothermal fluids.

CHAPTER 7

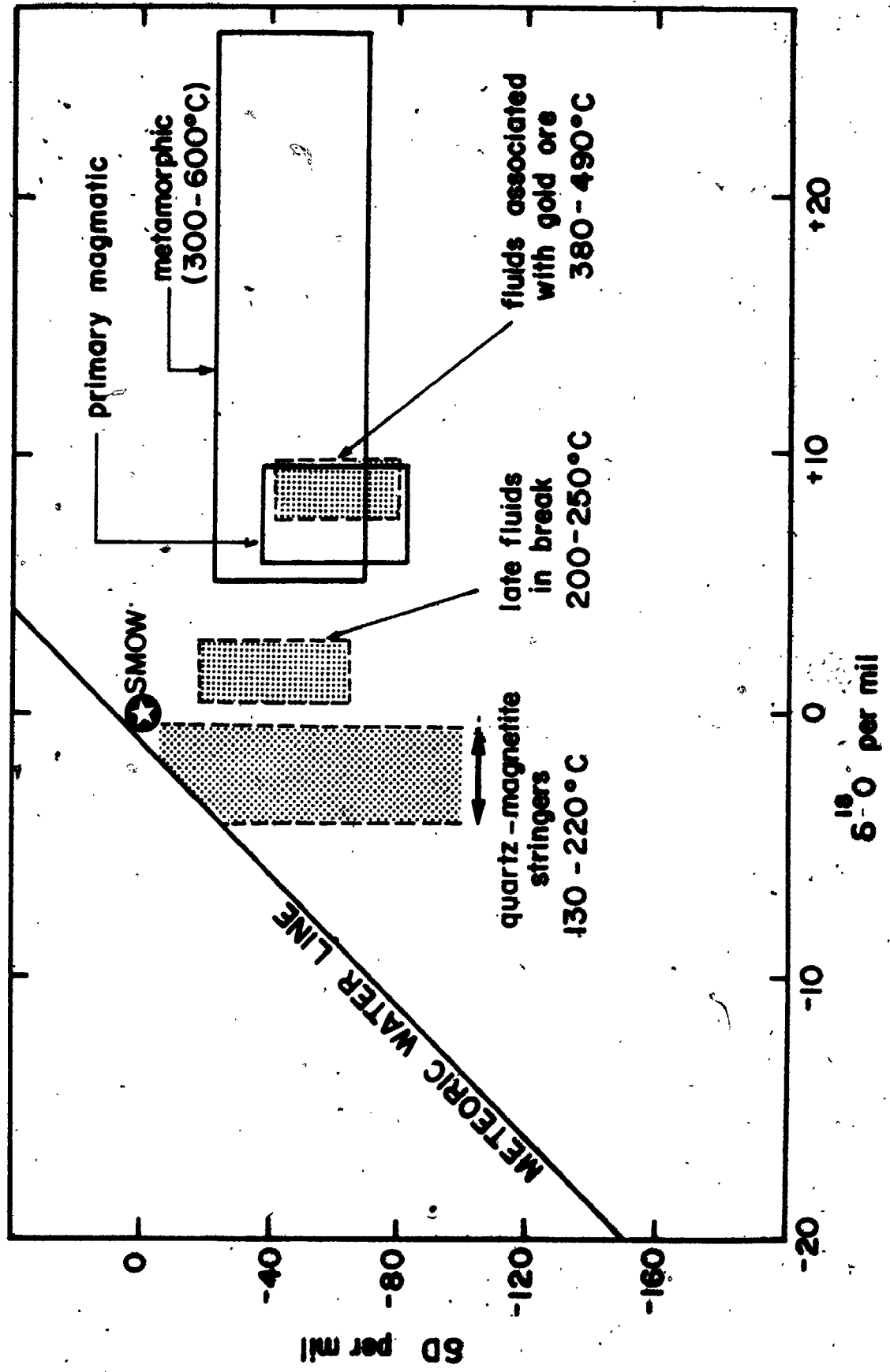
CONCLUSIONS FROM EVIDENCE

The following points summarize the important conclusions from this study:

- 1) Gold occurs as native metal and in precious metal telluride minerals in 3 types of ore at the Macassa Mine i) break ore, ii) vein ore and iii) breccia ore. Each type has a distinct relationship to major structures. The gold ores are enriched in varying amounts in Au, Ag, As, Sb, W, Sc and Te. The gangue minerals are quartz and Ca-, Fe-, Mg-carbonate minerals.
- 2) Mass balance consideration of rocks about ores indicate SiO_2 , S, and K_2O have been added to and Na_2O removed from wallrocks to gold ores. The carbonate gangue minerals do not appear to have formed by precipitation from solution, but rather by wallrock reactions in which Fe-, Mg-, Ca-, Mn-silicates are altered to Fe-, Mg-, Ca-, Mn-carbonate minerals by CO_2 -bearing hydrothermal fluids. Similarly, pyrite in wallrocks is formed by breakdown of iron-bearing silicates and addition of sulphur from the hydrothermal fluids.

- 3) Fe^{2+}/Fe_{Total} is 0.64 to 0.93. Hence, wallrocks to gold ores have been moderately to greatly reduced compared to unaltered rock. Some wallrock to the '04 and Narrows Breaks have Fe^{2+}/Fe_{Total} of less than 0.60, indicating more oxidizing conditions. It is suggested these data reflect two different hydrothermal fluids.
- 4) Gold ores were all precipitated from hydrothermal solutions $\delta^{18}O$ +7 to +9.6 per mil, δD -35 to -85 per mil at 380 to 490°C (Fig. 7-1). These fluids probably evolved by metamorphic dehydration reactions during the accumulation and burial of volcanic and sedimentary rocks of the Upper and Lower supergroups.
- 5) Rocks contained within sections of the '04 and Main Breaks have isotopic and mineral assemblage disequilibrium consistent with the above interpretation of Fe^{2+}/Fe_{Total} data. This has been interpreted to reflect downward penetration of oxidizing, sulphate-bearing fluids, $\delta^{18}O$ 0 to +2.2 per mil, δD -20 to -70 per mil, of probable marine or evolved meteoric water origin (Fig. 7-1) initially at temperatures of $\leq 200^{\circ}C$ (Watson and Kerrich, 1983).
- 6) Isotopic abundances in arrays of quartz-magnetite stringer veins indicate hydrothermal fluids of meteoric origin, $\delta^{18}O = -2$ per mil, at temperatures of 130° to 220°C (Fig. 7-1).

Figure 7-1. Isotopic composition of natural terrestrial fluid reservoirs in D, 180
co-ordinate space modified from Taylor (1974), with calculated fields for
hydrothermal solutions from the Macassa Mine superimposed. SMOW = Standard
Mean Ocean Water (from Kerrich and Watson, 1984).



- 7) The ore mineral assemblage and alteration mineral assemblage is consistent along the 3.2 km length and 1.4 km depth of the underground development of the Macassa Mine with no apparent spatial zonation. The large scale consistency is repeated at the smaller scale of individual areas within breccia ore.
- 8) Analysis of gold distribution within a type area of breccia-ore by geostatistics indicates zonal, geometric and proportional effect anisotropies interpreted to reflect a tectonically active environment of gold deposition. A related conclusion is that rock type does not control the distribution of gold within breccia-ore. Structural control is a more important factor.

SIGNIFICANCE OF MACASSA MINE DATA TO GOLD DEPOSITION
IN THE KIRKLAND LAKE DISTRICT

8.1 General Statement

Thomson et al. (1950) included within a summary of principal geologic events important to gold occurrence in Kirkland Lake an episode of "vein formation, mineralization and gold deposition from a deep-seated source". Hawley (1950), citing evidence first presented by Todd (1928), classified the gold deposits at Kirkland Lake as mesothermal and the result of "the infiltration of ores in hydrothermal solutions". Both the terminology and genetic suppositions reflect these authors' adherence to the classic magmatic hydrothermal theory of Lindgren (1933). According to this theory, epithermal vein-type deposits originated with fracture-filling by metal-rich hydrothermal fluids derived from late-stage crystallization of intrusive bodies (usually granitic). These fluids were thought to migrate along thermal gradients, upward and laterally away from their cooling magmatic source into suitable structural or chemical depositional sites. The model defined a direct

genetic link between the intrusion and the ore deposit contained within neighbouring country rocks. The magma was considered to be the source of both ore-forming fluids and metals.

Substantial increases in our understanding of the details of ore-forming processes in recent years has provided alternative explanations for the existence of epigenetic vein-type deposits in general and gold-bearing quartz veins in particular. Ore-forming metallic and gangue mineral elements are commonly described as being derived from country rocks which enclose the deposits or that are above, below, or lateral to the deposits. Emphasis has been placed on the important role of hot circulating waters external to the magma system (i.e. meteoric, ocean, connate and metamorphic waters) as transporting agents. The fault and fracture systems which become the loci of deposition for epigenetic vein-type deposits are considered to have an active role through the mechanism of seismic pumping and are not merely passive receptors or conduits for mineral-bearing hydrothermal fluids.

Three basic elements of any mineralizing process are: 1) existence of a suitable source area or reservoir for metallic and gangue mineral elements; 2) transporting and concentrating agents and media which have access to the source area; and 3) depositional sites and efficient precipitation mechanisms which result in the formation of an

ore-body. These elements will be discussed, in light of geologic data from the Macassa Mine and environs with reference to appropriate recent research on Archean gold deposits.

8.2 Source of gold

The close spatial association of gold ores with intrusive syenite in the Kirkland Lake district led early workers to assume a magmatic source for the gold. A similar correspondence has been recognized between felsic epizonal intrusions, and lode-gold deposits throughout the Abitibi greenstone belt. Hodgson (1982) from a compilation of geologic records of 725 past and present gold deposits in the Ontario part of the Abitibi belt stated that 40 percent of the occurrences are associated with felsic alkaline suites of rocks and 14 percent with quartz porphyries (Marmont, 1983). Cherry (1983) described a consistent association between gold deposits and felsic intrusive rocks in the Kirkland Lake-Larder Lake area (17 of 33 deposits, 69.9 percent of total Au production) and the Porcupine mining area (15 of 48 deposits, 60.3 percent of total Au production) and suggested the importance of this association had been overlooked since hypotheses of syngenetic gold mineralization had become popular. Despite recognition of this spatial association, implications regarding the genesis of lode gold deposits are unresolved.

8.2.1 Magmatic Fluid Source

Some explanations for the spatial association of Archean lode gold deposits with intrusive rocks are based on supposed anomalous primary concentrations of Au in these rocks. Ploeger (1980, 1981) in his regional study of alkalic intrusive rocks in the Kirkland Lake district noted normal to subnormal background abundances of Au in syenites and concluded that the original gold content of these rocks was not a factor responsible for subsequent enrichment. Similar conclusions were drawn by Kwong and Crocket (1978) for various Archean rocks in northwestern Ontario. Tilling et al. (1973) demonstrated that the gold content of unaltered igneous rocks is restricted and not normally greater than crustal abundances. They also observed no particular relationship between the gold content of igneous rocks and the presence of gold-ore bodies.

There is little evidence to support the original contention that gold deposited at Kirkland Lake or elsewhere was derived from residual magmatic fluids. Tilling et al. (1973) concluded that gold becomes depleted in residual silicate melts during differentiation of calc-alkalic magmas. Kwong and Crocket (1978), in a study of the gold content of various rocks in Northwestern Ontario, noted that quartz and feldspar are poor retainers of gold in comparison to ferromagnesian minerals and if gold does not separate from a melt along with the earlier-formed

mafic minerals it would not be retained in a felsic residua. Boyle (1979) asserts there is considerable difficulty on chemical grounds in deriving many metallic and gangue elements which accompany gold by magma differentiation from basic to intermediate to acid components. These elements tend to be enriched in basic and not acidic rocks and any differentiation during magmatic processes would be to reduce their concentration in residual fluids (Boyle, 1979).

It is suggested that the spatial association of gold in Kirkland Lake with alkalic intrusive rocks does not imply that the gold was derived directly from residual fluids associated with the syenitic melts nor is it related to an intrinsic primary enrichment of Au within the intrusive rocks themselves. It is noteworthy, however, that the two important Canadian occurrences of precious metal telluride minerals are associated with syenites (the Kirkland Lake deposits and the Lower H orebody of the Horne Mine at Noranda (Price, 1948)). It therefore seems possible that late syenite magmatism has somehow provided the tellurium for these ores (Hutchinson and Burlington, 1984).

8.2.2 Country Rock Source

Boyle (1961) introduced the source-bed concept to explain the genesis of Archean epigenetic gold occurrences. This concept held that gold was derived by lateral sece-

tion from surrounding volcanic rocks. Viljoen et al. (1979) suggested that the ultimate source of gold is in "primitive" mafic to ultramafic volcanic rocks from which it was mobilized during regional metamorphism and emplacement of granitic intrusions.

Others have suggested that source areas or source-beds should contain above normal abundances. However, in many gold provinces, no elevated gold concentrations can be detected in the proposed source rocks (Saager et al., 1982).

Keays and Scott (1976) stressed that the suitability of any rock as a source bed for gold is largely determined by the presence of "excess" or "reactive" gold, i.e. by the occurrence of gold in sulphide minerals, as native metal along grain boundaries, or in mesostasis phases. All available data on gold contents of minerals indicate that sulfide minerals can possess pronounced large abundances of Au relative to silicate minerals (Boyle, 1979). The siting of gold in sulfide minerals including those which occur as common accessory rock minerals (eg. pyrite, arsenopyrite, pyrrhotite, chalcopyrite) is unresolved. However, irrespective of the specific mode of occurrence, as lattice substitution, crystal defect structure or submicroscopic inclusions, gold contents from 1 to >2000 ppm have been reported in common sulfide minerals (cf. Boyle, 1979, Table 11). Thus, supraerustal rocks generally contain gold

available to leaching by hydrothermal solutions. A rough estimation, based on gold solubility data in sulfide minerals has gold abundances of up to 5 ppb in a rock that can be accounted for by sulfide mineral contents of less than 0.002 wt. %.

It has been commonly argued that any given ore-body can be created by efficient hydrothermal leaching of a sufficiently large volume of any rock, given average crustal elemental abundances. Although the argument may be appropriate for base metal deposits, it is less suitable for gold deposits. Given that the gold deposits of the Kirkland Lake district contain Au at the 10-15 ppm level and have produced in excess of 710,000 kg Au since 1913 (Lovell and Ploeger, 1980; Bertoni, 1983), the volume of rock with normal average Au content (2 to 5 ppb) required as a source reservoir for these deposits would be in the range of 10 to 100 km³. This assumes an extraction mechanism that is 100% efficient and ignores the amount of gold remaining in the Kirkland Lake district that could not be profitably mined.

Similar considerations discussed in Fyfe and Kerrich (1984) suggest that any source rock abnormally rich in Au would be of great significance. As stated, Keays and Scott (1976) proposed that the suitability of any rock as a source for vein-type gold is largely dependent on the presence of Au which is readily accessible to migrating

hydrothermal solution. Recent papers by Keays (1982, 1984) have proposed that komatiitic and related extrusive rocks and interflow chemical sediments resulting from the seawater alteration of these rocks are particularly important source rocks in that they contain elevated gold abundances within reactive sulfide minerals.

Keays (1984) suggests that komatiitic and related magmas have enhanced levels of Au and platinoid elements relative to other magmas. Because gold is preferentially hosted in sulfide minerals, it is proposed that the precipitation of gold from any crystallizing magma is essentially determined by its sulphur fugacity. The large precious metal contents of komatiitic rocks is probably related to their high temperature of magma generation and subsequent late-stage saturation with respect to immiscible sulfide liquids. In some cases, sulphur-saturation of komatiitic magmas may occur just prior to eruption. If so, small droplets of immiscible sulfides are kept in suspension within the silicate magma as it is erupted (Keays, 1982). As the magma crystallizes, immiscible sulfide melts separate from the intercumulus silicate liquid. Precious metals would be scavenged by the sulfide melts. At the end of the magmatic stage, the resulting disseminated sulfide minerals would be strongly enriched in Au relative to concentrations in silicate and oxide mineral phases. These sulfide minerals generally reside along grain boundaries

and are very reactive compared to silicate and oxide mineral phases.

As the freshly extruded hot lavas cool, shrink, and crack they are invaded by heated, convectively circulating seawater. Simple reaction of the sulfide minerals with near-neutral aqueous solutions would generate the reduced sulphur species (cf. Ewers, 1977) required to form the stable $\text{Au}(\text{HS})_2$ complex (Seward, 1973, 1984). The Au liberated at the sea-floor alteration stage is incorporated into interflow chemical sediments and intra-pillow sites during lulls in volcanic activity (Keays, 1984).

Given the large volumes of komatiitic rocks present in both the upper and lower supergroup volcanic cycles in the Kirkland Lake district, they plausibly represent a significant source of Au for subsequent mineralizing processes. The mechanisms described above would effectively pre-concentrate Au in these rocks and the mineralogical setting of that Au would ensure later access to potential leaching solutions. Jensen (1980) has already described the probable existence of various zones of gold enrichment by Archean sedimentary and volcanogenic processes operative in the Timmins-Kirkland Lake region.

8.3 Transport Agents and Media.

Almost all gold concentration processes involve the interaction of fluids with rocks and the dominant component

of such fluids is water. Fluid inclusions from gangue minerals and stable isotope abundance show that such fluids can and do transport gold and provide solutions from which gold can be precipitated (Roedder, 1984). Such models have been confirmed by direct measurements of gold concentrations in natural thermal waters. Data presented earlier from the Macassa Mine showed that fluids involved with the transport and deposition of gold were isotopically similar to either metamorphic waters or magmatic waters. The interpretation of these fluids as metamorphic waters is preferred here primarily because of the lack of geologic evidence for a significant volume of strictly late-stage magmatic fluids. At the Macassa Mine and throughout the mines of Kirkland Lake, the gold ore types occupy faults and fractures which cut and offset all of the igneous rocks down to the deepest level of mining. This indicates these rocks were fully consolidated and any processes of differentiation that might have resulted in late-stage magmatic fluids had ceased when the gold ores were formed. Also, the contact zones between the composite syenite stock and the Timiskaming Group volcanic and sedimentary rocks are not characterized by extensive alteration of any sort. Rather, it is the norm for all mines in the Kirkland Lake district that the wallrock alteration is controlled by and directly related to the fault and fracture system which transects all rock types. If one can judge from the lack

of chemical and mineral changes in wallrocks adjacent to the syenite, it is probable that the magmas that produced these rocks did not contain appreciable quantities of volatiles, metallic or gangue mineral elements during late stages of differentiation.

One process whereby large volumes of metamorphic fluids are mobilized involves prograde metamorphic dehydration and degassing. The general features of this process are summarized in Fyfe et al. (1978). During progressive metamorphism, at all major facies boundaries, large quantities of fluids are released from reacting minerals and fluids are produced, prior to their escape, on at least 50% of all mineral grain boundaries of the reactive rock (Fyfe and Kerrich, 1984). In the context of the preceding discussion on the development of Au-enriched zones within komatiitic volcanic rocks and associated chemical sediments, very efficient extraction of all trace metals held interstitially or in solid solution within reactive mineral phases (i.e. auriferous sulfide minerals) can occur in this environment. At most major facies changes, i.e. zeolite facies to greenschist, greenschist to amphibolite, the amount of water released is normally several percent. Except at extreme temperatures, near melting, the metamorphic fluid will have $H_2O > CO_2 \gg Cl$. The CO_2 content (and CO) will rise exponentially with the temperature of metamorphism, as will the HCl concentrations (Kerrich and

Fyfe, 1981).

A possible objection to the involvement of metamorphic fluids in the formation of the gold ores in the Kirkland Lake district is the lack of evidence for prograde regional metamorphism in the vicinity of the mine. However, fluids are continuously released from hydrated minerals during prograde metamorphism (Fyfe et al., 1978). The presence of metamorphic isograds indicating higher-grade conditions around the gold deposits is not a necessary condition (Kerrick, 1983).

Gold is usually in one of three oxidation states: 0 (native), +1 (aurous) and +3 (auric). The presence of the free ions, Au^+ and Au^{3+} , are unknown in aqueous media. Both are very complexed or hydrolysed and the mobility of gold is dependent on suitable available complexing species (Boyle, 1979). The chemistry of gold complexes has been summarized by Puddephatt (1978). Gold can form a wide range of complexes with such ligands as halide ions, sulphur species, carbonyls based on CO and nitrogen-containing species. All may be present in hydrothermal solutions (Fyfe and Kerrich, 1984).

The exact nature of gold-complexing species capable of attaining sufficient concentrations of Au in hydrothermal fluids is a matter of continuing debate. A thorough understanding of hydrothermal transport and deposition of gold is inhibited by the paucity of experimental data for high

temperature and pressure conditions (Seward, 1984).

8.4 Deposition - The role of structures

In the study by Hodgson (1982, 1983) previously cited, another clear association recognized was the influence of structural control on gold occurrences in the Abitibi greenstone belt. Out of 449 auriferous zones in the Timmins-Kirkland Lake area, 343 or 76.4 percent were described as being controlled by or occurring within shear zones, fractures and faults. Clearly the gold-bearing zones at the Macassa Mine and others in Kirkland Lake are prime examples of this structural association.

Early workers in the Kirkland Lake district concluded that two types of structures had particular importance in controlling the gold occurrences: 1) Mine scale system of faults and fractures directly related to the emplacement and cooling of the composite syenite complex within Timiskaming Group rocks; and 2) Regional scale structures which influenced the location of the mining district, i.e. the Kirkland Lake Main Break. The latter type has been expanded in more recent years by others to include the significance of the Main Break and the Kirkland Lake - Larder Lake Break (Fault Zone) in terms of regional stratigraphic development.

8.4.1 Mine Scale

At this scale, the control exerted by structures is commonly described as "ground preparation", the development of faults and fractures in and around the syenite intrusion which subsequently became conduits for hydrothermal fluids. Solidification of the syenitic melt to crystalline rock and further thermal contraction upon cooling probably resulted in a 10 percent volume reduction. Internal stresses set up by this volume reduction created sets of joints, fractures and faults. A preferred orientation of these structures would have been approximately parallel to contact surfaces of the intrusion with Timiskaming Group rocks.

Similarly, fracture and joint surfaces were created within Timiskaming Group rocks during the emplacement of the rising magma. Development of particular curvilinear structures and associated fractures has already been described along the 4250' level and related to drag-folding of country rocks adjacent to the intrusion.

8.4.2 Regional Scale

The spatial association of Archean lode gold deposits with long linear and curvilinear zones of intensely folded and faulted, schistose and altered rock, termed 'breaks', has been recognized for decades (Thomson, 1948; Thomson, 1948). These have most commonly been interpreted

as major faults.

It has been suggested recently that some parts of the larger breaks are faults which were active at the time the volcanic and sedimentary rocks were deposited. Jensen (1980), in considering the gold deposits of the Kirkland Lake - Larder Lake area, proposed that the formative processes operated in several stages along and around a regional fault and fracture zone - the Kirkland Lake - Larder Lake Break - that first developed during accumulation of the second volcanic cycle. The fault zone is interpreted as listric normal faults associated initially with crustal rifting and basinal development.

In this context, the Kirkland Lake Main Break may be considered a branch of the more extensive regional system. The zone of weakness now represented by the Main Break system probably existed prior to, during and after the emplacement of the composite syenite stock, controlled the locus of emplacement of these rocks and their subsequent fracturing and faulting and acted as a focussed discharge zone for hydrothermal fluids.

8.5 Seismic Pumping - The Active Role of Structure

In considering the role of regional and local fault and fracture systems during the operation of hydrothermal ore-forming processes, most models assume these structures play a passive role, merely providing very permeable zones

or conduits for fluids moving in response to thermal or pressure gradients. Here it is suggested that the fault and fracture systems themselves may be key factors in transporting significant volumes of mineralizing fluids from one crustal environment to another via the mechanism of seismic pumping.

8.5.1 Seismic Pumping Model

Fluid movement in active modern fault zones is an established phenomenon from the observation of the periodic surface effusion of hydrothermal waters following moderate to large shallow-focus earthquakes in consolidated rock (Sibson, 1981). This phenomenon has been explained by the dilatancy/fluid-diffusion model for energy release in shallow earthquakes. The following synopsis is condensed from Sibson et al., 1975.)

In its simplest form, the model supposes that prior to seismic shear failure along an existing fault, the region for considerable distance around the focus of the subsequent earthquake dilates in response to rising tectonic shear stress. This results in the opening of extension cracks and fractures normal to the least principal compressive stress. The development of this fracture porosity causes the fluid pressure (p) in the dilatant zone to decrease, inducing a slow, inwards migration of fluid from surrounding rocks.

At the onset of dilatancy, the drop in fluid pressure causes a rise in the frictional resistance to shear along the fault. As the migrating fluids fill the dilatant zones, fluid pressure again rises and frictional resistance decreases. Seismic failure eventually occurs when the rising shear stress equals the frictional resistance.

The rapid, partial release of shear stress which accompanies earthquake faulting allows the cracks in the dilatant zone to relax and the fluids they contain must be expelled rapidly upward in the direction of easiest pressure relief. Upflow from the collapsing dilatant zone must take place through the fault and fracture system.

Major displacement along fault and shear zones is normally accomplished by a large number of individual seismic events related to localized shear dislocations which are discontinuous over the entire surface of the fault-shear zone. The dilatancy/fluid-diffusion model provides an explanation for the intermittent flow of hydrothermal fluids in and around fault zones and suggests that seismic faulting acts as a pumping mechanism whereby individual earthquakes are capable of moving large volumes of fluids.

8.5.2 Geologic Evidence for Seismic Pumping

Textural features and structures within many hydrothermal vein-type deposits commonly indicate a series of

mineralization episodes as opposed to a discrete event. Two inferences result from such evidence: 1) that incremental deposition of minerals occurred when pulses, rather than a steady flow of hydrothermal fluid, passed through the fault-fracture system; and 2) that the fluid pulses were associated in time with increments of shear and extensional displacement on these fault-fracture systems (Sibson et al., 1975).

There are several aspects of the gold occurrences at the Macassa Mine which indicate both multi-stage movement along the fault and fracture planes and multi-stage fluid flow associated with the gold emplacement. Fracturing, comminution and incorporation of wallrocks adjacent to major faults followed by re-fracturing of these materials, into coarse breccias and even later fracturing of this secondary breccia (Thomson et al., 1950) shows clear evidence of complex, sequential episodes of deformation. The sequential development of different structural age groups in the mine in relation to the main ore-forming period, i.e. pre-ore, post-ore with varying degrees and senses of movement also is evidence of multi-stage deformation. The general paragenetic sequence defined by Hawley (1950) suggests gold-bearing veins incorporate 4 to 5 episodes of quartz deposition. It is interesting in this regard to note that although Hawley assigned native Au and precious metal tellurides to late stages of the mineraliz-

ing sequence, it is equally possible that gold mineralization was associated with several stages of mineral deposition and was subsequently "refined" by the later tectonic reworking. This supposition is supported by the common observation of leaf-gold occupying fractures normal to vein and fault margins indicating the ductile native metal had migrated during late deformation. Further support is given by the observation of Bloomfield et al. (1936) that early generations of auriferous pyrite at the former Lake Shore Mine tended to be silver-rich (lesser fineness) whereas later generation of native gold were silver-poor (greater fineness).

A notable feature of the gold occurrences in the Kirkland Lake district generally is the large scale homogeneity of mineral occurrences throughout the considerable length and depth of the Kirkland Lake Main Break system. Thomson et al. (1950) and Hawley (1950) have commented on the unchanging nature of the ore minerals and associated gangue minerals. The consistent spatial relationships suggest that mineralizing fluids were not only moving in response to ambient thermal or pressure gradients but rather were pumped into the structures en masse and gold deposition occurred essentially in situ as the system cooled and stabilized.

CHAPTER 9

GENETIC MODEL FOR THE KIRKLAND LAKE DISTRICT

9.1 General Statement

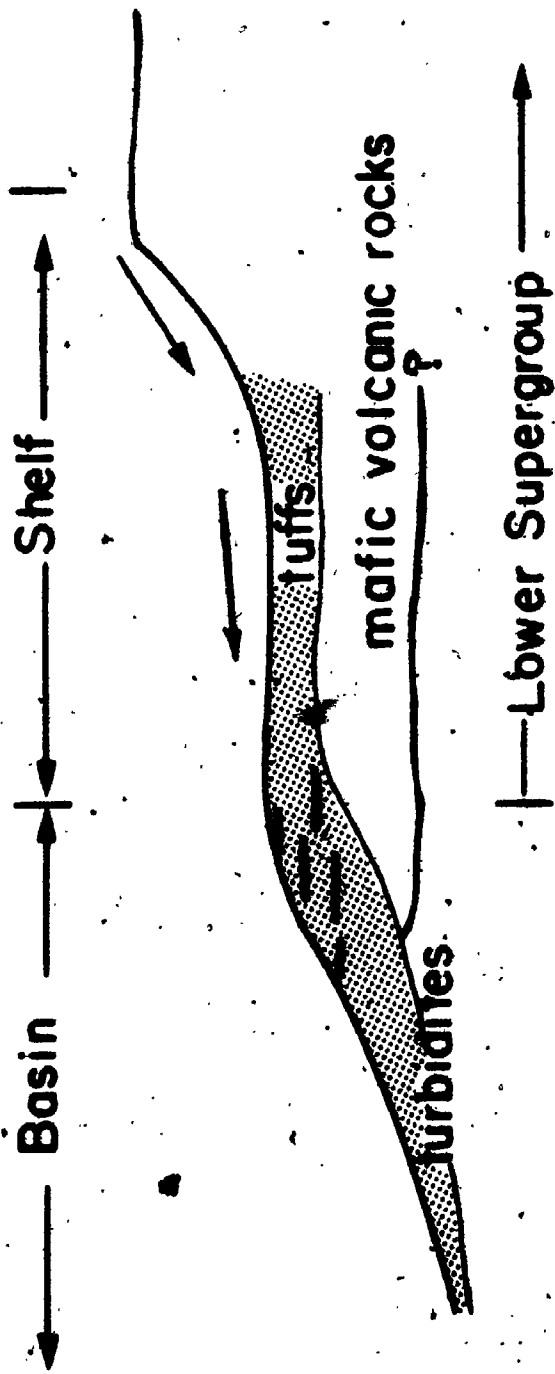
Jensen (1980) described the evolution of the Kirkland Lake - Larder Lake Break during the deposition of volcanic and sedimentary rocks of the Upper Supergroup. This description has been adapted to form a framework for a model for gold deposition in the Kirkland Lake district.

9.2 A Sequence of Events

By the end of the first complete volcanic cycle, Lower Supergroup rocks consisted of calc-alkalic strata volcanoes surrounded by a shallow marine shelf which extended toward a deep water basin. Turbidites, chemical sediments and tuffaceous rocks deposited on the shelf and in the nearby basin represent the erosional debris from the existing volcanic pile. The eroding terrain may have contributed clastic gold and gold in solution derived from pre-existing, primary volcanogenic exhalative deposits. This gold would have accumulated in troughs and chemical traps along the early shelf margins (Fig. 9.1a).

Figure 2-1. Schematic diagrams of proposed sequence for gold deposition in the Kirkland Lake district.

2-1a) Erosion of Lower Supergroup rocks and deposition of turbidite, tuffaceous rocks and chemical sediments on marginal shelf and in basin. Potential Au accumulations marked in black (after Jensen, 1980).



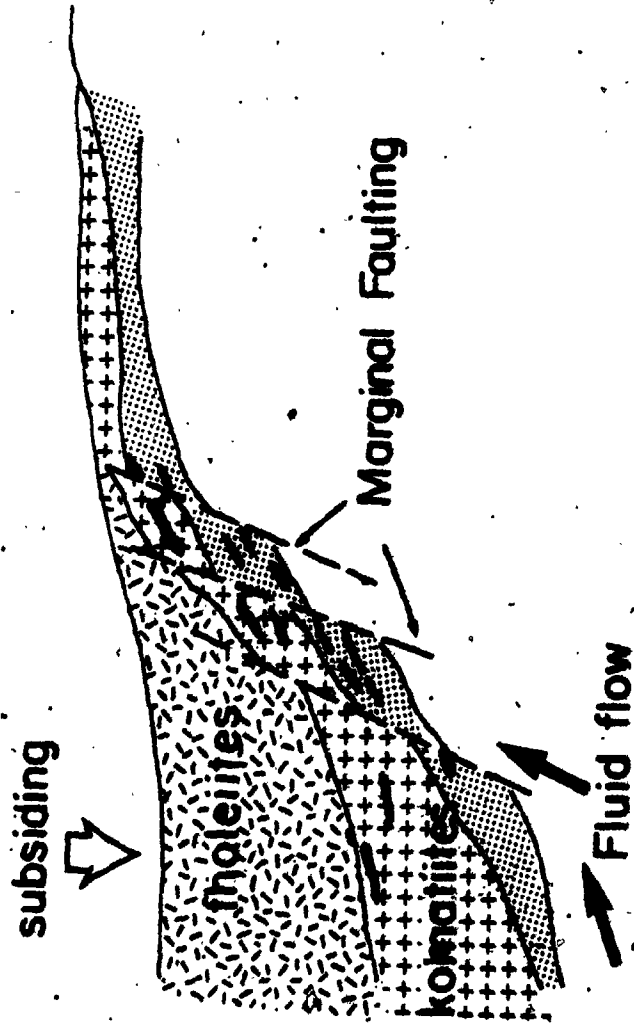
Deposition of the second volcanic cycle, the Upper Supergroup, commenced with the emplacement of ultramafic rocks on the floor of the deep water basin and the sedimentary and calc-alkalic volcanic rocks along shelf areas. Ultramafic and mafic lavas began to fill the basin and engulf the rocks along the shelf. During quiescent periods between volcanic episodes, gold contained within the lower komatiitic lavas would be leached by convectively circulating heated seawater brines and deposited in cherty, pyritic chemical sediments (cf. Hutchinson, 1976; Keays, 1982, 1984).

As lavas accumulated in the basin, their increasing weight depressed the basin floor inducing tension related faulting, fracturing and slumping along the margins of the underlying Lower Supergroup. These structures may have become zones of focussed discharge of fluids related to early metamorphic dewatering reactions or hydrothermal convective circulation (Fig. 9-1b).

Fluid flow along the marginal zone precursor to the Kirkland Lake - Larder Lake Break caused extensive carbonate alteration of rocks adjacent to major structures. This flow of altering fluids was apparently operative for a considerable length of time as evidenced by the presence of carbonate-altered ultramafic, spinifex-bearing clasts and fragments within Timiskaming conglomerates. This period of fluid flow may have been related to gold occurrences within

9-1b) Deposition of komatiitic and tholeiitic rocks of Upper Supergroup, depression of basin floor and marginal faulting (after Jensen, 1980).

Basin Shelf



the Larder Lake Group at Virginiatown.

As the basinal area was filled with komatiitic and tholeiitic volcanic and associated sedimentary rocks (Larder Lake and Kinojevis Groups); the accumulating weight continued to downwarp the basin floor. Much of the displacement probably occurred within the komatiitic and sedimentary rocks near the margin of the shelf and was accommodated by movement along marginal growth faults. Both the movement and fluid flow resulted in serpentinized komatiitic rocks and the formation of talc-chlorite schists along the Kirkland Lake - Larder Lake Break (Jensen, 1980).

Downward displacement of rocks on the basin side of the marginal fault zone, relative to the same rocks resting on the shelf area of the older volcanic pile accounts for the general north-dipping, north-facing attitude of pillow lavas from the Kinojevis Group north of Kirkland Lake.

Emplacement of calc-alkalic volcanic rocks of the Blake River Group toward the core of the newly formed volcanic pile was probably associated with an inward collapse of the older volcanic rocks toward the center of the original basin. This collapse resulted in dilation of the marginal faults and creation of a graben-like structural zone which was subsequently in-filled with high energy clastic and volcanoclastic sediments and trachytic volcanic rocks of the Timiskaming Group (Fig. 9-1c).

The graben zone probably encompassed a wide area and

175

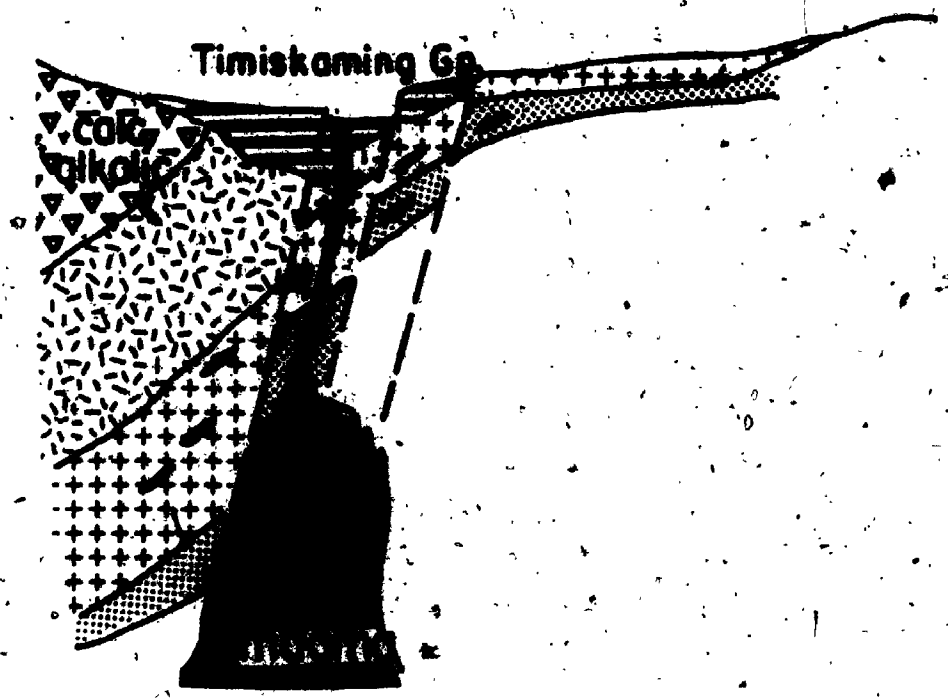
Figure 9-1c. Basin collapse, formation of graben zone and subsequent in-filling by Timiskaming group rocks. Later injection of magmas (after Jensen, 1980).

Basin
Collapse

Graben
Zone



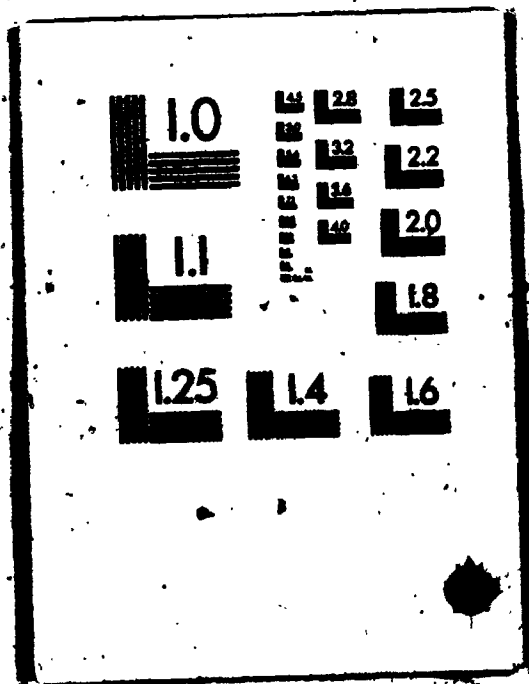
← tensional



4

4

OF / DE



included a number of normal faults subsidiary to the original locus of deformation and alteration along the Kirkland Lake - Larder Lake Break (ie, Kirkland Lake Main Break, Narrows Break, Amalgamated Kirkland Mud Break).

Differential movement along these fault structures resulted in the rotation of major units of Timiskaming Group rocks into their present south-dipping, south-facing attitude.

Pressure release associated with deep penetration of the marginal growth faults and graben block-bounding faults may have caused anatexis of downdropped volcanic and sedimentary rocks. Alternatively, the major faults may have created zones of crustal weakness allowing upward penetration of mantle-derived syenitic magmas. These melts intruded along and around the structural zone now represented by the Kirkland Lake Main Break. Fracturing and faulting associated with cooling and solidification of these melts in addition to subsequent episodes of fault movement along the Main Break system created a very continuous zone of brittle deformation within the syenites and Timiskaming Group rocks.

Continuing, intermittent seismic activity and fault movement on these major fault systems accomodating crustal compression along the basin margin resulted in mass movement of potentially ore-forming fluids via the dilatancy/fluid-diffusion mechanism. These fluids may have been derived from a variety of primary fluid reservoirs, princi-

pally metamorphic with or without a magmatic component. They were repeatedly drawn down and into the active fault systems, possibly to depths exceeding 10 km to allow for heating to 450°C, assuming an Archean geothermal gradient of 30°C/km, and expelled upwards following an undetermined residency period into the very fractured and broken rocks around the Kirkland Lake Main Break. These hydrothermal fluids were characterized by low redox, low salinity (< 3%), low pH; and had elevated CO₂ contents coupled with sodium to potassium ratios near unity (Kerrick, 1983). The fluids repeatedly leached and scavenged Au from various potential, primary and secondary sources within the volcanic and sedimentary rocks of the Lower and Upper Supergroups and deposited gold within quartz-carbonate ores in the Main Break system (Fig. 9-1d).

At some point, the upward flux of these hydrothermal fluids decreased, possibly during a period of crustal relaxation. The fault and fracture system was affected in places by an incursion of oxidizing, sulphate-bearing marine (or meteoric) waters.

A final, compressive regional event, possibly associated with the emplacement of large batholithic complexes, resulted in closure of the basin, uplift of the faulted margin and shelf areas above sea-level, reverse or thrust motion along major faults accompanied by a change in attitude and formation of major crossfault systems. Fluid


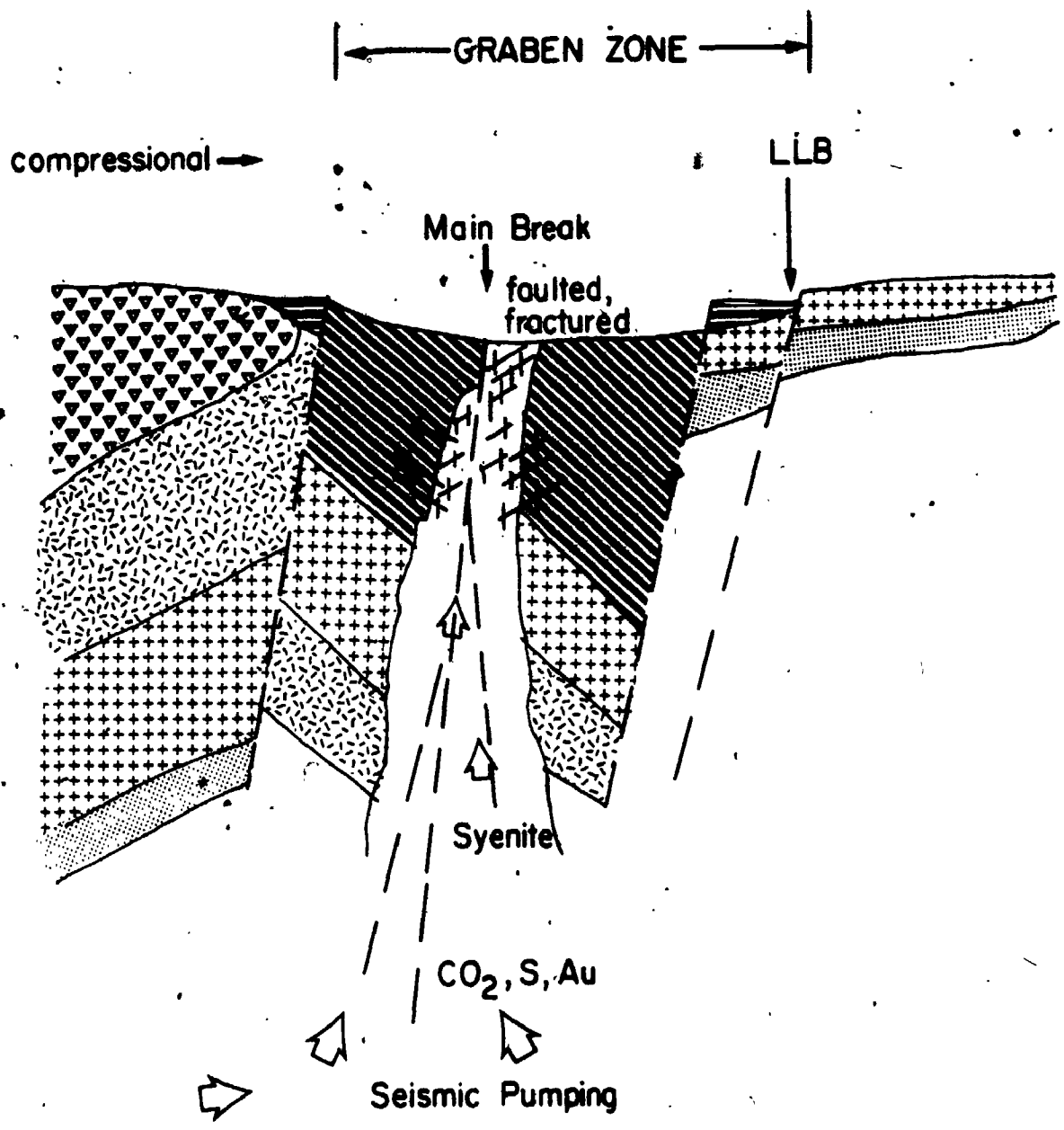


Figure 9-1d. Compression of graben zone, seismic pumping of hydrothermal fluids which leach Au and deposit in fractured syenites and Timiskaming Group rocks. Previous, normal, margin faults become sub-vertical reverse faults with continued compression. LLB = Larder Lake Break.



flow within the fault systems diminished and was eventually restricted to downward percolation of surface waters.

APPENDIX A

ANALYTICAL METHODS

Conventional procedures were used for the extraction of oxygen from minerals with bromine pentafluoride and quantitative conversion to CO₂ prior to mass spectrometric analysis (Clayton and Mayeda, 1963). Isotopic data are reported as $\delta^{18}\text{O}$ values in per mille relative to Standard Mean Ocean Water (SMOW). The overall reproducibility of $\delta^{18}\text{O}$ values has averaged +0.18 per mil (two standard deviations) (R. Kerrich, pers. comm., 1983).

Fractionations, or differences in $\delta^{18}\text{O}$ among minerals, are quoted as Δ defined as:

$$\Delta_{A-B} = 1000 \ln \alpha_{A-B} \quad \delta_A - \delta_B$$

where α_{A-B} is the fractionation factor for the coexisting minerals A and B.

Mineral separates for isotopic analysis were obtained using standard techniques based on relative magnetic susceptibility, and utilising a Franz isodynamic separator. Pure quartz was recovered from quartz-feldspar mixtures by means of a selective digestion of the latter in hydrofluorosilicic acid (H₂SiF₆). Quartz and chlorite were

intimately intergrown in samples A and G-82-150, such that pure chlorite separates could not be made. For these samples the $\delta^{18}\text{O}$ chlorite was estimated from that of the chlorite-quartz mixture, knowing their relative proportions and the $\delta^{18}\text{O}$ of quartz. In each case relative proportions were estimated from (a) XRD, (b) visual counting and (c) the oxygen yield of the mixture as compared to that of the two end members.

Whole rock major element abundances reported in this study were determined by X-ray fluorescence spectrometry by X-Ray Assay Laboratories in Toronto. Most samples were analysed once to avoid excessive costs in duplication. Five random samples within the 48 sample group were analysed twice in order to establish the reproducibility of analyses. All duplicate analyses were found to agree within 5% of each other.

X-Ray Assay Laboratories reports a standard detection limit of 0.010 wt. percent for major elements. Table A-1 summarizes other data on precision and accuracy routinely achieved by the X-Ray Labs.

Transition metal abundances were determined by Barringer Magenta Laboratories, Toronto, using induction coupled argon plasma spectrometry. Published detection limits supplied by Barringer-Magenta Labs range from 1 ppm for Cu and Ni to 5 ppm for Pb.

Au, As, Sc, Sb, W and Th abundances together with rare

Table A-1

<u>WHOLE ROCK ANALYSIS - XRF - PW1600 - REFERENCE STANDARDS</u>									
	<u>SY-1</u>	<u>SY-3</u>	<u>MRS-1</u>	<u>AGU-1</u>	<u>DTG-1</u>	<u>G-2</u>	<u>W-1</u>	<u>69a</u>	
SiO ₂	60.1 (60.10)	59.5 (59.68)	38.9 (39.32)	59.4 (59.61)	40.1 (40.61)	68.8 (69.22)	52.4 (52.78)	5.90 (6.01)	SiO ₂
Al ₂ O ₃	12.1 (12.12)	11.7 (11.80)	8.41 (8.50)	17.2 (17.19)	0.23 (0.25)	15.4 (15.40)	14.9 (15.02)	55.4 (55.0)	Al ₂ O ₃
CaO	7.99 (7.98)	8.21 (8.26)	14.8 (14.77)	4.99 (4.94)	0.13 (0.14)	1.95 (1.96)	11.1 (10.98)	0.31 (0.29)	CaO
MgO	2.71 (2.70)	2.69 (2.67)	13.4 (13.49)	1.52 (1.52)	49.3 (49.80)	0.72 (0.75)	6.59 (6.63)	0.01 (0.02)	MgO
Na ₂ O	4.38 (4.34)	4.10 (4.15)	0.71 (0.71)	4.35 (4.32)	0.00 (0.017)	4.10 (4.06)	2.20 (2.15)	0.00 (0.00)	Na ₂ O
K ₂ O	4.40 (4.48)	4.14 (4.20)	0.18 (0.18)	2.88 (2.92)	0.00 (0.00)	4.40 (4.46)	0.62 (0.64)	0.01 (0.00)	K ₂ O
Fe ₂ O ₃	6.30 (6.28)	6.43 (6.42)	17.7 (17.82)	6.77 (6.78)	8.61 (8.70)	2.70 (2.69)	11.2 (11.11)	5.91 (5.80)	Fe ₂ O ₃
MnO	0.32 (0.32)	0.32 (0.32)	0.16 (0.17)	0.10 (0.10)	0.12 (0.12)	0.03 (0.03)	0.17 (0.17)	0.02 (0.02)	MnO
TiO ₂	0.15 (0.14)	0.15 (0.15)	3.80 (3.69)	1.11 (1.06)	0.01 (0.007)	0.50 (0.48)	1.10 (1.07)	2.85 (2.78)	TiO ₂
P ₂ O ₅	0.43 (0.43)	0.53 (0.54)	0.06 (0.06)	0.49 (0.51)	0.00 (0.007)	0.13 (0.13)	0.13 (0.14)	0.07 (0.08)	P ₂ O ₅

Note: () are usable values as per Sydney Abbey, 1979.
This represents only part of the group of 40 reference materials used for calibrating the simultaneous spectrometer. Others are available on request.

INSTRUMENT STABILITY

(10 replicate analyses)

	<u>Mean (%)</u>	<u>SD (%)</u>	<u>Mean (%)</u>	<u>SD (%)</u>
SiO ₂	75.52	0.05	49.37	0.05
Al ₂ O ₃	12.85	0.02	13.70	0.03
CaO	0.74	0.00	11.68	0.04
MgO	0.00	0.00	7.36	0.03
Na ₂ O	3.76	0.04	2.04	0.04
K ₂ O	4.56	0.01	0.48	0.005
Fe ₂ O ₃	1.19	0.005	12.41	0.02
MnO	0.05	0.00	0.17	0.00
TiO ₂	0.09	0.00	2.87	0.01
P ₂ O ₅	0.01	0.00	0.28	0.00

SAMPLE PREPARATION REPRODUCIBILITY

(42 replicate analyses)

	<u>Mean (%)</u>	<u>SD (%)</u>	<u>Mean (%)</u>	<u>SD (%)</u>
SiO ₂	49.5	0.30	52.3	0.25
Al ₂ O ₃	17.5	0.10	16.8	0.10
CaO	8.56	0.05	8.58	0.05
MgO	2.38	0.04	5.97	0.05
Na ₂ O	3.91	0.04	2.52	0.02
K ₂ O	0.64	0.01	0.78	0.01
Fe ₂ O ₃	13.0	0.10	8.42	0.08
MnO	0.19	0.005	0.10	0.005
TiO ₂	1.47	0.01	0.93	0.01
P ₂ O ₅	0.14	0.005	0.11	0.005

Note: Mean is the arithmetic mean.
SD is standard deviation.

earth element abundances, were determined by Neutron Activation Services, Hamilton, by INAA and Ag by atomic adsorption spectrophotometry. Analytical precision routinely achieved by this laboratory is stated to be \pm 0.02%.

Trace element abundances, including S, V, Cr, Co, Ni, Cu, Zn, Pb, Rb, Sr, Y, Zr, Nb and Ba were analysed by x-ray fluorescence spectrometry by the writer at the University of Western Ontario. Table A-2 provides some comparative data on estimated precision, accuracy and detection limits achieved on this instrument (T. W. Wu, pers. comm., 1984). Macassa Mine samples were analysed with reference to Sy-2 rock standard.

Ferrous iron abundances reported in this study were determined by the writer titrimetrically using the meta-vanadate method described by Wilson (1955) with reference to Sy-2 rock standard.

Carbon dioxide was measured in a manometer, from CO₂ evolved by exposure of rock powders to HCl.

Feldspar mineral analyses were determined on 25 mm diameter polished thin sections coated with carbon, using a MAC 400 electron microprobe, featuring three spectrometers with KRISSEL automation. An excitation voltage of 15 kV was used, with a beam current of 0.05 A and a counting time of 30 seconds or 20,000 counts. The standards used were well analysed natural minerals and synthetic glasses, selected

Table A-2 The estimated precision, accuracy and detection limit from standard rocks for trace element analysis

Element	UWO-1				G-2			
	Mean(10)*	S.D.	R.D.(%)	R.V.	Mean(5)	S.D.	C.V.(%)	LLD
Nb	22.8	1.78	7.8	13	12.9	1.17	9.07	2.0
Zr	240.7	1.27	0.5	300	299.1	1.75	0.59	2.0
Y	27.1	0.70	2.6	11	11.1	0.21	1.90	1.5
Sr	210.7	3.00	1.4	480	478.7	1.33	0.28	3.0
Rb	198.0	1.50	0.8	170	170.7	2.42	1.42	3.0
Pb	32.7	2.73	8.4	30	30.2	2.16	7.16	5.0
Zn	50.1	2.39	4.8	84	85.7	3.10	3.62	2.0
Cu	9.3	0.40	4.3	10	10.2	0.40	3.92	0.5
Ni	7.7	1.57	20.3	3.5	3.9	1.07	26.88	1.0
Co	24.9	3.32	13.4	5	5.1	0.77	15.16	2.5
Cr	13.3	1.72	13.0	8	7.8	1.28	16.45	1.5
Ba	566.1	16.83	3.0	1900	1784.5	30.15	1.69	8.0
V	42.1	3.61	8.4	36	38.7	4.82	12.45	4.5
Ga	21.4	2.36	11.0	23	22.9	1.63	7.10	4.5

* Number of analyses;

R.V. = Recommended values from Abbey (1980);

S.D. = Standard deviation;

C.V. = Coefficient of variation;

LLD = Lower limit of detection (in ppm).

to minimize necessary corrections. All compositions were
calculated using MAGIC corrections.

APPENDIX B

Criteria for Distinguishing the Origin of Fluid-Inclusions (After Roedder, 1979)

1. Criteria for Primary Origin

- I. Based on occurrence in a single crystal with or without evidence of direction of growth or growth zonation.
 - A. Occurrence as a single (or a small three-dimensional group) in an otherwise inclusion-free crystal.
 - B. Large size relative to that of the enclosing crystal e.g., with a diameter of ≥ 0.1 that of crystal, and particularly several such inclusions.
 - C. Isolated occurrence, away from other inclusions, for a distance of ≥ 5 times the diameter of the inclusion.
 - D. Occurrence as part of a random, three-dimensional distribution throughout the crystal.
 - E. Disturbance of otherwise regular decorated dislocations surrounding the inclusion, particularly if they appear to radiate from it.
 - F. Occurrence of daughter crystals (or accidental solid inclusions) of the same phase(s) as occur as solid inclusions in the host crystal of as contemporaneous phases.

II. Based on occurrence in a single crystal showing evidence of direction of growth:

- A. Occurrence beyond (in the direction of growth), and sometimes immediately before extraneous solids (the same or other phases) interfering with the growth, where the host crystal fails to close in completely. (Inclusion may be attached to the solid or at some distance beyond, from imperfect growth).
- B. Occurrence beyond a healed crack in an earlier growth stage, where new crystal growth has been imperfect.
- C. Occurrence between subparallel units of a composite crystal.
- D. Occurrence at the intersection of several growth spirals, or at the center of a growth spiral visible on the outer surface.
- E. Occurrence, particularly as relatively large, flat inclusions, parallel to an external crystal face, and near its center (i.e., from "starvation" of the growth at the center of the crystal face), e.g. much "hopper salt".
- F. Occurrence in the core of a trigonal crystal (e.g., beryl). This may be merely an extreme case of previous item.
- G. Occurrence, particularly as a row, along the edge from the intersection of two crystal faces.

- III. Based on occurrence in a single crystal showing evidence of growth zonation (as determined by color, clarity, composition, X-ray darkening, trapped solid inclusions, etch zones, exsolution phases, etc.).
- A. Occurrence in random, three-dimensional distribution, with different concentrations in adjacent zones (as from a surge of sudden, feathery or dendritic growth).
 - B. Occurrence as subparallel groups (outlining growth directions), particularly with different concentrations in adjacent growth zones, as in previous item.
 - C. Multiple occurrence in planar array(s) outlining a growth zone. (Note that if this is also a cleavage direction, there is ambiguity.)
- IV. Based on growth from a heterogeneous (i.e., two-phase), or a changing fluid.
- A. Planar arrays (as in III-C), or other occurrence in growth zones, in which the compositions of inclusions in adjacent zones are different (e.g., gas inclusions in one and liquid in another, or oil and water).
 - B. Planar arrays (as in III-C) in which trapping of some of the growth medium has occurred at points where the host crystal has overgrown the surrounded adhering globules of the immiscible, dispersed phase (e.g., oil droplets or steam bubbles).

C. Otherwise primary-appearing inclusions of a fluid phase that is unlikely to be the mineral-forming fluid, e.g., mercury in calcite, oil in fluorite or air in sugar.

V. Based on occurrence in hosts other than single crystals.

A. Occurrence on a compromise growth surface between two nonparallel crystals. (These inclusions have generally leaked; and could also be secondary.)

B. Occurrence within polycrystalline hosts, e.g., as pores in fine grained dolomite, cavities within chalcedony-lined geodes ("enhydros"), vesicles in basalt, or as crystal-lined vugs in metal deposits or pegmatites. (These latter are among the largest "inclusions", and have almost always leaked.)


C. Occurrence in noncrystalline hosts (e.g., gas bubbles in amber; vesicles in pumice).

VI. Based on inclusion shape or size.

A. In a given sample, larger size and/or equant shape.

B. Negative crystal shape - this is valid only in certain specific samples and is a negative criterion in others.

VII. Based on occurrence in euhedral crystals, projecting into vugs (suggestive, but far from positive).



2. Criteria for Secondary Origin

- I. Occurrence as planar groups outlining healing fractures (cleavage or otherwise) that come to the surface of crystal (note that movement of inclusions with recrystallization can cause dispersion - see also III-C above).
- II. Very thin and flat; in process of necking down.
- III. Primary inclusions with filling of representative of secondary conditions.
 - A. Located on secondary healed fracture, hence presumably refilled with later fluids.
 - B. Decrepitated and rehealed following exposure to higher temperatures or lower external pressures than at time of trapping; new filling may have original composition but lower density.

3. Criteria for Pseudosecondary Origin

- I. Occurrence as with secondary inclusions, but with fracture visibly terminating within crystal. (See also III-C under "Primary", above.)
- II. Generally more apt to be equant and of negative crystal shape than secondary inclusions in same sample (suggestive only).
- III. Occurrence as a result of the covering of etch pits cross-cutting growth zones.

APPENDIX C

Geostatistical Concepts

Geostatistics - A conceptual overview

Etymologically, the term "geostatistics" designates the statistical study of natural phenomena. G. Matheron (1963) was the first to use the term extensively, and his definition will be retained: "Geostatistics is the application of the formalism of random functions to the reconnaissance and estimation of natural phenomena". In common usage, geostatistics refers to the application of the Theory of Regionalized Variables (first developed by Matheron) to problems in geology and mining although successful applications in such different fields as bathymetry and forest management continue to be demonstrated. Here, a brief introduction to the conceptual framework of the Theory of Regionalized Variables and mining geostatistical language is provided. The synopsis is taken in large part from Journel (1975).

Regionalized Variables

A quantified natural phenomenon is characterized by the development in space (or time) of certain measurable

quantities called Regionalized Variables (ReV.). A pertinent example is ore grade in 3-dimensional space. From a mathematical point of view, a ReV is simply a function $f(x)$ which takes a number at every point x of co-ordinates (x_u, x_v, x_w) in 3-D space. The definition of a ReV as a variable distributed in space is purely descriptive and does not involve any probabilistic interpretation.

The real variation of this function in space is commonly so irregular as to preclude its direct mathematical study. However, in many instances, a characteristic behaviour or structure of the spatial variability of the ReV can be discerned behind a locally erratic aspect. Generally, in most mineral deposits, in spite of local fluctuations, there exists:

1) rich and poor zones - the function $f(x)$ depends on the position of x .

2) phenomena of progressive enrichment or impoverishment.

A proper formalization must then take these two apparently contradictory characteristics of randomness and structure into account in such a way as to provide a simple representation of the spatial variability. This can be achieved with the probabilistic language of Random Functions.

Random Variables and Functions

A random variable (RV) is one that can take a certain number of values with a certain law of probability. For

example, the result of one throw of an unbiased die is a random variable that can take six values (1-6), each with an equal probability (1/6). If a particular throw gave the result 5, then 5 would be one particular realization of the random variable "result of throwing the die".

Similarly, an ore grade $y(x_1) = 0.5 \text{ oz. Au}$ at a precise point x_1 is a particular realization of a random variable $y(x_1)$, positioned at point x_1 . Consequently, the group of grades $y(x_1)$, for all points within a given deposit ($x \in \text{Deposit}$), i.e. the regionalized variable $y(x)$, is one particular realization of the set of all the random variables $y(x)_1, x \in \text{Deposit}$. This infinite set of random variables is called a Random Function - denoted $Y(x)$.

The expression "random function" contains the double aspect of a regionalized variable: locally $y(x_1)$ is a random variable; but $Y(x)$ is a random function, i.e. the two random variables $y(x_1)$ and $y(x_1 + h)$ are linked by correlation (the function).

Hypothesis of Stationarity

Thus a regionalized variable is interpreted as one particular realization $y(x)$ of a certain random function $Y(x)$. However, the knowledge of one realization limited to a certain discrete sample set (i.e. the number of drill holes) does not permit the determination of a probability law of $Y(x)$. In the same manner that many more than one

throw of our unbiased die would be necessary to deduce the probability law, we would need several realizations $y_1(x)$, $y_2(x)$, $y_3(x)$... etc., of our random function $Y(x)$ to infer the law. In most situations, particularly in mining applications, there is only a single limited realization - the actual set of sample data for example. The cost of obtaining even a second realization - i.e. a totally different sample set, normally precludes its achievement. This very real problem is circumvented through the Hypothesis of Stationarity.

In practice, even if only over a certain region, the ReV under study can very often be considered as homogenous, i.e. repeating itself in space. This homogeneity or repetition provides the equivalent of many realizations of the same random function $Y(x)$ and permits a certain amount of statistical inference.

Intrinsic Hypothesis

Geostatistics requires a weaker hypothesis. Interest is not focussed on the values of the random variables $y(x)$ and $y(x + h)$, but only on their differences $[y(x) - y(x + h)]$ and it is the stationarity of these increments that geostatistics requires. Thus, two pairs of data $[y(x_1) - y(x_1 + h)]$ and $[y(x_2 + h)]$ are considered as two different realizations of the same random increment $[y(x) - y(x + h)]$. This stationary hypothesis, limited to the incre-

ments, is called the Intrinsic Hypothesis.

The Variogram

The variogram function in geostatistics is defined as the second-order moment (the variance) of the increment $[Z(x) - Z(x + h)]$, and is written as

$$2\delta(x, h) = \text{Var} \cdot Z(x) - Z(x + h)$$

In general, the variogram $2\delta(x, h)$ is a function of both the point (x) and the vector h that separates (x) from $(x + h)$. Thus, the estimation of this variogram would require several different realizations of the pair of random variables $[Z(x), Z(x + h)]$. In practice, at least in mining applications, only one such realization is available, the actual measured pair of values (ie. assays) at points x and $x + h$. This problem is overcome through the assumption of the Intrinsic Hypothesis discussed previously. Under this assumption, the variogram function $2\gamma(x, h)$ depends only on the separation vector \vec{h} (modulus and direction), and not on the location of point x . It is then possible to estimate the variogram $2\gamma(h)$ from the available data. The estimator $2\gamma^*(h)$ is defined as the arithmetic mean of the squared differences between experimental measures at any two points separated by the vector \vec{h} . For each \vec{h} and $|\vec{h}|$:

$$2\gamma(h) = \frac{1}{N(h)} \sum_{i=1}^{N(h)} [Z(x_i) - Z(x_i + h)]^2$$

In practice, it is usual to plot the function as a graph of γ versus $|h|$. This function is equal to one-half of the variogram function and is termed the semi-variogram.

In the definition of the semi-variogram $\gamma(h)$, h represents a vector of modulus $|h|$ and direction α . For a given α , a semi-variogram begins at $\gamma(0) = 0$ and increases in general with the modulus $|h|$. This is simply an expression of the fact that, on average, the difference between two values measured at two points increases as the distance $|h|$ between them increases. The manner in which this semi-variogram increases for small values of $|h|$ characterizes the degree of spatial continuity of the variable studied.

Often, the semi-variogram stops increasing beyond a certain distance and becomes more or less stable around a limit value called a "sill" value. The distance beyond which $\gamma(h)$ remains stable is the range and it represents a transition from the state in which spatial correlation exists ($|h| < a$). When such a sill exists, the sill value C is equal to the normal sample variance of the distribution.

Thus the semi-variogram may be viewed as a quantified summary of all the available structural information which can then be used in resource and reserve estimation procedures.

Theoretical Semivariogram Models

The experimental semivariogram is a data summary technique describing the behaviour of a variable in 3d space. Conclusions must be produced by a process of inference. This process is analogous to constructing a histogram from a set of sample values and then inferring from the histogram a theoretical distribution for the entire population represented by the sample set. Thus, experimental semivariograms must be related to some theoretical model if conclusions are to be made.

There are only a few simplistic models for a theoretical semivariogram. These divide into two groups, those in which the semivariogram $\gamma(h)$ increases with distance h and those that increase at first and then tend to level off at a constant value of γ . The latter are said to have a sill, usually denoted by C .

Of the models without a sill, the most frequently used is the linear model. This is simply a straight line passing through the origin of the graph and is defined by its slope p . A generalization of this model exists in which the value of γ is related to the distance h raised to some power λ that lies between zero and 2.

There are three models that possess a sill: The two most commonly used are the spherical and the exponential model. Both models are virtually linear for small values of h , but the slope at the line is different. The

spherical model rises rapidly, then gradually curves until it reaches a sill (c) beyond a certain distance. This distance, generally denoted by a , is the range. The exponential model is also defined by these two parameters (sill and range), but it rises more slowly than the spherical model and never quite reaches its sill. The other model with a sill does not behave linearly near the origin but is parabolic. It takes the same shape as the spherical model in that it rises steeply toward the sill, but it reaches the sill in a smooth curve, rather than with the definitive break of the spherical model.

One other model element of note, particularly in geostatistical study of gold-bearing deposits, is termed the nugget effect. In gold-bearing deposits this is due to large differences in grades in two samples that are very close together when one of them contains grains or "nuggets" of gold and the other does not. A nugget effect appears on the semivariogram as an apparent discontinuity at the origin of amplitude C_0 , which is termed the nugget constant.

APPENDIX D

FORTRAN IV PROGRAM LISTINGS

PROGRAM ENTRY, FOR

A DATA ENTRY PROGRAM WHICH CREATES INDIVIDUAL FILES
OF CHEMICAL DATA FROM WHOLE ROCK ANALYSES FOR USE
WITH COMPANION CHEMICAL MASS BALANCE PROGRAM MUCK1, FOR

THIS VERSION BY G.P. WATSON, UNIVERSITY OF WESTERN ONT., 1963.

DOUBLE PRECISION FILEOUT, SAMPLE

INTEGER NAME(50)

REAL VALUE(50)

DATA VALUE/50*0./

DATA NAME/'SIO2','TIQ2','AL2O3','FE2O3','MNU','MGO',
1 'CAU','K2O','NA2O','P2O5','LOI','CO2','S','AU','AG','LI',
2 'BE','B','F','CL','AS','SB','SC','V','CR','CO','NI','CU',
3 'ZN','MU','SN','W','HG','PB','TH','RB','SR','Y',
4 'ZR','NB','CD','BA','B'/'

TYPE 100

THE PROGRAM REQUIRES A NAME FOR THE DATA FILE THAT WILL
CONTAIN THE ANALYTICAL DATA=NAME UP TO 6 CHARACTERS WITH
OPTIONAL 3 CHARACTER EXTENSION.

100 FORMAT(/' ENTER THE NAME OF THE FILE TO BE CREATED: ',8)
ACCEPT 101,FILEOUT

101 FORMAT(A10)
OPEN(UNIT=2,FILE=FILEOUT)
2000 IND=0
TYPE 999

SAMPLE NUMBER CAN BE UP TO 10 CHARACTERS

999 FORMAT(///,' ENTER THE SAMPLE NUMBER : ',8)
ACCEPT 998,SAMPLE
998 FORMAT(A10)
TYPE 1000

ANALYTICAL DATA IS ENTERED FREE FORMAT

IF ANY ELEMENTS NOT DETERMINED IN ANALYSIS, ENTER 0.0 VALUE.

1000 FORMAT(///,' PLEASE ENTER THE ANALYTICAL RESULT FOR EACH',
' ELEMENT',/)
1 CONTINUE
IND=IND+1
IF(NAME(IND).EQ.' ') GO TO 10

```

1010 TYPE 1010,NAME(IND)
      FORMAT(' ',A5,3X,8)
      ACCEPT *,VALUE(IND)
      GO TO 1
10 CONTINUE
      TYPE 1030
1030 FORMAT(/' SPEC. GRAV.= ?',8)
      ACCEPT *,SPG
      IND=IND+1
      PRINT 1052,SAMPLE
1052 FORMAT(5X,A10)
      PRINT 1050,(NAME(I),VALUE(I),I=1,IND)
1050 FORMAT(' ',A5,5X,F10,3)
      PRINT 1051,SPG
1051 FORMAT(' SPEC. GRAV.',3X,F10,3)
C
C
C THE PROGRAM WILL ASK IF USER IS SATISFIED DATA
C IS CORRECT AS DISPLAYED.
C
C IF DATA IS NOT CORRECT ANSWER NO (N) AND BEGIN AGAIN
C
      TYPE 1060
1060 FORMAT(/' IS THIS DATA CORRECT (Y/N) ?',8)
      ACCEPT 1061,IANS
1061 FORMAT(A1)
      IF(IANS.EQ.'N') GO TO 2000
      WRITE(2,990) SAMPLE
990 FORMAT(1X,A10)
      WRITE(2,1071)(VALUE(I),I=1,IND)
      WRITE(2,1071)SPG
1071 FORMAT(F10,3)
      CLOSE(UNIT=2)
      PRINT 1080,FILOUT
1080 FORMAT(/' DATA FILE WRITTEN ON DISK FILE: ',A10)
      STOP
      END

```

PROGRAM ROCK1

A REVISED VERSION OF CHEMICAL MASS BALANCE PROGRAM FOR
WHOLE ROCK DATA

THIS PROGRAM WILL ONLY DEAL WITH DATA FILES
PREVIOUSLY CREATED BY PROGRAM ENTRY, FOR

THIS VERSION BY G.P. WATSON, UNIVERSITY OF WESTERN ONT., 1983

DOUBLE PRECISION PARFIL, PROFIL, PAR, PROD, FILOUT

INTEGER NAME(50)

REAL PARENT(50), PRODCT(50), FV(50), GAL(50), POP(50)

LOGICAL NO(50)

DATA PARENT/50*0./, PRODCT/50*0./

DATA NAME/'SIO2', 'TIO2', 'AL2O3', 'FE2O3', 'MNO', 'MGO',

2 'CAO', 'K2O', 'NA2O', 'P2O5', 'LOI', 'CO2', 'S', 'AU', 'AG', 'LI',

3 'BE', 'B', 'F', 'CL', 'AS', 'SB', 'SC', 'V', 'CR', 'CO', 'NI', 'CU', 'ZN',

4 'MO', 'SN', 'W', 'HG', 'PB', 'TH', 'RB', 'SR', 'Y',

5 'ZR', 'NB', 'CD', 'BA', 'S'

100 TYPE 900

900 FORMAT(/' ENTER NAME OF THE PARENT ROCK DATA FILE : ', 8)

ACCEPT 901, PARFIL

901 FORMAT (A10)

TYPE 902

902 FORMAT (/ ' ENTER THE NAME OF THE PRODUCT ROCK DATA FILE : ', 8)

ACCEPT 903, PROFIL

903 FORMAT (A10)

THE PROGRAM WILL CREATE AN OUTPUT FILE CONTAINING
ORIGINAL PARENT/PRODUCT ANALYTICAL DATA AND RESULTS
OF ALL THE FOLLOWING CALCULATIONS

100 TYPE 904

904 FORMAT (/ ' ENTER THE NAME OF OUTPUT FILE : ', 8)

ACCEPT 905, FILOUT

905 FORMAT (A10)

OPEN (UNIT=2, FILE=PARFIL)

OPEN (UNIT=3, FILE=PROFIL)

OPEN (UNIT=4, FILE=FILOUT)

READ(2, 802) PAR

802 FORMAT (1X, A10)

READ(3, 804) PROD

804 FORMAT (1X, A10)

WRITE(4, 1009)

1009 FORMAT(' ', 20X, ' PARENT ', 11X, ' PRODUCT ', //)

WRITE(4, 1010) PAR, PROD

TYPE 1009

TYPE 1010, PAR, PROD

IND=0

CONTINUE

IND=IND+1

IF(NAME(IND).EQ.' ') GO TO 10

```

1010  FORMAT(' ',20X,A10,13X,A10,///)
      READ (2,1020) PARENT(IND),
      READ (3,1020) PRODC(T(IND)
1020  FORMAT(F)
      WRITE(4,1011)NAME(IND),PARENT(IND),PRODC(T(IND)
1011  FORMAT(' ',A5,10X,F12.3,10X,F12.3)
      TYPE 1011,NAME(IND),PARENT(IND),PRODC(T(IND)
      GO TO 1
10   CONTINUE
      READ(2,1030)SGPAR
      READ(3,1030)SGPRD
1030  FORMAT(F)
      WRITE (4,1012)SGPAR,SGPRD
1012  FORMAT(// ' ', 'SPEC. GRAV.', '4X,F12.3,10X,F12.3)
      TYPE 1012,SGPAR,SGPRD
C.....CALCULATE THE VOLUME FACTORS.....
      WRITE(4,1045)
1045  FORMAT(//, ' VOLUME FACTORS',/)
      TYPE 1045
      IND=IND-1
      DO 20 I=1,IND
      IF (PARENT(I).EQ.0.0) PARENT(I)=0.001
      IF (PRODC(T(I).EQ.0.0) NO(I)=.TRUE.
      IF (NO(I)) GO TO 20
      FV(I)=(PARENT(I)/PRODC(T(I))*(SGPAR/SGPRD)
      WRITE(4,1050)NAME(I),FV(I)
1050  FORMAT(' ',A5,F16.8)
      TYPE 1050,NAME(I),FV(I)
20   CONTINUE
40   CONTINUE
      TYPE 1060

1060  FORMAT(//, ' PLEASE GIVE VOLUME FACTOR (CTRL) Z TO STOP) ',8)
      READ(5,1070,END=999)FVC
1070  FORMAT(F)
C.....CALCULATE THE GAINS AND LOSSES.....
      WRITE(4,1071)FVC
1071  FORMAT(// 'FOR A VOLUME FACTOR OF: ',F10.6,8)
      WRITE(4,1075)
1075  FORMAT(//, ' GAINS AND LOSSES',/)
      TYPE 1075
      DO 50 I=1,IND
      IF (NO(I)) GO TO 50
      GAL(I)=(FVC*SGPRD*PRODC(T(I)/SGPAR)-PARENT(I)
      WRITE(4,1080)NAME(I),GAL(I)
      TYPE 1080,NAME(I),GAL(I)
50   CONTINUE
C.....CALCULATE THE PERCENT OF PARENT...
      WRITE(4,1090)
1090  FORMAT(//, ' PERCENT OF PARENT',/)
      TYPE 1090
      DO 60 I=1,IND
      IF (NO(I)) GO TO 60
      POP(I)=GAL(I)*100./PARENT(I)
      POP(I)=ABS(POP(I))
      WRITE(4,1050)NAME(I),POP(I)
      TYPE 1050,NAME(I),POP(I)
60   CONTINUE
      GO TO 40
999  TYPE 99,FILOUT

99   FORMAT(/// ' DATA WRITTEN ON FILE: ',A10)
      CALL EXIT

      END

```

PROGRAM HISTO

AN INTERACTIVE PROGRAM DESIGNED TO SELECT DATA FROM INPUT FILE (FILIN) CALCULATE AVERAGE, VARIANCE, COEFFICIENT OF VARIATION, MAXIMUM AND MINIMUM VALUES OF THE GIVEN POPULATION AND THEN PRINT A HISTOGRAM.

THIS VERSION ADAPTED FOR USE WITH FILES CREATED BY COMPANION PROGRAM COMPOS.F10.

THE FOLLOWING VARIABLES WILL BE USED:

FILIN = NAME OF INPUT FILE
 NVAR = NUMBER OF VARIABLES ON EACH LINE OF INPUT FILE
 NHIST = NUMBER OF HISTOGRAMS REQUIRED
 IX(I) = # OF VARIABLE(S) TO BE USED IN HISTOGRAM(S)
 LAB(I) = NAME(S) ASSIGNED TO VARIABLE(S)
 DTEST(I) = LOWER LIMIT FOR VARIABLE(S)
 CHAN = VALUE OF FIXED CHANNEL WIDTH (OPTIONAL)
 PROGRAM WILL ASSIGN CHANNEL WIDTH BY DEFAULT
 NK = NUMBER OF SORTING VARIABLES (OPTIONAL)
 KEY(IK) = # OF VARIABLE(S) USED TO SORT DATA
 LOW(IK) = LOWER LIMIT OF SORTING VARIABLE(S)
 UP(IK) = UPPER LIMIT OF SORTING VARIABLE(S)

....PROGRAM HAS OPTIONAL LOG-TRANSFORMATION OF DATA.....

ORIGINAL PROGRAM PROVIDED BY R. FROIDEVEAUX
 MODIFIED BY G.P. WATSON, DEPT. GEOLOGY, UWO.

```

dimension z(25),x(9500),ivec(51),KAN(300)
DIMENSION PM(7),IX(50),LAB(25,2),IFM(80)
DIMENSION KEY(25),UP(25),DTEST(25),UTEST(25)
INTEGER TITLE(80)
DOUBLE PRECISION FILIN,FILOUT
REAL LOW(25)
100 PRINT 500
500 FORMAT(' ENTER TITLE')
ACCEPT 290,TITLE
PRINT 501
501 FORMAT('/' ENTER NAME OF INPUT DATA FILE: ',8)
ACCEPT 502,FILIN
502 FORMAT(A10)
OPEN (UNIT=2,FILE=FILIN)
PRINT 499
499 FORMAT('/' ENTER NAME OF OUTPUT FILE ',/
1' (WITH EXTENSION .DAT): ',8)
ACCEPT 502,FILOUT
OPEN (UNIT=3,FILE=FILOUT)
PRINT 503
503 FORMAT('/' ENTER NO OF VARIABLES ON FILE: ',8)
ACCEPT 504,NVAR
504 FORMAT(I5)
110 CONTINUE
PRINT 505
505 FORMAT('/' HOW MANY HISTOGRAMS? '8)
ACCEPT 504,NHIST

```

```

506 PRINT 506
    FORMAT(/' ENTER VAR NUMBERS ',/
1' ' (ALL ON ONE LINE, SEPARATED BY COMMAS): ')
    ACCEPT *,(IX(I),I=1,NHIST)
    PRINT 508
508 FORMAT(/' ENTER NAME OF EACH VARIABLE (MAX. 10 CHAR.),/
1' ONE PER LINE')
    DO 10 I=1,NHIST
10 ACCEPT *,LAB(I,1),LAB(I,2)
509 FORMAT(2A5)
    PRINT 510
510 FORMAT(/' ENTER LOWER AND UPPER LOWER LIMITS FOR EACH VARIABLE'/
1' ONE SET OF LIMITS PER LINE, EACH SEPARATED BY COMMAS')
    DO 15 I=1,NHIST
15 ACCEPT *,DTEST(I),UTEST(I)
    PRINT 511
511 FORMAT(/' DO YOU WANT TO LOG-TRANSFORM THE DATA (Y/N) ? ')
    ACCEPT 512,IANS
512 FORMAT(A1)
    IF (IANS.NE.'Y') GO TO 111
    DO 5 I=1,NHIST
5 DTEST(I)=AMAX1(DTEST(I),0.00001)
111 CONTINUE
    PRINT 513
513 FORMAT(/' DO YOU WANT TO FIX THE CHANNEL WIDTH (Y/N) ? ',)
    ACCEPT 512,IANS2
    IF (IANS2.NE.'Y') GO TO 112
    PRINT 514
514 FORMAT(/' ENTER WIDTH: ',)
    ACCEPT *,CHAN
112 CONTINUE

    PRINT 515
515 FORMAT(/' HOW MANY SORTING VARIABLES ? ')
    ACCEPT *,NK
    IF (NK.LE.0) GO TO 113
    PRINT 516
516 FORMAT(/' ENTER VAR #, LOWER AND UPPER LIMITS FOR EACH SORTING #,
1' /, VARIABLE, ONE SET PER LINE, EACH NUMBER SEPARATED BY ',
1' A COMMA')
    DO 17 IK=1,NK
-17 ACCEPT *,KEY(IK),LOW(IK),UP(IK)
113 CONTINUE
    DO 220 IH=1,NHIST
    XMIN=1.0E35
    XMAX=XMIN
    SX=0.
    SX2=0.
    KMAX=0
    DO 130 I=1,150
130 KAN(I)=0
    N=0
1 HEAD(2,400,END=2) PH
400 FORMAT(A6,4X,5F12.3,F10.0)
    ND=PH(7)
    DO 3 I=1,ND
    READ(2,401) (Z(J),J=1,NVAR)
401 FORMAT(10F12.3)
    IF (NK.LE.0) GO TO 115
    DO 4 IK=1,NK

```



```

IF (2(KEY(IK)).LT.LOW(IK).OR.2(KEY(IK)).GE.UP(IK)) GO TO 3
4 CONTINUE
115 CONTINUE
V=Z(IX(IH))
IF (V.LT.OTEST(IH).OR.V.GE.UTEST(IH)) GO TO 3
IF (IANS.EQ.'Y') V=ALOG(V)
N=N+1
X(N)=V
SX=SX+X(N)
SX2=SX2+X(N)*X(N)
XMAX=AMAX1(XMAX,X(N))
XMIN=AMIN1(XMIN,X(N))
3 CONTINUE
GO TO 1
2 XN=N
TYPE 101, XN
101 FORMAT(/' AT 2 XN=',F12.3)
VAR=SX2-SX*SX/XN
XBAR=SX/XN
VAR=VAR/(XN-1.0)
COEF=SQRT(VAR/(XBAR*XBAR))
IF (IANS2.EQ.'Y') GO TO 135
CHAN=(XMAX-XMIN)/(10.*ALOG10(XN))
F=10.*INT(-ALOG10(CHAN)+1)
CHAN=INT(CHAN+F+0.5)/F
135 CONTINUE
XINF=INT(XMIN/CHAN)*CHAN
IF (XINF.LT.0) XINF=XINF-CHAN
XSUP=(INT(XMAX/CHAN)+1)*CHAN
NINTER=(XSUP-XINF)/CHAN+1
DO 100 I=1,N
IFLAG=(X(I)-XINF)/CHAN+1
KAN(IFLAG)=KAN(IFLAG)+1
KMAX=MAX0(KMAX,KAN(IFLAG))
160 CONTINUE
IDIV=KMAX/51+1
WRITE(3,230) TITLE
WRITE(3,240) LAB(IH,1),LAB(IH,2)
IF (IANS.EQ.'Y') WRITE(3,320)
WRITE(3,250) XBAR,VAR,COEF,XMIN,XMAX,N
WRITE(3,260)
CUM=0.0
DO 200 J=1,51
170 IVEC(J)=1H*
200 CONTINUE
DO 210 I=1,NINTER
IFLAG=KAN(I)/IDIV
IF (IFLAG.EQ.0.AND.KAN(I).GT.0) IFLAG=1
XLIM=(I-1)*CHAN+XINF
IF (ABS(XLIM).LT.0.0001) XLIM=0.
PER=(FLOAT(KAN(I))/XN)*100.0
CUM=CUM+PER
IF (IFLAG.EQ.0.) WRITE(3,270) KAN(I),PER,CUM,XLIM
IF (IFLAG.NE.0) WRITE(3,270) KAN(I),PER,CUM,XLIM
1 IVEC(K),K=1,IFLAG)
210 CONTINUE
NEWIND 2
220 CONTINUE
WRITE(3,280)
PRINT 520

```

```

520  FORMAT(/' DO YOU WANT TO DO ANOTHER RUN ? (Y/N)',8)
      ACCEPT 512,IANS
      IF (IANS,NE,'Y') GO TO 221
      PRINT 521
521  FORMAT(/' USING THE SAME FILE ? (Y/N)',8)
      ACCEPT 512,IANS
      IF (IANS,EQ,'Y') GO TO 110
      IF (IANS,NE,'Y') GO TO 100
221  CONTINUE
      PRINT 600,FILEOUT
600  FORMAT(/' HISTOGRAMS ON FILE ',A10)
      STOP
230  FORMAT(20A4)
240  FURMAT(///21X,'SAMPLE STATISTICS FOR ',2A5)
250  FURMAT(/21X,'AVERAGE',23X,G15.6/21X,'VARIANCE',22X,G15.6/21X,
      1 'COEF. OF VARIATION',13X,G15.6/
      1 21X,'MINIMUM',23X,G15.6/21X,'MAXIMUM',23X,G15.6,
      1 /,21X,'NB OF SAMPLES',17X,I10///)
260  FURMAT(50X,'CHANNEL',/21X,'FREQ.',5X,'%',6X,'CUM. %',6X,
      1 'LOWER',/50X,'LIMIT'///)
270  FURMAT(20X,I5,2(3X,F6.2),3X,G15.6,2X,50A1)
280  FURMAT(1H1)
290  FURMAT(80A1)
310  FURMAT(1H1,20X,'PROJECT : ',80A1)
320  FURMAT(1H+,52X,'(LOGTRANSFORMED DATA)')
      END

```

PROGRAM DRILL

AN INTERACTIVE PROGRAM THAT WILL CREATE DATA FILES FROM
DIAMOND DRILL HOLE LOGS.

INTEGER DHN,R(40),ANS
REAL II(40),IF(40),U(40),NR,ES,EL,DP,AZ,IM(40),IW(40),
I IV(40),INR(40),IES(40),IEL(40),COSDP
DOUBLE PRECISION OFILE,RFILE

THE FOLLOWING VARIABLES WILL BE USED IN THE PROGRAM:

DHN - DRILL HOLE NUMBER
NR - NORTH
ES - EAST
EL - ELEVATION
AZ - AZIMUTH
DP - INCLINATION
THE FOLLOWING ARRAYS HOLD THE INFORMATION CONCERNING EACH INTERSECTION
II - BEGINNING OF THE INTERSECTION
IF - END OF THE INTERSECTION
U - THE ASSAY VALUE
R - THE ROCK TYPE (DESIGNATED BY A 3 CHARACTER CODE)
IM - THE MIDPOINT OF THE INTERSECTION
IW - WIDTH OF THE INTERSECTION
IV - WIDTH X ASSAY VALUE
INR - NORTHING OF THE INTERSECTION
IES - EASTING OF THE INTERSECTION
IEL - ELEVATION OF THE INTERSECTION

N - THE NUMBER OF INTERSECTIONS
COSDP - HOLDS THE COS(ABSOLUTE VALUE OF DP)

PROGRAM WRITES A REPORT OF CALCULATIONS ON A FILE NAMED
BY THE USER (RFILE)
PROGRAM WRITES THE CALCULATIONS TO A FILE NAMED BY THE USER (OFILE)
PROGRAM ALLOWS UP TO 40 INTERSECTIONS FOR EACH DRILL HOLE

PROGRAM WRITTEN BY D.GOLDSTEIN, UWO COMPUTING CENTER FOR
G.P. WATSON, DEPT. GEOLOGY, UWO.

TYPE 9000
FORMAT(' OUTPUT DATA TO FILE NAME?',/' (UP TO 6 CHAR. NAME ".",
1 * 3 CHAR EXTENSION) ',8)

ACCEPT 8000, OFILE
FORMAT(A10)
OPEN(UNIT=1,FILE=OFILE)

TYPE 9005
FORMAT(' OUTPUT REPORT TO FILE NAME? ',8)
ACCEPT 8000,RFILE
OPEN(UNIT=2,FILE=RFILE)

CONTINUE

TYPE 9010
FORMAT(' INPUT DRILL INFORMATION',/' DRILL HOLE NUMBER:',8)
ACCEPT 9010,DHN

```

8010  FORMAT(15)
      TYPE 9020
9020  FORMAT(' NORTH:',8)
      ACCEPT 8020,NR
      TYPE 9030
9030  FORMAT(' EAST:',8)
      ACCEPT 8020,ES
8020  FORMAT(F7.1)
      TYPE 9040
9040  FORMAT(' ELEVATION:',8)
      ACCEPT 8040,EL
8040  FORMAT(F5.0)
      TYPE 9050
9050  FORMAT(' AZIMUTH:',8)
      ACCEPT 8050,AZ
8050  FORMAT(F6.2)
      TYPE 9060
9060  FORMAT(' INCLINATION:',8)
      ACCEPT 8060,DP
8060  FORMAT(F3.0)
      TYPE 9070
9070  FORMAT(//,' INPUT THE INTERSECTIONS')
      N=0
C
200  CONTINUE
C
      N=N+1
      IF (N.GT.40) GO TO 500
      TYPE 9080
9080  FORMAT(' BEGINNING OF THE INTERSECTION:',8)
      ACCEPT 8080,II(N)
8080  FORMAT(F6.2)
      TYPE 9090
9090  FORMAT(' END OF THE INTERSECTION:',8)
      ACCEPT 8080,IF(N)
      TYPE 9100
9100  FORMAT(' ASSAY VALUE:',8)
      ACCEPT 8080,O(N)
      TYPE 9110
9110  FORMAT(' ROCK TYPE:',8)
      ACCEPT 8110,R(N)
8110  FORMAT(A3)
C
      TYPE 9120
9120  FORMAT(//,' ARE THERE MORE INTERSECTIONS? (Y OR N):',8)
      ACCEPT 8120,ANS
8120  FORMAT(A1)
      IF (ANS.EQ.'Y') GO TO 200
C
C CHECK INTERSECTION DATA
C
      TYPE 9700,DHN,NR,ES,EL,AZ,DP
9700  FORMAT(//,' DRILL HOLE: ',15,4X,' NORTH: ',F7.1,4X,' EAST: ',F7.1,
1 //,4X,' ELEVATION: ',F5.0,4X,' AZIMUTH: ',F6.2,4X,' INCLINATION: ',
1 F4.0)
      TYPE 9710
9710  FORMAT(//,5X,' INTERSECTION',5X,' BEGINNING',5X,' END',5X,' ASSAY',
1 5X,' TYPE')
DU 250 I=1,N
TYPE 9720,I,II(I),IF(I),O(I),N(I)

```

```

9720  FORMAT(10X,I2,11X,F7.2,7X,F7.2,9X,F7.2,8X,A3)
250   CONTINUE
      TYPE 9730
9730  FORMAT(/,' DATA OKAY? (Y OR N):',6)
      ACCEPT 9730,ANS
9730  FORMAT(A1)
      IF (ANS.EQ.'Y') GO TO 280
      TYPE 9740
9740  FORMAT(/,' DRILL HOLE INFORMATION AND INTERSECTION DATA NOT',
1 ' WRITTEN TO THE FILE OR REPORT',/, ' CONTINUE INPUTTING DATA',//)
      GO TO 10

```

```

C
C START CALCULATIONS

```

```

C
280   CONTINUE
      COSDP=COSD(ABS(DP))
      DO 300 I=1,N
        IM(I)=(II(I) + IF(I))/2.0
        IW(I)=IF(I) - II(I)
        IV(I)=IW(I) * O(I)
        INR(I)=NR + (IM(I) * COSDP + COSD(AZ))
        IES(I)=ES + (IM(I) * COSDP + SIND(AZ))
        IEL(I)=EL - (IM(I) * SIND(DP))
300   CONTINUE

```

```

C
C OUTPUT THE REPORT AND THE DATA FILE

```

```

C
      WRITE(2,9500)
9500  FORMAT(1H1,/,/,3X,'DRILL HOLE',6X,'AZIMUTH',4X,'INCLINATION',5X,
1 'NORTH',11X,'EAST',10X,'ELEVATION',/,4X,'NUMBER',//)
      WRITE(2,9510) OHN,AZ,DP,NR,ES,EL

9510  FORMAT(5X,I5,10X,F6.2,7X,F4.0,8X,F8.2,8X,F8.2,9X,F5.0)
      WRITE(2,9520)
9520  FORMAT(/,45X,'NORTHING',8X,'EASTING',8X,'ELEVATION',9X,'WIDTH',
1 17X,'WIDTH',/,7X,'INTERSECTION',29X,'OF',14X,'OF',14X,'OF',
1 14X,'OF',9X,
1 'ASSAY',6X,'X',6X,'ROCK',/,10X,'NUMBER',27X,'INTERSECTION',
1 4X,'INTERSECTION',4X,'INTERSECTION',4X,'INTERSECTION',4X,
1 'VALUE',4X,'ASSAY',4X,'TYPE',//)

```

```

C
      DO 400 I=1,N
        WRITE(2,9530) I,INR(I),IES(I),IEL(I),IW(I),O(I),IV(I),R(I)
9530  FORMAT(12X,I2,31X,F8.2,8X,F8.2,8X,F8.2,8X,F8.2,6X,F5.2,3X,
1 F7.3,4X,A3,/)
        WRITE(1,9540) INR(I),IES(I),IEL(I),IW(I),O(I),IV(I),R(I)
9540  FORMAT(4(F8.2,2X),F5.2,2X,F7.3,2X,A3)
400   CONTINUE

```

```

C
C ASK USER IF THERE ARE ANY MORE DRILL HOLES TO ENTER

```

```

C
      TYPE 9600
9600  FORMAT(' ANY MORE DRILL HOLES? (Y OR N):',6)
      ACCEPT 9600,ANS
8600  FORMAT(A1)
      IF (ANS.EQ.'Y') GO TO 10

```

```

C
      CLOSE(UNIT=2)
      CLOSE(UNIT=1)
      TYPE 9620, RFILE, OFILE

```

```
9620  FORMAT( //° REPORT ON DISK FILE = °,A10, //,
      1° DATA FILE WRITTEN ON DISK FILE = °,A10)
      STOP
500   TYPE 510
510   FORMAT(° PROGRAM SET UP TO DEAL WITH ONLY 40 INTERSECTIONS PER°,
      1° DRILL HOLE //,° ---MUST CHANGE PROGRAM TO ACCEPT MORE THAN°,
      1° 40 INTERSECTIONS°)
      CLOSE(UNIT=1)
      CLOSE(UNIT=2)
      TYPE 520
520   FORMAT(//,° REPORT AND DATA FILE WRITTEN WITH ALL BUT LAST°,
      1° DRILL HOLE INFORMATION°)
      TYPE 9620
      STOP
      END
```

PROGRAM COMPOS

AN INTERACTIVE PROGRAM DESIGNED TO USE DATA FILES CREATED BY COMPANION PROGRAM DRILL,IO FROM DIAMOND DRILL HOLE LOGS.

PROGRAM WILL CREATE A NEW FILE FOR EACH DRILL HOLE BY ASSIGNING VALUES FOR LOCATION, GRADE, ROCK TYPE ETC. TO SEGMENTS OF FIXED LENGTH (USER DEFINED) ALONG THE DRILL HOLE FROM KNOWN VALUES.

EACH NEW FILE (FILOUT) WILL FIRST RECORD LOCATOR INFORMATION FOR THE COLLAR OF THE REAL DIAMOND DRILL HOLE. THIS IS FOLLOWED BY LISTING OF COMPOSITE SAMPLES WITH CARTESIAN COORDINATES, GRADE, ROCK TYPE AND INDICATOR VALUE FOR EACH.

FINAL OUTPUT N1= NUMBER OF INTERVALS IN ORIGINAL LOG FILE.
N2= NUMBER OF COMPOSITE INTERVALS IN NEW FILE

USER ASKED TO INPUT THE FOLLOWING INFORMATION :

FILIN = NAME OF INPUT FILE CREATED PREVIOUSLY BY DRILL,IO
FILOUT= NAME OF OUTPUT FILE TO BE CREATED BY COMPOS,IO
H = DESIRED LENGTH OF COMPOSITE SAMPLE
NVAR = NUMBER OF DESCRIPTOR VARIABLES PER INTERSECTION IN INPUT FILE

ORIGINAL VERSION SUPPLIED BY H.FROIDEVEAUX
MODIFIED FOR G.P. WATSON, DEPT. GEOLGY , UNO.

```

double precision filout,HOLE,FILIN
dimension up(3000),down(3000),v(3000,5),T(6)
TYPE 901
901  FORMAT(' NAME OF INPUT FILE? ',8)
ACCEPT 801,FILIN
801  FORMAT(A10)
TYPE 900
900  FORMAT(' OUTPUT DATA TO FILE NAME? ',8) (UP TO 6 CHAR. NAME ".","
    3 CHAR EXTENSION):',8)
ACCEPT 800,FILOUT
800  FORMAT(A10)
OPEN(UNIT=2,FILE=FILOUT)
OPEN(UNIT=1,FILE=FILIN)
TYPE 910
910  FORMAT('/' ENTER COMPOSITE LENGTH: ',8)
ACCEPT 810,H
810  FORMAT(F15.5)
TYPE 920
920  FORMAT('/' ENTER NUMBER OF VARIABLES: ',8)
ACCEPT 820,NVAR
820  FORMAT(I10)
N1=0
N2=0
100  CONTINUE
C.....READ LOCATOR INFORMATION FOR ORIGINAL DRILL HOLE COLLAR....
C
C

```

```

READ(2,401,END=130)HOLE,X,Y,Z,B,D,ND
N1=N1+ND
B=450-B
IF (B.GT.180.0) B=B-360
PHI=0+.0174533
ALPHA=B*.0174533
NT=0
TOLAST=-9999999.
DO 110 I=1,ND

```

```

C
C.....READ INFORMATION SET DESCRIBING ORIGINAL INTERSECTIONS.....
C

```

```

READ(2,410)FROM,TO,(T(J),J=1,NVAR)

```

```

C.....TEST THAT INTERSECTIONS IN ORIGINAL FILE ARE CONSECUTIVE....
C

```

```

IF (FROM.LT.TOLAST) TYPE 600,HOLE
IF (FROM.LT.TOLAST) PRINT *, FROM,TOLAST
IF (1.LE.1.OR.FROM.EQ.TOLAST) GO TO 101
NT=NT+1
UP(NT)=TOLAST
DOWN(NT)=FROM
DO 1 J=1,NVAR
1
101 V(NT,J)=0.
CONTINUE
NT=NT+1
UP(NT)=FROM
DOWN(NT)=TO

DO 2 J=1,NVAR
2
V(NT,J)=T(J)
TOLAST=TO
CONTINUE
110 Z1=INT(UP(1)/H)*H
ZL=(INT(DOWN(NT)/H)+1)*H
NS=(ZL-Z1)/H
N2=N2+NS

```

```

C
C.....WRITE DDH COLLAR LOCATOR INFORMATION HEADER TO OUTPUT FILE....
C

```

```

WRITE(1,300) HOLE,X,Y,Z,B,D,NS
IS=1
DO 3 IZ=1,NS
Z1=ZT+(IZ-1)*H
Z2=Z1+H
DO 10 J=1,NVAR
10 T(J)=0.
4 E=AMIN1(Z2,DOWN(IS))-AMAX1(Z1,UP(IS))
DO 5 J=1,NVAR
5 T(J)=T(J)+E*V(IS,J)
IF (DOWN(IS).GE.Z2) GO TO 6
IS=IS+1
IF (IS.LE.NT) GO TO 4
6 DO 7 J=1,NVAR
7 T(J)=T(J)/H

```



```

C=Z2-H/2
XO=X+C*COB(PHI)*COB(ALPHA)
YO=Y+C*COB(PHI)*SIN(ALPHA)
ZO=Z-C*SIN(PHI)

```

```

CCCC...WRITE SET OF ASSIGNED DATA FOR ALL COMPOSITE INTERVALS TO OUTPUT FILE.

```

```

3      WRITE(1,200)XO,YO,ZO,(T(J),J=1,NVAR)
      CONTINUE
      GO TO 100
130    CONTINUE
      CLOSE(UNIT=1)
      TYPE 951,FILOUT
951    FORMAT(// ' DATA FILE WRITTEN UN DISK FILE - ',A10)
      PRINT 500,N1,N2
300    FORMAT(A10,5F12.3,I10)
200    FORMAT(10F12.3)
400    FORMAT(1X,A10,2(I10,2F10.3),F10.2)
500    FORMAT(1X,'TOTAL',3X,2(I10,20X))
600    FORMAT(///' *** ERROR IN HOLE ',A10,2X,
      *'(INTERVALS NOT IN SEQUENCE)')
401    FORMAT(A10,5F12.3,I10)
410    FORMAT(7F12.3)
      END

```

PROGRAM GAMMA1

A GEOSTATISTICS PROGRAM FOR CALCULATING
ONE DIMENSIONAL SEMI-VARIOGRAM DATA FROM
DIAMOND DRILL HOLES.

THIS VERSION MODIFIED BY G.P. WATSON,
UNIVERSITY OF WESTERN ONT., 1983, FROM
ORIGINAL PROVIDED BY R. PROIDEVEAUX.

THE PROGRAM USES DATA FROM DRILL HOLE LOGS IN
FILES CREATED BY COMPANION PROGRAM COMPOS.F10.
THE FILES CONTAIN INFORMATION ABOUT COLLAR LOCATION
AND ATTITUDE OF EACH DRILL HOLE, 3-DIMENSIONAL
COORDINATES OF COMPOSITED SAMPLES, GRADE VALUE FOR
EACH SAMPLE AND ROCK TYPE CODE.

THE FOLLOWING VARIABLES ARE USED:

NVAR= # OF DESCRIPTORS PER COMPOSITE (MAX.=8)
IV = VARIABLE # FOR WHICH VARIOGRAM IS DESIRED
STEP= LENGTH OF COMPOSITE SAMPLE
KMAX= # OF LAGS TO BE CALCULATED
ZMIN= LOWER THRESHOLD VALUE ALLOWED
ZMAX= UPPER THRESHOLD VALUE ALLOWED
IS = USER PROGRAM OPTION: 0= PRINT
VARIOGRAM FOR EACH DRILL HOLE;
1= PRINT AVERAGE VARIOGRAM FOR ALL HOLES.
BMIN= LOWER LIMIT FOR DRILL HOLE AZIMUTH
BMAX= UPPER LIMIT FOR DRILL HOLE AZIMUTH
DMIN= LOWER LIMIT FOR DRILL HOLE DIP
DMAX= UPPER LIMIT FOR DRILL HOLE DIP

```

DOUBLE PRECISION FILIN,FILOUT,LAB
DIMENSION T(10),X(7)
DIMENSION VR(1000),NC(100),G(100),GM(100),NEF(100)
INTEGER TITLE(80)
10  TYPE 900
900  FORMAT (/ ' ENTER NAME OF INPUT DATA FILE: ',8)
    ACCEPT 901,FILIN
901  FORMAT (A10)
    OPEN (UNIT=2,FILE=FILIN)
    TYPE 903
903  FORMAT (/ ' ENTER NAME OF OUPUT FILE: ',8)

    ACCEPT 901,FILOUT
    OPEN (UNIT=3,FILE=FILOUT)
20  TYPE 920
920  FORMAT (/ ' ENTER TITLE: ',8)
    ACCEPT 921,TITLE
    TYPE 930
930  FORMAT (/ ' ENTER PARAMETER NAME: ',8)
    ACCEPT 931,LAB
931  FORMAT (A10)
    TYPE 940
940  FORMAT (/ ' ENTER NVAR,IV,STEP,KMAX,ZMIN,ZMAX,IS: ',/

```

```

1  *(ALL ON ONE LINE, SEPARATED BY COMMAS):',8)
ACCEPT *,NVAR,IV,STEP,KMAX,ZMIN,ZMAX,IS
TYPE 950
950  FORMAT ('/ ENTER TOLERANCE LIMITS (LOWER AND UPPER), FOR
2  BEARING AND DIP:',8)
ACCEPT *,DMIN,DMAX,DMIN,DMAX
TYPE 960
960  FORMAT ('/ DO YOU WANT TO WORK ON LOGTRANSFORMED DATA (Y/N)?:',8)
ACCEPT 961,IAN5
961  FORMAT (A1)
DO 30 I=1,50
GAM(I)=0.
NEF(I)=0.
30  CONTINUE
XBAR=0.
VAR=0.
NTOT=0.
NDH=0.
PRINT 9001, FILIN
9001  FORMAT(' INPUT FILE' *,2A5)
40  READ (2,300,END=70)X
300  FORMAT (A6,4X,5F12.3,F10.0)
HOLE=X(1)
ND=X(7)
DO 50 I=1,ND
READ (2,301) (T(J),J=1,NVAR)
301  FORMAT (10F12.3)
VR(I)=T(IV)
50  CONTINUE
IF (X(5).LT.DMIN.OR.X(5).GE.DMAX) GO TO 40
IF (X(6).LT.DMIN.OR.X(6).GE.DMAX) GO TO 40

IF (ND.LE.1) GO TO 40
NDH=NDH+1
DO 5 I=1,ND
V=VR(I)
IF (V.LT.ZMIN.OR.V.GE.ZMAX) GO TO 5
IF (IAN5.EQ.'Y') V=ALOG(V)
XBAR=XBAR+V
VAR=VAR+V*V
NTOT=NTOT+1
5  CONTINUE
CALL GAM1 (VR,ND,KMAX,STEP,NC,G,IS,ZMIN,ZMAX,HOLE,LAB,TITLE,
IAN5)
DO 60 I=1,KMAX
GAM(I)=GAM(I)+NC(I)*G(I)
NEF(I)=NEF(I)+NC(I)
60  CONTINUE
GO TO 40
70  VAR=(VAR-XBAR*XBAR/NTOT)/NTOT
XBAR=XBAR/NTOT
WRITE (3,90)TITLE,LAB,NDH
WRITE (3,100) XBAR,VAR,NTOT
IF (IAN5.EQ.'Y') WRITE (3,120)
DO 80 I=1,KMAX
DI=STEP
GAM(I)=GAM(I)/MAX0(NEF(I),1)
WRITE (3,110) I,D,NEF(I),GAM(I)
80  CONTINUE
TYPE 970

```

```

970  FORMAT(/ DO YOU WANT TO RUN ANOTHER JOB (Y/N)? :',8)
      ACCEPT 961, IANS
      IF (IANS.EQ.'Y') GO TO 1000
      TYPE 980
980  FORMAT (/ USING THE SAME FILE (Y/N)? :',8)
      ACCEPT 961, IANS
      REWIND 2
      IF (IANS.EQ.'Y') GO TO 20
      GO TO 10
1000 PRINT 1001, PLOUT
1001  FORMAT (// 'SEMI-VARIOGRAM DATA ON FILE: ', A10)
      STOP
90   FORMAT (1H1, 53X, 'SEMI-VARIOGRAM'/54X, 14(1H=)/48X, 'REGULAR GRID',
1    1X, '1 DIMENSION'//10X, 'PROJECT : ', 80A1/10X, 'PARAMETER: 'A5/
2    10X, 'NUMBER OF DRILL HOLES : ', I3//)
100  FORMAT (10X 'AVERAGE : ', F12.8/10X, 'VARIANCE : ', F12.8/10X,
3    'NB OF DATA : ', I5//21X, 'LAG', 9X, 'DISTANCE', 4X, 'NC', 10X,
4    'GAMA'//)
110  FORMAT (20X, I3, 7X, F8.2, 3X, I6, 4X, F12.5)
120  FORMAT (48X, '(LOG TRANSFORMED DATA)'//)
921  FORMAT (80A1)
140  FORMAT (1H1)
      END
      SUBROUTINE GAMA1(VR, ND, KMAX, STEP, NC, G, IS, ZMIN, ZMAX, HOLE,
1    LAB, TITLE, IANS)
      DIMENSION VR(1000), NC(100), G(100)
      INTEGER TITLE(80)
      DO 10 I=1, KMAX
      NC(I)=0
      G(I)=0
10   CONTINUE
      IF (VR(ND).LT.ZMIN.OR.VR(ND).GE.ZMAX) GO TO 810
      GO TO 800
810  U=0.
      V=0.
800  VRR=VR(ND)
      IF (IANS.EQ.'Y') VRR=ALOG(VRR)
      U=VRR
      V=VRR+VRR
      N=1
      ND1=ND-1
      DO 30 I=1, ND1
      IF (VR(I).LT.ZMIN.OR.VR(I).GE.ZMAX) GO TO 30
      VRI=VR(I)
      IF (IANS.EQ.'Y') VRI=ALOG(VRI)
      N=N+1
      U=U+VRI
      V=V+VRI+VRI
      I=I+1
      JM=MIN0(I+KMAX, ND)
      DO 20 J=I, JM
      K=J-I
      IF (VR(J).LT.ZMIN.OR.VR(J).GE.ZMAX) GO TO 20
      VRJ=VR(J)
      IF (IANS.EQ.'Y') VRJ=ALOG(VRJ)
      NC(K)=NC(K)+1
      VRR=VRI+VRJ
      G(K)=G(K)+0.5+VRR+VRR
20  CONTINUE
30  CONTINUE

```

```

IF (N.EQ.0) GO TO 110
V=(V-U*U/N)/N
UUU/N
DO 40 IK=1,KMAX
G(IK)=G(IK)/MAXO(1,NC(IK))
40 CONTINUE
50 IF (IS.EQ.1) GO TO 110
WRITE (3,80) TITLE,LAB,HOLE
WRITE (3,90) U,S,N
DO 60 K=1,KMAX
DK=STEP
60 WRITE (3,100) K,D,NC(K),G(K)
70 CONTINUE
80 FORMAT (1H1,53X,"SEMI-VARIOGRAM "/1H,53X,14(1H=)/48X,
2 "REGULAR GRID"
3 " 1 D 1 DIMENSION"//,10X,"PROJECT : ",80A1,10X,"PARAMETER : "
4 ",A8/10X,"DRILL HOLE : ",A6//)
90 FORMAT (10X,"AVERAGE : ",F12.5/40X,"VARIANCE : ",F12.5/10X,
5 "NB OF DATA: ",15//21X,"LAG",9X,"DISTANCE",4X,"NC",10X,
6 "GAMA"//)
100 FORMAT (20X,13,7X,F8.2,4X,14,4X,F12.5)
110 RETURN
END

```

```

PROGRAM GAMMA2
DIMENSION LAB(2),V(20),NOM(20,2)
DOUBLE PRECISION FILIN,FILOUT
INTEGER TITLE(20),FMT(80)
COMMON/DATA/Z(1000),X(1000),Y(1000),PHI(10),N,KMAX,STEP,DP,
1 IDIR,PSI
100 TYPE 101
101 FORMAT (/' ENTER NAME OF INPUT DATA FILE: ',8)
ACCEPT 102,FILIN
102 FORMAT(A10)
TYPE 10
10 FORMAT (/' ENTER THE NAME OF OUTPUT FILE: ',8)
ACCEPT 11,FILOUT
11 FORMAT (A10)
TYPE 103
103 FORMAT (/' ENTER TITLE: ',8)
ACCEPT 110,TITLE
110 FORMAT (20A4)
120 TYPE 111
111 FORMAT (/' ENTER NO.S OF X, Y, AND Z: ',8)
ACCEPT *,IX,IY,IZ
TYPE 112
112 FORMAT (/' ENTER STEP, MAX. NB. OF LAGS, LOWER AND ',
1 'UPPER LIMIT FOR Z: ',8)
ACCEPT *,STEP,KMAX,BINF,BORN
TYPE 113
113 FORMAT (/' ENTER NB. OF VARIOGRAMS DESIRED: ',8)
ACCEPT *,IDIR
IF (IDIR.GT.10)IDIR=10
IF (KMAX.GT.20)KMAX=20
TYPE 900,IDIR

900 FORMAT (/' IDIR= ',15)
TYPE 114
114 FORMAT (/' ENTER DIRECTION FOR EACH VARIOGRAM: ',8)
ACCEPT *,(PHI(I),I=1,IDIR)
TYPE 115
115 FORMAT (/' ENTER WIDTH OF ANGLE AND WIDTH OF DISTANCES: ',8)
ACCEPT *,PSI,DP
TYPE 116
116 FORMAT (/' DO YOU WANT TO LOG TRANSFORM Z (Y/N) ?: ',8)
ACCEPT 117,IAN5
117 FORMAT (A1)
OPEN (UNIT=2,FILE=FILOUT)
OPEN (UNIT=3,FILE=FILOUT)
TYPE 118
118 FORMAT (/' ENTER THE NUMBER OF VARIABLES ON INPUT FILE: ',8)
ACCEPT 119,NVAR
119 FORMAT (15)
READ (2,170)((NOM(I,J),J=1,2),I=1,NVAR)
LAB(1)=NOM(12,1)
LAB(2)=NOM(12,2)
PRINT 990,LAB(1),LAB(2)
990 FORMAT (2A4)
I=0
130 HEAD (2,20,END=140,ERR=150)(V(J),J=1,NVAR)
20 FORMAT (10F12,3)
IF (V(12).LE.BINF.OR.V(12).GT.BORN)GO TO 130
IF (IAN5.NE.'Y') GO TO 131
IF (V(12).LE.0.0)GO TO 130

```

```

V(IZ)=ALOG(V(IZ))
131 I=I+1
X(I)=V(IX)
Y(I)=V(IY)
Z(I)=V(IZ)
GO TO 130
140 N=1
CALL VARIO(TITLE,LAB)
TYPE 190
REWIND 2
TYPE 141
141 FORMAT (/ ' DO YOU WANT TO RUN ANOTHER JOB ? (Y/N): ',8)
ACCEPT 142, IANS
142 FORMAT (A1)
IF(IANS.NE.'Y') GO TO 100
TYPE 143
143 FORMAT (/ ' USING THE SAME FILE ? (Y/N): ',8)
ACCEPT 142, IANS
IF(IANS.EQ.'Y') GO TO 120
IF(IANS.NE.'Y') GO TO 100
GO TO 160
150 PRINT *, I, (V(J), J=1, NVAR)
160 PRINT 161, FILEOUT
161 FORMAT (// ' DATA FILE WRITTEN ON DISK FILE : ', A10)
STOP
170 FORMAT(IX, 20A4)
190 FORMAT(1H1)
END
SUBROUTINE VARIO(TITLE,LAB)
DIMENSION LAB(2), AS(20), AG(20), AH(20), AD(20), AV(20)
DIMENSION CAN(10), SAN(10), G(20,10), D(20,10), NC(20,10)
DIMENSION N1(20,10), U1(20,10), V1(20,10)
INTEGER TITLE(20)
COMMON/DATA/VH(1000), X(1000), Y(1000), ALP(10), ND, KMAX, STEP, DP,
1 NDI, DA
PI=3.14159265
IS=0
TOL=DP
IF(TOL.LE.0.) TOL=STEP/2.0
DALPHA=DA
IF(DA.LE.0.) DALPHA=45.
TYPE 901
901 FORMAT(/ ' AT 100 DO LOOP IN VARIO ',8)
TYPE 905, NDI
905 FORMAT(/ ' NDI = ', I20)
NDI=1
DO 100 KD=1, NDI
ALPHA=PI*ALP(KD)/180
TYPE 902, ALPHA
902 FORMAT(/ ' ALPHA = ', F7.3)
ALPHA=0.524
CAN(KD)=COS(ALPHA)
SAN(KD)=SIN(ALPHA)
100 TYPE 900, (CAN(KD), SAN(KD), KD=1, NDI)
900 FORMAT (/ ' CAN AND SAN ARE: ', F7.5, 5X, F7.5)
THETA=PI-DALPHA/180.
CDA=COS(THETA)
TYPE 950, THETA, CDA
950 FORMAT(/ ' THETA AND CDA ARE: ', F7.5, 5X, F7.5)
KMM=KMAX

```

```

DO 110 IK1=1,NDI
DO 110 IK2=1,KMM
NC(IK,IK1)=0
D(IK,IK1)=0.0
110 G(IK,IK1)=0.0
DO 120 I=1,KMM
AS(I)=0.
AG(I)=0.
AD(I)=0.
AV(I)=0.
120 AM(I)=0.
N=0
U=0.
V=0.
ND1=ND-1
PRINT *,ND1
DO 160 I=1,ND1
N=N+1
U=U+VR(I)
V=V+VR(I)*VR(I)
I1=I+1
DO 150 J=I1,ND
DX=X(J)-X(I)
DY=Y(J)-Y(I)
H=SQRT(DX*DX+DY*DY)
IF(N.GT.1.E-03)GO TO 121
PRINT 210,I,X(I),Y(I),J,X(J),Y(J)
GO TO 150
121 K=INT(H/STEP+0.5)+1
H1=ABS(H-(K-1)*STEP)
IF(K.GT.KMAX.OR.H1.GT.TOL)GO TO 150

DO 130 KD=1,NDI
COSD=(DX*CAN(KD)+DY*SIN(KD))/H
IF(ABS(COSD).GE.CDA)GO TO 140
TYPE 960,COSD
960 FORMAT(7' COSD= ',F7.5)
130 CONTINUE
GO TO 150
140 CONTINUE
NC(K,KD)=NC(K,KD)+1
D(K,KD)=D(K,KD)+H
VRR=VR(J)-VR(I)
G(K,KD)=G(K,KD)+0.5*VRR*VRR
N1(K,KD)=N1(K,KD)+2
U1(K,KD)=U1(K,KD)+VR(J)+VR(I)
V1(K,KD)=V1(K,KD)+VR(J)*VR(J)+VR(I)*VR(I)
150 CONTINUE
160 CONTINUE
IF(N.EQ.0)GO TO 180
V=V-U*U/N)/N
U=U/N
DO 170 IK1=1,KMAX
DO 170 IK2=1,NDI
D(IK1,IK)=D(IK1,IK)/MAXO(1,NC(IK1,IK))
170 G(IK1,IK)=G(IK1,IK)/MAXO(1,NC(IK1,IK)).
180 CONTINUE
IF(I8.EQ.1)RETURN
DO 190 IM=1,NDI
WRITE (3,220)

```



```

WRITE (3,240)TITLE,LAB
WRITE (3,250)U,ALP(IM),DALPHA,V,STEP,TOL,N
WRITE (3,260)
DO 190 IK=1,KMM
AS(IK)=AS(IK)+NC(IK,IM)
AG(IK)=AG(IK)+G(IK,IM)+NC(IK,IM)
AD(IK)=AD(IK)+D(IK,IM)+NC(IK,IM)
DUM1=(IK-1)*STEP-TOL
XLOW=AMAX1(DUM1,0.)
UP=(IK-1)*STEP+TOL
DUM2=(V1(IK,IM)-U1(IK,IM)+U1(IK,IM))
DUM3=MAXO(1,N1(IK,IM))
V2=(DUM2/DUM3)/DUM3
U1(IK,IM)=U1(IK,IM)/MAXO(1,N1(IK,IM))
AV(IK)=AV(IK)+NC(IK,IM)*V2
M2=U1(IK,IM)+U1(IK,IM)
AM(IK)=AM(IK)+M2*NC(IK,IM)
190 WRITE (3,271)XLOW,UP,NC(IK,IM),D(IK,IM),G(IK,IM)
WRITE (3,290)
TYPE 191
191 FORMAT (' DO YOU WANT AN AVERAGE VARIOGRAM (Y/N) ?',8)
ACCEPT 192, IANS2
192 FORMAT (A1)
IF (IANS2.NE.'Y') GO TO 195
WRITE (3,220)
WRITE (3,240)TITLE,LAB
WRITE (3,260)
DO 200 I=1,KMM
XLOW=AMAX1((I-1)*STEP-TOL,0.)
UP=(I-1)*STEP+TOL
AG(I)=AG(I)/AMAX1(1.,AS(I))
AD(I)=AD(I)/AMAX1(1.,AS(I))
VAR=AV(I)/AMAX1(1.,AS(I))
M2=AM(I)/AMAX1(1.,AS(I))
200 WRITE (3,270)XLOW,UP,AS(I),AD(I),AG(I)
195 CONTINUE
210 FORMAT (5X,'**DOUBLY DEFINED POINT**',2(I10,2F13.2))
220 FORMAT (1H1,///44X,'S E M I - V A R I O G R A M '/44X,27(1H=))
240 FORMAT (/42X,'(IRREGULAR GRID-2-DIMENSIONS)')///20X,'PROJECT : ',
1 20A4/20X,'PARAMETER : ',2A4///)
250 FORMAT(20X,'AVERAGE : ',F10.5,25X,'DIRECTION : ',F5.1,11X,
1 'TOLERANCE : ',F5.1/20X,'VARIANCE : ',F10.5,25X,'LAG : ',
1 F6.2,10X,'TOLERANCE : ',F6.2/20X,'NB OF DATA : ',I4///)
260 FORMAT (1H0,10X,'DISTANCE',13X,'NU. OF PAIRS',10X,
1 'AVERAGE DISTANCE',4X,'GAMMA',/)
270 FORMAT(1H ,4X,F7.2,'---',F7.2,10X,F8.0,8X,2(5X,F13.4))
271 FORMAT (1H,4X,F7.2,'---',F7.2,10X,18,8X,2(5X,F13.4))
280 FORMAT(1H ,1X,I3,'/',5(I3,1X,F7.2,1X,F11.5,'/'))
290 FORMAT(1H1)
300 FORMAT(50X,'A V E R A G E '/50X,13(1H=))
RETURN
END

```

REFERENCES

Bass, M. N., 1961, Regional tectonics of part of the southern Canadian Shield: *J. Geol.*, v. 69, p. 668-702.

Bertoni, C. H., 1981, Gold production in the Superior Province of the Canadian Shield. *CIM Bull.*, v. 76, no. 857, p. 62-69.

Bloomfield, A. L., Rood, H. S., Crocker, B. S., and Williamson, C. L., 1936, Milling investigations into the ore as occurring at the Lake Shore Mine. *Can. Inst. Min. Metall., Trans.*, v. 39, p. 279-434.

Bottinga, Y. and Javoy, M., 1975, Oxygen isotope partitioning among the minerals in igneous and metamorphic rocks: *Rev. Geophys. Space Phys.*, v. 13, p. 401-418.

Boutcher, S.M.A., Davis, G. L., and Moorhouse, W. W., 1966, Potassium and uranium lead ages from two localities. *Can. Mineralogist*, v. 8, p. 198-203.

_____, Edhorn, A. S., and Moorhouse, W. W., 1966, Archean conglomerates and lithic sandstones of Lake Timiskaming, Ontario: *Geol. Assoc. Can. Proc.*, 17, p. 21-42.

Boyle, R. W., 1961, The geology, geochemistry and origin of the gold deposits of the Yellowknife district. *Geol. Surv. Com. Mem.* 310, 193 p.

_____, 1979, The geochemistry of gold and its deposits. *Geol. Surv. Can., Bull.* 280, 584 p.

- _____, 1941, Rock Alterations by Hydrothermal Solutions in Certain Canadian Localities. Trans. Bruce, E. L., 1935, Little Long Lac gold area. Ont. Dept. Mines, Annual Report, pt. III, p. 1-58. Roy. Soc. Can., 3rd series, v. 35, sect. 4, pt. 1.
- Burrows, A. G., and Hopkins, P. E., 1914, The Kirkland Lake and Swastika Gold Areas: Ont. Bur. Mines, v. 23, pt. 2.
- _____, and Hopkins, P. E., 1920, The Kirkland Lake Gold Area (second report): Ont. Dept. Mines, v. 29, pt. 4, p. 1-48.
- _____, and Hopkins, P. E., 1923, Kirkland Lake Gold Area: Ont. Dept. Mines, v. 32, pt. 4, p. 1-52.
- Charlewood, G. H., 1964, Geology and Deep Developments on the Main Ore Zone at Kirkland Lake: Ont. Dept. Mines, Circ. No. 11, 49 p.
- Cherry, M. E., 1983, The association of gold and felsic intrusions - examples from the Abitibi Belt. in The Geology of Gold in Ontario, A. C. Colvine ed., Ont. Geol. Surv. Misc. Pap. 110, p. 48-55.
- Clayton, R. N., and Mayeda, T. K., 1963, The use of brominepentafluoride in the extraction of oxygen from oxides and silicates: Geochim. et Cosmochim. Acta, v. 27, p. 43-52.
- _____, O'Neil, J. R., and Mayeda, T. K., 1972, Oxygen isotope exchange between quartz and water:

- Jour. Geophys. Res., v. 77, p. 3057-3067.
- Condie, Kent C., 1981, Archean Greenstone Belts; Developments in Precambrian Geology, v. 3. Elsevier Scientific Publishing Co., Amsterdam, 434 p.
- Cooke, D. L., 1966, The Timiskaming volcanics and associated sediments of the Kirkland Lake area: Unpub. Ph.D. thesis, Univ. Toronto, 147 p.
- _____, and Moorhouse, W. W., 1969, Timiskaming volcanism in the Kirkland Lake area, Ontario, Canada: Can. Jour. of Earth Sciences, v. 6, p. 117-132.
- Costa, U. R., 1980, Footwall alteration and ore formation at Mattagami Mine, Quebec: Unpub. Ph.D. thesis, Univ. Western Ontario, London, Canada, 289 pp.
- Dyer, W. S., 1936, Geology and ore deposits of the Matachewan-Kenogami area: Ont. Dept. Mines, v. 44, pt. 2.
- Ewers, G. R., 1977, Experimental hot water-rock interactions and their significance to natural hydrothermal systems in New Zealand. Geochim. Cosmochim. Acta, v. 41, p. 143-150.
- Floyd, P. A. and Winchester, J. A., 1978, Identification and discrimination of altered and metamorphosed volcanic rocks using immobile elements: Chem. Geol., v. 21, p. 291-306.
- Freidman, I., and O'Neil, J. R., 1977, Compilation of Stable Isotope Fractionation Factors of Geochemical

Interest: U.S.G.S. Prof. Pap. 440-KK, Data of
Geochemistry, 6th Ed. 12 p.

Fyfe, W. S., Price, N. J., and Thompson, A. B., 1978,
Fluids in the Earth's Crust. Elsevier, Amsterdam, 383
p.

_____, and Kerrich, R., 1984, Gold: natural concen-
tration processes. in Gold '82: The geology, geo-
chemistry and genesis of gold deposits. R. P. Foster
ed., Geol. Soc. of Zimbabwe Spec. Publ. No. 1, p. 99-
127.

Gates, T. M., and Hurley, P. M., 1973, Evaluation of Rb-Sr
dating methods applied to Matachewan, Abitibi,
Mackenzie, and Sudbury dike swarms in Canada: Canadian
Journal of Earth Science, v. 10, p. 900-919.

Gerasimovsky, V. I., 1974, Trace elements in selected
groups of alkaline rocks, in Sorenson, H., ed., The
Alkaline Rocks: John Wiley and Sons, Ltd., p. 402-412.

Goodwin, A. M., 1965, Mineralized volcanic complexes in
the Porcupine-Kirkland Lake - Noranda region, Canada.
Econ. Geol., Vol. 60, p. 955-971.

_____, and Ridler, R. H., 1970, The Abitibi
orogenic belt, in Symposium on Basins and Geosynclines
of the Canadian Shield: Geol. Surv. Can., Pap. 70-40,
p. 1-30.

_____, and Ridler, R. H., 1977, The Abitibi Orogenic
Belt, in McCall, G.J.H., ed., The Archean: Dowder,

- Hutchinson and Ross Inc., Pennsylvania, 508 p.
- Graham, C. M., and Sheppard, S.M.F., 1978, Hydrogen isotope fractionation between aluminous hornblende and water: Prog. Exp. Petrol. Natural Environment Research Council Publ. Ser. D, No. 11, p. 152-153.
- _____, and Sheppard, S.M.F., 1980, Experimental hydrogen isotope studies. II. Fractionations in the systems epidote-NaCl-H₂O, epidote-CaCl₂-H₂O, and epidote seawater, and the hydrogen isotope composition of natural epidotes: Earth Planet. Sci. Lett., v. 49, p. 237-251.
- Gresens, R. L., 1967, Composition-volume relationships of metasomatism: Chem. Geol., v. 2, p. 47-65.
- Hawley, J. E., 1950, Mineralogy of the Kirkland Lake Ores, in Geology of the Main Ore Zone of Kirkland Lake: Ont. Dept. Mines, Ann. Rept. 1948, v. 57, pt. 5, p. 108-124.
- Hewitt, D. F., 1949, Geology of Skead Township, Larder Lake area: Ont. Dept. Mines, v. 58, pt. 6, 43 p.
- _____, 1963, The Timiskaming Series of the Kirkland Lake area: Can. Mineral., v. 7, pt. 3, p. 497-523.
- Hildreth, W., 1979, The Bishop Tuff: evidence for the origin of compositional zonation. In: Chapin, C. E., and Elston, W. G. (eds.), Ash-Flow Tuffs: G.S.A. Special Paper 180, p. 43-75.

Hodgson, C. J., 1982, Gold deposits in the Abitibi Belt, Ontario. in Summary of Field Work, 1982, by the Ontario Geological Survey, J. Wood, O. L. White, R. B. Barlow and A. C. Colvine, eds. Ont. Geol. Surv. Misc. Pap. 106, p. 192-197.

_____, 1983, Preliminary report on a computer file of gold deposits of the Abitibi Belt, Ontario. in The Geology of Gold in Ontario, A. C. Colvine, ed., Ont. Geol. Surv. Misc. Pap. 110, p. 11-37.

Hutchinson, R. W., 1976, Lode Gold Deposits: the Case for Volcanogenic Derivation. in Proceedings Volume, Pacific Northwest Mining and Metals Conference, Portland Oregon, 1975, Oregon Department of Geology and Mineral Industry, p. 64-105.

_____, and Burlington, T. L., 1984, Some broad characteristics of greenstone belt gold lodes. in Gold '82: The geology, geochemistry and genesis of gold deposits, R. P. Foster, ed., Geol. Soc. of Zimbabwe, Spec. Pap. No. 1, p. 339-372.

Hyde, R. S., 1978, Sedimentology, volcanology, stratigraphy and tectonic setting of the Archean Timiskaming Group, Abitibi Greenstone Belt, Northeastern Ontario, Canada: Unpub. Ph.D. thesis, McMaster Univ., Hamilton, 422 p.

_____, 1980, Sedimentary Facies in the Archean Timiskaming Group and their Tectonic Implications, Abitibi Greenstone Belt, Northeastern Ontario, Canada:

Precambrian Res., v. 12, p. 161-195.

_____, and Walker, R. G., 1977, Sedimentary environments and the evolution of the Archean greenstone belt in the Kirkland Lake area, Ontario: Geol. Surv. Can., Paper 77-1A, p. 185-190.

Irvine, T. N., and Baragar, W.R.A., 1971, A guide to the chemical classification of the common volcanic rocks. Can. Jour. Earth Sci., v. 8, p. 523-548.

Javoy, M., 1977, Stable Isotopes and Geochemistry: Jour. Geol. Soc., v. 133, p. 609-636.

Jensen, L. S., 1976, Regional Stratigraphy and Structure of the Timmins-Kirkland Lake Area, District of Cochrane and Timiskaming and Kirkland Lake Area, District of Timiskaming, in Milne, V. G., Cowan, W. R., Card, K. D., and Robertson, J. A., eds., Summary of Field Work, 1976, by the Geological Branch: Ont. Dept. Mines, Misc. Paper 67, 183 p.

_____, 1978a, Archean komatitic, tholeiitic, calc-alkalic, and alkalic volcanic sequences in the Kirkland Lake area. in Currie, A. L., and Mackasey, W. O., eds., Toronto '78 Field Trip Guidebook: Geol. Assoc. of Canada, 361 p.

_____, 1978b, Regional stratigraphy and structure of the Timmins-Kirkland Lake area, District of Cochrane and Timiskaming and the Kirkland-Larder Lake area, District of Timiskaming, in Summary of Field Work,

- 1978: Ont. Geol. Surv. Misc. Paper 82, p. 67-72.
- _____, 1980, Archean gold mineralization in the Kirkland Lake-Larder Lake area, in Roberts, R. G., ed., Genesis of Archean, Volcanic-hosted Gold Deposits: Ont. Geol. Surv., Open File Rept. 5293, p. 280-302.
- Jensen, L. S., and Pyke, D. R., 1980, Komatiites in the Ontario portion of the Abitibi belt, in Komatiites, N. T. Arndt and E. G. Nisbet (eds.), Allen and Unwin, London.
- _____, and Langford, F. F., 1983, Geology and Petrogenesis of the Archean Abitibi Belt in the Kirkland Lake Area, Ontario: Ont. Geol. Surv. Open File Report 5455.
- Jolly, W. R., 1974, Regional metamorphic zonation as an aid in study of Archean terrains; Abitibi Region, Ontario: Canadian Min., v. 12, p. 499-508.
- _____, W. R., 1978, Metamorphic history of the Archean Abitibi Belt, in Metamorphism in the Canadian Shield. Geol. Surv. Can. Paper 78-10, p. 63-78.
- Journel, A. G., 1975, Ore grade distributions and conditional simulations - two geostatistical approaches. Proceedings of the NATO A.S.I. "Geostat 75" Reidal Publishing Corp., Dordrecht, pp. 137-161.
- _____, and Huijbregts, Ch. J., 1978, Mining Geostatistics. Academic Press, London, 600 p.

_____, and Froideveaux, R., 1982, Anisotropic
hole-effect modeling. *Mathematical Geology*, Vol. 14,
No. 3, p. 217-239.

Keays, R. R., 1982, Palladium and iridium in komatiites and
associated rocks: application to petrogenetic
problems, in *Komatiites*, N. T. Arndt and E. G. Nisbet
(eds.). Allen and Unwin, London, p. 435-457.

_____, 1984, Archean gold deposits and their source
rocks: the upper mantle connection. in *Gold '82: The
geology, geochemistry and genesis of gold deposits*,
R. P. Foster, ed., Geol. Soc. of Zimbabwe Spec. Pub.
No. 1, p. 17-51.

_____, and Scott, R. B., 1976, Precious metals in
ocean-ridge basalts: implications for basalts as
source rocks for gold mineralization. *Econ. Geol.*,
v. 71, p. 705-720.

Kerrich, R., and Fryer, B. J., 1979, Archean precious-
metal hydrothermal systems, Dome Mine, Abitibi green-
stone belt, II. REE and oxygen isotope relations:
Can. J. Earth Sci., v. 15, p. 440-458.

_____, and Fyfe, W. S., 1981, The gold-carbonate
association: source of CO₂ and CO₂-fixation reactions
in Archean lode deposits. *Chem. Geol.*, v. 33, p.
265-294.

_____, 1983, *Geochemistry of Gold Deposits in the
Abitibi Greenstone Belt*: Canadian Institute of Mining

- and Metallurgy Special Paper, Volume 27, 75 pp.
- _____, and Watson, G. P., 1984, The Macassa Mine Archean lode gold deposit, Kirkland Lake, Ontario: geology, patterns of alteration and hydrothermal regimes. Econ. Geol. (in press).
- Krogh, T. E., Davis, D. W., Nunes, P. D., and Korfu, F., 1982, Archean evolution from precise U-Pb isotopic dating: GAC/MAC Progs. with Abstracts, Winnipeg, v. 7, p. 61.
- Kwong, Y.T.S., and Crocket, J. H., 1978, Background and anomalous gold in rocks of an Archean greenstone assemblage, Kakagi Lake area, Northwestern Ontario. Econ. Geol., v. 73, p. 50-63.
- Lindgren, W., 1933, Mineral Deposits, 4th ed. McGraw-Hill, New York.
- Lovell, H. L., 1967, Geology of the Matachewan area: Ont. Dept. Mines, Geol. Report 51, 61 p.
- _____, and Ploeger, F. R., 1980, 1979 Annual Report of the Kirkland Lake Resident Geologist, in Annual Report of the Regional and Resident Geologists: Ont. Geol. Surv., Misc. Paper 91, p. 77-96.
- MacLean, A., 1944, Geology of Lebel township, East Kirkland Lake area: Ont. Dept. of Mines Ann. Rept., v. 53, pt. 2.
- Harmont, S., 1983, The role of felsic intrusions in gold mineralization. in The Geology of Gold in Ontario,

A. C. Colvine, ed., Ont. Geol. Surv. Misc. Pap. 110,
p. 38-47.

Marshall, H. I., 1947, Geology of Midlothian Township.

Ontario Dept. of Mines, Annual Rep., Vol. '56, Part 5:
24 p.

Marumo, K., Nagasawa, K., and Kurodo, Y., 1980, Mineralogy
and hydrogen isotope geochemistry of clay minerals in
the Ohnuma geothermal area, Northeastern Japan: Earth
Planet. Sci. Letts., v. 47, p. 255-262.

Mathéron, G., 1962, Traite de Geostatistique Appliquee.
Vols. 1 and 2.

_____, 1963, Principles of geostatistics. Econ.
Geol., v. 58, p. 1246-1266.

Maynard, J. B., 1983, Geochemistry of sedimentary ore
deposits: Springer Verlag, New York, 305 pp.

Meyn, H. D., 1977, Iron deposits of Ontario, in Ont. Geol.
Surv. Misc. Pap. 75, p. 190.

Miller, W. G., and Knight, C. W., 1914, The Precambrian
geology of southeastern Ontario. Ont. Dept. of Mines,
Annual Report, Vol. 22, pt. 2.

Nemcsok, G., 1980, Geology of the Macassa Gold Mine:
Unpub. Company report.

Nunes, P. D., and Jensen, L. S., 1980, Geochronology of the
Abitibi metavolcanic belt, Kirkland Lake Area -
Progress Report. In: E. G. Pye (ed.), Summary of
Geochronology Studies 1977-1979: Ontario Geological

Survey Misc. Paper 92, p. 40-45.

O'Neil, J. R., and Taylor, H. P., Jr., 1967, The oxygen isotope and cation exchange chemistry of feldspar: *Am. Mineral.*, v. 52, p. 1414-1437.

Ploeger, F. R., 1980, Kirkland Lake Gold Study, District of Timiskaming. in Milne, V. G., White, O. L., Barlow, R. B., Robertson, J. A., and Colvine, A. C., eds., Summary of Field Work, 1980, by the Ontario Geological Survey: *Ont. Geol. Surv.*, Misc. Paper 96, p. 188-190.

_____, 1981, Kirkland Lake Gold Study, District of Timiskaming. in Wood, J., White, O. L., Barlow, R. B., and Colvine, A. C., eds., Summary of Field Work, 1981, by the Ontario Geological Survey. *Ont. Geol. Surv. Misc. Pap.* 100, p. 248-250.

_____, and Crockett, J. H., 1982, Relationship of Gold to Syenitic Intrusive Rocks in Kirkland Lake, in *Geology of Canadian Gold Deposits: Can. Inst. of Min. Met.*, Spec. Vol. 24, p. 69-72.

Price, P., 1948, Horne Mine. in *Structural Geology of Canadian Ore Deposits*, v. 1, Jubilee Volume, *Can. Inst. Min. Metall.*, p. 763-772.

Puddephatt, R. J., 1978, *The Chemistry of Gold*. Elsevier, Amsterdam, 274 p.

Purdy, J. W., and York, D., 1968, Rb-Sr whole rock and K-Ar mineral ages from the Superior Province near

Kirkland Lake, northeastern Ontario, Canada: Can. Jour. Earth Sci., v. 5, p. 699-705.

Pyke, D. R., 1975, On the relationship of gold mineralization and ultramafic volcanic rocks in the Timmins area. Ont. Div. Mines, Misc. Pap. 62, 23 p.

_____, and Jensen, L. G., 1976, Preliminary Stratigraphic Interpretation of the Timmins-Kirkland Lake Area, Ontario: Geol. Assoc. Canada Program with Abstracts, v. 1; p. 71.

Ridler, R. H., 1969, The relationship of mineralization to volcanic stratigraphy in the Kirkland Lake area, Northern Ontario, Canada: Unpub. Ph.D. thesis, Univ. Wisconsin.

_____, 1970, Relationship of mineralization to volcanic stratigraphy in the Kirkland Lake-Larder Lake area, Ontario: Proceedings, Geol. Assoc. Canada, v. 21, p. 33-42.

_____, 1975, Regional metallogeny and volcanic stratigraphy of the Superior Province, in Report of Activities, Part A: Geol. Surv. Can. Paper 75-1A, p. 353-358.

_____, 1976, Stratigraphic keys to the gold metallogeny of the Abitibi Belt: Can. Min. J., v. 97, No. 6, p. 81-87.

Roberts, R. G., 1981, The Volcanic-Tectonic Setting of Gold Deposits in the Timmins Area, Ontario, in Genesis of

Archean, Volcanic-Hosted Gold Deposits, Symposium held at University of Waterloo, Mar. 7, 1980: Ont. Geol. Surv. Misc. Pap. 97, p. 16-29.

Roedder, E., 1967, Fluid inclusions as samples of ore fluids. In Barnes, H. L. (ed.), *Geochemistry of Hydrothermal Ore Deposits*: New York, Holt Rinehart and Winston, p. 515-574.

_____, 1976, Fluid inclusion evidence on the genesis of ores in sedimentary and volcanic rocks. in *Handbook of Stratiform and Stratiform Ore Deposits*, K. H. Wolfe, ed., v. 2, p. 67-110.

_____, 1979, Fluid inclusions as samples of ore fluids. in *Geochemistry of Hydrothermal Ore Deposits* (2nd Edition), H. L. Barnes, ed., p. 684-737.

_____, 1984, Fluid inclusion evidence bearing on the environments of gold deposition. in *Gold '82: The geology, geochemistry and genesis of gold deposits*, R. P. Foster, ed., Geol. Soc. of Zimbabwe Spec. Pub. No. 1, p. 129-163.

Saager, R., Meyer, M., and Muff, R., 1982, Gold distribution in supracrustal rocks from Archean greenstone belts of Southern Africa and from Paleozoic ultramafic complexes of the European Alps: metallogenic and geochemical implications. *Econ. Geol.*, v. 77, p. 1-24.

Seward, T. M., 1973, Thio complexes of gold in hydrothermal ore solutions. *Geochim. Cosmochim. Acta*, v. 73, p. 379-399.

_____, 1984, The transport and deposition of gold in hydrothermal systems. in *Gold '82: The geology, geochemistry and genesis of gold deposits*, R. P. Foster, ed., Geol. Soc. of Zimbabwe Spec. Pub. No. 1, p. 165-180.

Sibson, R. H., Moore, J. McM., and Rankin, A. H., 1975, Seismic pumping - a hydrothermal fluid transport mechanism. *Journ. Geol. Soc. Lond.*, v. 81, p. 653-659.

_____, 1981, Fluid flow accompanying faulting: field evidence and models. in *Earthquake prediction and International Review*, D. W. Simpson and P. G. Richards, eds., American Geophys. Union; Morris Ewing Series, 4, p. 593-604.

Smith, R. L., 1979, Ash flow magmatism. In: Chapin, C. E., and Elston, W. E. (eds.), *Ash-Flow Tuffs*, G.S.A. Special Paper 180, p. 5-27.

Sorenson, H., 1974, Alkali syenites, feldspathoidal syenites and related lavas, in Sorenson, H., ed., *The Alkaline Rocks*: John Wiley and Sons, Ltd., p. 22-52.

Stricker, S. J., 1978, The Kirkland Lake - Larder Lake stratiform carbonatite. *Mineral. Depos. (Berl.)*, v. 13, p. 355-367.

Suzuoki, S. R., and Epstein, S., 1970, Hydrogen isotope fractionation factors (δ 's) between muscovite, biotite, hornblende and water: Am. Geophys. Union Trans., v. 51, p. 451-452.

_____, and Epstein, S., 1974, Hydrogen isotope fractionation between OH-bearing silicate minerals and water: Geochim. Cosmochim. Acta, v. _____, p. _____.

Taylor, H. P., 1968, The oxygen isotope geochemistry of igneous rocks: Contrib. Mineral. Petrol., v. 19, p. 1-17.

_____, 1974, The application of oxygen and hydrogen isotope studies to problems of hydrothermal alteration and ore deposition: ECON. GEOL., v. 69, p. 843-883.

_____, 1978, Oxygen and hydrogen isotope studies of plutonic granite rocks: Earth Plan. Sci. Letts., v. 38, p. 177-210.

_____, 1979, Oxygen and hydrogen isotope relations in hydrothermal mineral deposits. In Geochemistry of Hydrothermal Ore Deposits, 2nd Edition, ed. by H. L. Barnes. John Wiley and Sons, New York, p. 236-277.

Taylor, R. P., Strong, D. F., and Fryer, B. J., 1981, Volatile control of contrasting trace element distributions in peralkaline granitic and volcanic rocks. Contrib. Mineral. Petrol., v. 77, p. 267-271.

Thomson, J. E., 1941, Geology of McGarry and McVittie townships, Larder Lake area: Ont. Dept. of Mines,

Ann. Rept., v. 50, pt. 7.

_____, 1946, The Keewatin-Timiskaming unconformity in the Kirkland Lake district: Trans. Roy. Soc. Can., Ser. 3, v. 40, p. 113-124.

_____, 1948, Regional structure of the Kirkland Lake-Larder Lake area, in Structural Geology of Canadian Ore Deposits: CIM Special Vol., p. 627-632.

_____, 1950, Geology of Teck Township and Kenogami Lake area, Kirkland Lake Gold Belt: Ont. Dept. of Mines, v. 57, pt. 5, p. 1-53.

Thomson, J. E., Charlewood, G. H., Griffin, K., Hawley, J. E., Hopkins, H., MacIntosh, C. G., Ogrizio, S. P., Perry, O. S., and Ward, W., 1950, Geology of the Main ore zone at Kirkland Lake: Ont. Dept. of Mines, v. 57, pt. 5, p. 54-196.

Tihor, L. A., and Crocket, J. H., 1977, Gold Distribution in the Kirkland Lake-Larder Lake area with Emphasis on Kerr Addison Type Ore Deposits - a Progress Report, in Report of Activities, Part A: Geol. Surv. of Canada, Paper 77-1A, p. 363-369.

Tilling, R. I., Gottfried, D., and Rowe, J. J., 1973, Gold abundances in igneous rocks, bearing on gold mineralization. Econ. Geol., v. 68, p. 168-186.

Todd, E. W., 1928, Kirkland Lake Gold Area: Ont. Dept. of Mines, v. 37, pt. 2.

Turekian, K. K. and Wedepohl, K. H., 1961, Distribution of the elements in some major units of the earth's crust: Geol. Soc. America Bull., v. 7, p. 175-192.

Tyrrell, J. B., and Hore, R. E., 1926, The Kirkland Lake Fault: Trans. Roy. Soc. Can., 3rd series, v. 20, pt. 1, sect. 4.

Viljoen, R. P., Saager, R., and Viljoen, M. J., 1970, Some thoughts on the origin and processes responsible for the concentration of gold in the early Precambrian of southern Africa. Mineral. Dep., v. 5, p. 164-180.

Ward, W., and Thomson, J. E., 1950, Geology of the Macassa Mine, in Geology of the Main Ore Zone of Kirkland Lake: Ont. Dept. Mines, Annual Rept. for 1948, v. 57, pt. 5, p. 125-132.

Watson, G. P. and Kerrich, R., 1983, Macassa Mine, Kirland Lake - Production history, geology, gold ore types and hydrothermal regimes, in The Geology of Gold in Ontario, A. C. Colvine (ed.), Ont. Geol. Surv., Misc. Pap. 110, p. 56-74.

Wenner, D. B. and Taylor, H. P., 1971, Temperatures of serpentinitisation of ultramafic rocks based on ¹⁸⁰/₁₆₀ fractionations between co-existing serpentine and magnetite: Contr. Mineral. Petrol., v. 32, p. 165-185.

Wilson, A. D., 1955, A new method for the determination of ferrous iron in rocks and minerals, Great Britian. Geol. Surv. Bull., v. 9, p. 56-58.

Wilson, D. B., Andrews, P., Moxham, R. L., and Ramel, K.,
1965, Archean Volcanism in the Canadian Shield: Can.
Jour. Earth Science, v. 2, p. 161-175.

END

2	4	0	3	8	5
---	---	---	---	---	---

FIN